Comparison Of Two Hydrological Models On A Virginia Piedmont Watershed

by

Youtong Fu

The thesis submitted to the Faculty of the
Virginia Polytechnic Institute and State University
for approval of the research for the degree of

MASTER OF SCIENCE
in
Agricultural Engineering

APPROVED:

V.O.Shanholtz, Chairman

S.Mostaghimi

G.V.Loganathan

J.Perumpral, Department Head

December , 1994
Department of Biological Systems Engineering
Virginia Tech
Blacksburg, Virginia

.2

COMPARISON OF TWO HYDROLOGICAL MODELS ON A VIRGINIA PIEDMONT WATERSHED

by

Youtong Fu

Dr. V. O. Shanholtz , Chairman

(ABSTRACT)

KINEROS and PSRM-QUAL , two distributed parameter event-based hydrologic models, were applied to Foster Creek Watershed, Louisa County, Virginia. The simulations of the two models were conducted using published data and a ten year database from the Foster Creek Watershed, Louisa County, Virginia. Data management and analysis was supported through the use of PC-VirGIS, a DOS based GIS package developed by the Information Support Systems Laboratory, Virginia Tech.

The performance of the two models were based on the criteria established to compare the simulated and recorded peak discharge rates , total runoff volumes and time to peak. Goodness of fit criteria were based on graphic comparison, relative error, model efficiency, linear regression, hypothesis testing and variance. Based on these measurements, the simulated results by both models were acceptable. KINEROS generally made better predictions of peak discharge rate and time to peak. Hydrograph shapes also

generally matched the recorded sequence more closely. PSRM-QUAL simulated the total runoff volume slightly better than KINEROS.

The sensitivity of KINEROS and PSRM-QUAL to the model input parameters was evaluated. For KINEROS, peak discharge rate and runoff volume were very sensitive to changes in rainfall amount, saturated hydraulic conductivity and effective capillary drive. For PSRM-QUAL, peak discharge rate and total runoff volume were very sensitive to changes in SCS CN, initial abstraction coefficient and rainfall amount.

ACKNOWLEDGMENTS

I wish to acknowledge the influence and effort of Dr. Vernon Shanholtz. I would like to thank him for his patience, continuous support and great assistance.

Thanks are also due to Dr.Saied Mostaghimi, Dr.G.V.Loganathan for their guidance and support.

Special thank goes to Dr.D.A.Woolhiser for his valuable comments and suggestions on KINEROS model. I also wishes to thank Jan Carr and Dr. D.F. Kibler for their dedication and assistance with the data source of Foster Creek Watershed and PSRM-QUAL model package, respectively. Without their help, this work would not have been possible. In addition, I would like to thank Dr. Yahui Zhuang, Mr. Wes Kleene, Dr. Faycal Bouraoui, Mr. Chetan Desai, Mrs. Tina Strealy-Colom, Mr. Gene Yagow, Mr. Mike Justice, Mr. Aguilar Oscar and the staffs working at ISSL, for their input in the way of comments, assistance and suggestions. Many thanks to fellow students and friends for the good times and friendships.

I would like to thank Dr. Boyd Harshbarger and Mrs. Harshbarger for their encouragement.

I wish thank to my wife, Qun, for her love, help, patience and understanding since the beginning.

Finally, I would like to thank my relatives in Nanjing, my wife's parents and my parents for their love, encouragement and support.

TABLE OF CONTENTS

CHAPTER 5 BASIS FOR COMPARISON

CHAPTER 6 ANALYSIS AND RESULTS

LIST OF TABLES

LIST OF FIGURES

Chapter 1

INTRODUCTION

1.1 *BACKGROUND*

The hydrologic cycle and transport processes are always the center of environmental concerns in natural resource and biological systems. The hydrologic response of a catchment or a watershed is often measured in term of sediment and pollutants loads transported in both surface and subsurface pathways. Computer simulation models have been developed and demonstrated to be powerful tools in analyzing watershed hydrologic responses. Computer-based models have been used as predictive and forecasting tools.

Pollution from nonpoint sources (NPS) is a major contributor to poor stream water quality. Although the agricultural sector is generally considered to be a significant contributor to NPS pollution, other areas such as urban and forestry, can also provide significant pollutant loads. For several decades, the NPS pollution models have been developed and extensively applied to agricultural or urban watersheds. There is a growing need , however, for modeling procedures that operate equally well within both the urban and non-urban settings with the development of urbanization.

Two models, the Kinematics Runoff and Erosion Model (KINEROS) (Woolhiser et al., 1990) and the Penn State Runoff Quality Model (PSRM-QUAL) (Aron et al., 1992), were compare relative to their abilities to simulate storm flow sequences from a rural multiple land use watershed. The comparison involved the use of Geographic Information System (GIS) technology to calculate

model parameters and to display graphical results. The comparison of the two models was based on established criteria.

KINEROS is a distributed, event-based model developed in the Southwest for the Agricultural Research Service, United States Department of Agriculture (Woolhiser et al., 1990). Based on discussion with Dr. Woolhiser (D.A.Woolhier, personal communication, 1992), it has not been evaluated on Eastern United States watersheds. Components in KINEROS are based on physical principles such as the conservation of mass and momentum. The dimensional kinematic wave equation is used to calculate both overland and channel flows. The model includes procedure to provide peaks and volumes of runoff and sediment loads. The model does have components to simulate hydrologic responses and NPS pollution on less urban areas.

Penn State Runoff Quality Model (PSRM-QUAL) was developed in the mid-1970's at Pennsylvania State University (Aron et al., 1992). PSRM-QUAL is a distributed, event-based and urban-oriented model. An urban drainage system is sub-divided into sub-areas and each sub-area is further sub-divided into impervious and pervious overland flow planes. Surface runoff is routed across the plane surfaces using the kinematic wave equation. The PSRM-QUAL simulates peak discharge, runoff volume and pollutants such as suspended solids, trace metals and nutrients from either urban or non-unban watersheds (Aron et al., 1992).

Distributed-parameter models such as KINEROS and PSRM-QUAL include input parameters that are used to represent the relevant physical characteristics of a watershed. These types of models, however, require significant time to collect and organize data sets. Computation

time also can be expensive. The availability and cost of assembling detailed data sets has hampered widespread use of these type models.

GISs have been demonstrated as effective and efficient tools for handling spatial and non-spatial data and for performing such tasks as data inventory, management and spatial analysis (Shanholtz et al., 1988). The integration of GIS with distributed parameter models is expected to overcome some of the previous barriers contributing to their limited use.

1.1 RESEARCH OBJECTIVES

The basic goal of this research was to compare the simulation capabilities of KINEROS and PSRM-QUAL hydrologic models. This study provided support to a major study of the impact of development on the quality of surface and groundwater in the Thomas Jefferson Planning District, which includes Albemarle, Louisa, Green, Nelson and Fluvanna counties, Virginia. Both KINEROS and PSRM-QUAL models have been reported capabilities for simulating quantity and quality from both rural and urban areas (Woolhiser et al., 1990; Jackson, 1982; Kibler et al., 1982). Because of interest in evaluating models with historical hydrological data in this region, data for the Foster Creek Watershed (V.O.Shanholtz, personal communication , 1992) was selected for analysis.

The record included 10-years of hydrologic data but did not include water quality information.

The specific objectives of this research project included:

1. Compare the capability of KINEROS and PSRM-QUAL hydrologic model to simulate peak flow rate, time to peak, total runoff volumes and hydrograph shapes.

2. Conduct an analysis to determine relative sensitivity of simulated results to variation in model parameters.

Chapter 2

LITERATURE REVIEW

2.1 *INTRODUCTION*

Nonpoint source pollution (NPS) is one of the greatest concerns of environmental pollution of our times. It has significantly affected our environment. It is responsible for more than half of all water pollution. The EPA (1983) reported that 6 of 10 EPA regions found NPS pollution to be the principle remaining cause of water quality problems.

NPS pollution is diffuse pollution caused by man and his activities and emanates from such sources as agricultural farming, urban development, mining construction and transportation. NPS is the result of land use interaction with the hydrological transport system.

NPS pollution differs from point source (PS) pollution. PS pollution is defined as those sources which enter a watershed at a specific point, for example, effluent from industrial and sewage treatment plants, pollutants from farm buildings or solid waste disposal sites. It is discharged from pipe flows such as from municipal and industrial source.

Novotny and Chesters (1981) stated that " Nonpoint source pollution originates from nonpoint sources which are commonly regarded as those sources discharged to a watershed in a way that they depend upon the vagaries of the hydrologic cycle to transport them to the stream system". The major contribution of such pollution are sediments, nutrients, pathogenic bacteria, pesticides, heavy metals, auto emissions, PCBs, etc.

NPS pollution is categorized by Novotny and Chesters(1981) into rural and urban NPS pollution. The rural NPS pollution results from the sources related to agricultural cultural activities.

Soil types, climate, management practice and topography are the critical factors in determining the extent and magnitudes of rural NPS.

Urban NPS is closely related to the urbanization and hydrological modification above original or background levels. Storm water runoff has been recognized as a serious cause of water quality degradation in urban areas. Rapid urbanization, with its associated land clearing and paving of pervious area, has accelerated the problem recently. The USEPA Nationwide Urban Runoff Program (1983) reported " the urban nonpoint source water quality problems effect some 20% of the nation's river mileage". Thirty of 248 urbanized areas suffer priority runoff problems in USA as which indicated by Hearney and Huber (1982). An increase in volume and rate of runoff was due to an increase in impervious area and drainage improvement enhance the possibility of contamination to receiving waters.

There are differences between the rural NPS pollution such as the NPS pollution from agricultural land and urban NPS pollution from developed urban areas such as a city or, metropolitan areas because of the their different hydrologic characteristics. Urban NPS problems have unique characteristics related to concentration, distribution and decay.

There exists many localities which have both agricultural and urban landuse. The NPS pollution from such areas have the characteristics of both urban and agricultural areas.

The pollution from nonpoint sources have been considered as a hydrological problem. In general, the occurrence of meteorological events control the peak discharges of the sources. Many researchers report that two or three large storms each year are responsible for most of the total annual NPS pollutant yields. Nonpoint source pollution is almost nonexistent during droughts. The

hydrologic parameters such as rainfall volume and intensity, infiltration and storage, and the characteristics of a watershed have been considered closely related with NPS pollution (Novotny and Chesters, 1981). Hydrologic modifications of a watershed also can have a significant impact on NPS pollution. The objective to reduce the hydrological activity of lands are often effective for controlling excessive pollution . The NPS pollution is highly random because such nonpoint source is tied to random hydrologic process. Transport by surface water hydrological processes are often at the core of nonpoint sources pollution.

2.2 *NPS POLLUTION MODELING*

2.2.1 *The Usefulness and Classification of Models*

To better understand or explain the hydrological process, models have been developed to predict a watershed hydrological responses. Diskin (1970) defined models as: " simplified systems that are used to represent real-life systems and may be substitutes of the real systems for certain purpose. The models express formalized concepts of the real system.". Wight (1988) gave the definition of a model as the process of organizing, synthesizing, and integrating component parts into a realistic representation of the prototype. The model is a representation of reality but never a complete representation (Blackie et al., 1985). Watershed hydrologic models are approximations of the actual watershed system and obviously represent the hydrological cycle in various and appropriate ways (Woolhiser, 1982; Chow, 1988). Measurable or inferable hydrological and chemical variables are the inputs and outputs of hydrological or NPS models. The structure of the models is a set of equations linking with inputs and outputs (Chow, 1988). The best hope of the

hydrological model is that it will simulate with the reasonable accuracy the response of the system to a given input (Blackie et al., 1985).

The usefulness and importance of modeling have been illustrated by numerous investigators (e.g. Novotny and Chesters, 1981; Decousey, 1985). The various attributes or characteristics are given in the following list.

- Models have the capabilities to predict the effects of hydrological modification and impact of planned action on NPS.
- Models can shape the definition of hypothesis.
- Models can determine the critical area or process and areas of concerns of NPS pollution.
- Models can help the decision-maker to improve the informational background on which decisions are based and substantially reduce the cost of managing water resources.
- Models can generate and evaluate numerous alternatives for managing and controlling the pollution according to specific requirements.
- Models have significantly expanded the nation's ability to understand and manage large area NPS pollution.
- Models have the potential to provide even greater benefits for nonpoint sources pollution and water resource decision-makers both now and in the future.

Different criteria reflect different purposes which result in the classifications of models. Either material or formal (or mathematical) are the basic two types models used in any discipline including the hydrological science (Woolhiser, 1982 ; Haan , 1986).

Formal or mathematical models are commonly used in hydrological modeling. A formal model uses a symbolic and usually mathematical approximate representation of important structural properties of a real watershed (Woolhiser, 1982). Mathematical models have been used extensively on watershed hydrology and NPS pollution modeling since the late 1960s (DeCoursey, 1985). Because of popularity of computer technology, mathematical models coded in the computer are much more easily understandable and usable.

Stochastic, deterministic and parametric techniques are the generally accepted approaches to watershed modeling (DeCoursey, 1971; Woolhiser, 1971; Synder, 1972; McCuen and Snyder, 1986).

In stochastic models are the watershed outputs are considered as a time series of random events. An important element of the stochastic process is the nonpredictability of exact magnitudes of simulated objects (McCuen and Snyder, 1986).

Clark (1973), Woolhiser (1982), McCuen and Snyder(1986) and Chow (1988) pointed out that a common characteristic of deterministic models is that all variables of the model are assumed to be free of random variation. A set of input values will always simulate the same values. Deterministic models have evolved from the application of physical or chemical principles such as the laws of conservation of mass, energy, and momentum. Physical parameters used in deterministic models can be either measured, determined or derived. This type of model does not theoretically required

calibration. The deterministic models attempt to capture all aspects of the real system, which make them primary candidates for NPS pollution applications.

Parametric models contain both stochastic and deterministic processes (McCuen and Snyder, 1986). This approach is used when information or general knowledge of the process of real system is lacking. This approach starts from a conceptualization of the process on the real watershed. Each physical component of the system or process is modeled in a simpler manner.

Models can be categorized as static or dynamic models according to the role of time (Woolhiser, 1982):

" Static models include various empirical equations and regression models in which time is not independent, and dynamics models require different equations with time as an independent variable and thus can show time variability output."

Dynamic models can be classified as event-based or continuous-simulation models (Woolhiser, 1982). Event-based models simulate the hydrologic response for a single storm event. The event-based can not calculate the total annual water yield. It generally ignores or lumps evaporation and snow melt. Continuous models calculate the water balance, characterize long-term system response and account for meteorological variability. The event-based model generally does not have the capability to simulate long term processes. However, continuous models can represent the long term process of a simulated system. One of the disadvantage of continuous models is the individual events are ignored and some processes of interest may not be adequately described for storms.

Whether the model will employ a phenomenological or transfer function , i.e. "black box" leads to the classification of lumped and parametric-distributed models (Huggins and Burney, 1982). Thus, NPS pollution modeling can be categorized into lumped and parametric-distributed models according to the operation of models.

2.2.2 *Lumped Models*

To model the complete catchment hydrological system accurately requires a very detailed knowledge of the physical and biological characteristics of a watershed. Simplification must be made to model the watershed because of the complexity of natural systems. The most common and earliest simplification made in watershed is lumping or spatial averaging (Blackie et al., 1985). The lumped model approach is based on the law of the mean in differential calculus. The inputs and response of the watershed system can be represented mathematically using only the dimensions of depth and time. This approach assumes that the parameters have continuous functions, thus mean values can be used to evaluate the impact on a simulated response. The model does not consider spatial variability. Lumped models replace a spatial distributed process by one that is parameterized at a larger scale, e.g. the watershed. The successful application of a lumped model depends on stability of the watershed system i.e. uniform spatial distribution of precipitation, landuse and soil characteristics.

The characteristics of lumped models include the following:

- A single input to create a single output at a single point.
- The models require calibration, fitting and averaging of the parameter values.
- The models need historical data to conduct the calibration.

- The models are site specific and generally non transferable from watershed to watershed without calibration.

2.2.3 ***Distributed Models***

Spatial variability of the watershed characteristics are considered in distributed models. Huggins and Burney (1982) defined distributed models as: " to incorporate, to the degree practical, data concerning the area distribution of parameter variations together with computation algorithm to evaluate the influence of this distribution on simulated behavior".

In the use of distributed models, the watershed is discretized into hydrological homogenous units. Parameters for homogenous units are lumped. The distributed model therefore is a lumped process model at the computational element level but it is a distributed model at the watershed level. This type of model can avoid many of the errors attributed to spatial averaging or lumping over the whole watershed which may misrepresent the physical processes (Vieux, 1991).

The distributed models are generally associated with physical models. Physically based models are distributed because one or more space coordinates are involved in the equation defined in the models. The described equations for physically based models are generally nonlinear partial differential equations, which are solved using approximate numerical methods. The physical parameters of the distributed models can be measured, derived or extrapolated for other location or time periods. Theoretically, these parameters do not require calibration, which means the distributed-model can be used on ungaged watershed.

A model does not completely represent all factors of a watershed drainage because complex interactions are not fully understood. As a result, conceptual or empirical functions or laws are used

in some components of the models. A typical example is Manning's law for channel flows. These functions or laws have been extensively validated by experiment.

Distributed models are powerful tools to determine the efficiency of different management alternatives. Beven (1982) identified four major areas are appropriate to the application of distributed models. 1) Evaluating the effects of landuse change; 2) Evaluating the effects of spatially variable inputs and outputs; 3) Evaluating pollutant transport; 4) Forecasting the hydrological response of ungaged watersheds.

The spatial variables considered in the distributed models require extensive detailed information. The data availability and management are crucial to effective use of models.

2.3 *Existing Nonpoint Source Pollution Models*

2.3.1 *FESHM*

An event-oriented distributed parameter hydrological model, Finite Element Storm Hydrograph (FESHM) developed by Ross (1975; 1978), uses the finite element numerical technique to simulate runoff hydrograph (Judah, 1973; Judah et al., 1975). The model was based on a Hortonian infiltration excess concept of runoff generation (Shanholtz et al., 1981). Infiltration loss are predicted using the empirical Holtan equation with parameters that may vary between "hydrologic response unit" (HRU) based on the categories of soil types and landuse. The model was later modified to account for transmission from the overland flow plane (Heatwole, 1979; Heatwole et al., 1982). A sediment detachment and transport algorithm was incorporated into FESHM by Wolfe (1982). FESHM was developed and modified for simulating runoff in ungaged areas and for

NPS pollution control planning (Wolfe et al., 1983; Hession, 1988). Hession et al.(1994) reported on the use of FESHM in an ungaged context.

FESHM consists of two main components. The first component generates rainfall excess on discrete areas of the watershed. The second component then routes the excess rainfall to the watershed outlet. The model discretizes the watershed into homogenous HRUs. The finite element structure allows the model to route rainfall excess and sediment yield downstream. The movement of precipitation excess along overland flow and channel flow elements was solved by the finite element numerical technique. This model has the capability to predict and simulate peak discharge and sediment from watersheds under different landuse conditions.

FESHM was basically developed to simulate the hydrological responses from agricultural watersheds. The prediction of hydrological responses on nonagricultural watersheds has not been verified.

2.3.2 ***ANSWERS***

Aerial Nonpoint Source Watershed Environment Response Simulation (ANSWERS) is an event-oriented, deterministic and agricultural model, which was developed originally by Purdue University for EPA Great Lakes Program (Beasley, 1977). ANSWERS was designed to calculate peak flow rates and total surface runoff for single events and to compare the effectiveness of alternative land management practice on sediment yields. A phosphorus transport component has been incorporated into ANSWERS (Storm , 1986).

The hydrology component of ANSWERS simulates runoff, infiltration, interception, surface storage, subsurface drainage and groundwater seepage. Holtan's empirical infiltration equation was

used to calculate infiltration. The model discretizes the watershed into cells with uniform characteristics. For example, landuse, slope, soil type, management practices.

ANSWERS is spatially distributed, but lumped at the cell level of details. This means as the size of cell increases, the model becomes less representative of actual conditions. A typical maximum size for using the ANSWERS model would be a watershed smaller than 2000 ha. The components of ANSWERS do not support simulation of the hydrological responses for non-agricultural watersheds.

Identification and prioritization of critical areas is one of the major strong points of the ANSWERS model. A research version of ANSWERS has been developed to model individual fields without the need to simulate the entire watershed.

2.3.3 *AGNPS*

Agricultural Nonpoint Source Pollution Model (AGNPS) is a distributed watershed scale model for simulating runoff volume and peak rate, sediment detachment and transport, nutrient and oxygen concentration for single storm events on agricultural watersheds (Young et al., 1987).

The model requires that the watershed be divided into square cells. This allows the users to get the information for specific locations within analyzed watersheds. Subwatersheds determined by grouping appropriate cells are useful in providing further information on individual watershed sections.The Minnesota Land Management Information System (MLMIS), a Geographical Information System interfaced with the AGNPS is used to prepare input data for the model.

2.3.4 *HSPF*

The Hydrological Simulation Program Fortran (HSPF) is a continuous simulation model which was developed by Hydrocomp for the United States Environmental Protection Agency (Johanson et al., 1980; Decousey, 1985).

The HSPF model is a modification of the Stanford Watershed Model (Crawford and Linsley, 1966) and the Hydrocomp Simulation Program (Novotny, 1981). It simulates hydrographs, sediments, chemical pollutants and pesticides from land surface entirely through channel, reservoir, overland and groundwater sources. A set of modules are arranged in a hierarchical structure, which perform continuous simulation of a comprehensive range of hydrological and water quality processes. HSPF provides a method to determine the impacts of a wide range of BMPs.

Novotny and Chesters(1981) pointed out that the calibration of HSPF is difficult. The problem with field-to-stream delivery were also mentioned by the model developers. Additionally, a significant drawback of the model is the empirical base of many of its hydrologic parameters, which make it somewhat less reliable (Novotny and Chesters, 1981). HSPF is a lumped model and can not be used to identify areas within a watershed.

2.3.5 *SWMM*

The EPA Storm Water Management Model (SWMM) was developed in the early 1970s by a consortium consisting of the University of Florida, Metclf and Eddy, Inc. (Renard et al., 1981). It is the most widely used urban hydrological model (Jackson, 1982). The model was originally intended to provide comprehensive simulation capability for large metropolitan combined sewer system including dry weather flows and treatment-storage processes. This combined system is

complicated by the pressure of looping sewers, weir diversions, pump stations, submerged outfall, and expensive backwater throughout the system (Huber and Heaney, 1977).

It is the model which first attempted to simulate water quality. It was sponsored by EPA and developed during the period of 1969-1971. Watershed characteristics, pollutant accumulation, and runoff rate are used in the model. Suspended solids, biochemical oxygen demand, nitrogen, phosphorous, oil and grease are the pollutants considered .

The SWMM model is capable of representing drainage areas that range from 5 to 2000 ha. The SWMM model is intended for use on either complex separate or combined sewer systems where the impervious fraction is high (Kibler et al., 1982). It is not recommended for small highly simplified urban drainage networks (Kibler et al., 1982). The program is rather large, requiring an extensive amount of input data. Its use for simulating the NPS pollution process is limited (Novotny, 1981). Kibler et al. (1982) stated that because of the poor representation of the pervious fractions, SWMM was not recommended for use in undeveloped watersheds.

2.3.6 *STORM*

The Continuous Simulation Storage, Treatment, Overflow, Runoff Model (STORM) was developed in 1976, by the US Army of Engineering Hydrologic Engineering Center (HEC) (Novotny and Chesters, 1981). The program is capable of simulating quantity and quality of runoff from small-primarily urban-watersheds, however, nonurban areas also can be included. Water quality parameters include total and volatile particulate, biochemical oxygen demand (BOD), total nitrogen (N), and orthophosphate. The pollutant accumulation component for impervious surfaces assumes a uniform daily accumulation rate of pollutants during a dry period.

Pollutant wash-off from a pervious area is computed by an equation similar to that for impervious surfaces. Although the model has been used for all types of landuse all over the USA, no analysis of the availability of pollutants is made for non-urban areas (Novotny and Chesters, 1981).

2.3.7 *PSRM-QUAL*

PSRM-QUAL is the most recent modification of the Penn State Runoff Model (PSRM) (Aron et al., 1992). PSRM was developed in the mid-1970's in response to the need for urban runoff models which were less demanding in their data input and computer requirements, while offering acceptable hydraulic representation of the urban watershed (Kibler et al., 1982).

PRSM simulates runoff quantity on a single-event basis and has runoff quality routines (Kibler et. al., 1982). Two notable features of PRSM, which make it a design-oriented tool rather than a pure simulation model, are: tabular presentation of individual plane contribution to a composite flood peak at any point in the watershed and reservoir routing analysis for any plane.

PSRM-QUAL is a distributed urban runoff model. An urban drainage system is sub-divided into planes and each plane is further sub-divided into impervious and pervious overland flow planes. Surface runoff is routed across these plane surfaces using the kinematic wave equation. A uniform depth and runoff rate are determined for the entire planes. The SCS equation is used to calculate infiltration, which results in an abrupt stop to infiltration the moment precipitation starts (Aron et al., 1992).

PSRM provides a good simulation capability for small developing watersheds where sewer hydraulics do not include diversion structures and extensive backwater (Kibler et al., 1982). PSRM-QUAL includes a water quality routine which is described by Aron et al. (1992). The

PSRM-QUAL is simpler than EPA SWMM and has a good simulation capability for urban areas (Kibler et al., 1982). The model structure and components of PSRM-QUAL also allow it to be used for less developed and non-urban areas. The SCS curve number is used to calculate runoff from impervious and pervious surfaces. The Universal Soil Loss Equation (USLE) formulated by Wischmeier and Smith (1965) is used to calculate the sediment erosion from pervious areas.

2.3.8 *SLAMM*

The development of Source Loading and Management Model (SLAMM) began in the mid 1970s, primarily as a data reduction tool for use in an early street cleaning project sponsored by EPA's Storm and Combined Sewer Section (Pitt, 1989). Much of the information contained in SLAMM was obtained during the EPA's Nationwide Urban Runoff Program (NURP), especially the earlier Alameda Country, California, and the Bellevue, Washington projects (Pitt , 1989).

SLAMM was developed to evaluate the effects of development and control practices on urban runoff quality and quantity (Pitt,1989). Using the Soil Conservation Service runoff curve number approach and parameters empirically derived from past urban stormwater studies, the model calculates runoff characteristics and pollutant loading for individual rain events (Pitt, 1989).

SLAMM was developed to" assist water and land resource planners in evaluating the effects of alternative control practice and development characteristics on urban runoff quality and quantity" Pitt (1989). It is a planning tool which supplies the type of information most needed to make management decisions (Pitt, 1989). This model evaluates runoff characteristics at the source areas in the watershed at discharge outfall.

The disadvantage of the model is that it requires a substantial information for input data. It is not appropriate for less developed urban area since there is insufficient field data for such areas.

2.3.9 ***KINEROS***

Kinematic Runoff and Erosion Model (KINEROS) is a distributed, event-based, physically-based model which describes the process of surface runoff and erosion from small agricultural and urban watersheds (Woolhiser et al., 1992). The model has evolved from the work of Rovery, Woolhiser and Smith (Goodrich et al., 1988).

The watershed surface and channel network are represented by a cascade of planes and branching channels. Each plane and channel is described by appropriate parameters, initial conditions, and precipitation input.

The components in KINEROS are based on the conservation of mass and momentum equation. The model calculates surface runoff from given initial soil moisture conditions. Both overland and channel flow are approximated using the one dimensional kinemative wave equation. The Smith-Parlange infiltration model (Smith and Parlange, 1978) was used to calculate infiltration. The spatial variability of saturated hydraulic conductivity was incorporated into the physical rainfall-runoff model (Woolhiser et al., 1990). The simulation of erosion is optional and was based on work done by Smith (1978;1981).

KINEROS has been used in the Midwest and Southeast on range and urban conditions (Renard et al., 1982). It has been demonstrated to be applicable to natural and distributed rural and urban watersheds of arbitrary configuration (Woolhiser et al., 1990). It can be used to evaluate the

effects of various artificial features including less urban development, small detention pond and reservoir on flood hydrograph and sediment yield.

2.4 ***Geographic Information System (GIS)***

A Geographic Information System (GIS) is a computer-assisted tool for spatial and non-spatial creation, storage, retrieval, management, manipulation, analysis and display of data. GISs have been demonstrated to provide the effective and efficient functions for handling spatial and non-spatial data and performing spatial analysis (Shanholtz et al., 1988). The unique functions of GIS such as overlay and buffering are useful and important for developing derivative datasets that serve as proxies for unavailable variables (Kemp, 1993). Many researchers suggested GIS technology can advance the management of natural and transformed land areas. According to Judd (1993), GISs "have significant potential for analysis and modeling in those sciences dealing with spatially distributed phenomena."

The distributed, physical based models can, at least conceptually, identify the contributions of particular areas within a watershed to total watershed responses, such as runoff and sediment yield. The models are generally used to simulate the effects of spatial factors such as landuse, soil, topography on the quantity and quality of water resources of a watershed. However, most of distributed, physically-based hydrological and NPS models recorded in the literature have limited capability to integrate and interpret spatial data from different disciplines and sources. The preparation of definition of the input parameters of the models usually is time consuming and expensive (Vieux et al., 1988). The determination of the combination information, such as

"hydrological response unit" (Li , 1975), is limited and less accurate by manual methods (Vieux et al., 1988; Wolfe and Neale, 1988).

Most distributed, physically-based models do not have the visual capabilities to display the simulated results, i.e. their capabilities of information communication is limited. These shortcomings limit widespread use, especially for large watersheds, which need extensive data preparation.

The integration of GIS with the distributed, physically-based models improves data management issues. The integration has been shown to be more effective, less expensive and has the potential for reuse than manual methods. The integration enhances the capabilities of the models and offers a method to analyze the hydrological processes with the full information content of the data. Vieux (1990) stated that the integration will reduce the uncertainty caused by spatial averaging. The integration also improves the visual capabilities of the models. GIS is an effective and convenient tool for hydrologists to study the spatially distributed watershed characteristics and their influences on runoff generation (Chairat and Delleur, 1993).

GIS has been extensively applied to hydrological and NPS modeling in recent years. These applications of GIS have ranged from synthesis and characterization of hydrologic tendencies to simulation of response to hydrologic events (DeVantier and Feldman, 1993). Gupta and Solomon (1977) described a raster based GIS for use with a distributed process hydrological model. Vieux (1990) used vector GIS (ARC/INFO) to integrate with the FESHM model to calculate runoff. Stuebe et al. (1991), Muzik (1988) and Hill et al. (1987) estimated the runoff volume by SCS runoff curve number using GIS techniques. Young et al. (1987) used a raster GIS database along with the Agricultural Nonpoint Source Pollution Model (AGNPS) to model NPS pollution from large areas.

Chairate and Delleur (1993) integrated TOPMODEL, a physically-based hydrological model with a GIS software (GRASS). Maidment (1993) developed a spatially distributed unit hydrograph by using GIS.

Shanholtz et al. (1988) developed a user friendly interface using GIS (VirGIS) with FESHM to assist with data compilation and display of simulation results. Shanholtz et al. (1993) illustrated the use of a GIS in identifying agricultural NPS potential. Many organization such as USGS, EPA are more apt to recognize the utility of combining the model with GIS technology (Judd , 1993).

There are two forms of interfaces utilized in integrating GIS technology with models. One form is to couple an existing model with a GIS. Most discussions on GIS interfaces with a model involve with this form of integration. This approach is the data input and structure of the models are well understood , refined and documented (Judd, 1993). Also, the models such as TR-55, HEC2, PSRM-QUAL, FESHM, ANSWERS, KINEROS are commonly used and accepted in the public and private sector. Although this type of integration can enhance the model's performance, the full power of GIS can not be wholly implemented.

Another form of integration is to translate or migrate some types of models into the processing language of the GIS (Judd , 1993), such as the GRID extention. However, no research was found that demonstrate that all models types can be cost-effectively migrated into GIS .

2.5 *Summary*

Models are needed that have the capability to simulate NPS pollution from urban and nonurban sources. KINEROS and PSRM-QUAL have the capabilities to simulate sediment from both urban and non-urban areas. The two models are described in detail in Chapter 3.

Distributed models require an extensive databases and generally require large computational time and computer resources. The major deterrents to the use of the distributed-parameter models are data compilation and analysis. Some distributed-models not only deal with spatial information, such as topography and soil, but also with non-spatial information such as costs associated with the implementation of BMPs. A distributed model typically requires a large volume data to predict the effect of BMPs and to choose the most effective one to be implemented at least cost. The amount of data to be used will vary from site to site. It is a difficult task to design an system which stores, retrieves and updates data. KINEROS and PSRM-QUAL lack the capabilities to allow the users easy access for storage, updating and retrieval, i.e. each model's capabilities of handling and managing data are limited. GIS technology can improve the model's capability to conduct analyses and interpret the results.

Chapter 3

DESCRIPTION OF PSRM-QUAL AND KINEROS

3.1 PENN STATE RUNOFF QUALITY MODEL (PSRM-QUAL)

The Department of Civil and Environmental Engineering and Environmental Resources Institute of Pennsylvania State University in cooperation with the Pennsylvania Department of Environmental Resources and the United States Environmental Protection Agency developed the Penn State Runoff Quality Model (PSRM-QUAL), a modification of the Penn State Runoff Model (PSRM), to simulate storm water quality as well as quantity from urban watersheds (Aron et al., 1992).

PSRM-QUAL simulates runoff and pollutant transport as a cascade of sheetflows from consecutive drainage sub-areas along the flow path. Flow is then diverted into a channel which drains a sub-area. The model computes overland runoff using the kinematic wave equations which are solved by the method of characteristics. Routing through channels is done by the Muskingum method (Aron et al., 1992). A non-point source pollution transport algorithm is incorporated into the model so that it can simulate the transport of pollutants such as suspended solids, trace metals and nutrients.

Figure 3-1 is the flowchart which illustrates the hydrologic components of PSRM-QUAL. Sections 3.1.1 through 3.1.7 describe details of the hydrologic components of the model .

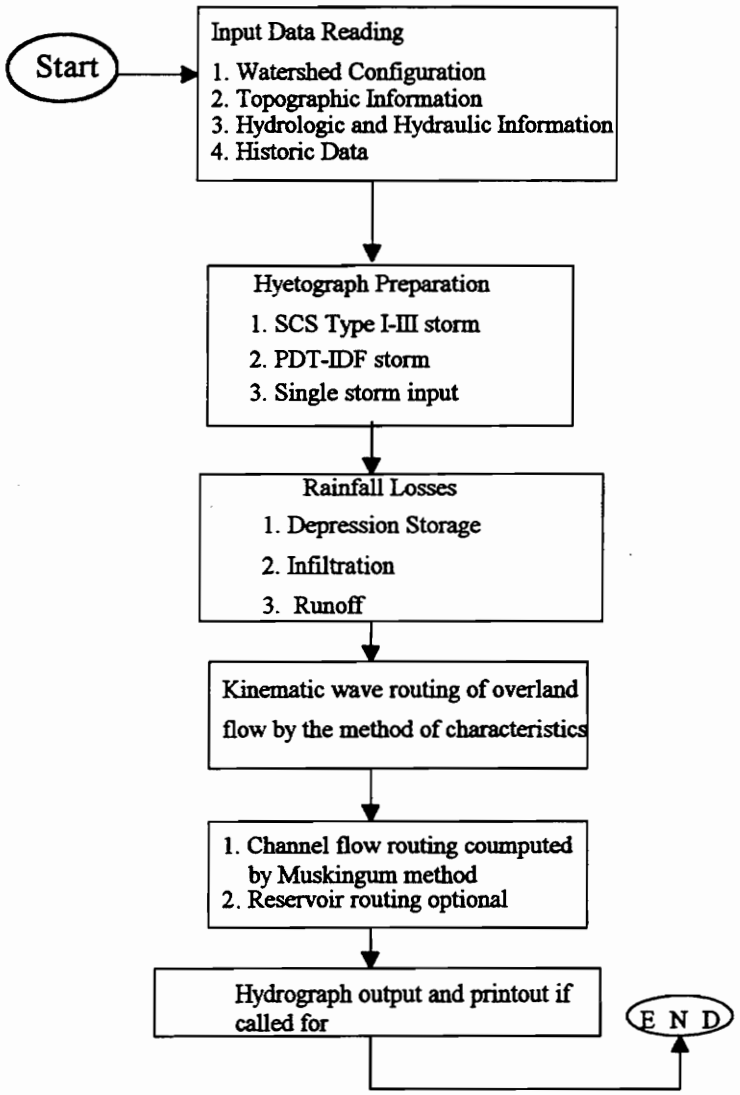

Figure 3-1 Flowchart of PSRM-QUAL hydrologic components

3.1.1 HYETOGRAPH PREPARATION

Rainfall input to the model is from either a design storm or a recording raingage record. Up to three design storms can be entered in the form of a specified number of rainfall increments for one or several gages (Aron et al., 1992). Design storm options include: (1) an SCS 24-hour rainfall amount; (2) the SCS rainfall distribution of TYPE I, II, or III; (3) a Pennsylvania design storm generated by the instruction of the PDT-IDF manual (Aron et al., 1986).

When rainfall is given for several nearby raingages, a rainfall weighting method must be applied (Aron et al., 1992). A weighing factor inversely related to the distance between raingages and subarea centroids is given by:

$$WT_{ij} = \frac{d_{ij}^{-m}}{\sum_{j=1}^{n} dij^{-m}} \qquad (3\text{-}1)$$

where:

WT_{ij} is weighing factor of gage j and subarea i

d_{ij} is distance between gages j and the centroid of subarea i, in any units measured from a map ;

m is inverse distance exponent. m=2 as recommended by Dean and Snyder (1977); and

n is the number of subareas.

The total depth and the temporal center of gravity of the storm is computed for each raingage and is used to maintain the shape of original rainfall hyetograph in the weighted rainfall distribution (Aron et al., 1992).

3.1.2 RAINFALL LOSSES AND RUNOFF

Runoff can be produced only when initial abstraction and available depression storage are satisfied. Infiltration and depression storage are the main losses considered in the PSRM-QUAL model (Aron et al., 1992).

The SCS curve number approach (SCS, 1985) is used in PSRM-QUAL (Aron et al., 1992) to calculate the runoff.

Soil storage capacity is given by:

$$S = \frac{1000}{CN} - 10 \tag{3-2}$$

where

S is soil storage capacity.

CN is SCS curve number.

The initial abstraction, I_a, which includes the depression storage in the model, is determined by the equation:

$$I_a = cS \tag{3-3}$$

where

c can assume the following conditions:

1.a value of 0.2 suggested by SCS

2.a value of 0.1 suggested by PSRM-QUAL manual for urban areas.

3.a value assigned by a user.

Runoff is calculated from the relationships:

$$Q = \frac{(P-I_a)^2}{(P-I_a)+S} \tag{3-4}$$

where

P is accumulative precipitation, inches
I_a is initial abstraction.

S is a soil storage capacity.

3.1.3 INFILTRATION

The infiltration algorithm is based on concepts developed by SCS (1972) and Horton (1935). By defining precipitation losses as the sum of initial abstraction, infiltration and runoff (Aron et al., 1992), the effective precipitation is defined as:

$$P_e = P - I_a = P - cS_c \tag{3-5}$$

where

P_e is the effective precipitation and

P, c, Sc are as previously defined.

Since a storm can include three period of no rainfall, the infiltration capacity is calculated as:

$$F = \frac{P_e S_c}{P_e + S_c} + \Sigma f_c \frac{CF}{S_c} \Delta t \tag{3-6}$$

where

CF is accumulated water in soil

Δt is time step used in calculation

f_c is equilibrium infiltration rate input as defined by the user.

The accumulative water in soil is calculated from the expression

$$CF = CF_o + \Sigma(f - d)\Delta t \tag{3-7}$$

where

CF_o/S is the initial ratio of soil water capacity filled; and

f is infiltration rate.

The following equation is used to limit the infiltration rate.

$$f = f_o - (f_o - f_c)\frac{CF}{S_c} \tag{3-8}$$

where

f_o is the maximum infiltration rate which is calculated from the relationship

$$f_o = 0.037 + 1.84 f_c - 0.075 f_c^2 \quad (3\text{-}9)$$

The equations (3-8) and (3-9) are derived from Hortan's (1935) concepts.

Infiltration rates tend to be high during very intense rainfall bursts. Infiltration is assumed to be zero immediately at the cessation of rainfall. The model considers the change of the water content in the soil between the storms.

3.1.4 *OVERLAND FLOW*

Overland flow is calculated by the kinematic wave method (Kibler, 1968). A set of ordinary differential equations which can be solved analytically by the characteristics method are used for calculation of overland flow. The equations are :

$$\frac{\partial y}{\partial t} + \partial y y^{\eta-1} \frac{\partial y}{\partial x} = i \quad (3\text{-}10)$$

$$\frac{\partial y}{\partial t} dt + \frac{\partial y}{\partial x} dx = dy \quad (3\text{-}11)$$

where

y is depth of flow, ft;

t is time, seconds;

a is kinematic wave parameter related to roughness, slope; and

n is kinematic wave parameter related to turbulent flow conditions.

The Manning hydraulic resistance law is used to determine the overland flow. The overland flow rates are computed separately for the impervious and pervious portion of each subarea by using the CN for the impervious and pervious areas.

3.1.5 *CHANNEL FLOW AND ROUTING THROUGH CHANNELS*

Full-flow capacity and travel time of the channels are required as input. The Muskingum method (Viessman et al., 1977) is used to compute the travel time of runoff through channels (Aron et al., 1992).

The Muskingum method is given by the relationship

$$S = K_m[X_m I + (1 - X_m)O] \tag{3-12}$$

where

K_m is storage time constant for the reach;

X_m is weighing factor which varies between 0 and 0.5 for a given tributary section;

I is inflow rate;

O is outflow rate from the reach, cfs; and

S is storage within the reach, cfs.

3.1.6 *ROUTING THROUGH RESERVOIRS*

The modified puls method (Viessman et al., 1977) is used to route flows through reservoirs:

$$I_n + I_{n+1} + (\tfrac{2S}{\Delta t} - O_n) = \tfrac{2S_{n+1}}{\Delta t} + O_n + 1 \tag{3-13}$$

where

I is inflow rate, cfs;

O is overflow rate, cfs; and

S is reservoir storage, cfs.

A maximum of one reservoir can be included in each plane.

3.1.7 THE INPUT AND OUTPUT FILES

Only one input file contains both the rainfall data and information for each channel and sub-areas are required. A procedure is included that can be used to create and edit the input file. One output file contains all pertinent information from a given computer run in tabular form for each plane. Planes can be chosen by the user. A procedure is included to plot hyetographs, hydrographs and pollutantgraphs for selected planes.

3.2 A KINEMATIC RUNOFF AND EROSION MODEL (KINEROS)

The Agricultural Research Service of United States Department of Agriculture developed the KINEROS model to simulate the quantity and quality of storm runoff (Woolhiser et al., 1990). It is an event-oriented, physically-based model describing the process of interception, infiltration, surface runoff, and erosion from small agricultural and urban watersheds. The model uses kinematic approximation and mass balance to estimate runoff, erosion and sediment transport from a cascade of planes and branching channels, which are derived from watershed topography.

The hydrologic components of the model are shown in Figure 3-2 and described in Section 3.2.1 through Section 3.2.7

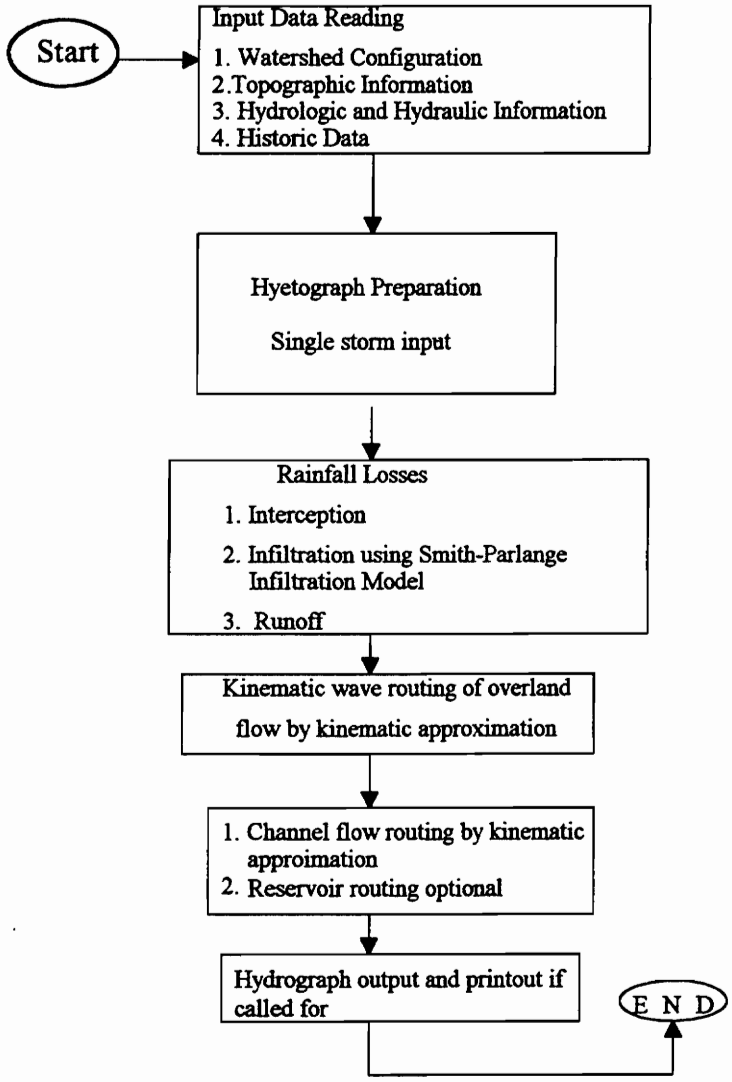

Figure 3-2 Flowchart of KINEROS hydrologic components

3.2.1 HYETOGRAPH PREPARATION

KINEROS is an event-based model. Rainfall from either a recorded event or a design storm is entered as a cumulative distribution. The rainfall from up to twenty rain gages with user defined weights can be input simultaneously.

3.2.2 INTERCEPTION

Interception is defined as rainfall retained on vegetable foliage. It ultimately evaporates back into the atmosphere. It is affected by the growth stage of vegetation, season of year, and wind velocity. Interception represents an abstraction from precipitation. The depth of interception which is usually given in inches or millimeters is used to quantify the interception. For example, 0.03 in was defined by Horton (1919) as the amount rainfall intercepted by corn. Interception is subtracted from the rainfall before infiltration is calculated.

3.2.3 INFILTRATION

Infiltration is process that many hydrologic models use to allocate rainfall into unrouted rainfall, soil water storage and percolation to groundwater.

The Smith-Parlange (1978) Infiltration Model is used in KINEROS to calculate infiltration. Smith and Parlange (1978) started with the Richards equation and derived an infiltration model for arbitrary rainfall rates. The model can be used to predict both ponding time and infiltration capacity. The equation is :

$$f_c = K_s \exp(F/B)/[\exp(F/B) - 1] \qquad (3\text{-}14)$$

where

f_c is the infiltration capacity;

K_s is effective saturated hydraulic conductivity;

F is the amount of rain already absorbed into the soil; and

B is the difference between the volumetric water-holding capacity of the soil and its initial water content calculated in equation 3-15.

$$B = G(\theta_s - \theta_i) \tag{3-15}$$

where

θ is saturated water content [L^3/L^3];

θ_i is the initial water content [L^3 / L^3]; and

G is the effective net capillary drive [L].

From the relationships above, the effective saturated hydraulic conductivity and effective net capillary drive are key parameters in determining infiltration. The relationship of the two parameters is described in the following equation:

$$G = \frac{1}{K_s}\int_{-\infty}^{0} K(\Psi)d\Psi \tag{3-16}$$

where

Ψ is soil matric potential [L];

$K(\Psi)$ is hydraulic conductivity potential [L]; and

K_s is previously defined.

The two parameters are determined by the types of soil. The spatial variables of the two parameter can be considered in the infiltration model of KINEROS. The values of both parameters for each type of soil may be calculated from measurable soil properties or determined from infiltration experiments (Woolhiser et al., 1990).

In KINEROS, the infiltration process is separated into infiltration during the rain period, called the "rain limited infiltration period" and infiltration when rain ceases or the rainfall rate is below the infiltration rate. KINEROS considers change of water content during significant intervals of no rainfall.

3.2.4 *OVERLAND FLOW*

Hortontian overland flow begins when the rainfall rate exceeds the infiltration capacity. In KINEROS, one dimensional flow on a plane surface is solved by the kinematic wave equations, because it has been shown that the kinematic wave formulation is an excellent approximation for most overland flow conditions (Woolhiser and Liggett, 1967; Morris and Woolhiser, 1980). The continuity equation used in KINEROS for a overland flow is:

$$\frac{\partial h}{\partial t} + \alpha m h^{m-1} \frac{\partial h}{\partial x} = q(x,t) \qquad (3\text{-}17)$$

where

h is the storage if water per unit area or depth if the surface is a plane;

α, m are parameters related to roughness, slope and the whether the flow is laminar or turbulent;

t is time;

x is spatial coordinate; and

$q(x,t)$ is the lateral inflow rate.

Four options for α and m in equation 3-17 are provided in KINEROS. These include: (1) The manning hydraulic resistance law; (2) A laminar law until the Reynolds number exceeds a critical value then Manning's law is used; (3) A laminar law until the Reynolds number exceeds a critical value then Chezy law is used; (4) The Chezy law. The user does not specify the critical

Reynolds number. The user only selects the applicable law and gives the appropriate values such as the Manning's N or Chezy C. It is commonly agreed that overland flow on a plane begins as laminar flow and eventually becomes turbulebnt. The Manning's law and the Chezy law are often selected for large watersheds. Optional 2) and 3) are only selected for very small watersheds with relatively smooth and plane surface such as the parking lots and streets.

3.2.5 *ROUTING THROUGH CHANNELS*

The kinematic approximation to the equations of unsteady, gradually varied flow is used to represent the unsteady, free surface flow in channels. The continuity equation for a channel with lateral inflow is:

$$\frac{\partial A}{\partial t} + \frac{\partial Q}{\partial x} = q_c(x,t) \tag{3-18}$$

where

A is the cross-sectional area;

Q is the channel discharge; and

$q_c(x,t)$ is the net lateral inflow per unit length included the flow from the overland and upstream channels

The relationship between channel and discharge and cross-section area represented by the kinematic approximation is as follows:

$$Q = \alpha R^{m-1} A \tag{3-19}$$

where

Q , A, α , m are defined in equation 3-18 and 3-17; and

R is the hydraulic radius.

Either Manning or Chezy law can be chosen by the user for channel flow conditions. The channel cross section may be approximated as trapezoidal or circular. In an urban environment, storm sewers are represented by only circular conduits and the discharge relationship for flow is defined by the Darcy-Wisbach formula:

$$S_f = \frac{f_d}{4R}\frac{u^2}{2g} \tag{3-20}$$

where

S_f is the friction slope ;

f_d is the Darcy-Weibach ;

u is the velocity (Q/A) ; and

g is the gravity.

The discharge for the flow in pipes is

$$Q = \frac{\alpha A^m}{p^{m-1}} \tag{3-21}$$

where

p is the wetted perimeter; Q, A are defined in equation 3-18;

α is the value equal to $[8gS_f/f_d]^{1/2}$; and

m is 3/2.

Both channels and storm sewers can be modeled with KINEROS.

3.2.6 *ROUTING THROUGH RESERVOIR*

Up to three reservoirs can be contained in a watershed. Rainfall falling on ponds or reservoirs and infiltration from the ponds or reservoirs are not considered. Since the outflow is solely regarded as a function of reservoir depth in the model, reservoir outflow is given by the mass balance relationship:

$$\frac{dV}{dt} = q_I - q_o \tag{3-22}$$

and

$$q_o = c_1(h_r - h_z)^{c2} \tag{3-23}$$

where

V is $V(hr)$ the reservoir volume [L^3];

h_r is reservoir surface elevation [L];

q_I is inflow rate [L^3/T];

q_o is outflow rate [L^3/T];

h_z is reservoir outflow weir elevation [L]; and

$c1$, $c2$ are weir coefficients.

3.2.7 THE INPUT AND OUTPUT FILE

Two input files are required. One is used to store watershed configuration, topographic, hydrologic and hydraulic information or sediment data if the model is used to simulate sediment. The second files is used to store rainfall data. Two output files are generated. One is used to store output hydrographs for each plane and channel. The detailed finite difference solution for planes and channels are stored in a second output file. KINEROS allows the user to specify the planes and channels and print the details for these planes and channels.

Chapter 4

DATA PREPARATION

4.1 *STUDY AREA*

The Foster Creek Watershed, located in Lousia County, Virginia (Figure 4-1) was chosen as the study area because of previously discussed interest in evaluating models with the Thomas Jeffeson Planning District for potential future applications. The watershed covers approximately 415 acres. Nason silt loam and Tatum silt loam are the dominated soil types comprising about 70% of the watershed area as shown in Table 4-1. The predominated landuse is woods and pasture covering approximately 27% and 50% of the total watershed, respectively as shown in Table 4-2. Hydraulic and hydrological characteristics related to soil and landuse are summarized in Tables 4-3 and 4-4, respectively. Continuous monitoring of rainfall and streamflow was conducted over the period 1960-1969 at the locations given in Figure 4-2 by USDA/ARS and the Department of Agricultural Engineering, Virginia Tech.

Topographic detail was available at a 1:2400 scale from the Department of Agricultural Engineering, Virginia Tech (V.O.Shanholtz, personal communication, 1992). Soil characteristic data was available for dominant soil types. Landuse mapping was available at a 1:7920 scale from a previous research project (V.O. Shanholtz, personal communication, 1992).

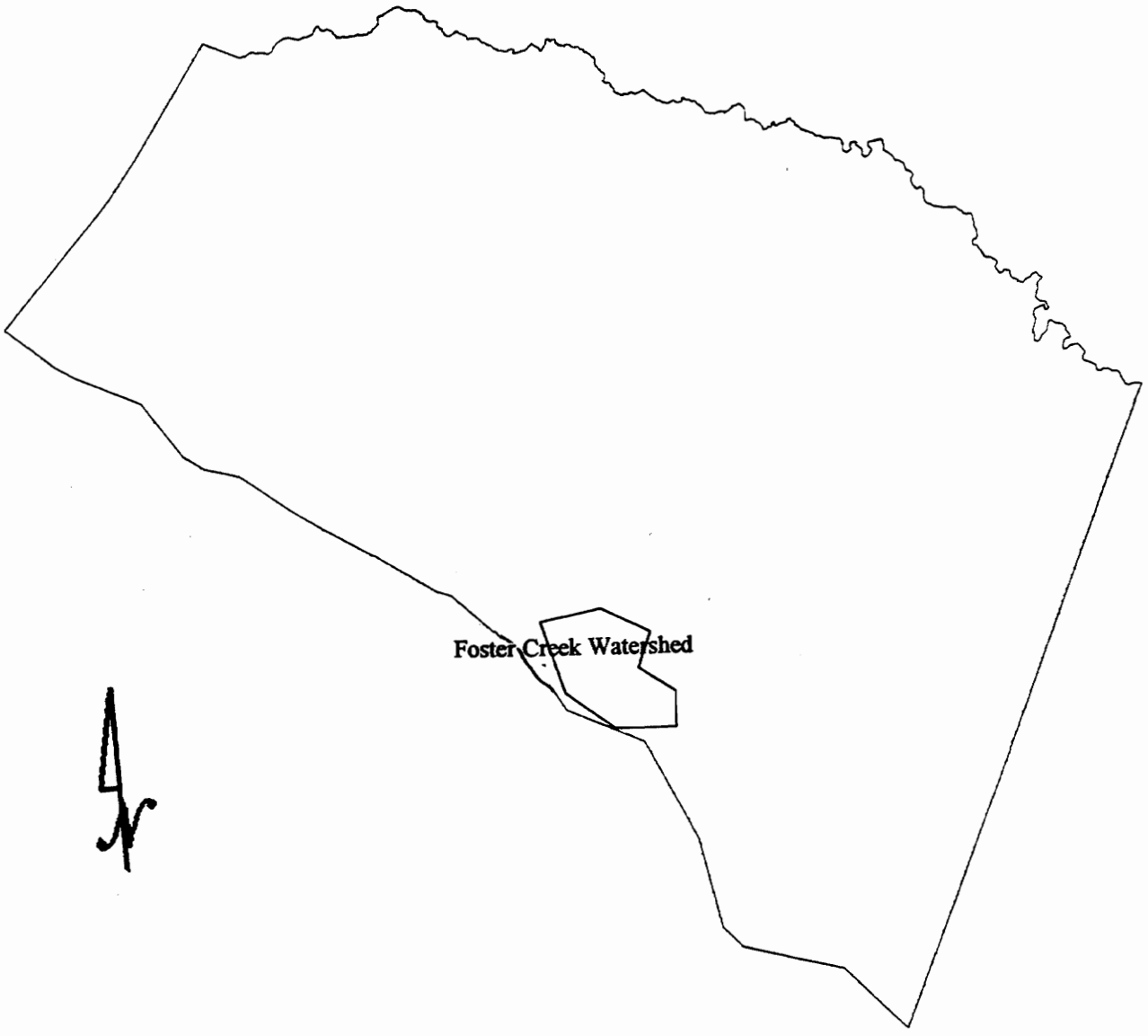

Figure 4-1 The schematic map of the location of Foster Creek Watershed at Louisa County, Virginia

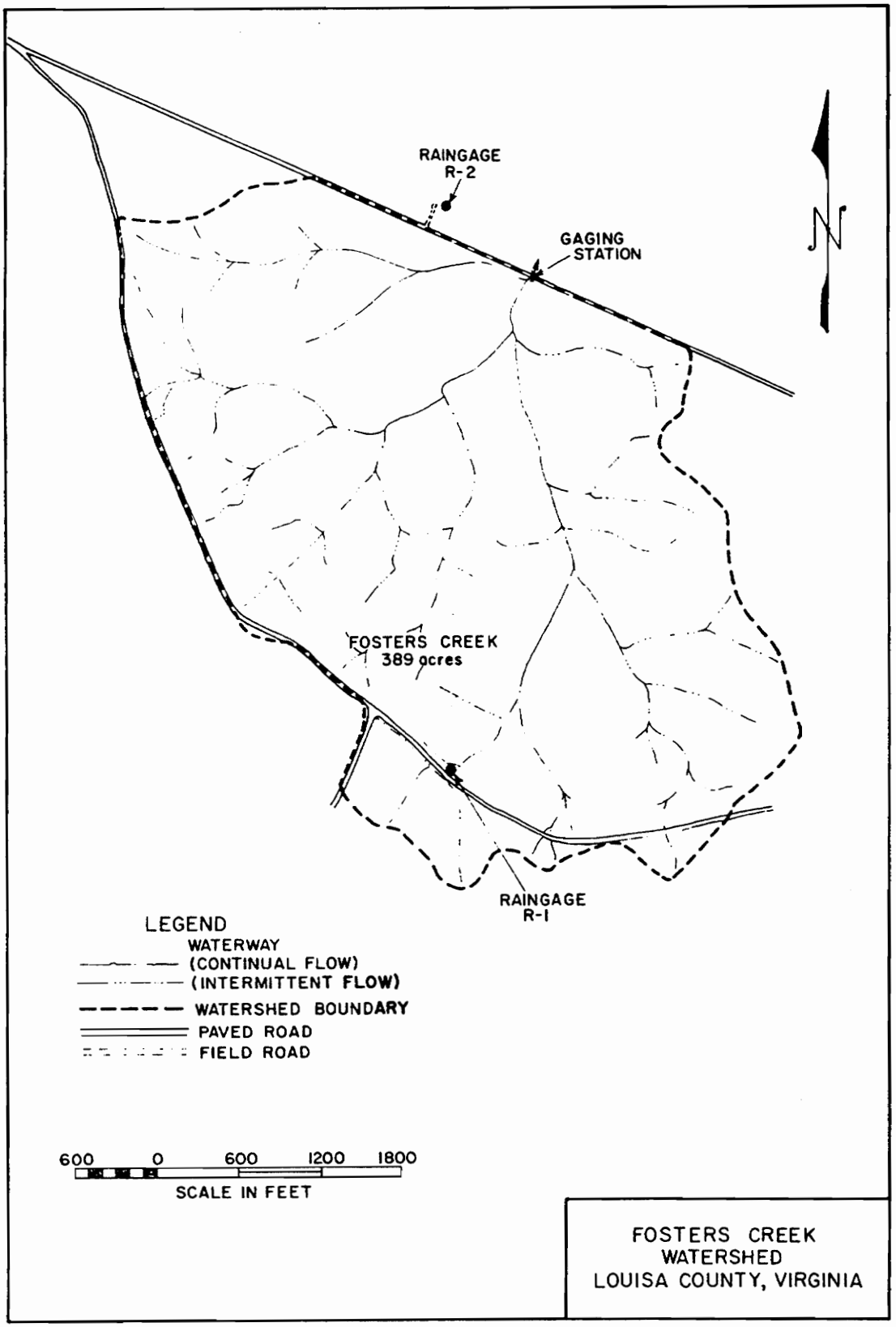

Figure 4-2 Foster Creek Watershed.

Table 4-1 Summary of the general soil information for Foster Creek Watershed

Soil Type	Mapping Symbol	Areas (Acres)	Proportionate Extent (%)	Slope Range (%)
Nason silt loam	1A	24.71	5.94	00-02
Nason silt loam	1B	148.54	35.73	02-07
Nason silt loam	1C	12.63	3.03	07-15
Tatum silt loam	2A	21.51	5.17	00-02
Tatum silt loam	2B	75.51	18.16	02-07
Tatum silt loam	2C	6.59	1.59	07-15
Senica silt loam	3A	1.1	0.26	00-02
Senica silt loam	3B	12.73	3.04	02-07
Senica silt loam	3C	0.27	0.07	07-15
Ligum loam	4A	0.55	0.13	00-02
Ligum loam	4B	19.49	4.69	02-07
Ligum loam	4C	0.55	0.13	07-15
Fluvanna very fine sandy loam	5A	4.12	0.99	00-02
Fluvanna very fine sandy loam	5B	29.65	7.13	02-07
Fluvanna very fine sandy loam	5C	4.11	0.99	07-15
Worsham silt loam	6A	0.82	0.20	00-02
Worsham silt loam	6B	8.24	1.98	02-07
Worsham silt loam	6C	1.10	0.26	07-15
Tatum silt loam	7A	0.55	0.13	00-02
Tatum silt loam	7B	16.75	4.03	02-07
Tatum silt loam	7C	6.31	1.52	07-15
Manteo silt loam	8B	1.92	0.46	02-07
Manteo silt loam	8C	1.92	0.46	07-15
Mixed alluvial land	9A	3.02	0.73	00-02
Mixed alluvial land	9B	10.43	2.51	02-07
Mixed alluvial land	9C	3.29	0.79	07-15

Table 4-2 Summary of landuse information for Foster Creek Watershed

Name of Landuse	Area (Acres)	Proportionate Extent
Natural Grasses; Hay Lesp	50.79	12.19
Pasture	110.37	26.48
Woods	195.76	49.97
Corn	4.67	1.12
Idle	46.95	11.27
Wheat ; Oats; Barley	8.24	1.98

Table 4-3 Hydraulic and hydrologic characteristics of soils in Foster Creek Watershed

Soil Types	Mean Saturated[1] Hydraulic Conductivity (in/hr)	Mean Effective Net Capillary Drive (in)	Total Porosity[2] (cm^3 / cm^3)	Hydrologic Soil Group
Nason silt loam	0.27	8.00	0.50	C
Tatum silt loam	0.27	8.00	0.50	B
Senica silt loam	0.27	8.00	0.50	C
Ligum loam	0.52	4.30	0.46	C
Fluvanna very fine sandy loam	1.00	5.00	0.45	C
Worsham silt loam	0.27	8.00	0.50	C
Tatum silt clay loam	0.06	10.20	0.50	B
Manteosilt loam	0.27	8.00	0.50	C
Mixed alluvial land	0.05	11.90	0.43	C

[1] Rawls et al. (1982)

[2] Ross (1978)

[3] SCS (1986)

Table 4-4 Hydraulic and hydrologic characteristics related to landuse for Foster Creek Watershed

Landuse Type	Overland[1] Manning's N	Depression[1] Storage (inches)	Interception (inches)	Curve Number for[2] Hydrologic Group B	Curve Number for[2] Hydrologic Group C
Hay, Natural Grasses	0.20	0.30	0.08	71.00	81.00
Pasture	0.25	0.40	0.02	70.00	80.00
Woods	0.40	0.50	0.03	65.00	77.00
Corn	0.10	0.15	0.03	78.00	85.00
Idle	0.30	0.30	0.01	60.00	73.00
Wheat, Oats & Barley	0.10	0.15	0.16	74.00	82.00

[1] From Ross (1978)

[2] From SCS (1986)

4.2 *INPUT PARAMETERS FOR KINEROS AND PSRM-QUAL*

The input data required by KINEROS and PSRM-QUAL are categorized into topographic, hydrologic and hydraulic, and historic data. The topographic data includes the geographic and physical information of channels, watersheds and sub-watersheds. The acquisition of topographic data consists of delineating the watershed boundary, conceptualizing the watershed, and determining physical attributes of the watershed, sub-watersheds and channels for the two models. The hydrologic and hydraulic data is the information related to soil, landuse or their combination such as saturated hydraulic conductivity, SCS curve number, etc. Historic data refers to the recorded rainfall and streamflow or the design storms for specific regions or locations.

Specific input data requirements for the two models are given in Table 4-5 and 4-6, respectively. Procedures used to assemble databases for the models and to test the models on a watershed are illustrated and discussed in the following sections.

4.3 *DIGITAL MAP DATA BASES*

To describe the spatial variability of soil, landuse and topography, both models require that the watershed be subdivided into numerous inter-connecting planes . The data requirements listed in Table 4-5 and 4-6 must be assembled for each plane and channel.

GIS technology was used extensively to prepare databases for both KINEROS and PSRM-QUAL. By digitizing base maps for soil, landuse, topography, watershed drainage and conceptual sub-units, GIS techniques can be used to quickly estimate parameters for each plane and channel. Note, however, that this study did not involve developing an interface between the models and a GIS.

Table 4-5 Summaries of input model parameter for KINEROS

Type of Information	Input Model Parameter
Topographic	
	number of plane, channel and pond elements defined by watershed conceptualization;
	width and overland flow length of a plane;
	slope of a plane;
	length and slope of a channel;
	channel section.
Hydrologic and Hydraulic	
	relative soil saturation defined by the soil porosity, soil depth and evapotranspiration;
	saturated hydraulic conductivity;
	effective net capillary drive;
	infiltration recession factor;
	manning's n of channel;
	manning's n of overland;
	interception.
Historic Data	a gage record or a design storm in form of a number of accumulative rainfall amount with accumulative time;
	streamflow records.

Table 4-6 Summaries of the input parameters for PSRM-QUAL

Type of Information	Input Model Parameter
Topographic	
	number of plane and channel defined by watershed conceptualization;
	area and overland flow length of a plane;
	slope of a plane;
	length and slope of a channel;
	full-flow capacity of a channel;
	full-flow travel time through a channel.
Hydrologic and Hydraulic	
	SCS curve number;
	SCS initial abstraction factor;
	equilibrium infiltration capacity;
	depression storage on pervious surface;
	initial of soil wetted defined by soil porosity, soil depth and evapotranspiration;
	manning's n of channel;
	manning's n of overland.
Historic Data	A gage record or up to three design storms options;
	A SCS 24-hour rainfall amount;
	The SCS rainfall distribution of type I, II and III;
	A Pennsylvania design storm.

Source maps were obtained for topography, soil and landuse from historical records for the Foster Creek Watershed, which were on file in the Department of Agricultural Engineering, Virginia Tech. Each map was digitized using VirGIS digitizing software. Each map feature was assigned an attribute appropriate for later analysis. Figures A1 and A2 , Appendix A show the digital soil and landuse maps, respectively.

The data were referenced to the Universal Transverse Mercator (UTM) coordinate system and stored in the USGS Digital Line Graph (DLG) format. The following data layers were created from historical records.

Soil mapping units

Landuse-landcover

Elevation Contours

Water features including drainage network and ponds

Roads

Building footprints

The watershed subdivision boundaries, which are discussed in the next section, were digitized, referenced to the UTM coordinate system and stored in DLG format.

4.4 *TOPOGRAPHIC DATA FOR KINEROS*

The topographic data for KINEROS are listed in Table 4.5. Sections 4.4.1 through 4.4.5 describe the procedures used to determine each parameter.

4.4.1 *Watershed Conceptualization for KINEROS*

In KINEROS, the watershed is subdivided into a series of cascading planes and channels. Descriptive information for cascading planes and channels includes geometry and surface conditions that affect flow.

The goal is to subdivide the watershed into elements with relatively homogenous characteristics. The procedures used to subdivide Foster Creek Watershed are detailed by Woolhiser et al. (1990). The first task was to highlight the drainage channels on a topographic map of the watershed. The boundary of planes to each channel was outlined by drawing dashed lines perpendicular to the contour lines to the watershed divide. According to Woolhiser et al. (1990), a first order channel has at last three contributing plane elements, i.e. one plane contributes to the upper end of the channel and two planes contribute channel flow. The remaining higher order channels should have at least two planes which contribute lateral flow. Figure 4-3 shows the schematic representation of the watershed configuration. A total of 77 planes and 32 channels were manually determined based on the watershed topographic maps. Additional subdivision can be made based on the spatial distribution of soils and land slope. As noted previously, the watershed elements were digitized and stored in a DLG format. A numeric number was assigned to each element.

After the watershed elements were digitized, the configuration of the elements was reviewed for additional sub-division based on the spatial distribution of soils and slopes. The procedure is outlined in the following steps:

1. GIS procedures were used to overlay the watershed element data layer onto the soil mapping unit data layer to determine if the spatial variation is sufficient to justify further subdivision.

2. If more than one soil type existed in a given plane element, the following criteria were used to determine additional subdivision of the element.

a). For the situation where one soil type occupied over 60% of the total area of the plane, the plane was not subdivided further.

b). For the situation where two soil types occupied approximately 40% and 60%, respectively, of the total area of the plane, two additional planes were added, i.e. , one for each soil type. Likewise, for the situation of three soil types each covering approximately 33% of the element, three additional planes were added.

c). A review of land slopes followed procedures similar to those described for soils. The slope data layer was grouped into four classes: 0-2%, 2%-7%, 7%-15%, over 15% and then overlaid onto the watershed element previously modified to include the variation in soils.

If one or more planes were subdivided, the additional boundaries were digitized and added to the digital map data file containing watershed plane boundary.

For the Foster Creek Watershed, the above review did not result in the creation of additional planes or channels. The final watershed configuration is given in Figure 4-4.

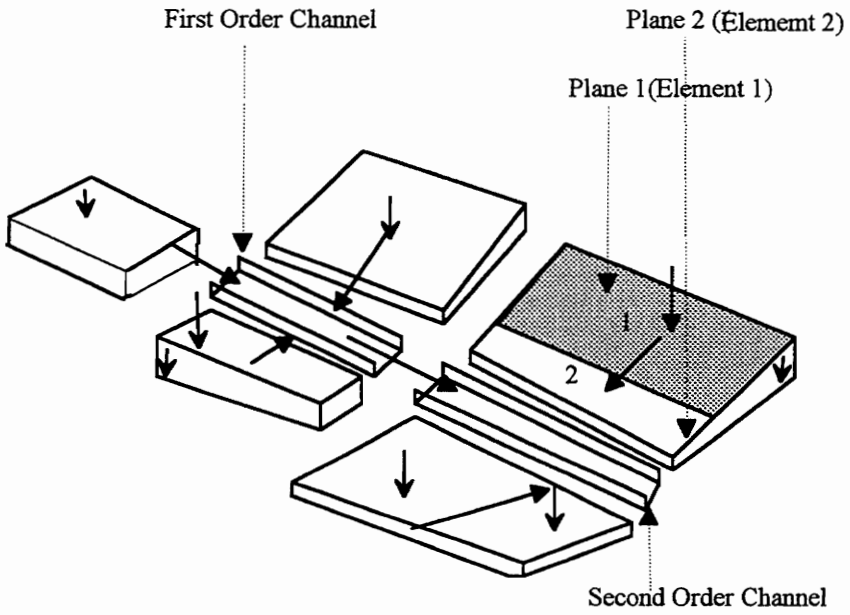

Figure 4-3 A schematic representation of the watershed conceptualization of KINEROS

4.4.2 *Slope of A Plane*

The average slope for each plane was determined as follows:

1.A Digital Elevation Model (DEM) was created from the elevation contour data layer using PC-VirGIS software. DEM were constructed determining elevation at 109 feet equally spaced intervals.

2. The average cell slope was calculated using a root mean square average of slopes between each neighbor in a 3 x 3 windows . The slope data layer is shown on Figure A1, Appendix A.

3. The slope data layer was overlaid on the plane data layer and the proportionate extent of each slope was determined for each plane.

4. The following equation was used to calculate the average slope for a plane based on the results of step 3.

$$KW_i = \frac{\sum_{i=1}^{n} AiK_i}{\sum_{i=1}^{n} A_i} \qquad (4\text{-}1)$$

KW_i is the area weighted slope for a plane in percent;

A_i is area in a plane for the slope i;

K_i is the value for the slope i ;

n is the number of unique slopes estimated in a plane; and

i is slope category.

The procedure used to calculate the area weighted slope is illustrate in Figure 4-5.

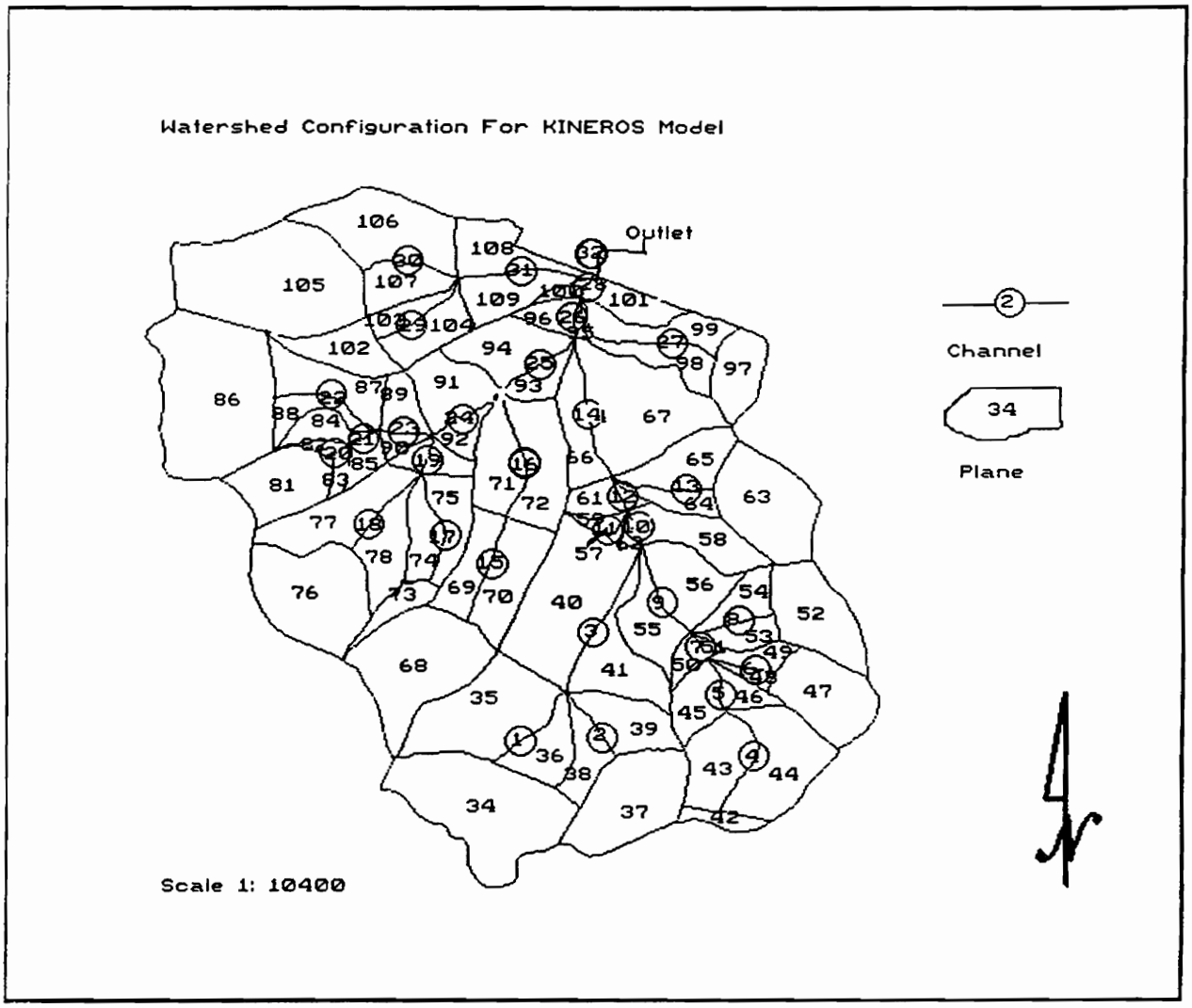

Figure 4-4 The watershed configuration of KINEROS

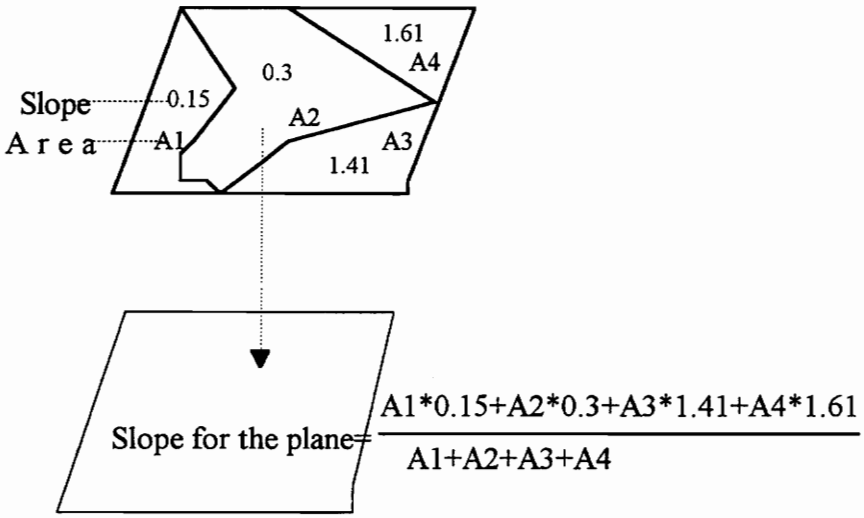

Figure 4-5 A schematic procedure to define the area weighted slope for a a plane.

4.4.3 *Overland Flow Length, Width And Area Of A Plane*

The area of each plane was calculated using the VirGIS software. The overland flow length of the plane was determined in the following steps:

1). The plane and contour map data layers were displayed by PC-VirGIS software.

2). Five points were randomly located on the up drainage boundary of the plane.

3).The overland flow paths for each point was determined by moving downslope perpendicular to the contours to the corresponding channel element and recording the distance given by the graphical ruler.

4). The overland flow length of the plane was defined as the average of the five flow paths.

The average width of each plane was determined from the relationship:

$$W = \frac{A}{L} \tag{4-2}$$

where

L is overland flow length;

A is area of a plane; and

W is width of a plane.

4.4.4 *Channel Section*

A trapezoidal channel cross-section was assumed based on pervious work by Ross (1978). The geometry of the channel section is shown on Figure 4-6.

4.4.5 *Slope And Length of A Channel.*

The length of the channel was defined using the VirGIS software to measure the distance between the two ends of the channel. The difference in elevation between the

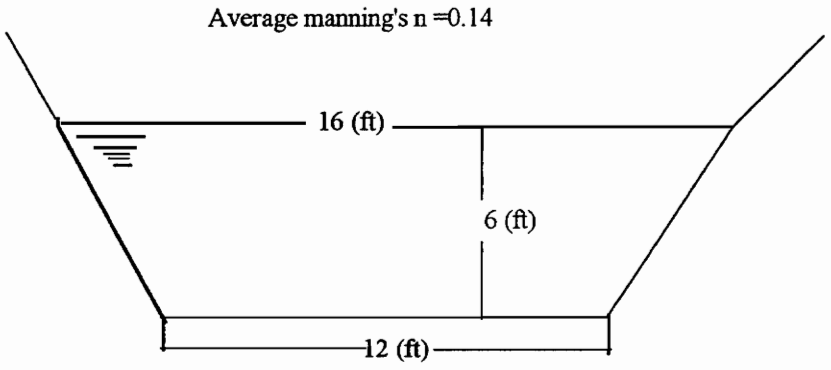

Figure 4-6 The channel cross section

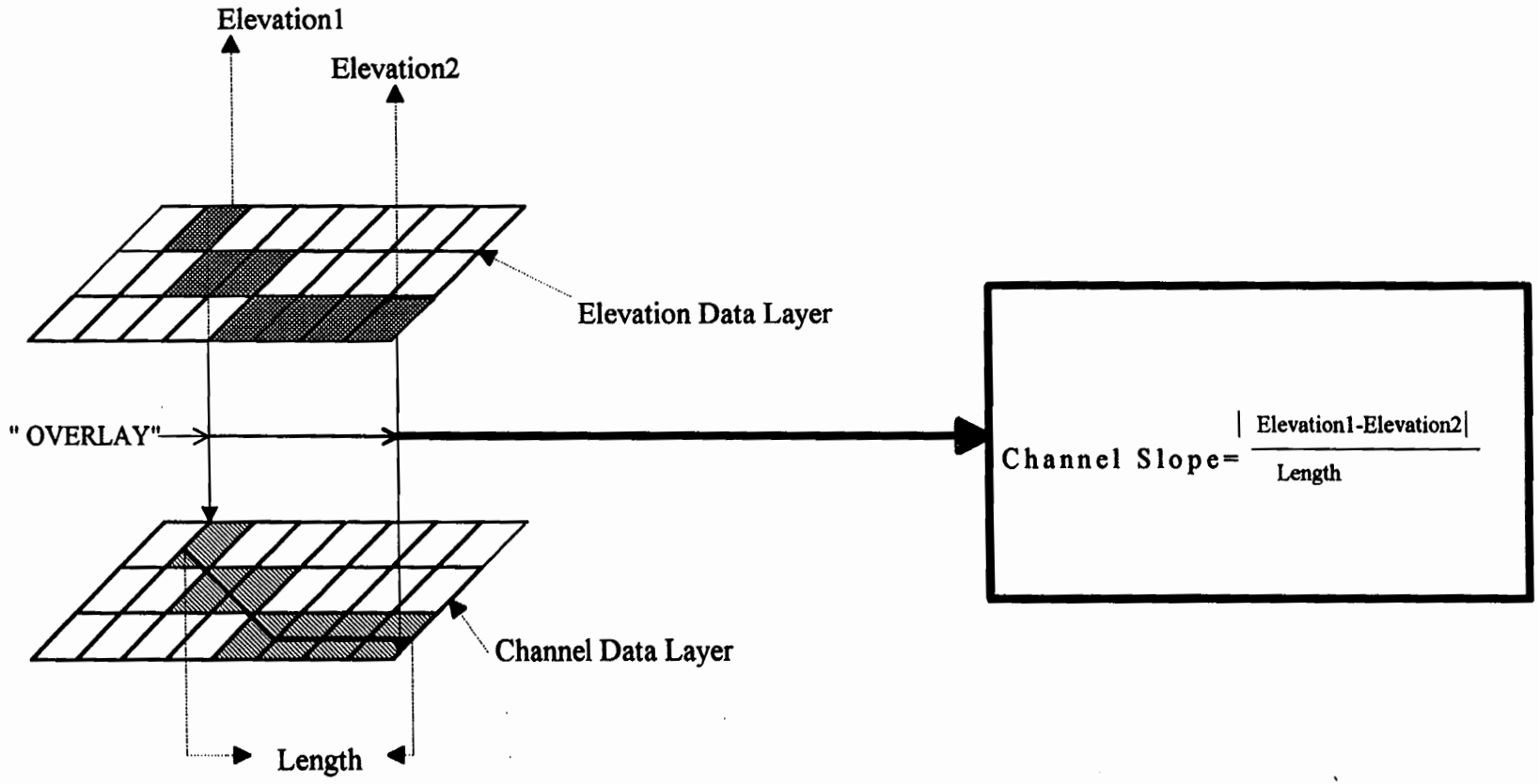

Figure 4-7 A schematic procedure to calculate the slope and length of a channel

upstream and downstream points of a channel element was determined by overlaying the elevation contour data layer with the channel data layer. Channel slope was calculated as the ratio of channel relief to channel length. The procedure is illustrated in Figure 4-7.

The topographic information for each channel and plane are summarized in Table A1 and A2, Appendix A, respectively.

4.5 *HYDROLOGIC AND HYDRAULIC DATA FOR KINEROS*

The hydrologic and hydraulic data requirements are listed in the Table 4.5. A description of the procedure used to calculate each parameter is given in Sections 4.5.1 through 4.5.6.

4.5.1 *Relative Soil Saturation*

The relative soil saturation is defined as the ratio of the initial moisture content to soil porosity (Woolhiser et al., 1990). The values of soil porosity for each soil type were obtained from Ross (1978). Estimation of the initial soil moisture content for the event simulated is defined in section 4.5.1.1.

The digitized soil data layer was reclassified to create the relative soil saturation data layer within VirGIS. The relative soil saturation data layer was overlaid on the plane data layer and an equation similar to equation 4-1 was used to calculate the area weighted relative soil saturation for each plane. The procedure is illustrated in Figure 4-8.

4.5.1.1 *Initial Soil Moisture Content*

The initial infiltration rate is significantly affected by antecedent soil moisture. Watersheds with low initial soil moisture tend to have less runoff over a given time interval. Whereas, watershed

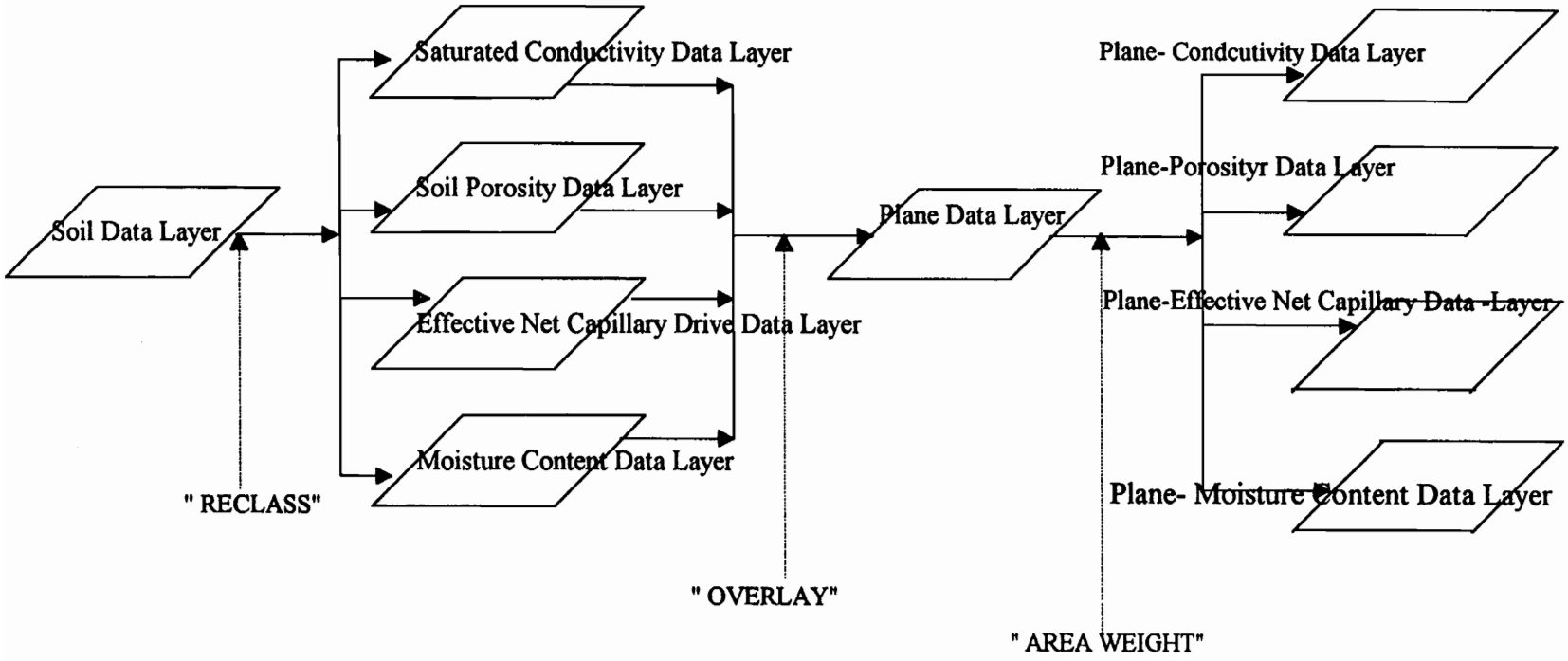

Figure 4-8 A schematic procedure of definition of values related to soil characteristics for a plane

with high initial moisture content tend to result in higher runoff (Ponce, 1989). Therefore, it is very important that good estimation of antecedent moisture content be used when attempting to compare simulated storm flow with corresponding recorded events.

The moisture content can be measured directly or indirectly. Direct measurement includes the determination of weight loss from oven-dried samples. This method provides a point measurement and gives little information on the soil moisture change with time. Soil moisture content can be measured indirectly with tensionmeter, however, Ponce (1989) pointed out that, although this method can be performed in situ, its application is limited.

The water balance method also can be used to provide an indirect measure of soil moisture. When sufficient information such as recorded rainfall and runoff data, potential evapotranspiration and percolation data are available, this method can provide useful and reliable results (Thornthwaite et al., 1955; Ross, 1978; Beasley, 1982). This procedure was followed to estimate initial moisture content. The following equation is used to calculate the moisture balance.

$$\theta_t = \theta_{t-1} + P_t - ET_t - DS_t - R_t \tag{4-3}$$

where

θ_t is antecedent soil moisture in inches at time t;

ETt is evapotranspiration losses in inches at time t;

Rt is runoff losses in inches at time t;

DS_t is percolation in inches at time t; and

t is time in days.

Ross (1978) recommended that antecedent moisture calculation should be started approximately one month before the event being simulated. Ross (1978) and Beasley et al. (1982) gave the details of the procedure and discussed its assumptions.

Estimation for initial soil moisture content for each plane required data for daily evapotranspiration, soil water holding capacity, and daily rainfall. The procedures used to estimate these data are given in the following sections.

4.5.1.1.1 ***Evapotranspiration***

Evapotranspiration (ET) is the process by which water on the land surface, soil and vegetable is converted into vapor state and returned to atmosphere. The potential evapotranspiration (PET) is defined by Saxton et al. (1982) as " an atmosphericly determined quantity, which assumes that the ET flux will not exceed the available energy from both radiant and convection sources". It is the amount of ET that will take place when water is not limiting.

Techniques for estimating PET are based on one or more atmospheric variables, such as air temperature, solar or net radiation and can be grouped into four categories: 1) temperature method; 2) radiation method; 3) combination method; and 4) pan-evaporation method (Saxton, 1982).

The availability of data determines the method of calculation of PET. The Thornwaite (1948) method was used to calculate the monthly evapotranspiration for this study because of the availability of daily temperature from the watershed. Calculation was based on the relationship:

$$PET = 0.63 L_d \left[10 \frac{T}{I} \right]^a \qquad (4\text{-}4)$$

where

PET is potential evpotranspiration, inch;

L_d is daytime hours in unit of 12;

T is mean monthly air temperature, ^{0}C;

I is heat index which is equal to $\sum_{i=1}^{12} (T_i/5)^{1.514}$; and

a is a constant calculated from the relationship :

$0.000000675I^3-0.0000771I^2+0.49239$.

Data for day length vs. latitude taken from Thornthwaite and Mather (1955) are given in Table A6, Appendix A.

The mean daily evapotranspiration rate was calculated as PET/30 and then translated into English units.

4.5.1.1.2 ***Soil Water Holding Capacity***

The soil water holding capacity of each soil type was required to calculate the daily soil moisture balance. It was calculated for the zone of maximum hydrologic activity, which was assumed by Ross (1978) to include the A and a portion of the B soil horizon. It generally coincides with the depth of significant root penetration of the vegetative. Soil physical properties, field capacity and saturated hydraulic conductivity were obtained from Ross (1978).

4.5.1.1.3 ***Percolation***

The saturated hydraulic conductivity for each soil type was used to define the value of percolation. Section 4.5.2 describes the procedure used to determine saturated hydraulic conductivity for each soil type.

In general, the soil moisture content for the event simulated was defined for each soil type after completing the calculation of equation 4-3. Relative moisture content for each soil type was thus determined by assigning the value of the ratio of soil moisture content with soil porosity for each soil type.

4.5.2 *Saturated Hydraulic Conductivity (FMIN)*

Saturated hydraulic conductivity is used in determining the infiltration by both KINEROS and PSRM-QUAL models. Neither field nor laboratory measurements for saturated hydraulic conductivity data existed for Foster Creek Watershed. The tabulations of Rawls et al. (1982) was used as the source to define the value for each soil type. VirGIS software was used to reclassify the soil data layer to create the soil hydraulic conductivity data layer. Then the saturated hydraulic conductivity data layer was overlaid on the plane data layer and a equation similar to equation 4-1 was used to determine the area weighted saturated hydraulic conductivity for each plane. Figure 4-8 illustrate the procedure.

4.5.3 *Effective Net Capillary Drive (G)*

Effective net capillary drive is a conceptually soil characteristic and can be defined as a net or effective value of capillary head (Woolhiser et al., 1990). The parameter was defined based on procedures given in Rawls et al. (1982). The procedure which was used to define values for each plane was similar to the method previously described for saturated hydraulic conductivity. The procedure is illustrated in Figure 4-8.

4.5.4 *Infiltration Recession Factor (REC)*

The infiltration recession factor is used by KINEROS to represent the local maximum average depth of surface water flow (h) for which the surface is essentially completely covered by the water. The ratio of h to REC is used to reduce the net rate of loss of surface water by infiltration during storm recession. A relative smooth surface generally is represented by low value of the REC. Woolhiser et al. (1990) gave the details of the parameter. The depression storage is defined by Shanholtz et al. (1994) as "Precipitation excess required to satisfy the requirements of surface irregularities". Because the concept and function of REC was analyzed similar to those of depression storage, the values of the depression storage from Ross (1978) was used to define REC. The procedure used to define REC for each plane was similar to that used for saturated hydraulic conductivity. Figure 4-9 illustrates the procedure.

4.5.5 *Interception (DINTR)*

Interception is the process by which precipitation is abstracted by vegetation or other forms of surface cover. Interception is very important for annual water balance calculation, however, it is relatively unimportant for event-based modeling (Woolhiser et al., 1990). Interception rates were obtained from Ross (1978). The landuse/land cover data layer was reclassified to create the interception data layer. The data layer then was overlaid onto the planes and the area weighted interception for each plane determined following the procedure previously outlined for REC. The procedure to determine the value of the parameter for each plane is illustrated in Figure 4-9.

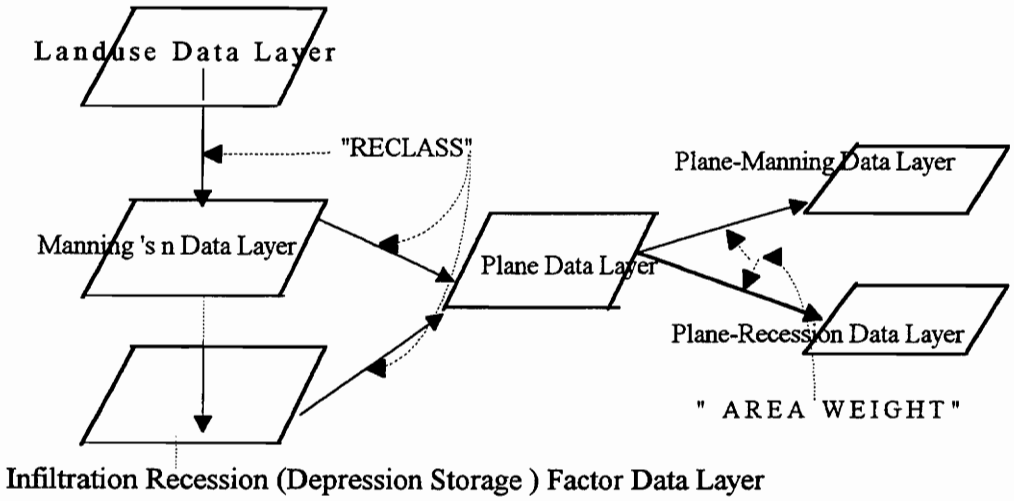

Figure 4-9 A schematic procedure for determining the information related to landuse for a sub-area or a plane

4.5.6 ***Manning's N of A Channel (R1)***

Chow (1964) pointed out that "it is uncommon for engineers to think of a channel as having a single value (manning's n) for all occasions". That is, n is highly variable. Such factors as vegetation, surface roughness and channel irregularity influence manning's n. Manning's n was obtained from the values reported by Ross (1978).

4.5.7 ***Overland Manning 's N of (R1)***

The manning's n of overland is defined by the types of landuse. The value of n for each type of landuse was obtained from values reported by Ross (1978). Manning's n was related to landuse and manning's n of overland data layer was created by reclassifying the landuse/land-cover data layer and overlaying onto the plane to determine the average value for each plane. The procedure similar to that of defining interception was used to determine the area weight Manning's n for each plane. Figure 4-9 illustrates the procedure.

The hydrologic and hydraulic information for each plane and channel are summarized in Table A1 and A3, Appendix A, respectively.

4.5.8 ***Modifications to KINEROS Computer Code***

Computer code was modified to increase the storage limitation relating to planes and channels. The current limitation are 115 elements and 110 time-depth pairs of rainfall.

4.5.9 ***Testing of KINEROS Data Sets***

The approach used to check data and basic flow logic was recommended by Woolhiser et al. (1990). The saturated hydraulic conductivity and effective net capillary drive for all the channels and planes were set to zero to simulate a completely impervious watershed. The rainfall input file

was set to a constant rate of 1.0 in/hr for a duration of 300 minutes when the model was executed with the above parameters. The data set is considered acceptable if the condition in the statement of Woolhiser et al. (1990) is met: "If the output hydrograph approaches steady state rate nearly equal to the input rate, all elements are contributing and numerical errors are acceptable". The results are given in Figure 4-10, which indicates that the watershed description met the above criteria.

4.6 *TOPOGRAPHIC DATA FOR PSRM-QUAL*

The procedures used to determine database for PSRM-QUAL are described in the remainder of this chapter.

4.6.1 *Watershed Conceptualization for PSRM-QUAL*

The procedures used to subdivide the Foster Creek Watershed are described by Aron et al. (1992). The first step involved tracing the channels on a topographic map. The second step involved constructing boundary lines for each plane.. These were created by moving laterally from each of the channel segmentation points, in such a way that each channel corresponds to only one plane immediately upstream. The plane and corresponding channel were labeled by the same number. Figure 4-11 illustrates the schematic representation of the watershed configuration for PSRM-QUAL. Following these procedures, the watershed was divided into 32 planes and 32 channels. The boundary for planes and channels were digitized following procedures previously described and stored in a DLG format for later analysis. The watershed subdivision is shown in Figure 4-12

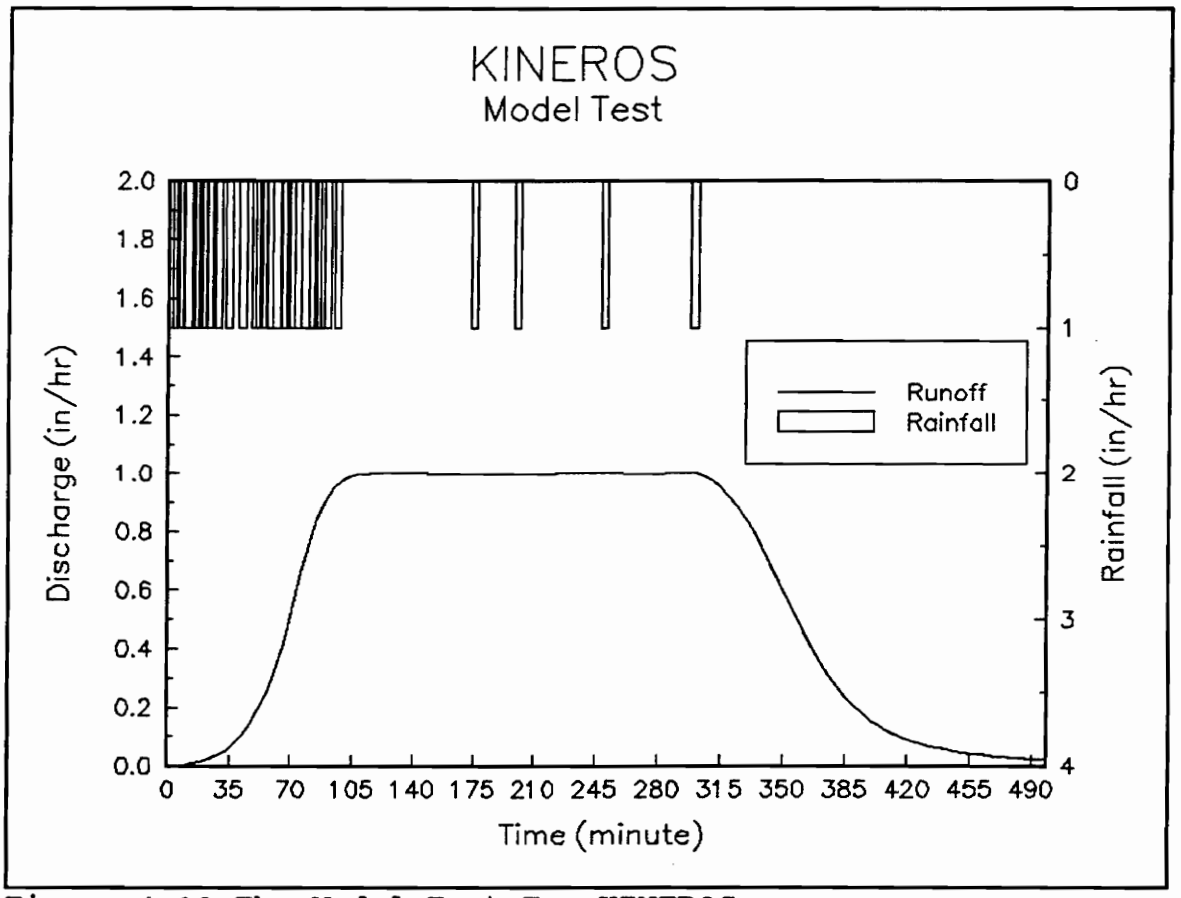

Figure 4-10 The Model Test For KINEROS

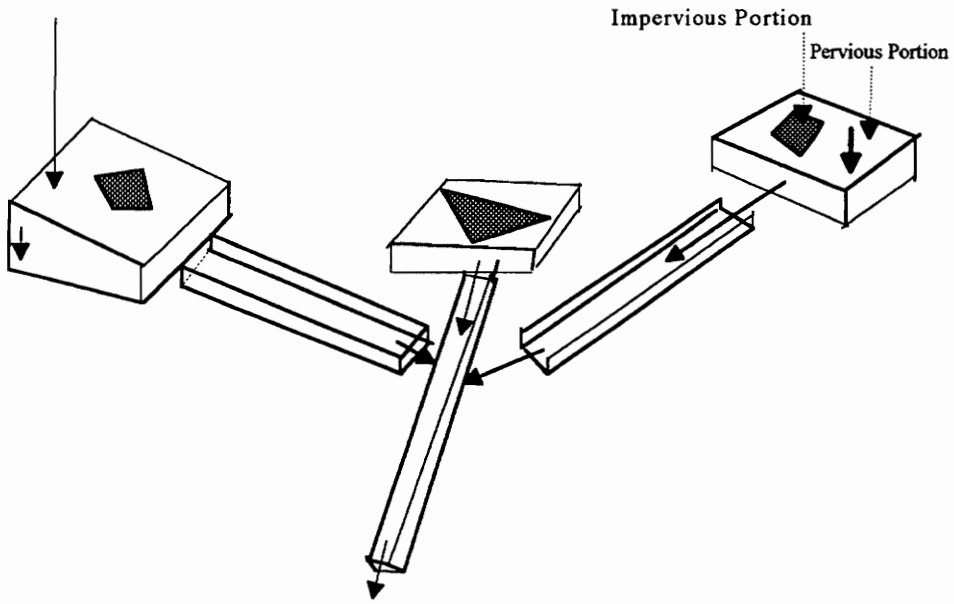

Figure 4-11 A schematic representation of the watershed conceptualization of PSRM-QUAL.

4.6.2 *Overland Flow Length, Width And Area Of A Plane*

The procedure used to define overland flow length, width and area for each sub-area was similar to the method described in Section 4.4.3.

4.6.3 *Slope Of A Plane*

The procedure used to determine the slope for each subarea is described in Section 4.4.2.

A description of the topographic information for each subarea and channel is summarized in Table A4 and A1, Appendix A, respectively.

4.7 *HYDROLOGIC AND HYDRAULIC DATA FOR PSRM-QUAL*

The procedures to define the hydrologic and hydraulic data for each plane and channel are described in Section 4.7.1 through Section 4.7.11.

4.7.1 *SCS Curve Number (CN)*

The SCS curve number was determined based on the hydrologic soil group and hydrological conditions (SCS , 1986). The soil type determines the soil hydrologic group and the hydrological conditions were determined based on landuse. The following procedures were used to determine the CN for a plane. 1) The hydrologic groups were determined for each soil type according to SCS (1986) and then the hydrologic group data layer was created by reclassifying the soil data layer. 2) Landuse was overlaid on the hydrologic group data layer and CN was defined based on the landuse-hydrologic group combination. 3) The CN for each plane was calculated using a relationship similar to equation 4-1. The procedure are illustrated in Figure 4-13 and 4-14, respectively.

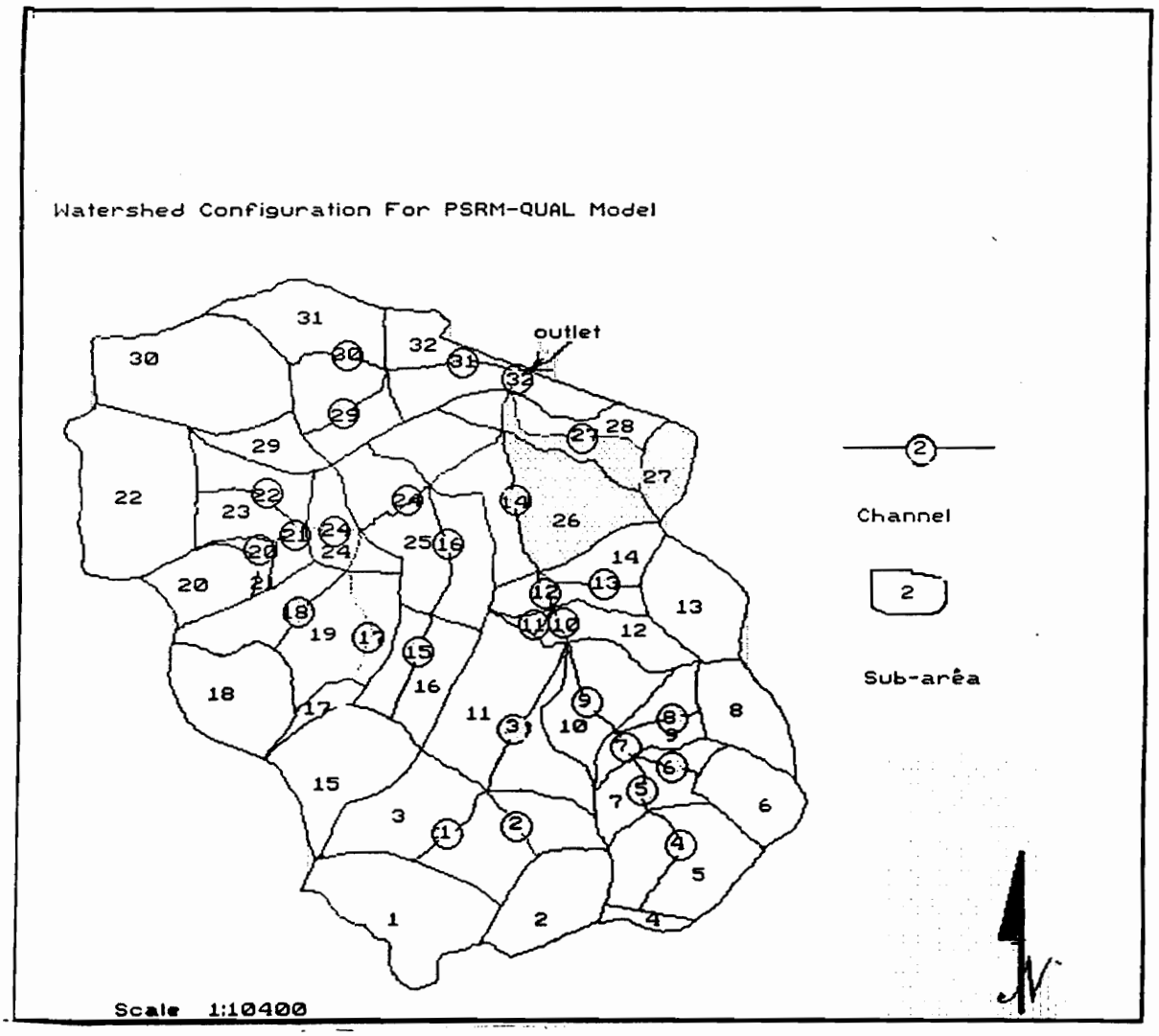

Figure 4-12 The watershed configuration of PSRM-QUAL

4.7.2 *Initial of Soil Wetted (STIS)*

STIS is the ratio of initial soil water content with soil storage capacity (S_c). A procedure similar to that use to determine the relative soil moisture content for KINEROS was utilized to determine STIS for each plane.

4.7.3 *Equilibrium Infiltration Capacity (STKS)*

The saturated hydraulic conductivity is considered equal to the equilibrium infiltration capacity in PSRM-QUAL (Aron et al., 1992). The value of the parameter for each soil was defined from the research work of Li (1975). A procedure similar to that used to determine the saturated hydraulic conductivity for KINEROS was used to define the values of the parameter for each plane.

4.7.4 *SCS Initial Abstraction Factor (STDIA)*

Initial abstraction is defined as excess rainfall lost before runoff begins. Water retained in surface depressions, intercepted by vegetation, evaporation and infiltration are included in the parameter. The STDIS value was assigned 0.2 initially for each plane (SCS, 1986).

4.7.5 *Depression Storage on Pervious Surface (STDS)*

In PSRM-QUAL, the depression storage on impervious and pervious surface are considered separately. Since over 98% of the area of the Foster Creek Watershed was pervious, impervious surface was ignored for this study. The values of depression storage on pervious surface was determined from Ross (1978). The landuse data layer was reclassified to create the depression storage data layer and then was overlaid on the plane data layer. An equation similar to equation 4-1 was used to define the value of the parameter for each plane.

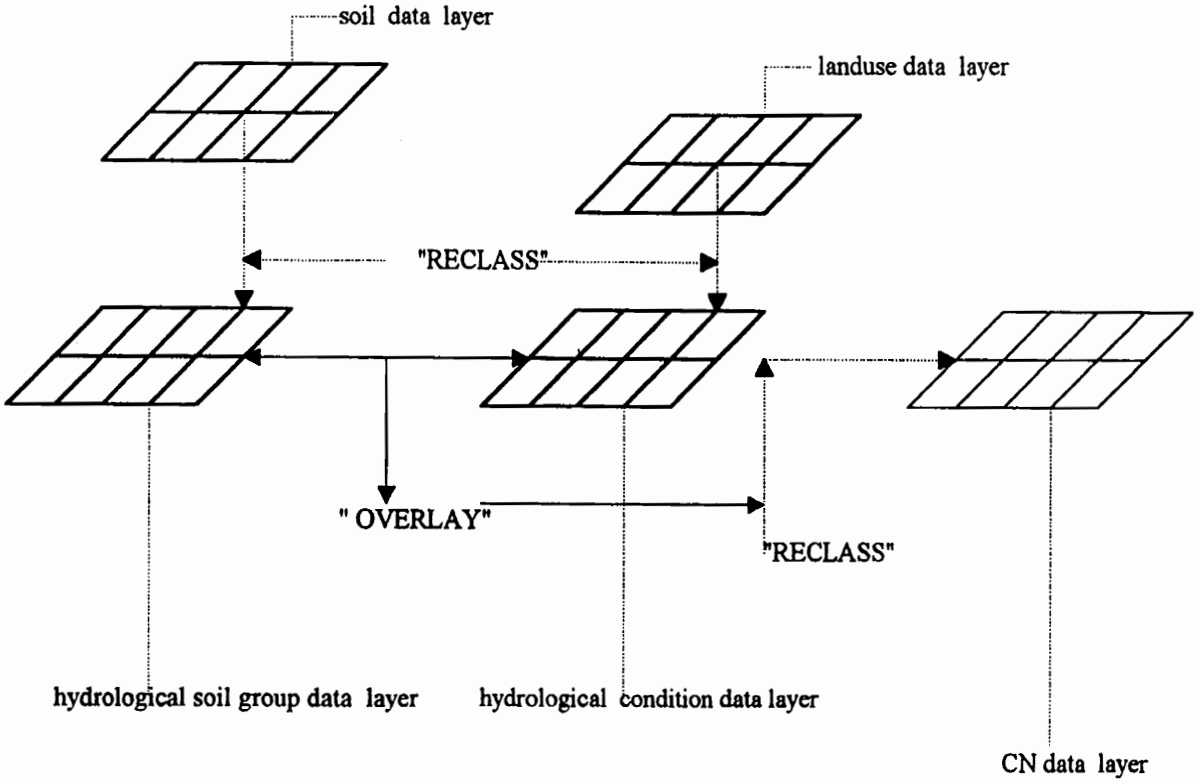

Figure 4-13 A schematic procedure of determination SCS curve number

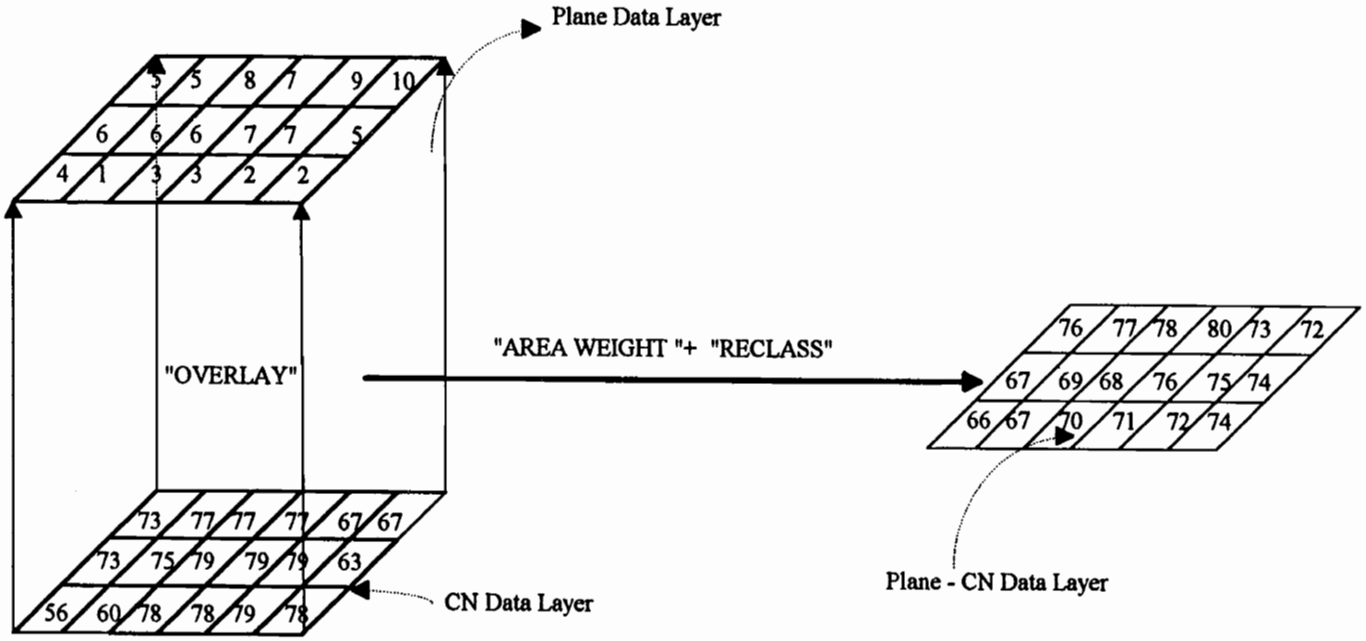

Figure 4-14 A schematic procedure of determination CN for a plane

4.7.6 *Weighting Factor of Muskingum Method (STMX)*

The weighting factor of Muskingum is used to define the amount of translation and the amount of attenuation of downstream discharge. Chow (1988) and Aron et al. (1993) suggest 0.2 as a mean value for a stream channel. This assumption was also used for this study.

4.7.7 *Full-flow Capacity of A Channel*

The Manning formula was used to calculate the full flow capacity for each channel. The channel section , channel length, slope, manning's n were determined following the same procedure as previously discussed for the KINEROS.

4.7.8 *Full-flow Travel Time Through A Channel*

The full-flow travel time through a channel was defined by the dividing the full-flow capacity of a channel with its length.

4.7.9 *Ratio of In-bank to Overbank Flow Velocities (CTS)*

The ratio of in-bank to overbank flow velocities is used to increase the travel time for surcharge flow. Aron et al. (1992) suggest that CTS should be determined by calibration, which was followed for this study.

4.7.10 *Sinuousity Factor*

The procedures illustrated in Section 4.4.3 implies that an overland length is measured as a straight line. In reality, the overland flow path is most likely undulating. A sinuousity factor is used in the model to increase the measured length of the flow path. Because no field data were available to define the value of the parameter, the determination of the value of this parameter, it was determined by calibration.

4.7.11 *The Manning's n of A Plane*

The procedures illustrated in Section 4.5.6 were used to define the value of the Manning's n for each plane.

Table A5, Appendix A contains the summaries of the hydrologic and hydraulic information for each plane, respectively.

4.7.12 *Testing of PSRM-QUAL Data Sets*

Care was exercised in the preparation of input data to minimize errors. The model also includes an internal routine to check the sequencing of the subareas, making sure that the connections of plane and channel are legitimate. The input file was tested by this routine and found to be correct.

4.8 *SELECTION OF STORM EVENTS*

The recorded rainfall and streamflow data covering the period 1960-1969 for Foster Creek Watershed, which are stored on mainframe computer of Agricultural Engineering Department, Virginia Tech, were used to evaluate the two model's capabilities. A computer program was used to download these data to a PC computer from the mainframe computer. The rainfall data were continuously recorded at rainfall gaging station 2, i.e. R2 in Figure 4-1. Runoff data were recorded with a Virginia V-notch weir (Burford and Lillard, 1963), which was located at the outlet of Foster Creek Watershed (Figure 4-2). The following criteria were used to select storm events to be used for calibration and verification analysis.

1. Events resulting from snowmelt were excluded because neither KINEROS nor PSRM-QUAL supports simulation of snow melt.

2. The storm events were selected from the period between April through October of each year.

3. Only rainfall events which resulted in runoff were chosen. A minimum peak flow rate of 0.017 in/hr (9.13 cfs) was established for all runoff events.

A computer program was developed based on the above criteria and used to select 29 events from the nine year record.

4.9 *Summary*

Both KINEROS and PSRM-QUAL have substantial input parameters that must be defined. The major source for data to define the input parameters were from previous research reported by Ross (1978), Rawls et al. (1982) and SCS (1986).

GIS technology was used extensively to assist with data preparation. VirGIS software was used to create and to organize the huge volume of topographic, hydrologic and hydraulic data for the two models.

Chapter 5

BASIS FOR COMPARISON

5.1 *PROCEDURES FOR COMPARISON*

The basis for assessing the performance of a hydrological model generally focuses on the comparison of the goodness-of-fit of a simulated hydrograph with a corresponding observed hydrograph (Green and Stephenson, 1986). A number of criteria have been set to judge the goodness-of-fit based on the objectives of the model user (Loague and Freeze, 1985; Sorooshian and Gupta, 1983; Green and Stephenson, 1986). No universal method was found that can be used to evaluate the performance of all aspects of a model. A given set of criteria highlights a particular aspect of a model or models. Therefore, it may be unfair to draw a conclusion that one model is best among the models which have similar domains. Consequently, several methods were selected from the literature (Loague and Freeze, 1985; Green and Stephenson, 1986; Hession, 1988), which provide criteria for evaluating a range of model's simulation capability. These include: 1) Graphical comparison; 2) Hydrograph shapes; 3) Relative errors; 4) Model efficiency; 5) Linear regression; and 6) Hypothesis testing.

As illustrated in Chapters 3 and 4, KINEROS and PSRM-QUAL are distributed models, which have many model parameters that need to be defined. Many parameters must be determined through calibration. Sensitivity analysis was used to determine the degree of variability of input model parameters to model simulated results. The most sensitive parameters were determined from sensitivity analysis and used in calibration. McCuen and Snyder (1986) give illustrations of sensitivity analysis as an aid in hydrologic modeling.

The results from sensitivity analyses were used to guide the calibration of model parameters. The available population of storm events was randomly separated into two groups. One group was used for calibration and the remaining group was used for verification analysis. These procedures are described in detail by James and Burges (1982), Loague and Freeze (1985) and Sasowsky and Gardner (1991).

In summary, the basis for model evaluation involved three general tasks: 1) sensitivity analysis for the two models; 2) calibration for the two models; and 3) verification for the two models. These tasks are discussed in Sections 5.1.1 through 5.1.3.

5.1.1 ***Sensitivity Analysis***

The objective of sensitivity analysis for this study was to improve the efficiency of calibration since sensitivity analysis provides a measure of the relative sensitivity of model parameters on the output generated by models (Osborn et al., 1982; Ponce, 1989). It also is a useful tool for all phases of model evaluation, calibration and verification (Osborn et al., 1982; McGuen and Snyder, 1986).

The following procedures were established to evaluate the relative sensitivity of model parameters.

Sensitivity analysis were conducted for the hydrological and hydraulic parameters listed in Tables 4-5 and 4-6. Because rainfall is the principle model input parameter, the variation of rainfall on model outputs response was also evaluated. The sensitivity analysis was divided into two stages. The most sensitive parameters were determined during the first stage. During the second stage, the selected parameters were further investigated as to their impact on simulated results, because

understanding the impact of changes in parameter values on simulated results facilitates the calibration process.

The following steps were followed during the first stage of sensitivity analysis.

- One storm event was randomly chosen from the rainfall storm event population.

- A base hydrograph was simulated using recommended parameter values.

- Most parameters were varied ±20% (Hession, 1988) within their hydrologic or hydraulic meaning while the remaining parameters remained unchanged from the base values. Rainfall amount and the SCS curve number were found to be very sensitive parameters to total runoff volume and peak discharge rate in studies by Hession, 1988 and Young, et al. 1987. Therefore, these two parameters were varied±10% to test the sensitivity in this study.

The selected parameters were varied at several intervals and same procedures were used to test the relative sensitivity to total runoff volume and peak discharge rate during the second stage.

- The relative sensitivity on simulated output was calculated using the relationship:

$$Relative\ Sensitity(\%) = \frac{Simulated-Base}{Base} * 100 \qquad (5\text{-}1)$$

The above procedures can be used to determine the most sensitive model parameters (McCuen and Snyder, 1986). However, the information on the level of certainty to be placed on the results of the modeling as well as the interactions between parameters is not provided by this procedure.

5.1.2 ***Calibration***

Calibration of hydrological models is the process of adjusting values of a parameter set that gives acceptable agreement between simulated and recorded flows (Ponce, 1989). The process

requires a procedure to evaluate the success of a given calibration and another procedure to adjust the parameter estimates for the next iteration. It is commonly recognized that the basic objective of model calibration is to minimize the differences between the observed and simulated values through optimization of parameters.

The overall importance of calibration varies with model type. Calibration is extremely important for the conceptual, stochastic or lumped modeling, since most parameters of these type models are indirectly related to the physical process of specific watershed characteristics (Ponce, 1989; James and Burges, 1982). The distributed parameter modeling approach evaluates the influences of the spatial variation of parameters on simulated behavior. Distributed parameter models incorporate data concerning the aerial distribution of parameter variations of the specific watershed with computational algorithms. Therefore, physically-based distributed models theoretically require little or no calibration if the field and experimental data are accessible. However, physically-based models are usually not entirely deterministic and experimental and field data are not available, therefore calibration is still often necessary.

The two approaches generally used to calibrate models are manual or automatic (Sorooshian et al., 1983). In the automatic calibration procedure, a computer program is used to determine the optimal set of parameters that result in the best fit of simulated versus observed records. The automatic calibration procedure is difficult to use with the distributed parameter models (Beven, 1985; Blackie, 1985; Sorooshian and Gupta., 1983; Ibbitt et al., 1971) because a) the definition of a distributed parameter model involves many parameters and extensive data. Some parameters have a degree of interdependence with each other; b) indifference of the objective

function to the values of threshold type parameters; c) discontinuities of the response surface; and d) nonuiqueness of the optimum values of parameters. The automatic calibration procedure may result in the best possible fit between the simulated and the observed hydrograph by sacrificing the physical meaningfulness of some parameters (Sorooshian et al., 1983). Therefore, the calibration of physically-based distributed models involving a large number of parameters and even more parameter values by automatic calibration is impractical and often misleading (James and Burges, 1982; Ponce, 1989).

The manual calibration procedure is used to calibrate the relatively important parameters based on "trial-and-error". The manual calibration procedure can apply the experience gained from sensitivity analysis and subjective judgment of the modeler (Blackie, 1985). Compared with the present automatic calibration procedure, the manual calibration procedure is more accurate but costly (James and Burges, 1982). James and Burges (1982) illustrated the details of the differences between automatic and manual calibration procedures and discussed some procedures to calibrate models.

The basis for calibration involved the following steps:

1. Define calibration objectives.
2. Establish objective function, i.e. determine the degree of goodness of the agreement.
3. Choose the most important input parameters to calibrate.
4. Define reasonable ranges for input parameter values.

5. Manually adjust the input parameters until output matches observed hydrograph within acceptable limit.

The basic calibration objective was to minimized the error between simulated and observed time to peak, peak discharge rate and total runoff volume based on the relationship:

$$RelativeError(\%) = \frac{Simulated - Observed}{Observed} * 100 \quad (5\text{-}2)$$

$$RelativeError_{timetopeak} = |Observed - Simulated| \quad (5\text{-}3)$$

The following criteria for relative percent error and relative error using equations 5-2 and 5-3 were assumed acceptable based on the research by James and Burges (1982), Hornberger et al. (1985) and Jewell (1978).

1. The difference between simulated peak rate and recorded rate should not exceed 15%.
2. The differences between runoff volume simulated and runoff volume observed should be less than 20%.
3. The differences between simulated time to peak and observed time to peak should not exceed 15 minutes.

Additional overall goodness of simulated results were based on the relationship:

$$MARE = \frac{\sum |RelativeError\%|}{n} \quad (5\text{-}4)$$

$$LMARE = \frac{\sum LOG(|RelativeError\%|)}{n} \quad (5\text{-}5)$$

where

MARE is the arithmetic mean relative error;

LMARE is the logarithmic mean absolute relative error; and

n is the number of calibrated events.

Equation 5-4 tends to emphasize outliers. Equation 5-5 tends to decrease the effect of outliers. The relationships given by Equations 5-4 and 5-5 provide outliers for evaluating calibrated results for the entire calibrated rainfall sample. The common accepted approach for a model calibration and verification is to split the available observed rainfall data into two groups. One group is used to calibrate the model and the second group to test the performance of the model, i.e. model verification. The physically based distributed models are expected to be applied to watershed with minimum calibration because of their characteristics. Good verifications with few calibrations will indicate that the so called physically based distributed model is adequate for use on the watershed. Therefore, proportion of data used for verification generally should be larger than the sample data used for calibration. As illustrated previously, thirty events were chosen to be used for calibration and verification. However, no literature was found to suggest the optimum ratio between the data sets used for calibration and verification. Thus, seven events were selected from the thirty storm samples and used in calibration analysis. No rainfall events occurring during 1963 met the rainfall selection criteria described in Section 4.8. The recorded rainfall information for the year of 1969 was not available. Each of the seven events were therefore picked randomly from sample population, which covered the period 1960 to 1968. The remaining storm events were used for the verification analysis discussed in Section 5.1.3. Tables D-1 and D-2, Appendix D contain the input data files used to calibrate KINEROS and PSRM-QUAL, respectively.

The range for each parameter was established from research reported by Rawls et al. (1982), Ross (1978) and SCS (1986). For example, the mean value of the effective capillary drive for sandy loam was defined by Rawls et al. (1982) as 5.0 inch. The minimum and maximum values

were defined as 1.2 and 21.3 inch, respectively. The range of the effective capillary drive for sandy loam was set to - 24% to 426% of the mean value. Calibration involved a systematic adjustment of each parameter running the model and comparing simulated and observed hydrograph until the criteria of goodness of fit were met or the allowable range of the parameter was encountered .

5.1.3 ***Verification***

Verification analysis were conducted to determine the goodness of fit between simulated and observed characteristics of storm flow hydrographs. The process involved using parameters determined by calibration to simulate storm flows for the verification storm sample. The mean value of the calibrated parameter from the seven events was used for the verification.

For a single event-based hydrological model, the peak discharge rate, runoff volume , time to peak and hydrograph shape are the hydrograph characteristics generally used to judge the performance of the model. Goodness of fit criteria were based on the following methods.

5.1.3.1 ***Graphic Comparison***

Visual comparison of the simulated and observed hydrographs provide a comprehensive means of judging the accuracy of the model output. The differences between the simulated and observed peak discharge rate and time to peak and the similarity of simulated and observed hydrograph shapes can be readily assessed by this technique. Although graphical comparison is a widespread method, the procedure is very subjective and usefulness is dependent on the experience of the user (Green and Stephenson, 1986).

5.1.3.2 ***Hydrograph Shape Index***

A measure of the extent that simulated and observed data match has been found to be a useful measure of goodness of fit (Green and Stephenson, 1986). It can be used to quantitatively judge the similarity of observed and simulated hydrograph shapes. The deviation of common points along the hydrograph is measured by variance as given in the following relationships.

$$S = \sqrt{\frac{1}{n}\sum_{i=1}^{n}[q_{0(t)}-q_s(t)]_i^2} \tag{5-6}$$

where

S is variance;

$q_o(t)$ is observed discharge rate at time t ;

$q_s(t)$ is simulated discharge rate at time t; and

n is number of ordinates;

The results of variance is regarded as the hydrograph shape index to judge the goodness-of-fit of simulated and observed hydrographs.

5.1.3.3 ***Relative Errors***

A measure of goodness of fit between simulated and observed peak rate, time to peak and total runoff volume is given by Equation 5-2. Relative error provides a measure of the goodness of fit of specific hydrograph characteristics such as peak flow rate and volume flow. It provides no information on hydrograph shape and similar shape characteristics. It also provides a distorted perspectives for low flows versus high flows.

5.1.3.4 ***Model Efficiency***

Two types of model efficiency were illustrated by Loague and Freeze (1985): the model efficiency on forecasting and prediction. Forecasting and prediction were defined by Lettenmaier and Wood (1992) as " the estimation of conditions at a specific future time, or during a specific time interval" or " the estimation of future conditions, without reference to a specific time". Loague and Freeze (1985) pointed out that the evaluation of model efficiency on forecasting should be based on a comparison of observed and predicted values of the summary variables for individual verification events on an event-by-event basis. For prediction, the evaluation should be based on a full suite of verification events.

The criteria set up by Nash and Sutcliffe (1970) was used to evaluate the model efficiency on both the forecasting and prediction of the models, since the Natural Environment Research Council (NEC) (1975) and Loague and Freeze (1985) suggested that the criteria be used as model fitting criteria. The equation is dimensionless, therefore the results are not affected by the sample size. The expression is given:

$$E = [\sum_{i=1}^{n} (Q_i - \bar{Q}_i)^2 - \sum_{i=1}^{n} (\hat{Q}_i - Q_i)^2] * [\sum_{i=1}^{n} (Q_i - \bar{Q}_i)^2]^{-1} \qquad (5\text{-}7)$$

where

$\hat{Q}_i$ is simulated value for event i ;

Q_i is observed value for event i ;

$\bar{Q}_i$ is mean value over the verification events; and

n is number of events.

5.1.3.5 ***Linear Regression***

Simple linear regression was used to describe the degree of association between simulated and observed values following a procedure recommended by (Hession, 1988). For the ideal situation, the simulated and corresponding observed results would be identical.

$$Y=X \tag{5-8}$$

5.1.3.6 ***Hypothesis Testing***

The purpose of hypothesis testing of the models focus on providing a more quantitative comparison of relative performance of models in a statistical sense (Loague and Freeze, 1985). Hypothesis testing of the mean and standard deviation of the peak rate, total runoff volume and time to peak were performed at a 5% level of significance. T-test and F-test were used for hypothesis testing for mean and standard deviation of the simulated results, respectively.

In summary, the above methods were found to be commonly used to evaluate the performance of distributed event-based models. The results from these methods were used to evaluate the capabilities of KINEROS and PSRM-QUAL models in this study.

The summaries of overall verification results are illustrated and discussed in Section 6.3.6, Chapter 6.

Chapter 6

ANALYSIS AND RESULTS

The results of sensitivity, calibration and verification analysis for KINEROS and PSRM-QUAL are summarized and discussed in this Chapter. Sensitivity analysis are discussed in Section 6.1 followed by calibration and verification analysis in Sections 6.2 and 6.3 , respectively.

6.1 *RESULTS AND DISCUSSION OF SENSITIVITY ANALYSIS*

Sensitivity analysis were performed to provide a basis for calibration of model parameters. The most sensitive parameters and the range of each parameter were objectives of the sensitivity study.

The procedures described in Section 5.1.1, Chapter 5 were used to test the relative sensitivity analysis for the two models. The major parameters included for each model were manipulated to test their sensitivities to the total runoff volume and peak discharge rate. The same procedure illustrated in Section 5.1.2, Chapter 5 was used to set the ranges of hydrologic parameters with their hydrologic meanings.

A rainfall event was randomly selected from the rainfall database, of which the hyetograph is shown in Figure 6-1. For this event, 1.35 inch rainfall occurred over a 2.45 hour duration with the recorded highest intensity 4.2 in/hr.

The mean values for hydraulic and hydrologic parameters of the models, which are shown in Tables 4-3 and 4-4, were employed to construct the base hydrograph. Discharge peak rate and the total runoff volume were determined by setting the parameter of interest

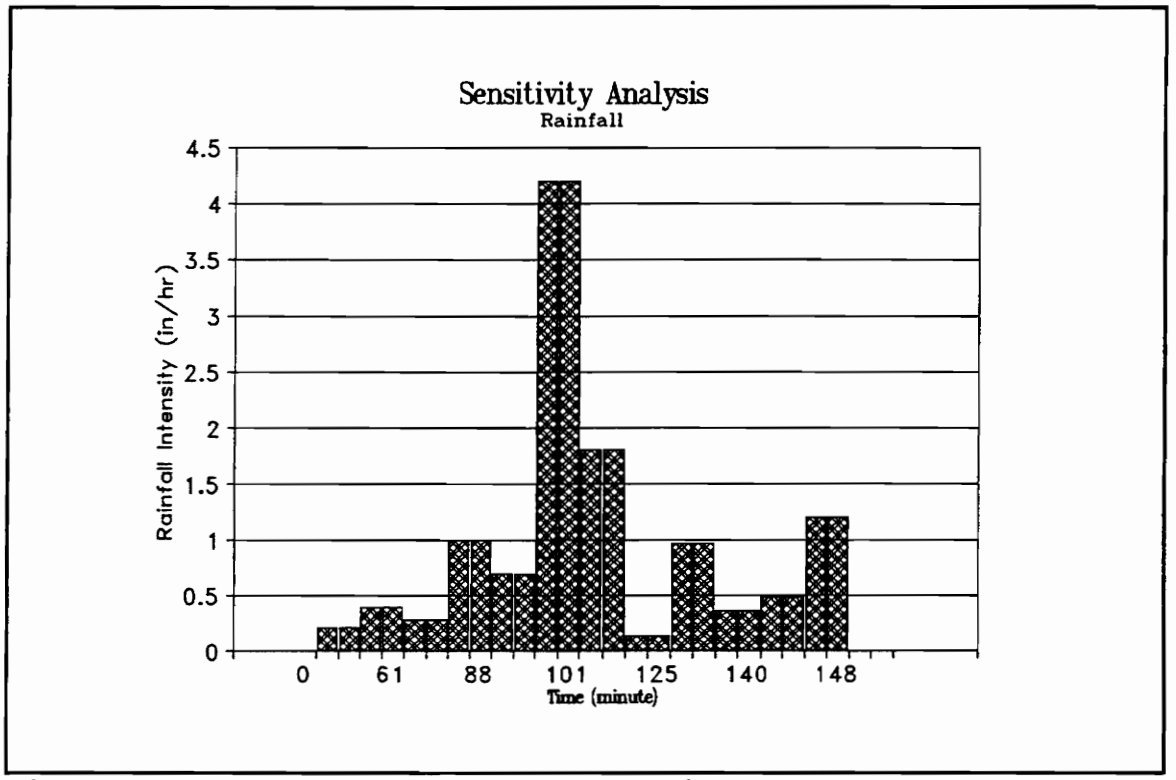

Figure 6-1 The hyetograph of the rainfall event used for sensitivity analysis

(e.g. saturated hydraulic conductivity, K_s) to a value equal to K_{s_base} /1.2 (lower range) and holding all remaining values constant. The process was repeated by setting the selected parameter to K_{s_base} x 1.2 to represent the upper range.

This procedure was followed for all parameters listed in Tables 6-1 through 6-2. The results are also summarized in the Tables 6-1 and 6-2, respectively.

After the most sensitive parameters were determined for the models, the procedures during the so called second stage in Section 5.1.1, Chapter 5 were used to further test the sensitivity of the selected parameters. The linear or non-linear relationships between each parameter and its response on total runoff volume and peak discharge rate were studied during this stage. The relationships can be very helpful during calibration of model parameters, since it indicates how parameter should be varied in calibration. The results of the second stage are summarized in Section 6.3.4.

6.1.1 *Results and Discussion----KINEROS*

The sensitivity of each input parameter to simulated results for KINEROS is described in Sections 6.3.1.1 through 6.3.1.9.

6.1.1.1 *Rainfall*

From Table 6-1, a variation of +10% in rainfall amount per time interval resulted in an increase in the simulated peak discharge rate of 6.84 % and an increase in simulated total runoff volume of 10.8 %. Reducing the rainfall amount per time interval by 10% resulted in the simulated peak discharge rate decreasing by 5.37% and a decrease in total runoff volume of 10.1%. The results showed both peak discharge rate and total runoff

Table 6-1 The summary of sensitivity analysis for KINEROS's model input parameter

Model Parameters	Variation	Base Ruonff Peaks (in/hr)	Runoff Peaks (in/hr)	Change %	Base Runoff Volumes (in)	Runoff Volume (in)	Change %
Rainfall Amount	+10%	0.818	0.87	6.84	0.47	0.52	10.80
	-10%		0.77	-5.37		0.42	-10.10
Saturated Hydaulic Conductivity	+20%		0.72	-11.60		0.43	-8.17
	-20%		0.85	3.79		0.47	1.72
Effective net Capillary Drive	+20%		0.76	-6.84		0.44	-6.23
	-20%		0.84	2.32		0.48	2.37
Relative Soil Saturation	+20%		0.83	1.71		0.47	1.51
	-20%		0.81	-1.22		0.46	-1.08
Soil Porosity	+20%		0.76	-7.21		0.43	-6.67
	-20%		0.87	6.85		0.50	7.31
Channel's Manning n	+20%		0.74	-10.00		0.46	-2.15
	-20%		0.92	12.20		0.47	1.94
Overland's Manning n	+20%		0.79	-3.91		0.46	-1.08
	-20%		0.86	5.50		0.48	2.15
Interception Depth	+20%		0.88	6.96		0.50	6.88
	-20%		0.80	-1.96		0.46	-1.94
Infiltration recession factor	+20%		0.82	0.48		0.47	0.43
	-20%		0.81	-0.73		0.46	-0.86

were very sensitive to rainfall amount. The total runoff volume is more sensitive to rainfall amount than peak discharge rate. The results also illustrated the quality of recorded rainfall is very important when evaluating model's simulation capability. The sensitivity of precipitation is illustrated in Figure 6-2.

6.1.1.2 ***Saturated Hydraulic Conductivity***

In general, the higher soil saturated hydraulic conductivity results in the lower peak discharge rate and total runoff volume. For this example, a 20% increase in saturated hydraulic conductivity resulted in a decrease in the simulated peak discharge rate of 11.6% and a decrease in total runoff volume of 8.17%. A 20% decrease in saturated hydraulic conductivity, however, resulted in the simulated peak discharge rate to increase by 3.79% and total runoff volume to increase by 1.72%. The results show that saturated hydraulic conductivity was sensitive to peak discharge rate and total runoff volume. However, the degree of sensitivity of peak discharge rate and total runoff volume to an increase or decrease of saturated hydraulic conductivity are obviously different. This may be due to the interdependence among this parameter with other model parameters. The sensitivity of this parameter is illustrated in Figure 6-3.

6.1.1.3 ***The Effective Net Capillary Drive***

From Table 6-1, an increase of 20% in the effective net capillary drive resulted in a decrease in simulated peak rate of 6.84 % and a decrease in total runoff volume of 6.23%. However, decreasing effective net capillary by 20% resulted in little change on simulated total runoff volume and peak discharge rate. The results showed both peak discharge rate

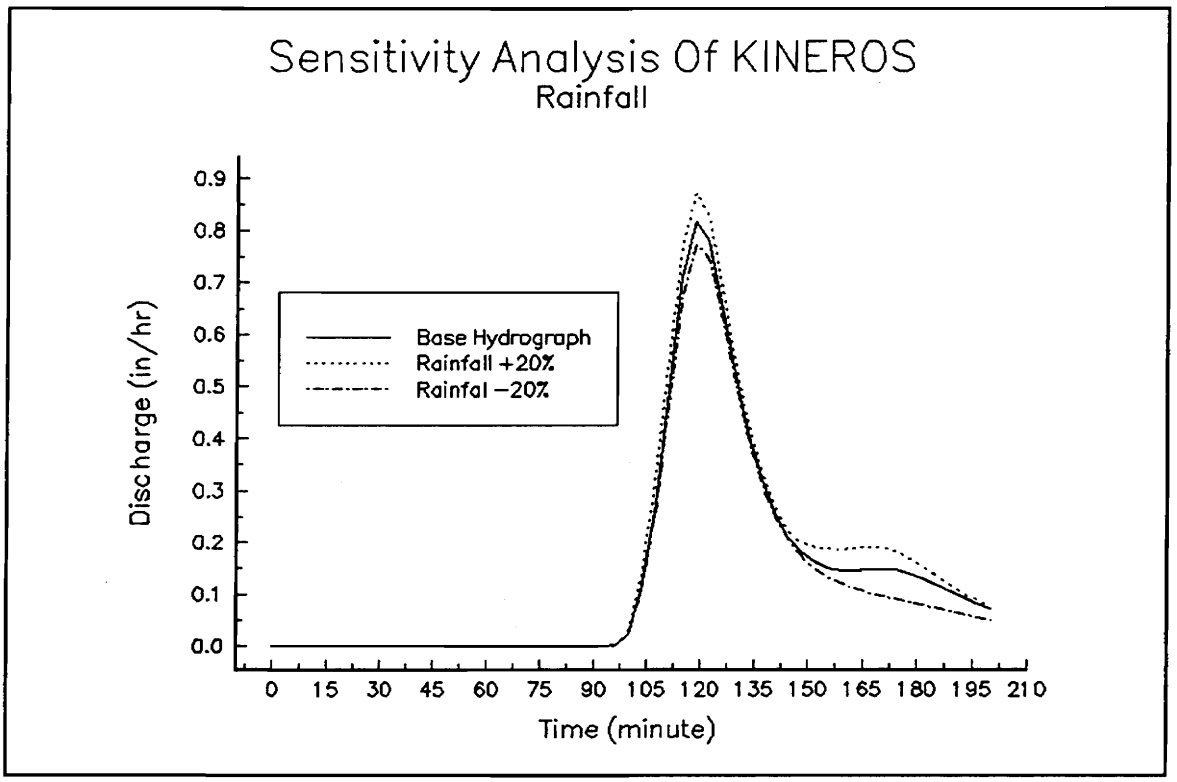

Figure 6-2 The effect of rainfall on simulated hydrographs (KINEROS)

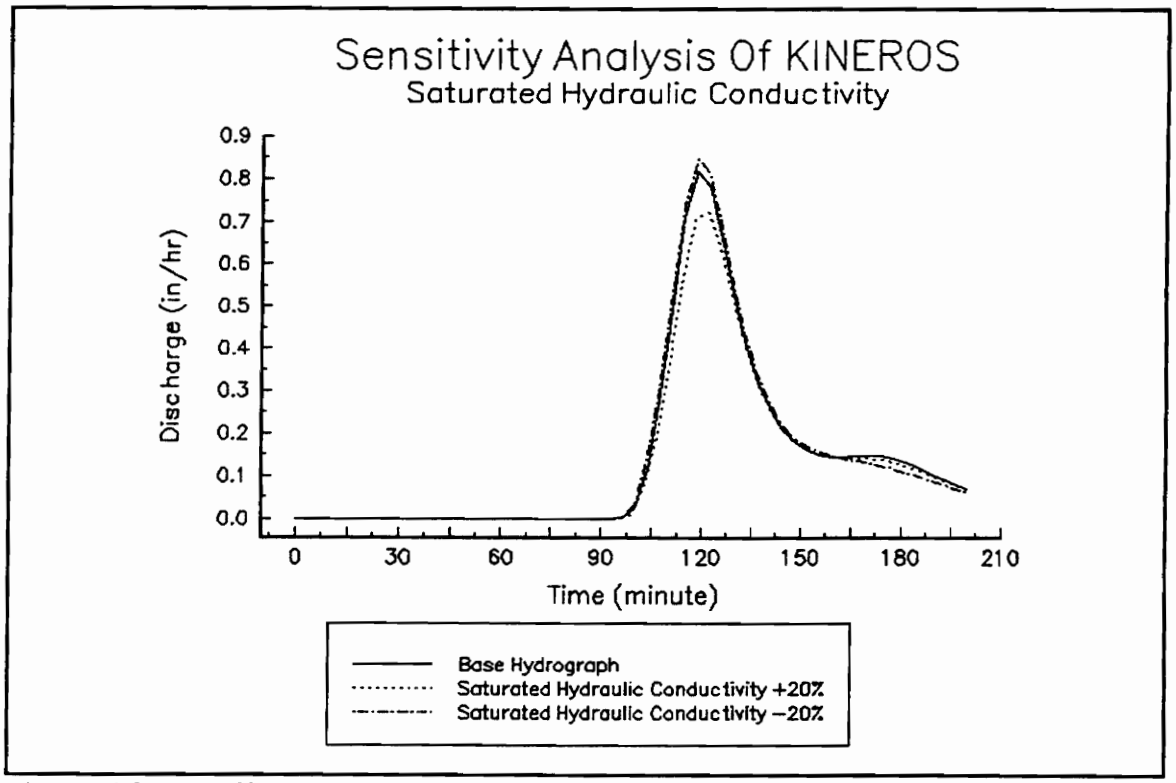

Figure 6-3 The effect of saturated hydraulic conductivity on simulated hydrographs (KINEROS)

and total runoff volume are sensitive to this parameter. Like saturated hydraulic conductivity, the increase in the effective capillary drive resulted in significant differences in the total runoff volume and peak discharge rate. This could be caused by the interactions among the parameter with other parameters. For example, equation 3-16 in Chapter 3 can be used to explain the interaction between the saturated hydraulic conductivity and the effective capillary drive. The effects of the parameter on hydrograph shapes are shown in Figure 6-4.

6.1.1.4 ***Relative Soil Saturation***

This parameter impacts the volume of water infiltrated. The higher the value, the less runoff volume and peak discharge rate produced. However, a variation of ± 20% in relative soil saturation resulted in little change on simulated runoff volume and peak discharge rate, which indicated the model was relatively insensitive to this parameter. The results also showed the parameter did not strongly affect the model outputs. The effects of the parameter on the hydrograph shapes are illustrated on Figure B-1, Appendix B.

6.1.1.5 ***Soil Porosity***

An increase of 20% in soil porosity resulted in a decrease in simulated peak discharge rate of 7.2% and a decrease in total runoff volume of 6.6.%. A decrease of 20% resulted in an increase in simulated peak discharge rate of 6.8% and an increase in total runoff volume of 7.3%. The higher value of soil porosity results in higher infiltration rate. The results shows the peak discharge rate and total runoff volume are sensitive to the parameter. The sensitivity of soil porosity is illustrated in Figure B-2, Appendix B.

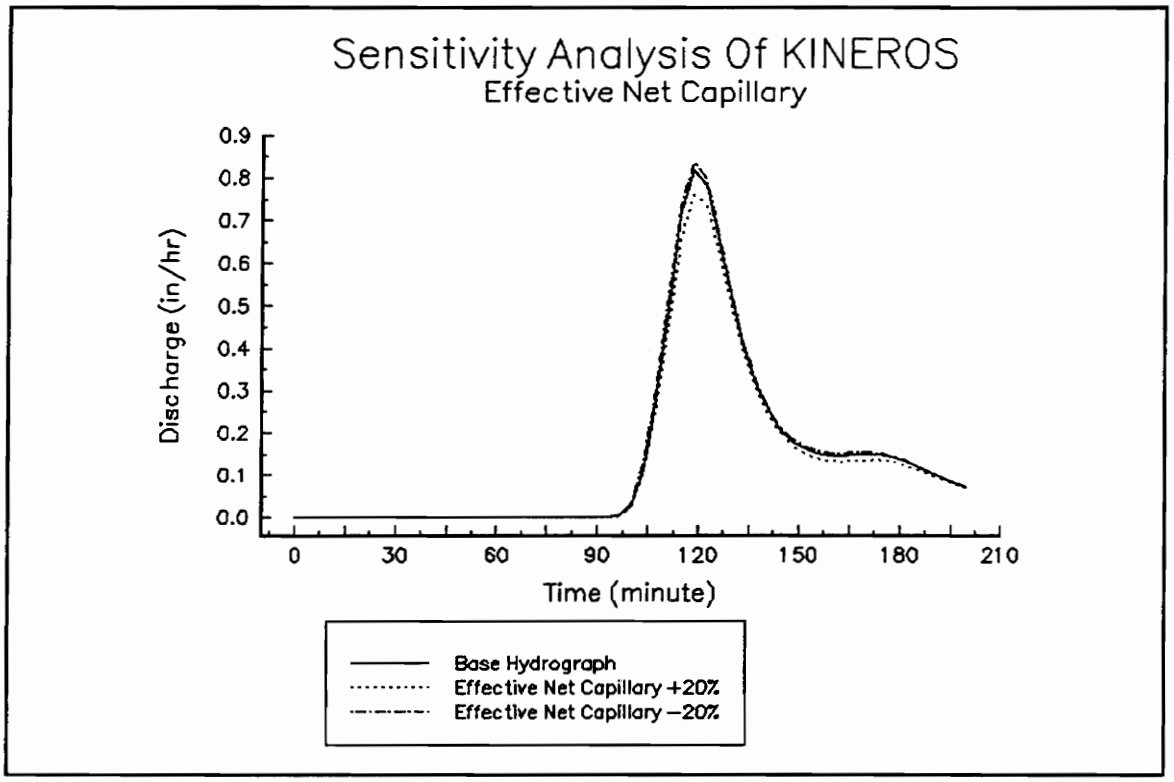

Figure 6-4 The effect of the effective net capillary driver on simulated hydrographs (KINEROS)

6.1.1.6 ***Channel Manning's N***

The peak discharge rate increased by 10% when channel manning's n was reduced 20%. The total runoff volume was reduced by 2.15%. When n was decreased 20%, the peak discharge rate and total runoff volume were increased 12% and 1.94%, respectively. This example shows the peak discharge rate is very sensitive to the variation of the channel manning's n but total runoff volume is relatively insensitive. The results can be explained by Manning's equation. The higher value of n , the lower velocity of channel flow, which results in lower peak discharge rate. A change in velocity of channel flow generally has little effect on total runoff volume. The sensitivity of this parameter is illustrated graphically in Figure B-3, Appendix B.

6.1.1.7 ***Overland Manning's N***

Increasing overland manning's n by 20% resulted in a decrease in simulated peak discharge rate of 3.9% and a decrease in total runoff volume of 1%. Decreasing overland manning's n by a similar percentage resulted in peak discharge rate of 5.5% and an increase in total runoff volume of 2.1%. This example shows both peak discharge rate and total runoff volume are relatively insensitive to changes in this parameter. The results illustrated that channel 's manning's n had much more effect on peak discharge rate than n for overland flow. The sensitivity of this parameter is illustrated graphically in Figure B-6, Appendix B.

6.1.1.8 ***Interception Depth***

The peak discharge rate increased by 6.96% when interception depth was increased by 20%. Total runoff volume was increased by 6.88%. When interception depth was reduced by 20%, peak discharge rate and the total runoff volume were decreased by 1.96% and 1.94%, respectively. The sensitivity of this parameter is graphically illustrated in Figure B-4 , Appendix B.

6.1.1.9 ***Infiltration Recession Factor***

Sensitivity analysis with the infiltration recession factor had little impact on simulated peak discharge rate and total runoff volume. The results are given in Tables 6-2 and 6-3 and illustrated graphically in Figure B-5, Appendix B.

6.1.2. ***RESULTS AND DISCUSSIONS ---- PSRM-QUAL***

Sections 6.3.2.1 through 6.3.2.9 describe the analysis of sensitivity of each input parameter to simulated results by PSRM-QUAL. The results of sensitivity analysis are summarized in Tables 6-2 and 6-3, respectively.

6.1.2.1 ***Rainfall***

From the Tables 6-2 and 6-3, a variation of +10% in the rainfall amount per time interval resulted in an increase in the simulated peak discharge rate of 21.4% and the simulated total runoff volume of 20.7%. Reducing the rainfall amount per time interval by 10% resulted in a decrease in the simulated peak discharge rate of 22.4% and a decrease in total runoff volume of 20.7%. The results show that rainfall amount are very sensitive to peak discharge rate and the total runoff volume. It illustrates the need for accurate

Table 6-2 Summary of sensitivity analysis for PSRM -QUAL 's input parameters (peak discharge rate)

Parameter	Variation	Base Peak Rate (in/hr)	Simulated (in/hr)	Change %
Rainfall	+ 10%	0.51	0.62	21.40
	-10%		0.40	-22.40
Curve Number N	+10%		0.89	73.90
	-10%		0.20	-60.70
Initial Moisture Content	+20%		0.57	10.31
	-20%		0.44	-13.62
Saturated Hydraulic Conductivity	+20%		0.50	0.14
	-20%		0.51	0.00
Overland Manning's N	+20%		0.48	-6.03
	-20%		0.55	6.42
Channel Manning's N	+20%		0.45	-13.42
	-20%		0.56	8.95
Initial Abstraction Coefficient	+20%		0.36	-29.96
	-20%		0.66	28.40
Muskingum's Weighting Facotr	+25%		0.53	3.11
	-33%		0.50	-3.21
Simuousity Factor	+1%		0.51	-0.58
	+3%		0.51	-1.36
	+10%		0.49	-4.47
	+20%		0.47	-9.14
	+40%		0.42	-17.51

Table 6-3 Summary of sensitivity analysis for PSRM-QUAL 's input parameters (total runoff volume)

Parameter	Variation	Total Runoff Volume (in)	Simulated (in)	Chang %
Rainfall	+ 10%	0.24	0.29	20.68
	-10%		0.19	-20.68
Curve Number	+10%		0.41	73.40
	-10%		0.10	-58.23
Intial Moisture Content	+20%		0.26	10.13
	-20%		0.21	-12.24
Saturate Hydraulic Conductivity	+20%		0.23	-2.53
	-20%		0.24	0.84
Overland Manning's N	+20%		0.23	-3.80
	-20%		0.25	3.80
Channel Manning's N	+20%		0.24	-0.84
	-20%		0.24	-0.42
The Muskingum 's Weighting factor	+25%		0.02	1.27
	-33%		0.02	-2.95
Initial Abstraction Coefficient	+20%		0.17	-26.70
	-20%		0.30	26.60
Simuousity Factor	+1%		0.24	-0.42
	+3%		0.24	-0.84
	+10%		0.23	-2.53
	+20%		0.23	-5.06
	+40%		0.21	-10.12

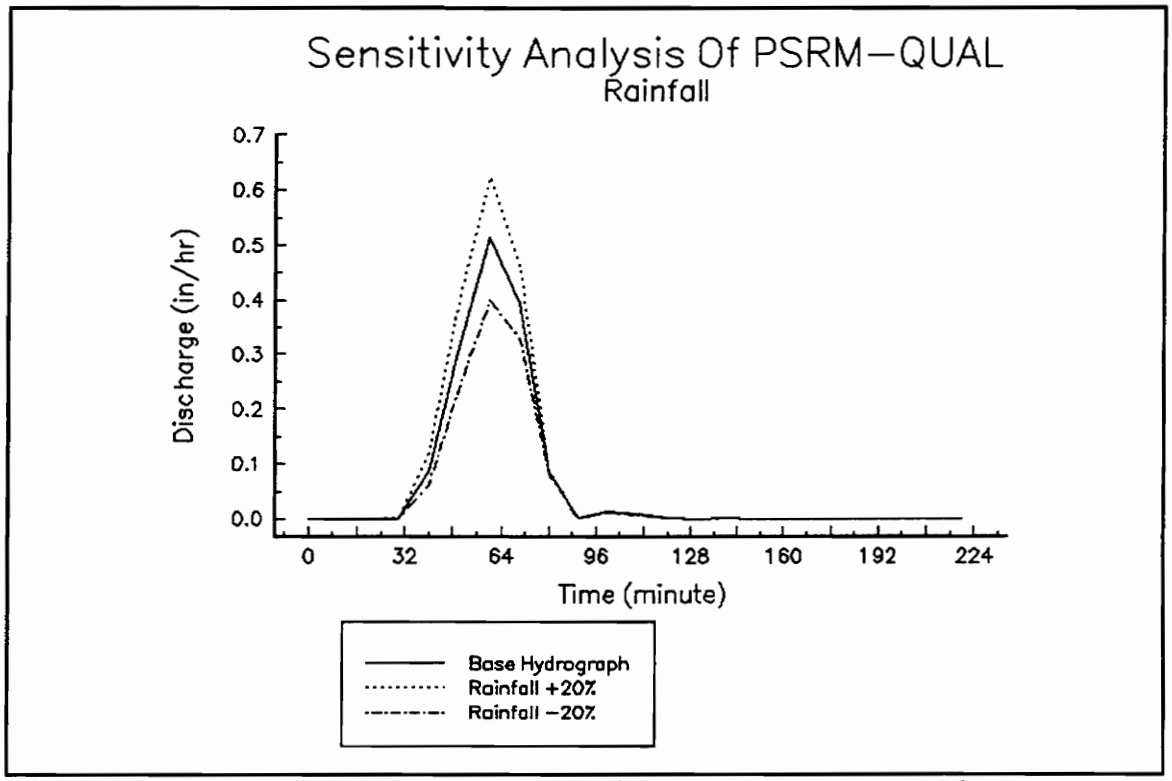

Figure 6-5 The effect of the rainfall amount on simulated hydrographs(PSRM-QUAL)

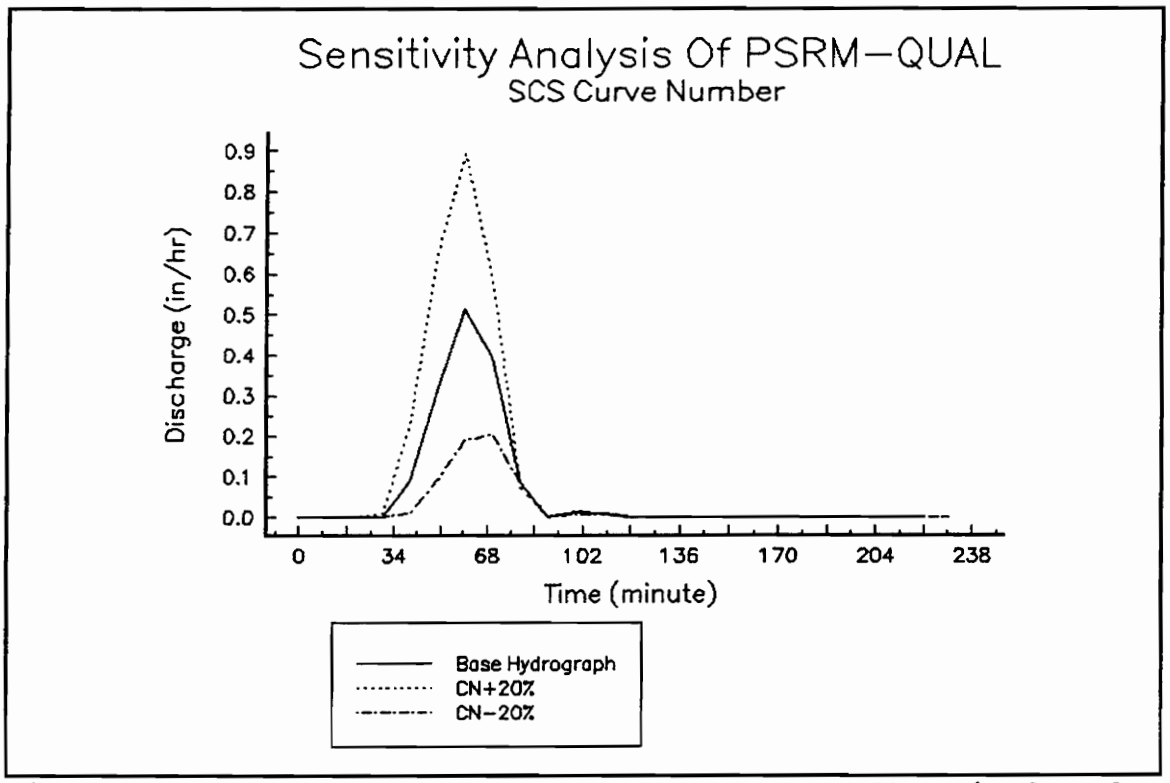

Figure 6-6 The effect of SCS curve number on the simulated hydrographs(PSRM-QUAL).

rainfall information when attempting to simulate a recorded runoff hydrograph. The sensitivity of this parameter is shown Figure 6-5.

6.1.2.2 ***SCS Curve Number***

From Table 6-2 and 6-3, an increase of 20% in the SCS CN resulted in an increase in the simulated peak discharge rate of 73.4% and an increase in total runoff volume of 58.2%. However, decreasing the CN by 10% resulted in a decrease in the simulated peak discharge rate of 60.7% and a decrease in total runoff volume of 58.2%. This example shows CN is very sensitive to peak discharge rate and total runoff volume. This illustrates it is very important to choose an accurate CN to represent the actual situation. The sensitivity of this parameter is illustrated graphically in Figure 6-6.

6.1.2.3 ***Saturated Hydraulic Conductivity***

A variation of 20% in saturated hydraulic conductivity resulted in little change on simulated total runoff volume and peak discharge rate. This example illustrates saturated hydraulic conductivity is insensitive input parameter to total runoff volume and peak discharge rate. The sensitivity of this parameter is illustrated graphically in Figure B-7 , Appendix B.

6.1.2.4 ***Initial Moisture Content***

This parameter impacts the volume of water infiltrated. From Tables 6-2 and 6-3, a variation of +20% in initial moisture content resulted in an increase in simulated peak discharge rate of 10.3% and an increase in total runoff volume increment of 10.1%. Reducing the initial moisture content by 20% resulted in a decrease in simulated peak

discharge rate of 13.6% and a decrease in the simulated total runoff volume of 12.2%. The sensitivity of this parameter is illustrated graphically in Figure B-8, Appendix B.

6.1.2.5 ***The Overland Manning's N***

Increasing overland manning's n± by 20% resulted in a decrease in the simulated peak discharge rate of 6.03% and a decrease in the simulated total runoff volume of 3.8%. Reducing overland manning's n by 20% resulted in an increase in the simulated peak discharge rate of 6.42% and an increase in the simulated total runoff volume of 3.8%. The sensitivity of this parameter is illustrated graphically in Figure B-9, Appendix B.

6.1.2.6 ***The Channel Manning's N***

The peak discharge rate decreased by 13.42% when manning's n of channel was increased 20%. The total runoff volume was decreased by 0.84%. When the manning's n of channel was decreased 20%, the simulated peak discharge rate was increased by 8.95%. Total runoff volume was decreased by 0.42%. This example shows the peak discharge rate is very sensitive to the channel manning's n. However, the total runoff volume is relative insensitive to the parameter. The sensitivity of this parameter is illustrated graphically in Figure B-10, Appendix B.

6.1.2.7 ***Initial Abstraction Coefficient***

From Table 6-2 and 6-3, a variation of +20% in initial abstraction coefficient resulted in a decrease in simulated peak discharge rate of 29.96% and a decrease in total runoff volume of 26.7%. Reducing the initial abstraction coefficient by 20% resulted in an increase in simulated peak discharge rate of 28.4%. Total runoff volume was increased by

26.6%. This example shows both peak discharge rate and total runoff volume are sensitive to initial abstraction coefficient. The sensitivity of this parameter was illustrated graphically in Figure 6-7.

6.1.2.8 ***Sinuousity Factor***

From Table 6-2 and 6-3, increasing the sinuousity factor from 1% to 10% resulted in slight decreases in simulated peak discharge rate and total runoff volume. An increase of sinuousity factor by 20% and 40% resulted in a decrease in the simulated peak discharge rate of 5.05% and 10.12%, respectively. The total runoff volume were reduced 9.14% and 17.51% respectively. These results suggest that this parameter can significant attenuate model results. The sensitivity of the parameter is illustrated graphically in Figure B-11, Appendix B.

6.1.2.9 ***Muskingum's Weighting Factor***

The results from Table 6-2 and 6-3 show both peak discharge rata and total runoff volume are not sensitive to changes in this parameter. The sensitivity of the parameter is illustrated graphically in Figure B-12, Appendix B.

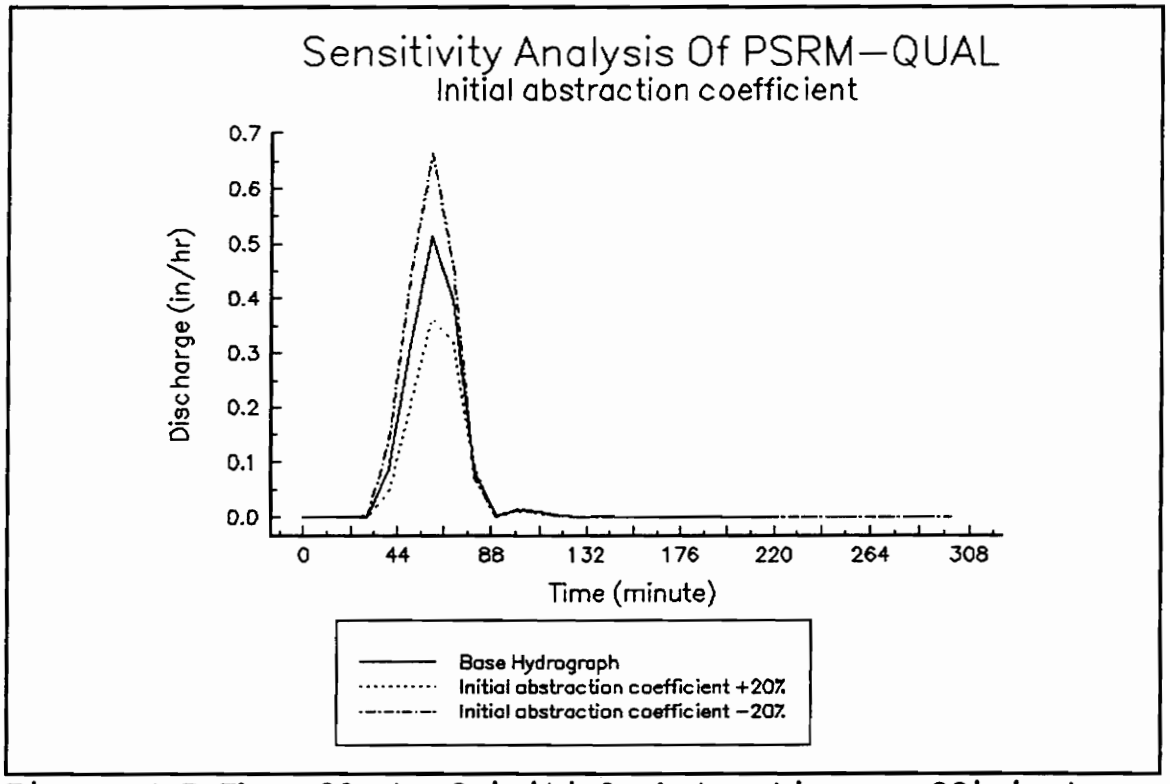

Figure 6-7 The effect of initial abstraction coefficient on simulated hydrographs(PSRM-QUAL)

6.1.3 *Summary of Sensitivity Analysis For KINEROS and PSRM-QUAL*

For KINEROS , both peak rate and runoff volume were found to be most sensitive to the rainfall amount, saturated hydraulic conductivity and effective net capillary drive. Changes in channel manning's n can greatly influence peak discharge rate but have little effect on total runoff volume.

For PSRM-QUAL , the rainfall amount, CN and initial abstraction coefficient were found to be most sensitive to both total runoff volume and peak discharge rate. The channel manning's n had significant influence on peak rate but little effect on total runoff volume. Unlike the KINEROS model, total runoff volume and peak discharge rate were not sensitive to changes in the saturated hydraulic conductivity. The rank of relative sensitivity of parameters to peak discharge rate and total runoff volume are listed in Tables 6-4 and 6-5, respectively.

6.1.4 *Investigation of Sensitivity of The Most Sensitive Parameters*

For KINEROS, the saturated hydraulic conductivity, the effective capillary drive and the channel manning's n were further tested as to whether or not changes resulted in a non-linear response in total runoff volume and peak discharge rate. Although soil porosity is very sensitive parameter to the total runoff volume and peak discharge rate, it was not selected for this phase of the analysis. The purpose of further investigation of the most sensitive parameters was to provide additional indications on how the response varied in order to hopefully expedite calibration. The data soil porosity used in this study was from a field survey. Therefore, it was considered inappropriate to calibrate this parameter. For

Table 6-4 The rank of sensitivity analysis of model parameters to peak discharge rate

	KINEROS	PSRM-QUAL
The sensitive parameters to peak discharge rate [1]	*Rainfall Amount, Saturatued Hydraulic Conductivity, Channel's Manning 's N, Soil Porosity, Effective Net Capillary Drive, Interception Depth, Relative Soil Saturation, Infiltration Recession Factor*	*Rainfall Amount, CurveNumber, Initial Abstraction Coefficient, Channel's Manning's N Initial Moisture Content, Overland's Manning's N, Muskingum's Weighting Factor, Sinuousity Factor, Saturated Hydraulic Conductivity*

[1] from most to least sensitive

Table 6-5 The rank of sensitivity analysis of model parameters to total runoff volume

	KINEROS	PSRM-QUAL
The sensitive parameters to total runoff volume [1]	*Rainfall Amount,* *Saturatued Hydraulic Conductivity,* *Soil Porosity,* *Effective Net Capillary Drive,* *Interception Depth,* *Relative Soil Saturation,* Cha*annel'sManning's N*, *Overland's Manning's N,* *Infiltration Recession Factor*	*CurveNumber,* *Initial Abstraction Coefficient,* *Rainfall Amount,* *Initial Moisture Content,* *Overland's Manning's N,* *Sinuousity Factor,* *Muskingum's Weighting Factor,* *Saturated Hydraulic Conductivity* *Channel's Manning's N*

[1] from most to least sensitive

PSRM-QUAL, the tests were done on SCS curve number, the initial abstraction coefficient and the channel manning's n. For the same reason, the soil porosity was not included in this phase of this study. The peak discharge rate and the total runoff volume were determined by setting each parameter (e.g., the effective capillary drive, G) to a series of values equal to G_{base} /1.15, 1.10, 1.05 and holding all remaining values constant. The procedures was repeated by setting the parameter to G_{base} x 1.15, 1.10, 1.05. This procedure was followed for all parameters. The results are discussed in the following sections.

6.1.4.1 ***The Saturated Hydraulic Conductivity***

The relative errors of all the tests for saturated hydraulic conductivity is illustrated in Figure 6-8. From Figure 6-8, the series of increases in the saturated hydraulic conductivity result in obvious changes of total runoff volume and peak discharge rate. The higher increase in the parameter results in larger changes of outputs. The relationships between the model outputs and increases in saturated hydraulic conductivity were found to be generally linear (Figure 6-8). However, the total runoff volume showed little change for decrease of -5% to 20% from the mean value. The decreases in the saturated hydraulic conductivity however, were found to change non linearly as the magnitude of change. The changes in total runoff volume show an irregular responses to a decrease in saturated hydraulic conductivity. As illustrated previously, these changes could be caused by unknown interactions between the saturated hydraulic conductivity and other model parameters. The interactions could cause difficulty in calibrating this parameter. This

example also demonstrates that the procedure used for the sensitivity analysis can not always provide adequate insights on the relationships between model parameters and outputs.

6.1.4.2 ***The Effective Capillary Drive***

From Figure 6-9, the changes±of 5%,10% and 15% in the effective capillary drive resulted in similar changes of total runoff volume and peak discharge rate. Within the ranges of -15% to 15% changes, the larger changes in the parameter resulted in greater differences in the model outputs. The relationships between the parameter with total runoff volume and peak discharge rate is generally linear. However, in contrast as shown in Figure 6-9, the trend in responses for total runoff volume and peak discharge rate resulted from the changes are more clearly defined. This implies that the calibration of this parameter could be more straight forward than that of saturated hydraulic conductivity. However, the relationship dramatically changed with a decrease of 20%. However, reason for the abrupt changes in unknown, but is most likely related to interaction between other parameters. The uncertainty of the parameter again could result in difficulty for its calibration.

6.1.4.3 ***The Channel Manning's N***

The relationships between changes in the channel manning's n with peak discharge rate is shown in Figure 6-10. The relationship is generally linear. The changes in this parameter resulted in large differences in the peak discharge rate. The total runoff volume, however, only changed slightly which was inticipated. The results generally

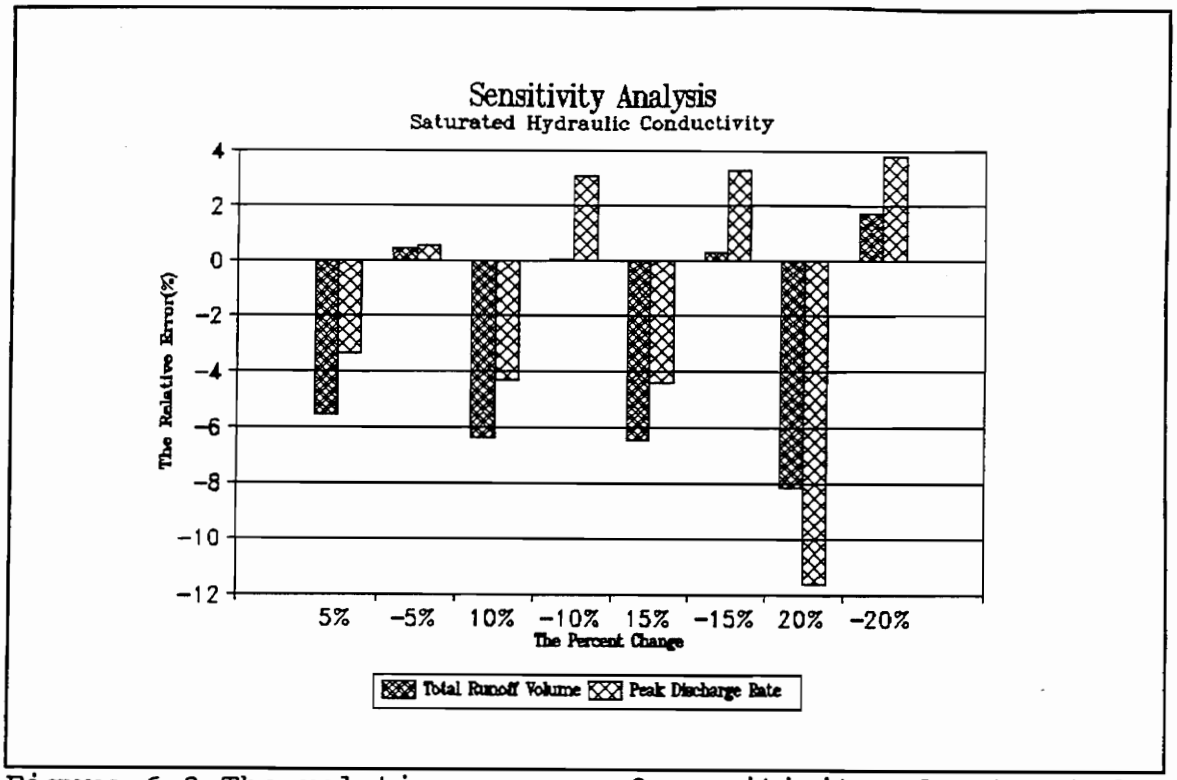

Figure 6-8 The relative errors of sensitivity of saturated hydraulic conductivity

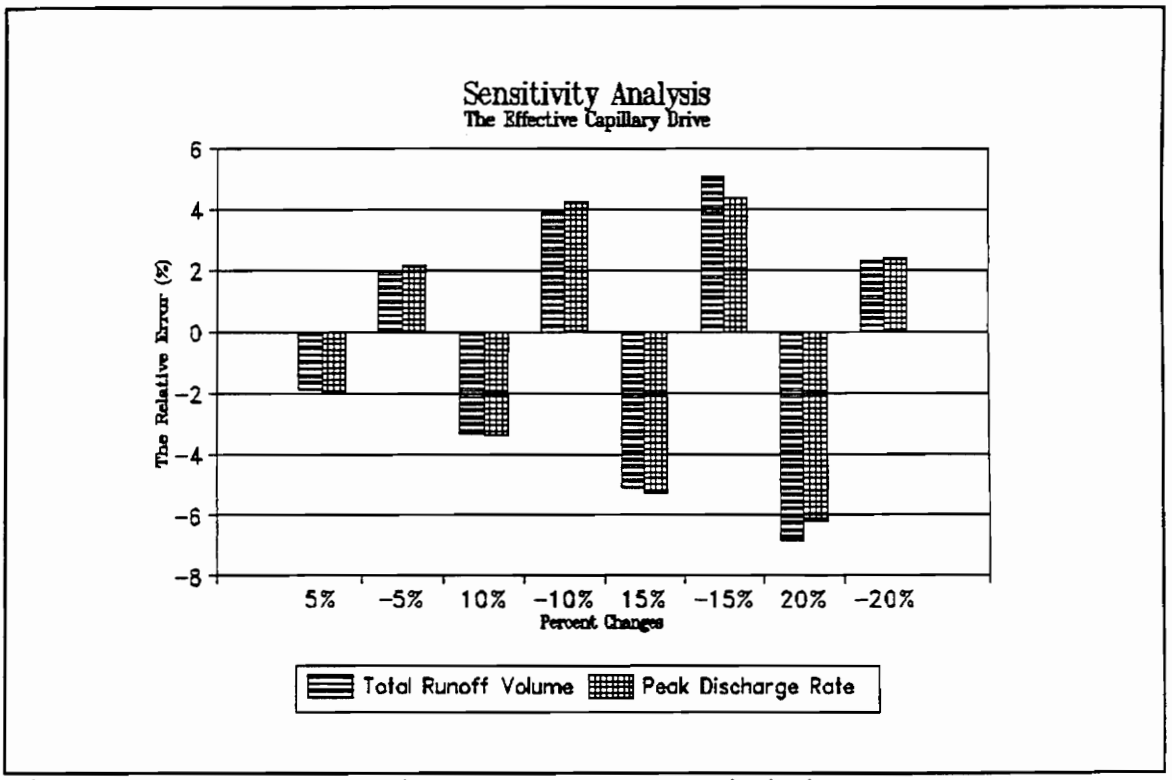

Figure 6-9 The relative error of sensitivity of the effective capillary drive

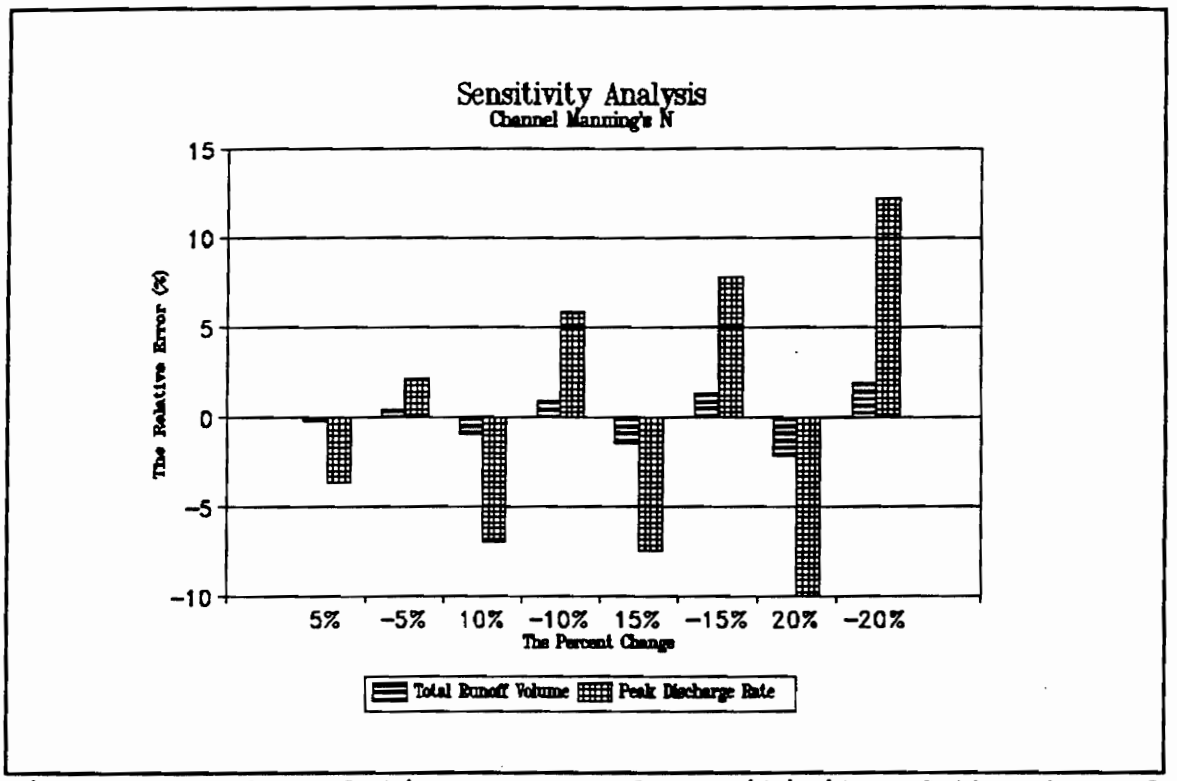

Figure 6-10 The relative errors of sensitivity of the channel manning's n (KINEROS)

suggest higher channel manning's n will result in lower flow velocities and longer travel time resulting in attenuation of peak. The results shown on Figure 6-10 indicate that the parameter can be used effectively to calibrate peak flow estimates.

6.1.4.4 ***The SCS Curve Number***

Several conclusions can be drawn from the Figure 6-11. One is that a slight variation in the SCS curve number results in large changes in total runoff volume and peak discharge rate. The other is that variations of the total runoff volume resulted from the changes are larger than those of peak discharge rate. The variations become larger with an increase in the magnitude of the parameter change. The results show that the SCS curve number is the dominate parameter which has great impacts on model outputs in the PRSM-QUAL model. Therefore, it is very important to select accurate values of the parameter and to have good samples to calibrate the parameter. The samples should be fairly distributed so that the results from calibration could be applied on verification events with much more confidence.

6.1.4.5 ***The Initial Abstraction Coefficient***

From Figure 6-12, increases in the initial abstraction coefficient resulted in corresponding decreases in total runoff volume and peak discharge rate. The increase in total runoff volume and peak discharge rate resulted from decreases in the parameter. The results shown in the Figure 6-12 indicate linear relations between the changes in the parameter with total runoff volume and peak discharge rate. The variations of peak discharge rate to changes in the parameter are slightly larger than those of total runoff

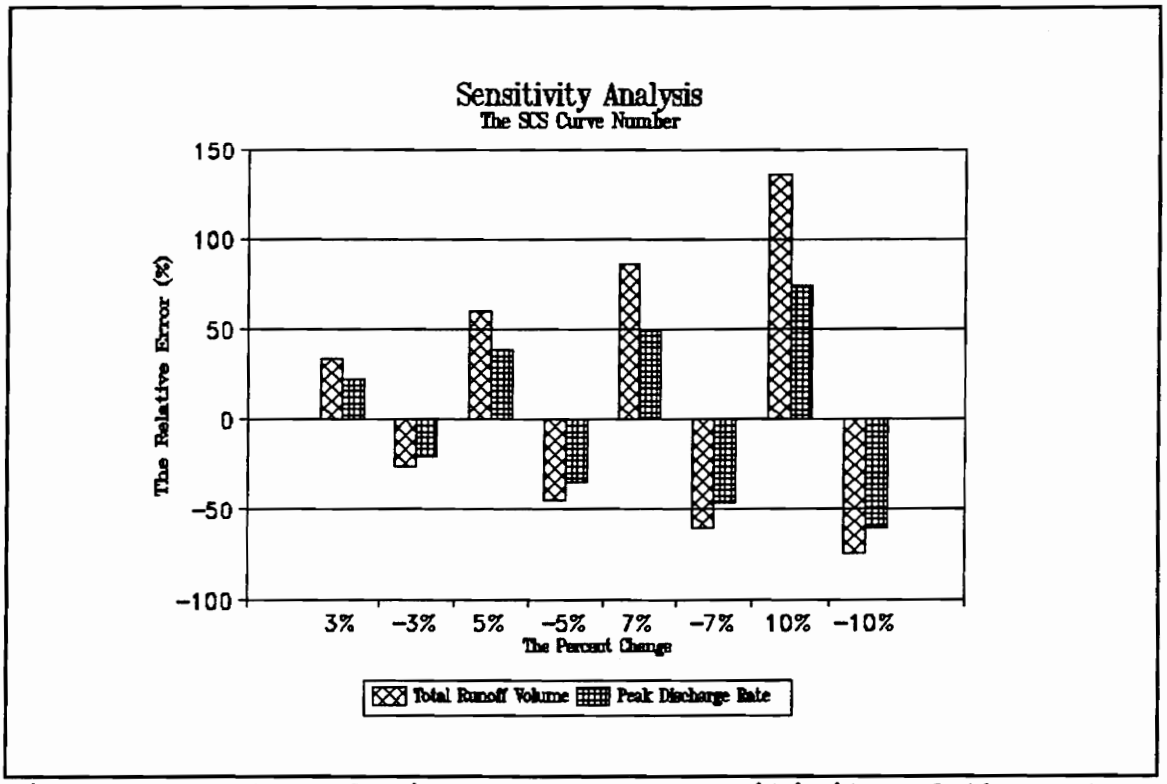

Figure 6-11 The relative errors of sensitivity of the SCS curve number

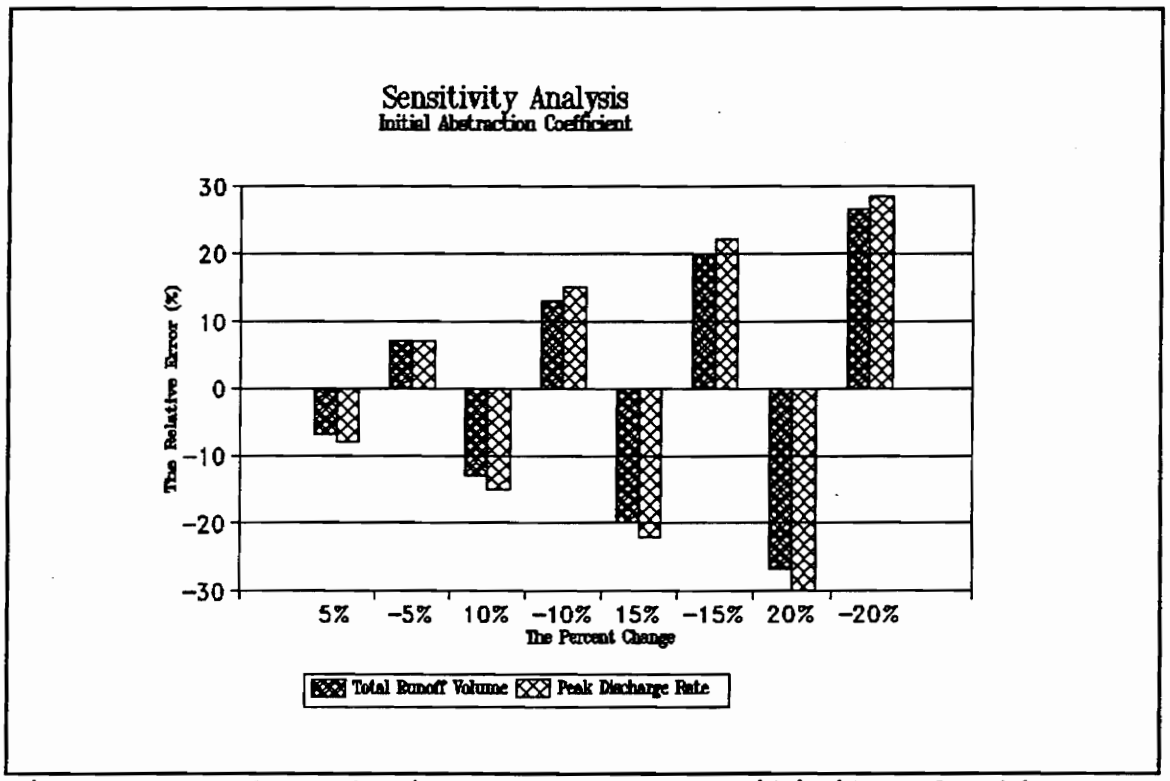

Figure 6-12 The relative errors of sensitivity of initial abstraction coefficient

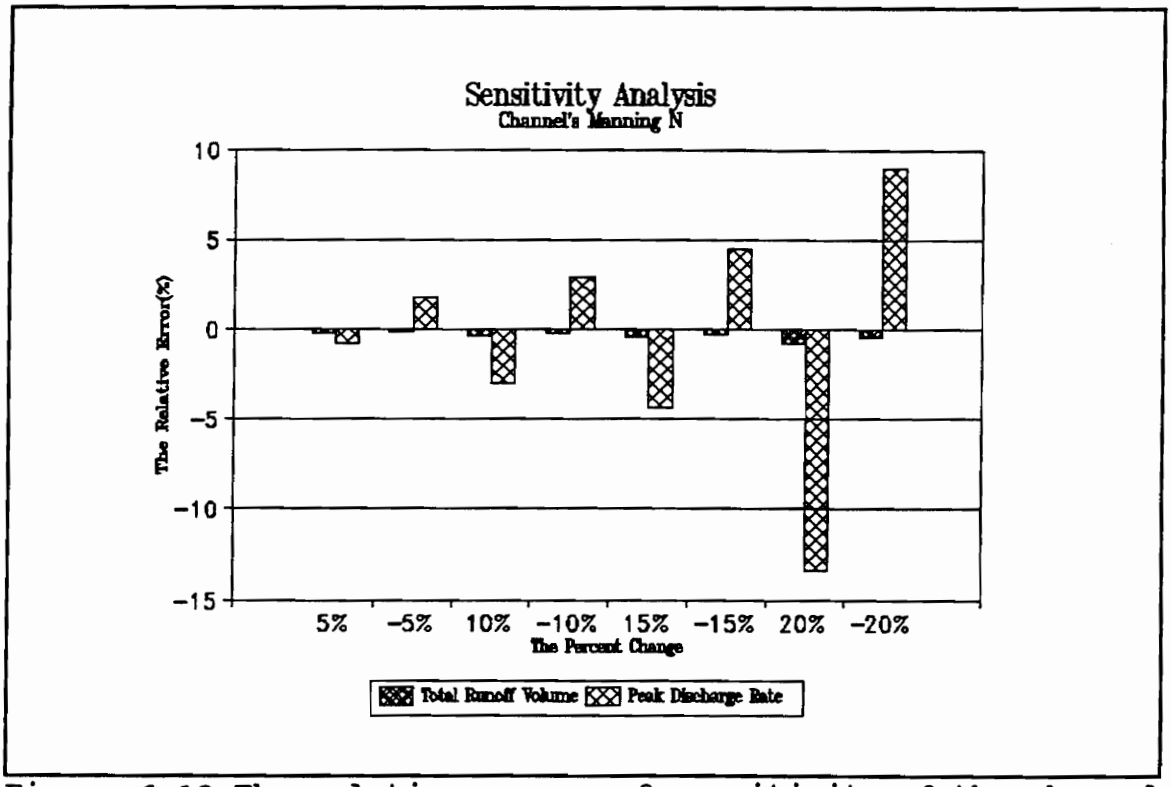

Figure 6-13 The relative errors of sensitivity of the channel manning's n (PSRM-QUAL)

volume. However, the impacts of the parameter on model outputs is much less than changes in the SCS curve number. The results show that the parameter could be used a minor parameter for model calibration.

6.1.4.6. ***The Channel Manning's N***

From the Figure 6-13, the increases in channel manning's n resulted in increases in the peak discharge rate. The relationship between them is generally a linear as shown in Figure 6-13. As expected, the total runoff volume is not affected by variations in this parameter.

In summary, the most sensitive parameters of the two models was evaluated. The interactions among the saturated hydraulic conductivity, the effective capillary drive and other model parameters resulted in variable impacts on model outputs. The impacts of the channel manning' s n on the total runoff volume and peak discharge rate for both models were consistent over the range of manning's n evaluated.

The dominant role of the SCS curve number in PSRM-QUAL model underlies the extremely importance of parameter selection for model calibration. This also illustrates that it is relatively easier to calibrate PSRM-QUAL than KINEROS model, although its performance for individual storms may be inconsistent.

6.2 *CALIBRATION ANALYSIS*

Seven rainfall events were selected from the rainfall sample following procedures outlined in Section 5.1.2 and used to conduct to calibrate. The rainfall events with resulting runoff hydrograph characteristics are given in Tables 6-6 though 6-11, Figure 6-14 and Appendix C. These events were used to calibrate parameters for both the KINEROS and PSRM-QUAL models.

A review of storm event sample available for analysis shows that two of the seven events had peak discharge rates less than 0.03 in/hr, three events had peak discharge rates between 0.04 to 0.06 in/hr. For the remaining, peak discharge rate averaged approximately 0.19 in/hr. The maximum peak discharge rate was 0.53 in/hr. For the remaining, the observed total runoff volume ranged between 0.1 and 0.2 inches. The analysis of the samples for time to peak showed two events with a time to peak less than 100 minutes. For the remaining events, the time to peak ranged between 200 and 700 minutes. Each of the rest five events had the time to peak with the range of 200 to 700 minutes. The average peak discharge rate for the seven calibration events was 0.087 in/hr, while the average peak discharge rate for the verification events was 0.078 in/hr. The average total runoff volume for the calibration samples was 0.16 in. For the verification samples, the average value of the total runoff volume was 0.26 in. For the seven calibration events, the average time to peak was 262 minutes. The average time to peak for verification events was 260 minutes.

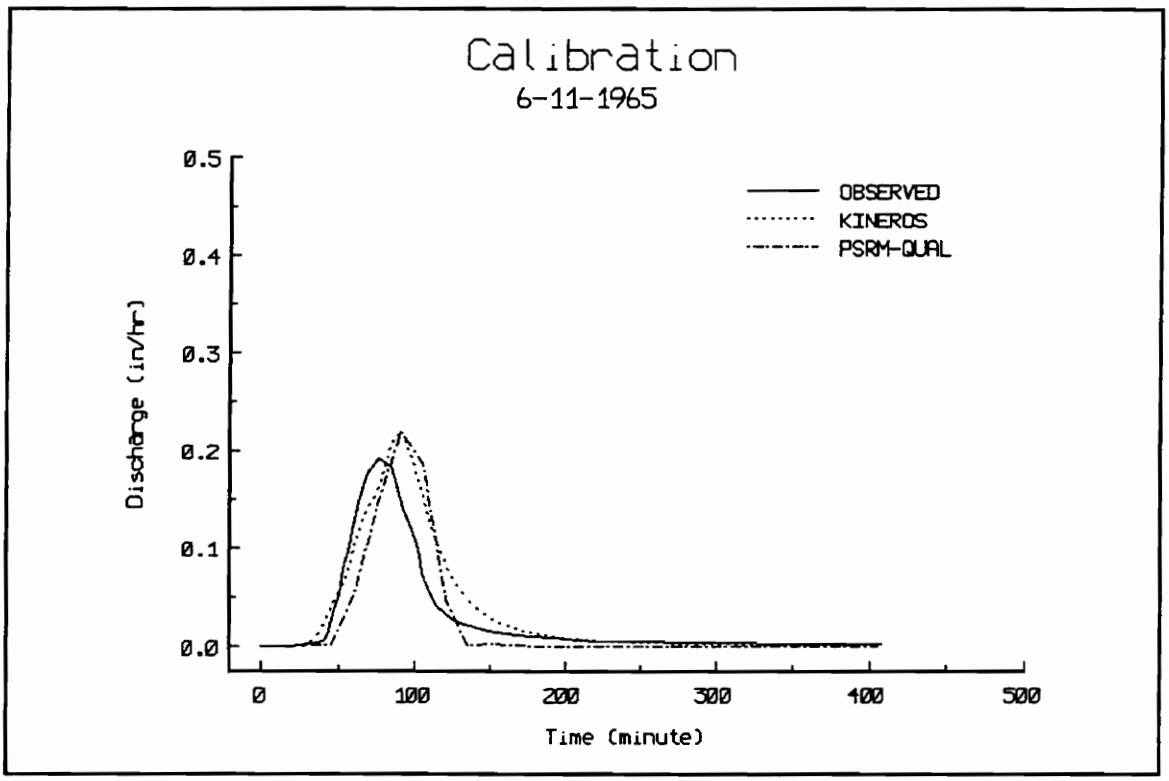

Figure 6-14 A sample calibration run (Event 6/11/1965)

Figure 6-15 describes the distribution of peak discharge rate for calibration and verification storm samples. The characteristics of the calibration sample appear to be representative of the verification samples. Additionally, similar characteristics of total runoff volume and time to peak are shown in Figures 6-16 and 6-17. As illustrated in Section 6.3.4, it is very important that the sample for calibration reflect the general characteristics of verification sample or storm events and conditions for which the model is to be used. Since the randomly selected storm sample appears to represent the major characteristics of the verification sample, the calibration should provide acceptable results when applied to the storms in the verification analysis.

The objective during calibration was to determine parameter values for each storm event that minimized the differences between simulated and recorded storm peak discharge rate, total runoff volume and time to peak.

Parameters identified during sensitivity analysis formed the basis for calibration. These included the saturated hydraulic conductivity, effective capillary drive and manning's n of channel for KINEROS and the SCS curve number, initial abstraction coefficient and the channel manning's n for PSRM-QUAL.

The steps followed were:

The Manning's n for all the channels were set up using the value described in Figure 4-6 for the calibration of the both models. The mean values illustrated in Table 4-3 for the saturated hydraulic conductivity and the effective capillary drive were employed using the procedures outlined in Sections 4.5.2 and 4.5.3 as the initial values for the

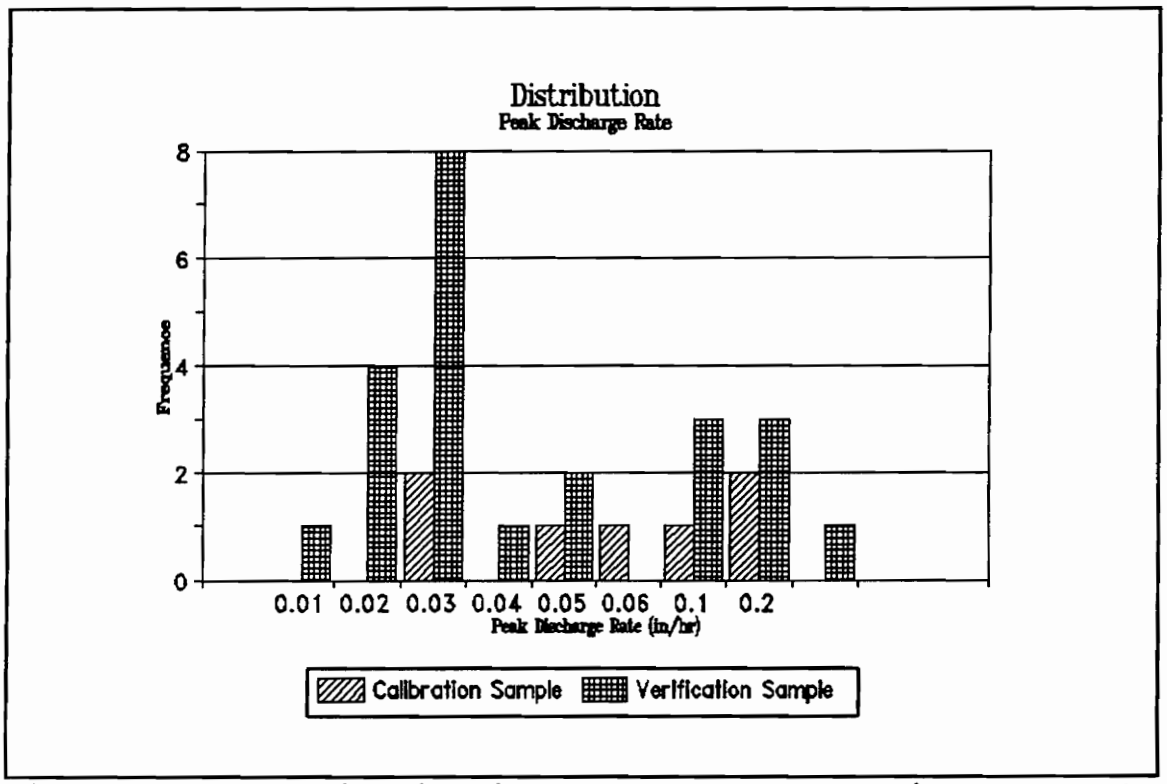

Figure 6-15 The distribution of observed peak discharge rate for calibration and verification samples

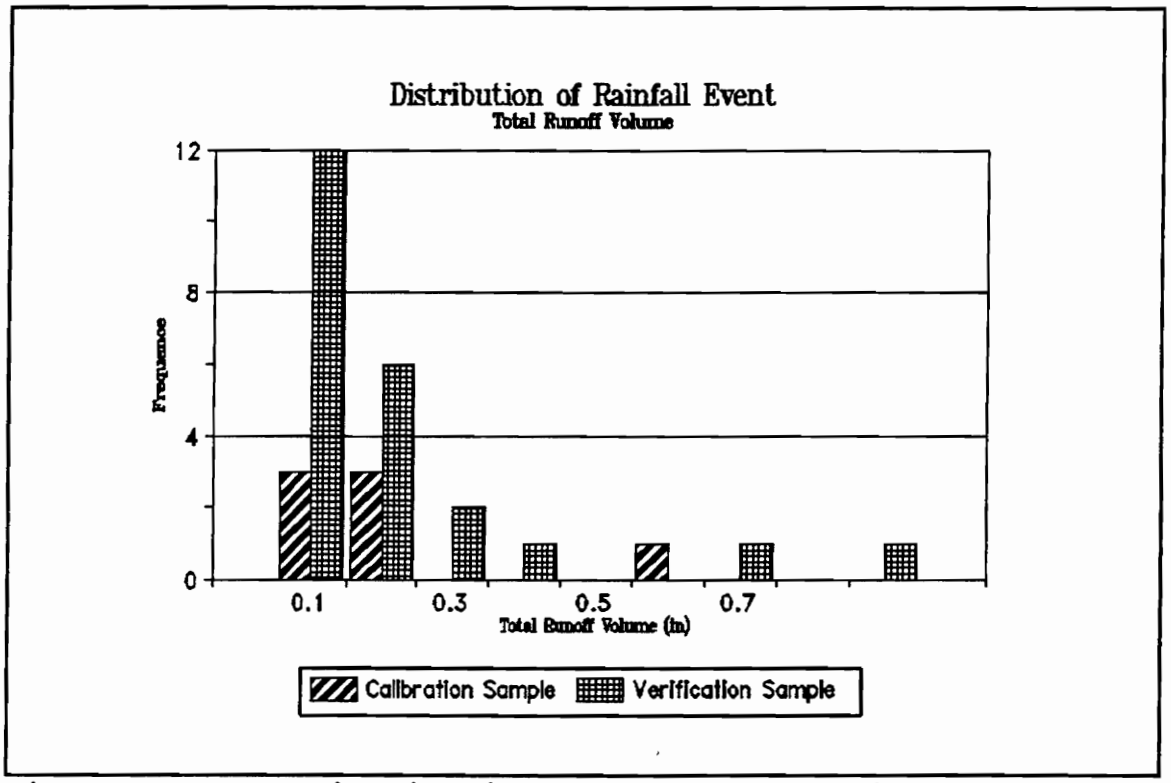

Figure 6-16 The distribution of observed total runoff volume of calibration and verification samples

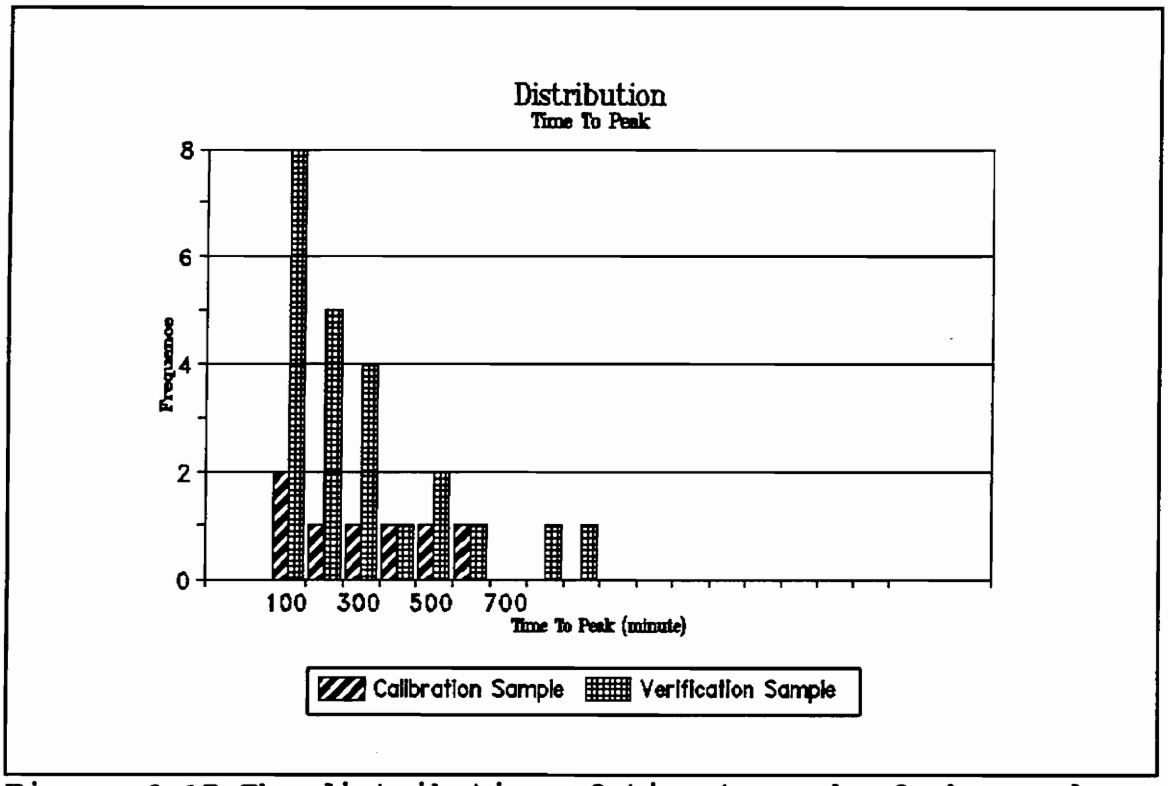

Figure 6-17 The distribution of time to peak of observed calibration and verification samples

calibration of KINEROS. Similarly, the initial values of the SCS curve number and the initial abstraction coefficient were determined for the calibration of PSRM-QUAL.

For subsequent simulation, parameters, such as the saturated hydraulic conductivity, the effective capillary drive, the channel manning's n, the SCS curve number, the initial abstraction coefficient, were adjusted until an acceptable response was achieved or no improvement could be obtained within the allowed ranges set for each parameter. The ranges set for the parameters were given in Section 5.1.2. The criteria for each objective were also described in Section 5.1.2.

The following scheme was used to adjust each parameter. After the initial calibration run for each sample, the simulated results were compared with the corresponding observed data. The comparison was judged based on the criteria established in Section 5.1.2. If one or more of the criteria were not acceptable, the following adjustments in the parameters were made. The results of sensitivity illustrated in Figures from 6-8 through 6-13 were used as the references to adjust the parameters. For example, if both the simulated time to peak and peak discharge rate did not meet the criteria , the channel manning's n was the first parameter to be adjusted, since the literature review in pervious chapters shows that the channel manning's n has direct impact on peak discharge rate and time to peak. For KINEROS, both saturated hydraulic conductivity and the effective capillary drive are very sensitive to the total runoff volume and peak discharge rate. An increases or decreases in the effective capillary drive had similar impacts on total runoff volume and peak discharge rate. However, the total runoff volume and peak

and peak discharge rate were very sensitive to a decrease in saturated hydraulic conductivity. The different impacts of the two parameters on total runoff volume and peak discharge rate were used to adjust the two parameters for the next calibration run based on the results from the pervious calibration run. For PSRM-QUAL, the SCS curve number is the dominate parameter on total runoff volume and peak discharge rate. The impacts of the parameter on the total runoff volume and peak discharge rate were used to adjust the parameter for each calibration. Initial abstraction coefficient also has strong impact on peak discharge rate and the total runoff volume. The parameter was used in PSRM-QUAL to be adjusted when simulated results did not meet the criteria but the differences were close.

A hydrograph resulting from calibration is compared with a recorded hydrograph in Figure 6-14. The results for the remaining six events are given in Appendix C. Based on visual comparison, simulated and observed hydrographs matched well. However, the graphical comparison can not provide quantitative results.

From Table 6-6, the differences between calibrated peak discharge rates of KINEROS and observed for the seven events were within 15%. As shown in Table 6-8, only 1 event of which calibrated discharge rate of PSRM-QUAL exceeded 15%. The remaining events met the established criteria. In general, the peak discharge rates of KINEROS and PSMR-QUAL were considered acceptable based on the criteria established for calibration analysis.

From Tables 6-7 and 6-10, total runoff volume established by KINEROS met the criteria for four events, which three event did not meet. Total runoff volumes for the three events were larger than corresponding observed total runoff volumes. These may be due to the errors of calculation of soil moisture content for the events or the uncertainty of model parameters. All the calibrated total runoff volumes of PSRM-QUAL were acceptable.

Tables 6-8 and 6-11 show that six of seven events where the calibrated time to peak for both models were within 15 minutes. Only one event did not meet the criteria. The results showed the calibrated time to peak of KINEROS and PSRM-QUAL are basically acceptable.

The arithmetic mean relative errors and the logarithmic mean absolute relative errors are also given in Tables 6-6 through 6-11. Tables 6-12 and 6-13 summarize the optimization range for the parameters calibrated for the two models, which was used for verification analysis in a later section.

The calibration results for PRSM-QUAL were slightly better than KINEROS. This could be attributed to the interaction between the saturated hydraulic conductivity and the effective capillary drive, which was illustrated in Section 6.3.4. The interaction of the parameters led to difficulty in calibrating the saturated hydraulic conductivity and took a longer time for some calibration events.

In summary, the manual calibration was time consuming. The sensitivity analysis provided information useful in calibration. The experiences were obtained and

accumulated from pervious calibration run. The manual calibration can provide the opportunity to understand the impacts of gradual changes of the model parameters on simulated results.

6.3 *RESULTS AND DISCUSSION OF VERIFICATION ANALYSIS*

The procedures and methods illustrated in Section 5.1.3, Chapter 5 were used to verify the remaining events. The mean values of calibrated parameter results, which are shown in Tables 6-12 and 6-13, with the other parameters determined in Chapter 4 were used for the verification.

Event-based models are generally designed to predict flood flows or events producing significant runoffs. KINEROS and PSRM-QUAL, however, have components to simulate pollutant transport. Because low flows events often contribute more pollutants than several large storms in a year in less or urban areas (Pitt, 1989), the event of May 17, 1964 with a peak discharge rate 0.96 cfs was randomly chosen and used to illustrate the performances of the two models with low runoff producing events. Therefore 23 events were used for verification. The results are summarized and discussed in Sections 6.3.1 through 6.3.6.

6.3.1 *Graphical Comparison*

Graphical comparison is used to judge the differences between simulated and observed peak discharge rate, time to peak and hydrograph shapes. If time bases for simulated and observed hydrographs are known, the difference between simulated and observed total runoff volume also can be compared by this method.

Table 6-6 Summary of calibration of peak discharge rate for KINEROS

Event	Peak Rate (in/hr)		
Date	**Observed**	**Simulated**	**Relative Error (%)**
June 26, 1968	0.02	0.023	15.00
July 3, 1962	0.024	0.024	0.00
Aug. 23, 1967	0.059	0.061	3.39
Sept. 14, 1966	0.073	0.072	-1.37
Oct. 21, 1961	0.192	0.195	1.56
Sept. 10, 1960	0.049	0.047	-4.08
June 11, 1965	0.192	0.216	12.50
MARE			5.41
LMARE			0.53

Table 6-7 Summary of calibration of total runoff volume for KINEROS

Event	**Total Runoff Volume (in)**		
Date	**Observed**	**Simulated**	**Relative Error (%)**
June 26, 1968	0.034	0.055	61.76
July 3, 1962	0.066	0.065	-1.52
Aug. 23, 1967	0.110	0.100	-9.09
Sept.14, 1966	0.134	0.12 0	-10.45
Oct. 21, 1961	0.53	0.46 0	-13.21
Sept. 10, 1960	0.055	0.070	27.27
June 11, 1965	0.175	0.22	25.71
MARE			21.2
LMARE			1.13

Table 6-8 Summary of calibration of time to peak for KINEROS

Event	**Time To Peak (minute)**		
Date	**Observed**	**Simulated**	**Relative Error (min)**
June 26, 1968	110	105	5
July 3, 1962	331	351	20
Aug. 23, 1967	278	280	2
Sept. 14, 1966	546	542	4.00
Oct. 21, 1961	486	490	4
Sept. 10, 1960	86	90	4
June 11, 1965	76	89	13.00
MARE			7.42
LMARE			0.74

Table 6-9 Summary of calibration of peak discharge rate for PSRM-QUAL

Event	Peak Rate (in/hr)		
Date	**Observed**	**Simulated**	**Relative Error (%)**
June 26, 1968	0.02	0.029	45.00
July 3, 1962	0.024	0.24	0.00
Aug. 23, 1967	0.059	0.051	-13.56
Sept. 14, 1966	0.073	0.081	10.96
Oct. 21, 1961	0.192	0.177	-7.81
Sept. 10, 1960	0.049	0.053	8.16
June 11, 1965	0.192	0.165	-14.06
MARE			14.22
LMARE			0.97

Table 6-10 Summary of calibration of total runoff volume for PSRM-QUAL

Event	**Total Runoff Volume (in)**		
Date	**Observed**	**Simulated**	**Relative Error (%)**
June 26, 1968	0.034	0.029	-14.71
July 3, 1962	0.066	0.073	10.61
Aug. 23, 1967	0.11	0.129	17.27
Sept.14, 1966	0.134	0.122	-8.96
Oct.21, 1961	0.53	0.61	15.09
Sept. 10, 1960	0.055	0.056	1.82
June 11, 1965	0.175	0.165	-5.71
MARE			10.59
LMARE			0.94

Table 6-11 Summary of calibration of time to peak for PSRM-QUAL

Event		**Peak time (minute)**	
Date	**Observed**	**Simulated**	**Relative Erro (min)**
June 26, 1968	110	130	20
July 3, 1962	331	320	-11.00
Aug. 23, 1967	278	280	2.00
Sept.14, 1966	546	540	-6.00
Oct.21, 1961	486	480	-6.00
Sept. 10, 1960	86	100	-14
June 11, 1965	76	90	-14.00
MARE			10.4
LMARE			0.93

Table 6-12 Optimization range of calibrated parameter for KINEROS

Parameter	Optimization Range From Mean Value[1]
Saturated Hydraulic Conductivity	111% ---- 251%
Effective Net Capillary Drive	74.5%----299%
Manning's N of Channels	157%----250%

[1] The values are percentage of the ratio of calibrated values to their mean values from Table 4-3.

Table 6-13 Optimization range of calibrated parameter for PSRM-QUAL

Parameter	Optimization Range From Mean Value[1]
SCS Curve Number	77.5%----109%
Initial Abstraction Factor	101%----109%
Manning's N of Channles	100%----214%

[1] The values are percentage of the ratio of calibrated values to their mean values from Table 4-3

Typical examples illustrating how well each model performed are given in Figure 6-18 through 6-21. The results for the remaining storm events are given in Appendix C, Figure C-7 through C-26.

From a visual inspection of the results, the KINEROS model appears to more closely match observed hydrographs. The performance of each model was compared for four events in the following discussion.

Event of October 20, 1961: This event is the largest event on the record for the watersheds. For this event, Figure 6-18, both KINEROS and PSRM-QUAL predicted peak discharge rate and time to peak reasonably well. Both of the two models overpredicted the total runoff volume.

Event of May 19, 1966: For this event, Figure 6-19, both KINEROS and PSRM-QUAL overpredicted the peak rate. KINEROS predicted the time to peak and total runoff volume well. PSRM-QUAL, however, was late on time to peak and underpredicted total runoff volume.

Event of July 2, 1968: For this event, Figure 6-20, KINEROS estimated time to peak well but slightly underpredicted the peak discharge rate. PSRM-QUAL also underpredicted peak discharge rate slightly and was late on time to peak. Both of the models simulated the total runoff volume well.

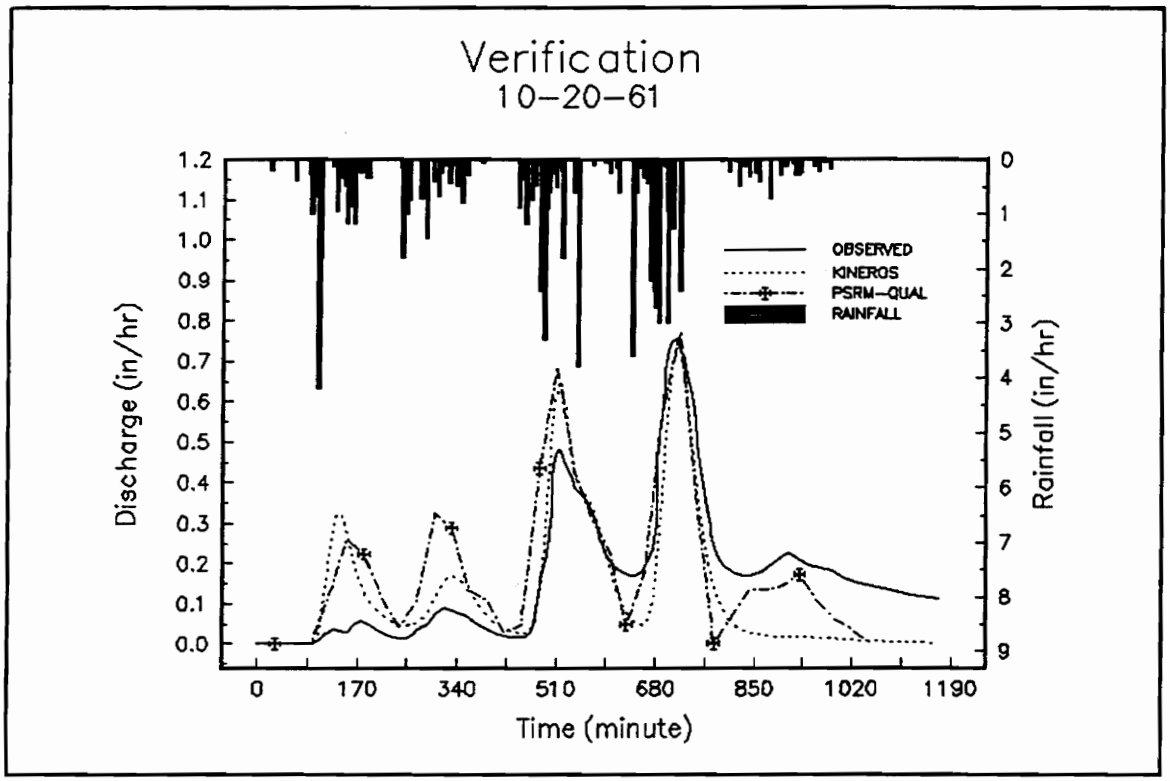

Figure 6-18 A sample verification run (event 10/20/1961)

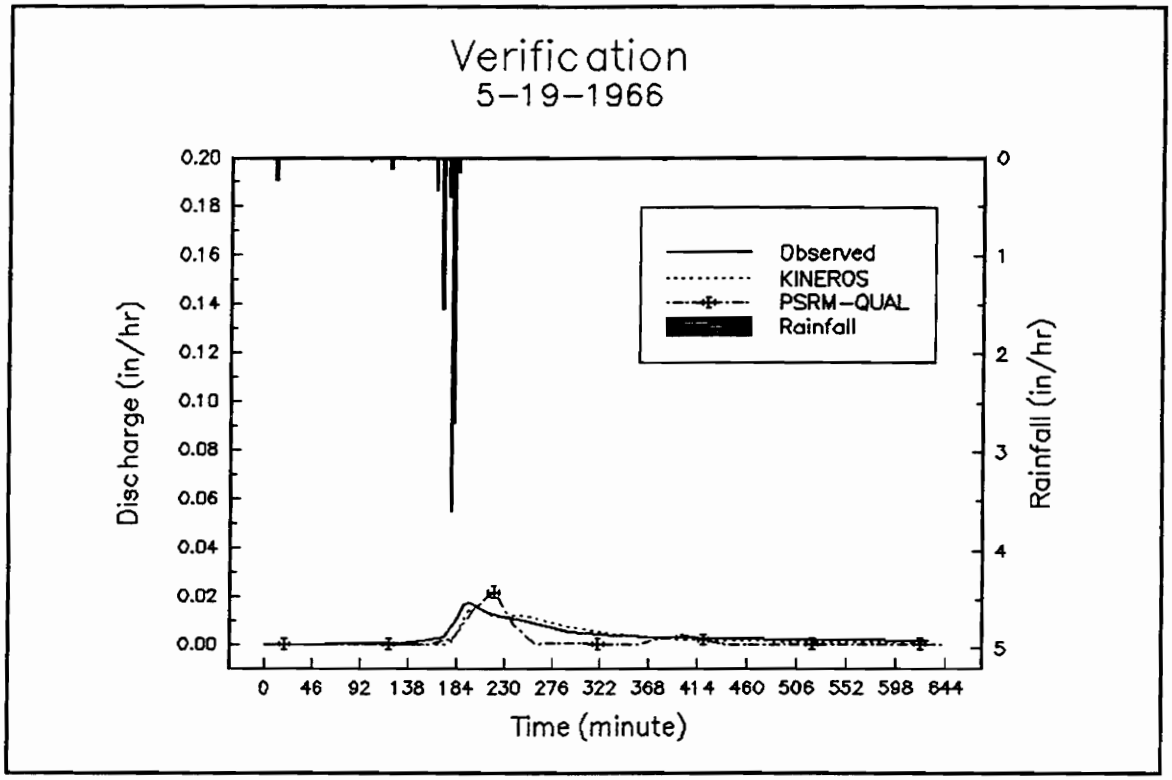

Figure 6-19 A sample verification run (event 5/19/1966)

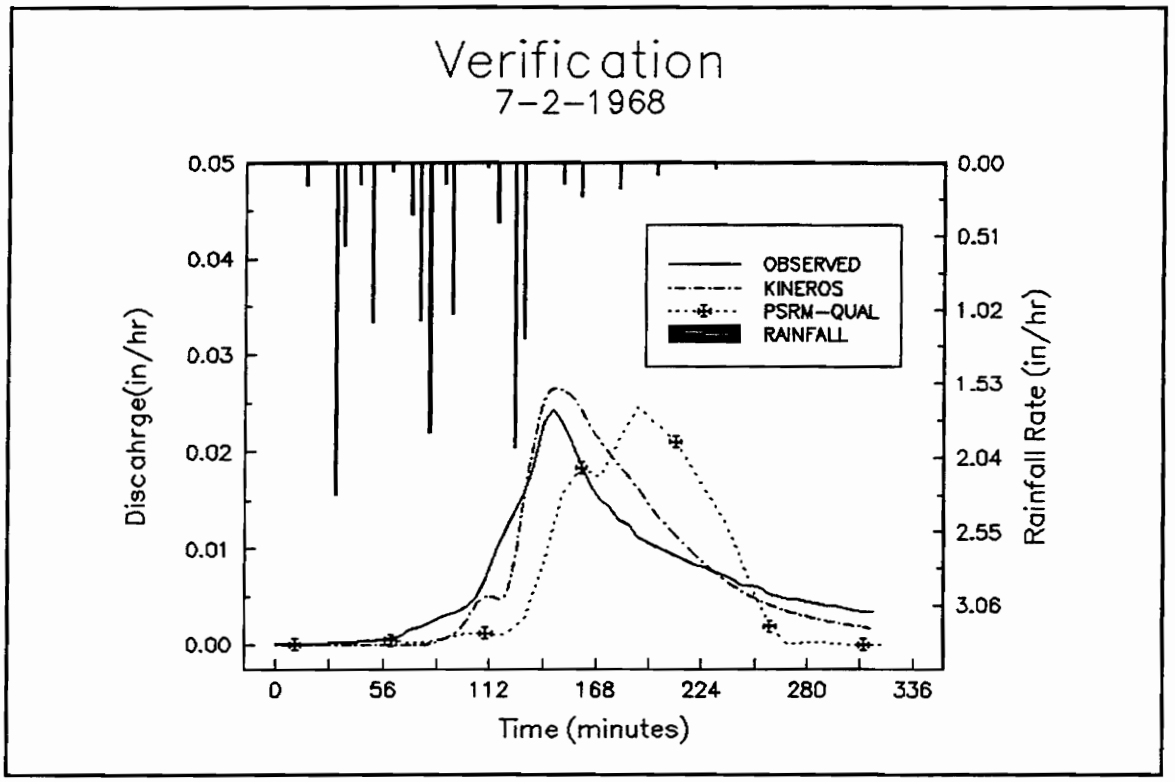

Figure 6-20 A sample verification run (event 7/2/1968)

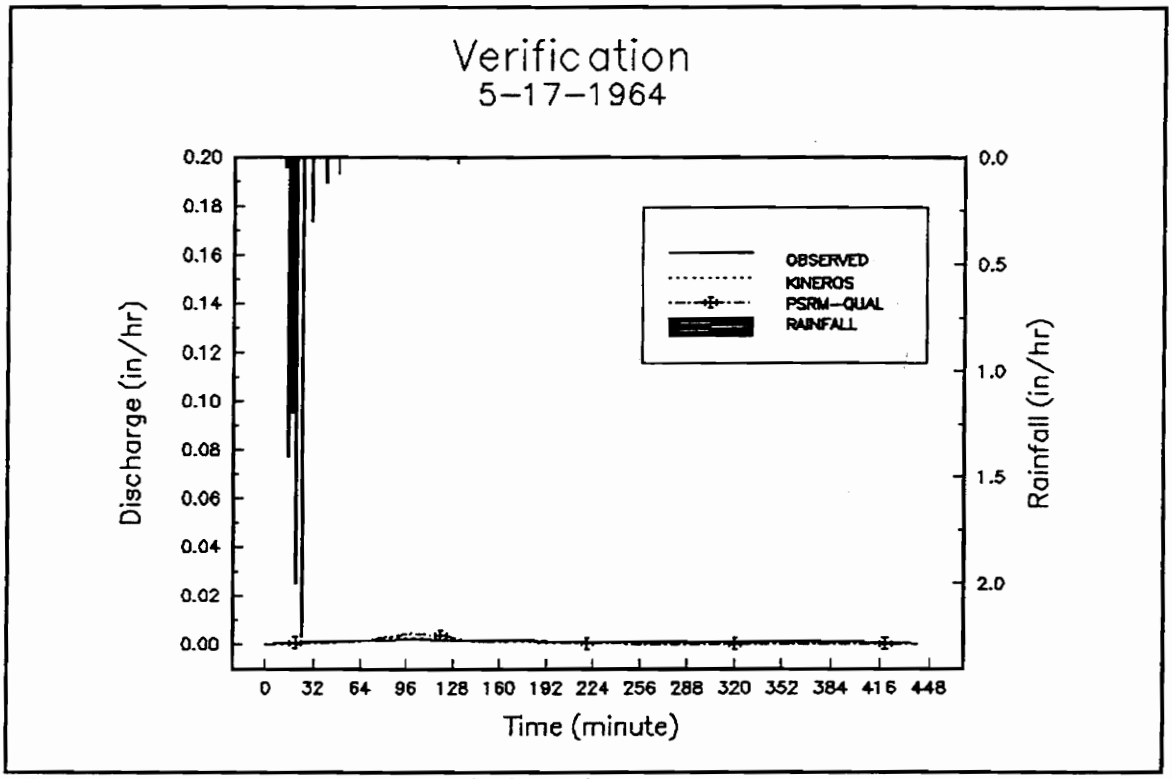

Figure 6-21 A sample verification run (event 5/17/1964)

Event of May 17, 1964: For this event, Figure 6-21, both models accurately estimated time to peak. Both models overpredicted the peak discharge rate. From a visual inspection, however, KINEROS appears to more closely match the observed hydrograph. The performances of the two models on total runoff volume are difficult to judge for this event.

6.3.2 ***Relative Error***

The method of relative errors is used to evaluate the model performance for individual events on a characteristic by characteristic basis.

The results for time to peak, peak discharge rate and total runoff volume for the two models are summarized in Table 6-14, 6-15 and 6-16, respectively.

The simulated peak discharge rate for eleven and six events, respectively by KINEROS and PSRM-QUAL were within 10% observed values. There are eight and one events, respectively, were within 10 % to 20% observed values. One event was simulated within 20% to 30% error by both models. Three events by KINEROS and fifteen events by PSRM-QUAL exceeded 30% error. The largest error for KINEROS was 117.6%. For PSRM-QUAL, it was 282.4%. The results shows KINEROS performed better on peak discharge rate than PSRM-QUAL.

The time to peak was simulated within 5 minutes for seventeen events by KINEROS while only 4 events where within this range by PSRM-QUAL. Four events by KINEROS were within the range of 10 minutes and five events by PSRM-QUAL where within this range. Two events by KINEROS were within the 10-20 minute range while

three events by PSRM-QUAL were within this range. Eleven events simulated by PSRM-QUAL differed by over 20 minutes. The biggest difference between the simulated and observed for KINEROS was 13.7 minutes. Two events simulated by PSRM-QUAL had differences of 104 and 106 minutes. The results shows KINEROS performed better on time to peak than PSRM-QUAL.

The total runoff volume was simulated within 10% for six events by KINEROS and for seven events by PSRM-QUAL. Six events by KINEROS and nine events by PSRM-QUAL were simulated within the range of 10% to 20%. Eight events by KINEROS fell within the range of 20% to 30% of observed volume while only five events by PSRM-QUAL were within this range. Three and two events, respectively exceeded error was 42.1% by KINEROS and 66.9 % by PSRM-QUAL.

6.3.3 *Model Efficiency*

Model efficiency is used to evaluate the overall model capabilities on forecasting and prediction. Equation 5-5 was used to calculate the model efficiency on forecasting for the parameters such as peak discharge rate, time to peak and total runoff volume. To evaluate model efficiency on prediction, the observed and simulated values of these parameters were ranked independently in decreasing order. Then equation 5-5 was used to calculate model efficiency on prediction for two models. The results are summarized in the Table 6-12.

Table 6-14 Observed and simulated time to peak with computed errors

Date	Observed (minute)	KINEROS		PSRM-QUAL	
		Simulated (minute)	Relative Error (minute)	Simulated (minute)	Relative Error (minute)
Sept.5, 1960	64	69	5	54	-10
Oct. 20, 1960	209	204.4	-4.6	210	1
April 9,1961	425	424	-1	420	-5
May 1, 1961	1062	1061	-1	1050	-12
May 12, 1961	85	91	6	120	35
Aug. 25, 1961	84	87	3	90	6
Aug. 26, 1961	378	384	6	420	42
Sept. 7, 1961	73	72.5	-0.5	140	67
Oct. 20, 1961	712	717	5	720	8
May 1, 1962	64	60	-4	60	-4
June 11-12, 1962[1]	458	464	6	352	-106
April 19, 1964	200	202	2	260	60
April 20, 1964	86	89	3	70	-16
May 17, 1964	99	96	-3	100	1
May 19, 1966	198	202	4	220	22
Sept. 20, 1966	201	200	-1	240	39
Sept. 21, 1966	192	195	3	200	8
Oct. 1, 1966	232	218.3	-13.7	336	104
May 7, 1967	565	564	-1	600	35
May 14, 1967	157	163	6	150	-7
May 15, 1967	88	92	4	75	-13
July 2, 1967	210	221	11	234	24
July 2, 1968	145	145.8	0.8	190	45

[1] The storm is between the two days.

Table 6-15 Observed and simulated peak rate with simulated relative errors

Date	Observed (cfs)	KINEROS		PSRM-QUAL	
		Simulated (cfs)	Relative Error (%)	Simulated (cfs)	Relative Error (%)
Sept.5, 1960	18.02	14.67	-18.60	19.70	9.30
Oct. 20, 1960	54.91	19.46	117.56	107.31	95.42
April 9,1961	37.72	39.40	4.44	24.31	-35.5
May 1, 1961	17.60	19.70	11.90	24.73	40.48
May 12, 1961	38.98	44.43	13.98	39.40	1.08
Aug. 25, 1961	6.71	7.13	6.25	7.54	12.50
Aug. 26, 1961	31.86	33.11	3.95	33.53	5.26
Sept. 7, 1961	8.80	7.96	-9.52	12.99	47.62
Oct. 20, 1961	316.05	314.37	-0.53	323.59	2.39
May 1, 1962	60.78	67.49	11.03	61.62	1.38
June 11-12, 1962[1]	11.74	11.53	-1.79	24.31	107.1
April 19, 1964	8.38	9.22	10.00	18.44	120.0
April 20, 1964	9.22	8.80	-4.55	23.05	150.0
May 17, 1964	0.96	1.26	30.43	2.01	108.7
May 19, 1966	7.13	6.71	-5.88	8.80	23.53
Sept.20, 1966	12.57	16.77	33.33	20.54	63.33
Sept.21, 1966	45.27	54.91	21.30	75.45	66.67
Oct.1, 1966	14.25	15.1	5.88	54.49	282.3
May 7, 1967	11.32	10.48	-7.41	22.22	96.30
May 14, 1967	9.22	10.90	18.18	14.25	54.55
May 15, 1967	6.71	7.96	18.75	19.28	187.5
July 2, 1967	10.06	8.80	-12.50	15.93	58.33
July 2, 1968	10.06	11.32	12.50	10.48	4.17

[1] The storm is between the two days

Table 6-16 Observed and simulated total runoff volume with computed relative errors

Date	Observed	KINEROS		PSRM-QUAL	
	(in)	Simulated (in)	Relative Error (%)	Simulated (in)	Relative Error (%)
Sept.5, 1960	0.038	0.054	42.11	0.035	-7.89
Oct. 20, 1960	0.684	0.449	-34.36	0.512	-25.15
April 9,1961	0.292	0.196	-32.88	0.24	-17.81
May 1, 1961	0.170	0.125	-26.47	0.167	-1.76
May 12, 1961	0.157	0.120	-23.57	0.052	-66.88
Aug. 25, 1961	0.025	0.022	-12.00	0.022	-12.00
Aug. 26, 1961	0.115	0.118	2.61	0.103	-10.43
Sept. 7, 1961	0.021	0.027	28.57	0.02	-4.76
Oct. 20, 1961	3.160	2.490	-21.20	3.31	4.75
May 1, 1962	0.205	0.155	-24.39	0.195	-4.88
June 11-12, 1962[1]	0.092	0.079	-14.13	0.102	10.87
April 19, 1964	0.048	0.046	-4.80	0.043	-10.23
April 20, 1964	0.040	0.045	12.50	0.034	-15.00
May 17, 1964	0.0071	0.0062	-12.68	0.0059	-16.90
May 19, 1966	0.032	0.031	-3.130	0.024	-25.00
Sept.20, 1966	0.140	0.099	-29.29	0.110	-21.43
Sept.21, 1966	0.310	0.284	-8.390	0.230	-25.81
Oct.1, 1966	0.159	0.126	-20.75	0.230	44.65
May 7, 1967	0.14	0.099	-29.29	0.110	-21.43
May 14, 1967	0.0071	0.0062	-12.68	0.0059	-16.90
May 15, 1967	0.044	0.039	-11.36	0.042	-4.55
July 2, 1967	0.051	0.049	-3.92	0.043	-15.69
July 2, 1968	0.038	0.0384	1.05	0.035	-7.89

[1] The storm is between the two days

The value of E generally should be less than 1 (Loague and Freeze, 1985). The simulation capability of a model is good if the value of E exceeds 0.97 (James and Burger, 1982). A review of the results in Table 6-17 shows that both performed reasonably well in simulating time to peak. PSRM-QUAL performed extremely well on total runoff volume for model efficiencies on forecasting and prediction. Although the values of E of the model efficiencies of forecasting and prediction on total runoff volumes for KINEROS are consistently lower than 0.97, according to Loague and Freeze (1985), KINEROS has strong powers in model forecasting and prediction. The lower values of KINEROS could be resulted from the interactions of saturated hydraulic conductivity, the effective capillary drive with the other model parameters. For the same reason, both KINEROS and PSRM-QUAL have fair simulating capabilities on peak discharge rate. However, the model efficiencies on forecasting and prediction for peak discharge rate and time to peak by KINEROS are slightly higher than PSRM-QUAL.

6.3.4 *Linear Regression*

The objective of using linear regression is to test the degree of association between simulated and observed values. The tests of linear regression between the simulated and observed peak discharge rate, time to peak and total runoff volume were run, respectively. The results are illustrated and discussed as follows.

The resulting regression describing the relationship between simulated and observed peak discharge rate by KINEROS and PSRM-QUAL are:

$$Peak_{kineros}=1.01Peak_{observed}+0.008 \quad (6\text{-}1)$$

Table 6-17 Summary of the model efficiencies of forecasting and prediction of KINEROS and PSRM-QUAL

Model	model efficiency on forecasting		
	Peak Rate	**Total Runoff Volume**	**Time to Peak**
KINEROS	0.95	0.94	1.00
PSRM-QUAL	0.94	0.99	0.97
	model efficiency on prediction		
	Peak Rate	**Total Runoff Volume**	**Time to Peak**
KINEROS	0.96	0.94	0.99
PSRM-QUAL	0.96	0.99	0.98

$$Peak_{psrm}=1.01Peak_{observed}+0.022 \quad (6\text{-}2)$$

R^2 values for KINEROS and PSRM-QUAL are 0.959 and 0.954 respectively, which indicates that both two models did equally well based on this parameter.

The linear regression relationships between simulated and observed total runoff volume for PSRM-QUAL and KINEROS are as follows:

$$Volume_{kineros}=0.781Volume_{observed}+0.002 \quad (6\text{-}3)$$

$$Volume_{psrm}=1.04Volume_{observed}-0.023 \quad (6\text{-}4)$$

The values of R^2 were 0.997 and 0.994 for KINEROS and PSRM-QUAL, respectively. Both models performed equally well.

The linear regression equations for time to peak of the two models are:

$$Time_{kineros}=0.999Time_{observed}+1.657 \quad (6\text{-}5)$$

$$Time_{psrm}=0.969Time_{observed}+22.1 \quad (6\text{-}6)$$

The values of R^2 were 0.999 and 0.973 for KINEROS and PSRM-QUAL, respectively, which indicated both of the two models performed well but the results suggest that KINEROS did slightly better. The scattplots of the line regression are shown on Figures 6-22 through 6-27.

6.3.5 *Hypothesis Testing*

Hypothesis testing of the mean and standard deviation of the peak discharge rate, total runoff volume and time to peak were performed using the procedures described in Section 5.1.2.7, Chapter 5. The results are summarized in Table 6-18.

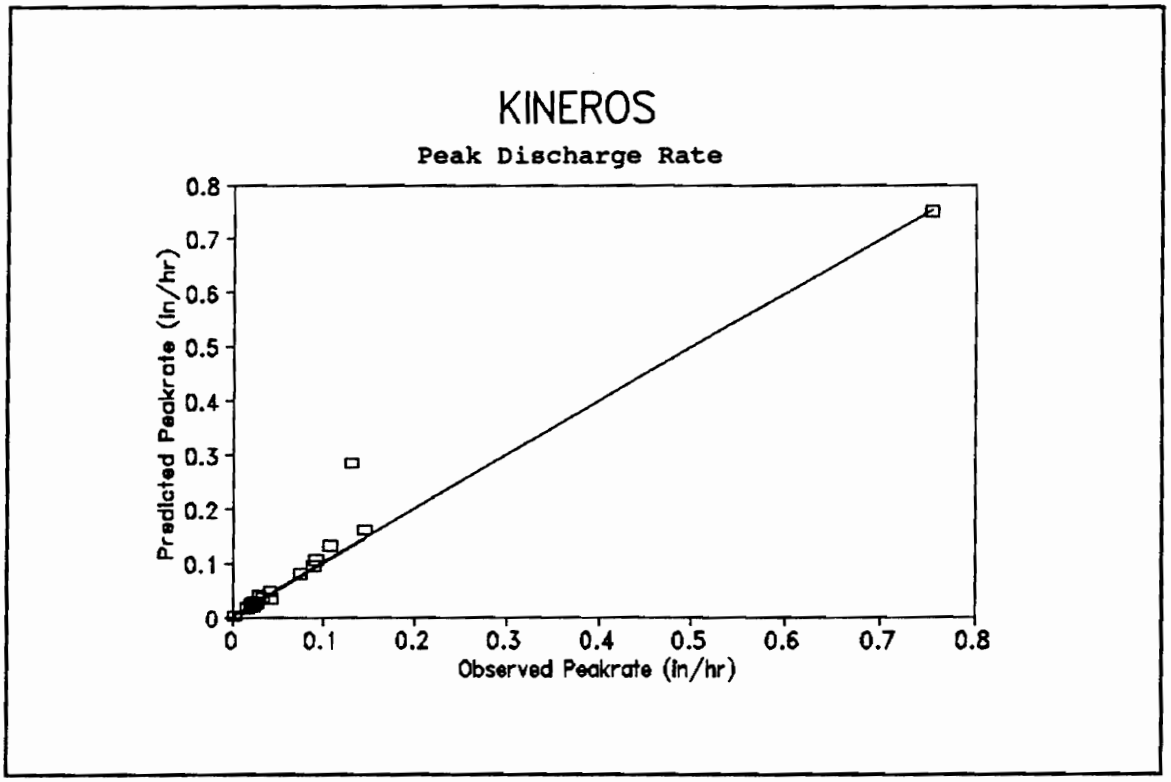

Figure 6-22 Comparison Of simulated and observed peak discharge rate and linear regression results (23event, KINEROS)

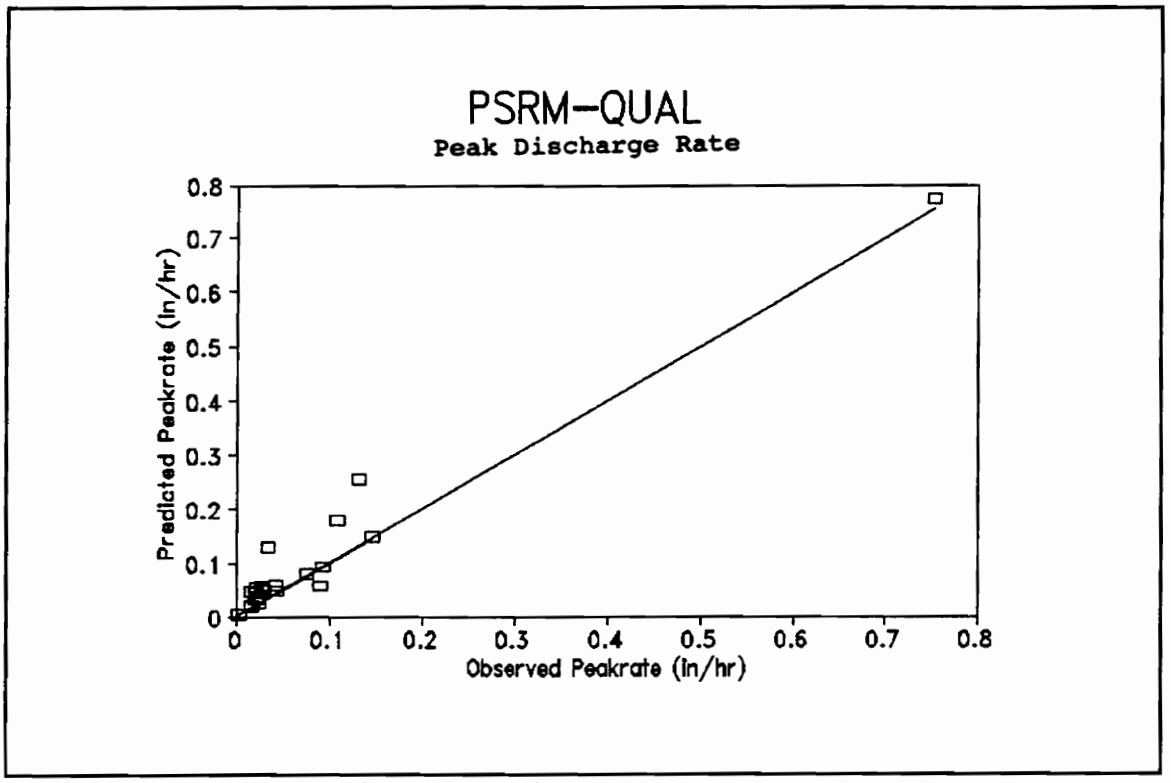

Figure 6-23 Comparison of simulated and observed peak discharge rate and linear regression results (23 events, PSRM-QUAL)

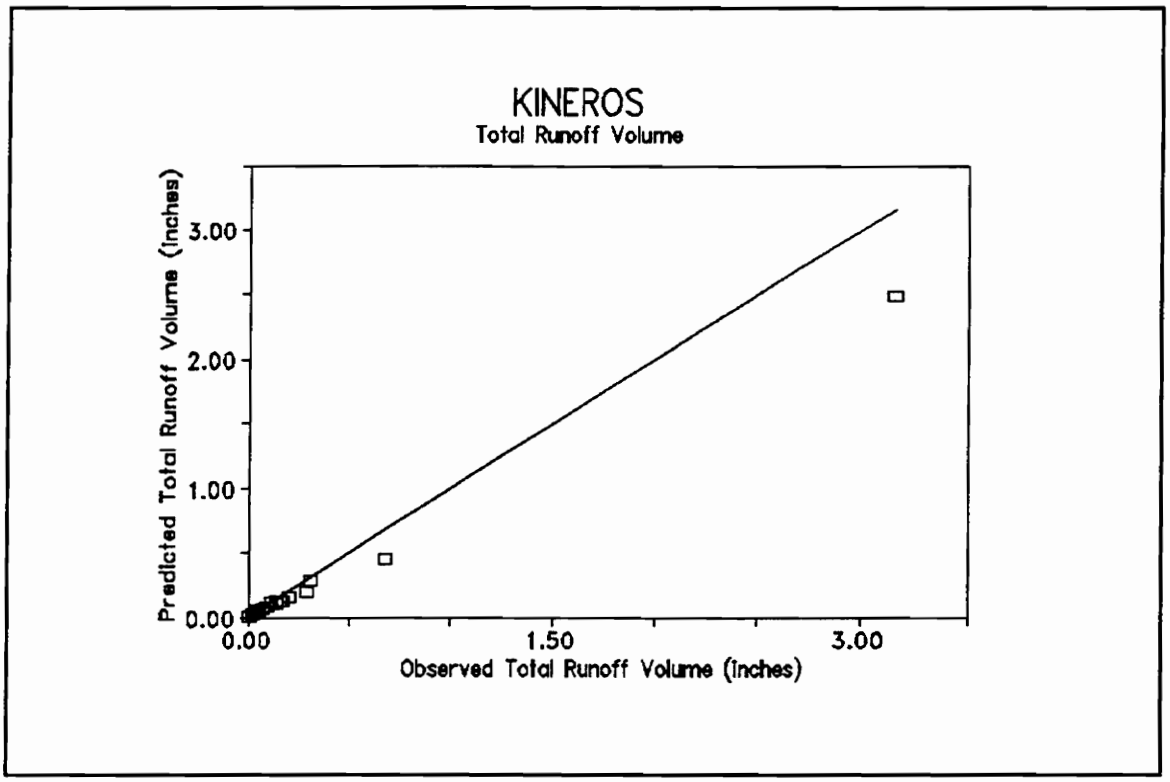

Figure 6-24 Comparison of simulated and observed total runoff volume and linear regression results (23 events, KINEROS)

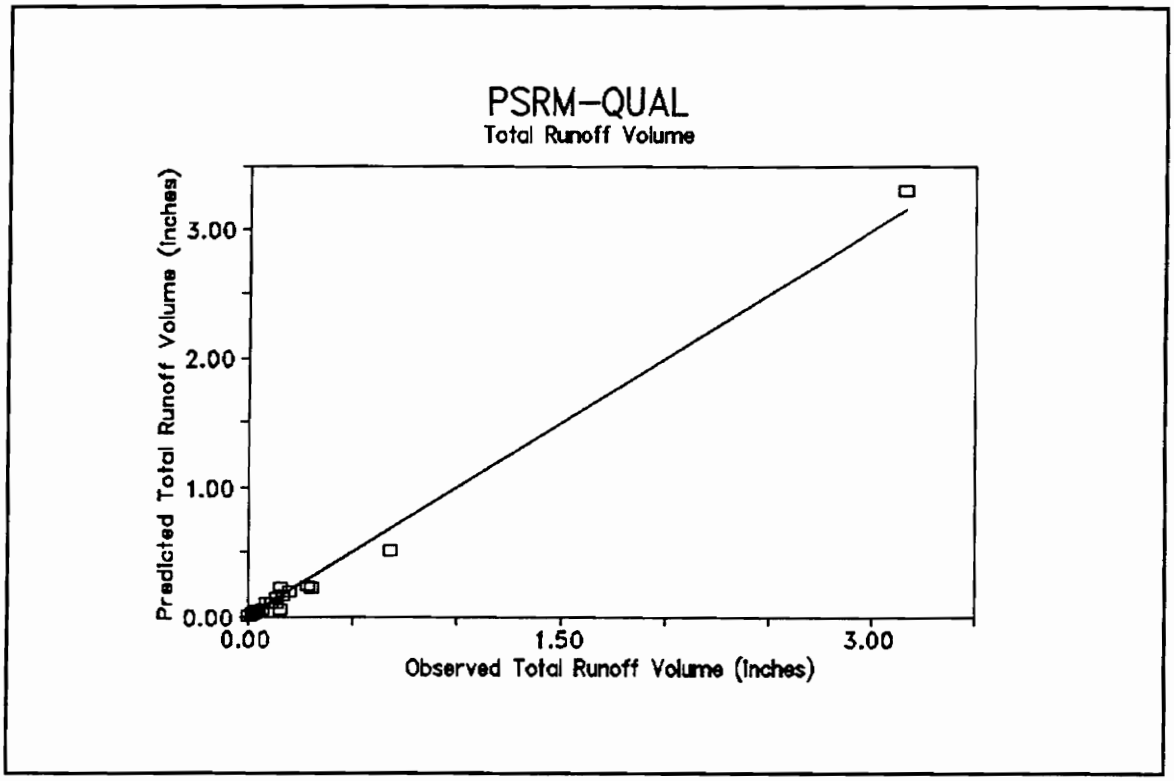

Figure 6-25 Comparison of simulated and observed total runoff volume and linear regression results (23 events, PSRM-QUAL)

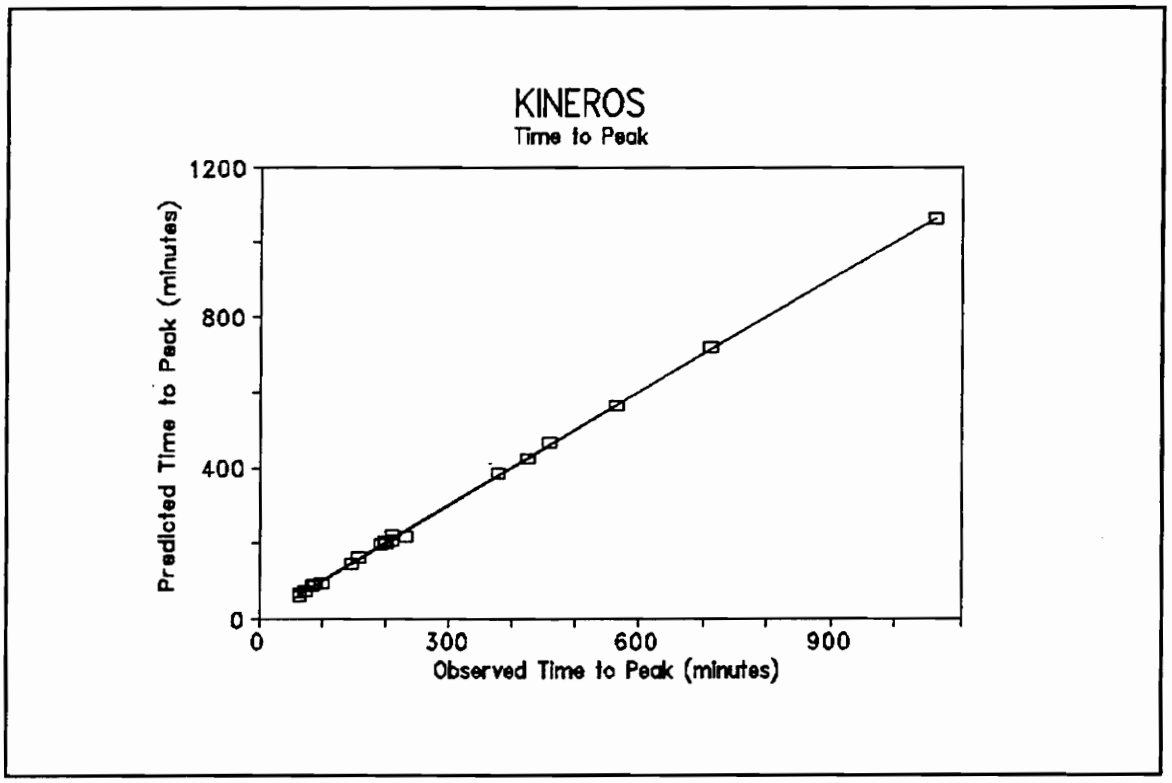

Figure 6-26 Comparison of simulated and observed time to peak and linear regression results (23 events, KINEROS)

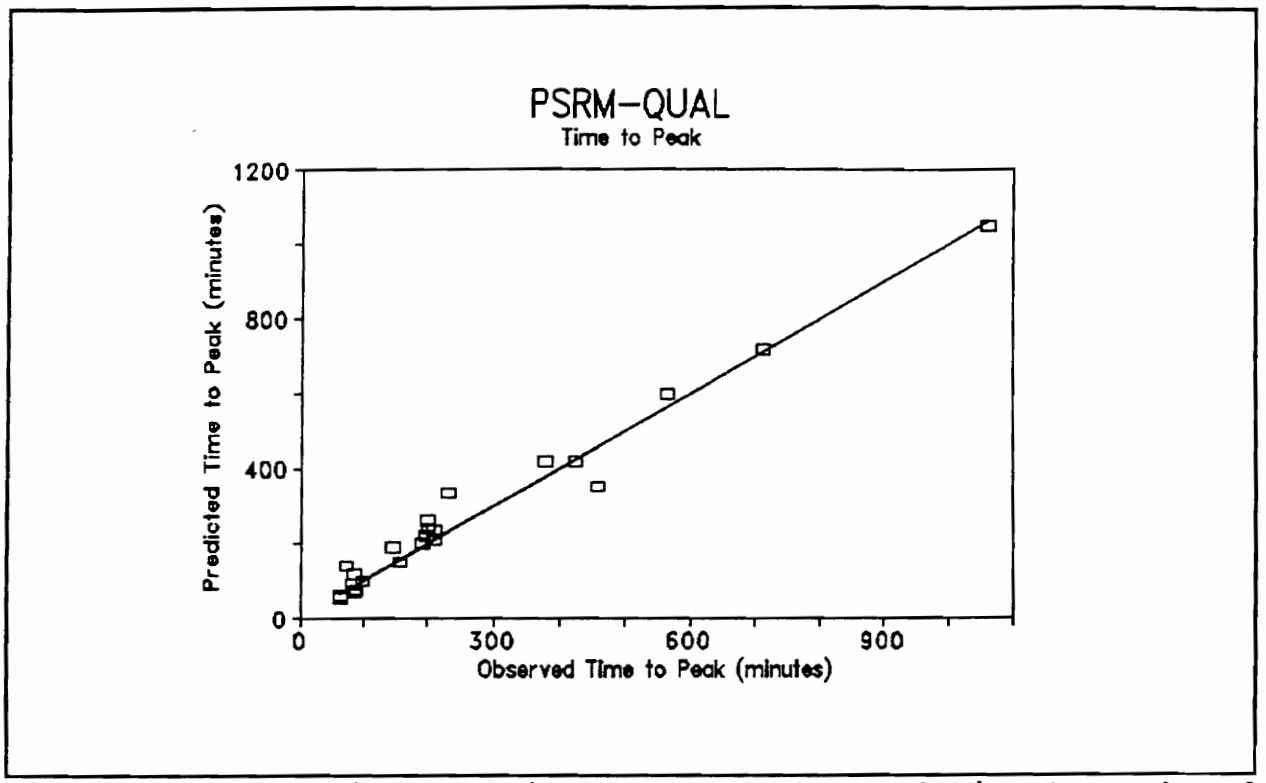

Figure 6-27 Comparison of simulated and observed time to peak and linear regression results (23 events, PSRM-QUAL)

From Table 6-18, all the hypothesis on means and the standard deviations of two models can not be rejected at the 5% siginificant level.

6.3.6 ***Hydrograph Shapes***

Equation 5-6 in Section 5.1.3.2, Chapter 5 was used to calculate variances of the hydrograph shapes for each verificated event. The results are summarized in Table 6-19 and discussed as follows.

From the Table 6-19, most of variances of events calculated for KINEROS are smaller than those for PSRM-QUAL. The mean variance for KINEROS is almost half of the variance calculated for PSRM-QUAL. A conclusion can be drawn the hydrograph shapes produced by KINEROS more closely match the observed hydrograph shapes.

6.3.7 ***Summaries and Discussions of Verification Analysis***

In summary, statistical tests and model efficiencies indicate that both models adequately simulated storm events. KINEROS performed better on time to peak and peak discharge rate while PSRM-QUAL simulated total runoff volume slightly better.

KINEROS is a physically based distributed parameter model. It defines the instantaneous rate of change of rainfall to runoff in terms of a rate parameter. The model considers time directly. This type of deterministic model is regarded as a rate parameter model which generally performs better on peak discharge rate and time to peak (Addiscott and Wagenet, 1985). PSRM-QUAL calculates the runoff using the SCS CN number by the amounts of rainfall. It considers the time indirectly during the change from rainfall to runoff. This type of deterministic model is regarded as a capacity model which

usually simulates the total runoff volume better (Addiscott and Wagenet, 1985). PSRM-QUAL has limitations as to the duration of time step that can be stored for a storm. Limiting the time step constrains the duration because, depending on the number of sub-areas, the incremental storm volumes must be consolidated. Thirty three sub-areas were determined for Foster Creek Watershed. A maximum of 35 time intervals could be used to represent a storm. For example, when the time step is set to 10 minutes, the duration of storm should be no more than 350 minutes. For some rainfall-runoff events which have longer duration, e.g. 700 or 1000 minutes, the time step would be set to 20 and 29 minutes, respectively. This resulted in the patterns of the rainfall events being significantly changed. Short, high intensity rainfall periods are reduced, which diminishes accuracy and the real characteristics of rainfall events can not be reflected in the simulation. The performances of PSRM-QUAL on peak discharge rate and time to peak, which are poorer compared with KINEROS, may be due to aggregating the rainfall time-rate distribution. However, the aggregation does not effect the total rainfall amount thus the total runoff volume calculated by SCS CN method is not significantly affected.

Table 6-18 Summary of hypothesis testing for the observed and simulated total runoff, peak discharge rate and time to peak on verification data sets

	Hypothesis					
	$u_e = u_e$			$\sigma_Q^2 = \sigma_{Q'}^2$		
Model	Q_{volume}	Q_{pk}	t_{pk}	Q_{volume}	Q_{pk}	t_{pk}
KINEROS	C	C	C	C	C	C
PSRM-QUAL	C	C	C	C	C	C

Level of significance is 5%; C, cannot reject; R, reject.

Table 6-19 Computed variances of observed and simulated hydrographs

Date	KINEROS 10^{-4}	PSRM-QUAL 10^{-4}
Sept. 5, 1960	1.1	2.0
Oct. 20, 1960	37.5	44.3
April 9,1961	4.2	5.9
May 1, 1961	0.5	2.4
May 12, 1961	1.6	4.9
Aug. 25, 1961	0.0	0.1
Aug. 26, 1961	0.6	1.8
Sept. 7, 1961	0.20	1.3
Oct. 20, 1961	162.5	346.4
May 1, 1962	4.1	5.1
June 11-12, 1962[1]	0.4	2.8
April 19, 1964	0.3	0.9
April 20, 1964	0.7	6.2
May 17, 1964	0.0	0.0
May 19, 1966	1.00	1
Sept. 20, 1966	6	1.9
Sept. 21, 1966	2.7	24.1
Oct. 1, 1966	0.3	10.6
May 7, 1967	0.1	0.9
May 14, 1967	0.10	1.2
May 15, 1967	0.1	2.1
July 2, 1967	0.2	0.7
July 2, 1968	0.1	0.4
Mean Variance	9.80	20.30

[1] The storm is between the two days.

Chapter 7

SUMMARY AND RECOMMENDATION

7.1 *SUMMARY AND CONCLUSION*

Increasing concerns about the affect of NPS pollution from localities with both agricultural and urban landuse require computer models which have the capability to simulate the status of stream water quality. The use of distributed models is becoming a feasible alternative because of rapid development of the PC-based hardware/software platforms. Two distributed models, the Kinematic Runoff and Erosion Model (KINEROS) and the Penn State Runoff Quality Model (PSRM-QUAL), were selected for this study, since both have the structure and components to simulate hydrologic responses and NPS pollution from agricultural and less developed urban areas. The Foster Creek Watershed was selected as the study area because of the availability of recorded hydrological data and its nearness to the Thomas Jefferson Planning District (TJPD).

The computational process and input requirements of the two event-based models, KINEROS and PSRM-QUAL were thoroughly reviewed. The computer code for the KINEROS model was modified to increase the storage limitation relating to planes, channels and time-depth pairs of rainfall. The modified model currently can support 115 elements and 110 time-depth pairs of rainfall.

GIS technology was employed to improve data management and modeling efficiency. PC-VirGIS, a GIS software package developed at the Information Supported Systems Laboratory (ISSL), Virginia Tech, was used for this study. Topographical

information, soil data and landuse source maps were digitized and stored in DLG format. Each data layer was rasterized for ease in performing spatial analysis. GIS technology was utilized in creating and deriving the topographic and hydrologic data layers such as slope data layer, SCS CN data layer, etc. The watershed configuration for KINEROS was assisted by GIS. GIS technology simplified data management and reduced time and effort to prepare required input data for the models.

GIS technology was not completely coupled with the two models. The watershed configuration for the two models were determined manually. Because of numerous detailed input information required for the two models, it is less easily linked to GIS. A significant data preparation was done manually.

Although the KINEROS model has structures to allow the watershed to be divided into relatively homogeneous units which can better represent the impacts of spatial variability, the preparation of input files for KINEROS were more time consuming than data preparation for PSRM-QUAL. PSRM-QUAL has limitations to store the duration and time step. The limitations results in consolidation of storm volumes, which changes the pattern of some rainfall events.

The sensitivity of KINEROS and PSRM-QUAL to the parameters of models was evaluated using the data bases for Foster Creek Watershed. Reference hydrographs were established for two models and selected parameters of the two models were varied while holding all others constant at their pre-defined reference values. For KINEROS, peak discharge rate and runoff volume were most sensitive to changes in rainfall amount,

saturated hydraulic conductivity and effective capillary drive. Changing manning's N of channels caused significant changes in peak discharge rate. For PSRM-QUAL, peak discharge rate and total runoff volume were most sensitive to changes in SCS CN, initial abstraction coefficient and rainfall amount. Changing manning's N of channels also significantly impacted the peak discharge rate.

Thirty rainfall-runoff events were selected from the database for the Foster Creek Watershed to validate KINEROS and PSRM-QUAL models. Seven events were randomly selected from this record and used for calibration. Saturated hydraulic conductivity, effective capillary drive and manning's N of channels, which were very sensitive model parameters, were used to calibrate for KINEROS model. SCS CN, initial abstraction coefficient and manning's N of channels were used to calibrate the PSRM-QUAL model. A "trial and error" method was adopted to calibrate the parameters for each model. Sensitivity analysis was helpful in obtaining an acceptable calibration. The saturated hydraulic conductivity and the effective capillary drive were found to have uncertain impacts on KINEROS model's output, which resulted in difficulties for the calibration of the two parameters.

Twenty-three rainfall-runoff events were used to evaluate the performance of each model. Model parameters were based on calibration results. The simulation results were evaluated using graphic comparison, relative error, calculation of hydrograph shape index, linear regression, model efficiency and hypothesis testing.

The discharge hydrographs simulated by KINEROS appeared to match recorded hydrographs better than those PSRM-QUAL. The calculation of hydrograph shape index confirmed this visual interpretation.

The model efficiency parameters on forecasting and prediction show excellent efficiencies for both models. However, KINEROS performed marginally better on peak discharge rate and time to peak while PSRM-QUAL performed slightly better on total runoff volume. The results from hypothesis tests show both of models predicted peak discharge rate, time to peak and total runoff volume within statistically acceptable limits.

The results of relative error and linear regression analysis show KINEROS performed better on peak discharge rate and time to peak while PSRM-QUAL performed better in predicting total runoff volume. The interaction between the saturated hydraulic conductivity and the effective capillary drive could result in the little poorer performance in predicting total runoff volume in contrast with PSRM-QUAL.

In general, the results from all analysis showed that simulated results from both models were acceptable. KINEROS generally gave better predictions for peak discharge rate, time to peak. The hydrograph shape also generally more closely matched the recorded sequence. The differences of the models may be due to differences between the rate parameter and capacity models. The poorer performance on peak discharge rate, time to peak and simulated hydrograph shapes by PSRM-QUAL may be attributed to its storage limitation.

The simulated results of both KINEROS and PSRM-QUAL on Foster Creek Watershed are encouraging. The performances of PSRM-QUAL illustrates that although, the model was originally developed to be used on urban areas, it may be applied to agricultural watersheds.

It is very important to remember, however, that this study was conducted on only one watershed and the samples used are small. More work is needed to improve our confidence in the application of KINEROS and PSRM-QUAL to agricultural and less urban areas.

7.2 *Recommendations*

The following recommendation are presented for further use of KINEROS and PSRM-QUAL on both agricultural and less urban areas.

1. Extensive evaluation of capabilities of KINEROS and PSRM-QUAL should be conducted on other watersheds within Virginia having gaged records. The criteria such as graphic comparison, model efficiency and statistical techniques should be employed to determine if both models, especially PSRM-QUAL, are applicable for simulating the hydrologic response from agricultural watersheds.

2. Evaluation of water quality routine of the two models should be conducted on the watersheds similar to the Foster Creek Watershed. This research work would be useful to evaluate the capabilities of the two models on predicting NPS pollution from agricultural watersheds. This would require the availability of observed data of rainfall, runoff, sediment and pollutants for several watersheds.

3. Future research work should focus on the evaluation of the simulation capabilities of KINEROS and PSRM-QUAL on watersheds which have both agricultural and urban landuse. The work should include the simulation of all the required hydrologic, sediment, and chemical characteristics in order to fully evaluate the two models capabilities.

4. The computer code for the PSRM-QUAL model must be modified to overcome the storage limitations in order to be applied to complex watersheds. This would involved using a higher level computer languages, such as C or FORTRAN 77.

5. The development of additional software to complete the data management and manipulations for creating input files for KINEROS and PSRM-QUAL with GIS technology is recommended. The software used to determine the watershed configurations for two models, especially for KINEROS, is particularly needed. GIS's spatial modeling capability could be utilized to delineate the boundaries of watershed and sub-watersheds and to determine channel junctions, topographic and hydrologic information.

6. Additional research should be conducted on the level of both certainty and uncertainty of the two models' parameters on results of modeling and the interactions within the model parameters.

Addiscott , T.M. and R.J. Wagenet. (1985) Concepts of Solute leaching in soils: a review of modeling approaches. Journal of Sciences, 36 pp.411-424.

Aron, G., D.J. Wall, E. L. White, C. N. Dunn, and D.M. Kotz. (1986) Field Manual of Pennsylvania Department of Transportation storm intensity-duration-frequency charts PDT-IDF. Department of Civil Engineering, The Pennsylvania State University, University Park, PA.

Aron, G., B. A. Dempsey and T. A. Smith III. (1992) Penn State Runoff Quality Model User Manual. Department of Civil and Environmental Engineering and Environmental Resource Research Institute. The Pennsylvania State University.

Beven, K. 1985. Distributed models. Hydrological Forecasting. Edited by M.G. Anderson and T.P. Burt. John Wiley & Sons Ltd. pp.405-432.

Beasley, D.B. (1977) ANSWERS: A mathematical model for simulating the effects of land use and management on water quality. Ph.D. Thesis, Purdue University, West Lafayette, IN. 266p.

Beasley, D.B. and L.F. Huggins. (1982) ANSWERS (Aerial Nonpoint Source Watershed Environment Response Simulation) User's Manual. EPA-905/9-82-001.

Blackie, J.R. and C.W.O. Eeles. (1985) *Lumped catchment models.* Hydrological Forecasting. Edited by M.G. Anderson and T.P. Burt. John Wiley & Sons Ltd. pp.311-345.

Burford, J.B. and J.H. Lillard. (1963) High-accuracy streamflow measurement with low-cost installations. Transactions of the ASAE 6(4): 276-278, 281.

Chairat, S. and J.W. Delleur. (1993) Integrating a physically based hydrological model with GRASS. HydroGIS 93: Application of Geographic Information Systems in Hydrology and Water Resources. IAHS Publ. no. 211, 1993.

Chow, V.T. (1964) Open-channel Hydraulics. McGraw-Hill, Inc. New York, NY.

Chow, V.T., D.R. Maidment and L.W. Mays.(1988) Applied Hydrology. McGraw-Hill Book Company.

Clark, R.T. (1973) A review of some mathematical model used in hydrology, with observation on their calibration and use. J. Hydrol., 19, 1-20.

Crawford, H.H. and R.K. Linsley. (1966) Digital simulation in hydrology: Stanford watershed model IV. TR No. 39. Stanford Univ., Stanford, Calif. pp. 210

Diskin, M.H.(1970) Objectives and techniques of watershed modeling. In Proceeding of ARS-SCS Watershed Modeling Workshop. U.S. Department of Agriculture. Tucson, AZ.

DeCoursey, D. G. (1985) Mathematical models for nonpoint water pollution control. J. of Soil and Water Conservation. September-October.

DeVantier, B.A. and A.D. Feldman (1993). Review of GIS applications in hydrologic modeling. J. of Water Resources Planning and Management, Vol.119, No.2, March/April.

EPA.(1983) Final report for the Nationwide Urban Runoff Program. Water Planning Division, Washington, D.C., December .

Goodrich, D.C., D.A. Woolhiser and S. Sorooshian. (1988) Model complexity required to maintain hydrologic response. Proceedings of 1988 National Conference of the Hydraulic Division, ASCE, Colorado Springs, CO, August 8-12, pp. 431-436.

Green, R.A. and D.Stephenson (1986) Criteria for comparison of single event models. J. of Hydrological Sciences. 31, 3, September.

Gupta, S.K. and S.I. Solomon (1977) Distributed numerical model for estimating runoff and sediment discharge of ungaged rivers, i. The information system. Water Resour. Res., 13(3).

Hann, C.T. (1986) Statistical method in hydrology. Iowa State University Press, Ames, Iowa.

Heatwole, C.D.(1979) A finite element model to describe transmission loss from overland flow. M.S. Thesis, Department of Agricultural Engineering, Virginia Polytechnic Institute and State University, Blacksburg, VA.

Healwole, C.D., V.O. Shanholtz, and B.B. Ross. (1982) Finite element model to describe overland flow on an infiltrating watershed. Transactions of the ASAE 25(3): 630-637.

Heaney, J.P. and W.C., Huber (1973) Storm water management models: refinements, testing and decision making. Department of Environmental Engineering, University of Florida, Gainsville.

Hession, W. C.(1988) Pre-mining hydrologic analysis using modeling and geographic information system technology. M.S. Thesis, Department of Agricultural Engineering, Virginia Polytechnic Institute and State University, Blacksburg, VA.

Hill, J.M., V.P. Singh and H. Aminian (1987) A computerized data base for flood prediction modeling. Water Resources Bulletin 23:21-27.

Hornberger, G.M., K.J.Beven, B.J.Cosby and D.E. Sappington (1985) Shenandoah Watershed Study: Calibration of a Topography-Based, Variable Contributing Area Hydrological Model to a Small Forested Catchment. Water Resources Research, Vol.. 21, No.12, Pages 1841-1850 , December .

Huggins, L.F. and J.R. Burney (1982) Surface runoff, storage and routing. In: Hann et al. (ed.) Hydrologic modeling of small watersheds. ASAE, St. Joseph, MI. pp. 169-228.

Horton, R.E. (1919) Rainfall interception. Monthly Weather Review 47:603-623.

Horton, R.E. (1935) Surface runoff phenomena: I. Analysis of the hydrograph. Horton Hydrology Laboratory Publication 101, Edwards Brothers, Inc. Ann Arbor, MI.

Ibitt, R.P. and T. O'Donnell (1974) Designing conceptual catachment models for automatic fitting models IASH-AISH. Pub., 101 461-475.

Jackon, T. J. (1982) Application and selection of hydrologic models. In: Hann et. al. (ed.) Hydrologic modeling of small watersheds. ASAE St. Joseph, MI. pp. 475-506.

James, L. D. and S. J. Burges (1982) Selection, calibration, and testing of hydrologic models. In: Hann et al. (ed.) Hydrologic modeling of small watersheds. ASAE, St. Joseph, MI. pp. 437-474.

Jewell, T.K., T.J. Nunno and D.D. Adrian. (1978) Methodology For Calibrating Stormwater Models. Journal of the Environmental Engineering Division. EE3, June.

Johanson, R.C., J.C.Imhoff, H.H. Davis (1980). Users manual for hydrological simulation program-FORTRAN (HSPF). EPA-600/9-80-015 .

Judd, D. (1993) Environmental Modeling. Earth Observation Magazine, June, 1993.

Judah, O.M. (1973) Simulation of runoff hydrographs from natural watersheds by finite element method. Ph.D. Dissertation, Department of Agricultural Engineering, Virginia Polytechnic Institute and State University, Blacksburg, VA.

Judah, O.M., V.O. Shanholtz and D.N. Contractor (1975) Finite element simulation of flood hydrographs. Transactions of the ASAE 18(3):518-522.

Kiber, D.F. and D.A. Woolhiser (1970) The kinematic cascade as a hydrologic model. Colorade State University Hydrologic Papers, No. 39, Fort. Collins, CO.

Kiber, D.F., K. A. Riley, G. Aron, G. Osei-kwadow and E.L. White (1982) Recommended hydrologic procedures for computing urban runoff from small developing watersheds in Pennsylvania. Institute for Research on Land and Water Resources The Pennsylvania State University Park, VA 16802.

Kemp, K.K. (1993) Environmental modeling and GIS:dealing with spatial continuity. HydroGIS 93: Application of Geographic Information Systems in Hydrology and Water Resources. IAHS Publ. No. 211.

Lettenmaier, D. P., E. F. Wood. (1993) Hydrologic Forecasting. Handbook of Hydrology. Edited by David R. Maidment. McGrwa-Hill, INC.

Li, E.A. (1975) A model to define hydrologic response units based on characteristics of the soil-vegetative complex within a drainage basin. M.S. Thesis, Department of Agricultural Engineering, Virginia Polytechnic Institute and State University, Blacksburg, VA.

Loague, K. M. and R. Freeze. (1985) A comparison of rainfall-runoff modeling techniques on small upland catchments. Water Resource Research, Vol. 21, No. 2 Pages 229-248.

Maidment, D.R. (1993) Developing a spatial distributed unit hydrograph by using GIS. HydroGIS 93: Application of Geographic Information Systems in Hydrology and Water Resources. IAHS Publ. No. 211, 1993.

McCuen , R. and W. M. Snyder (1986) Hydrologic modeling: Statistical methods and applications. Prentice-hall, Englewood Cliffs, New Jersey.

Morris, E.M. and D.A. Woolhiser. (1980) Unsteady one-dimensional flow over a plane: Partial equilibrium and recession hydrographs. Water Resource Research 16(2): 355-360.

Muzik, I.(1988) Application of a GIS to SCS procedure for design flood hydrographs. In: Proceedings of the International Symposium on Modeling in Agricultural, Forest, and Rangeland Hydrology, Chicago. ASAE, St. Joseph, MI. pp. 494-500.

Natural Environment Research Council (1975). Flood Studies Report, vol. 1. NERC, London.

Nash, J.E. and J.V. Sutcliffe (1970) River flow forecasting through conceptual models. Part I- A discussion of principles. J. Hydrology. 19, 282-290.

Novotny, V. and G. Chesters. (1981) Handbook of nonpoint pollution sources and management. Van Nostrand Reihold Company, New York.

Pitt, R. (1989) SLAMM 5. Source loading and management model : an urban nonpoint source quality model. Univ. of Alabama, Birmingham.

Ponce, V.M. (1989) Engineering Hydrology Principles and Practices. Prentice Hall, Englewood Cliffs, New Jersey.

Rawls, W.J., D.L. Brakensiek, and K.E. Saxton.(1982) Estimation of soil water properties. Transactions of the American Society of Agricultural Engineers 25(5): 1316-1320, 1328.

Renard, K.G., W.J. Rawls and M.M. Fogel. (1982) Currently available models. In: Hann et al. (ed.) Hydrological modeling of small watersheds. ASAE, St. Joseph, MI. pp. 507-522.

Ross, B.B. (1978) A spatially response catchment model for predicting stormwater runoff from unaged watersheds. Ph.D Dissertation, Department of Agricultural Engineering, Virginia Polytechnic Institute and State University, Blacksburg, VA.

Osborn, H.B. , L.J. Lane, C.W. Richardson and M.P. Molnau. (1982) Precipitation. In: Hann et al. (ed.) Hydrological modeling of small watersheds. ASAE, St. Joseph, MI. pp. 81-120.

Saxton , K.E. and J.L. McGuinness (1982) Evapotranspirtion. In: Hann et al. (ed.) Hydrologic modeling of small watersheds. ASAE, St. Joseph, MI. pp. 229-258.

Shanholtz, V.O and N. Zhang (1989) GIS/hydrologic model interface for local planning jurisdictions. ASAE meeting, St. Joseph, MI 49085-9659 USA.

Shanholtz, V.O, B.B. Ross and J.C. Carr. (1981) Effect of spatial variability on the simulation of overland and channel flow. Transactions of the ASAE 24(1):124-138.

Shanholtz, V. O., J.M. Flagg, C. Metz and C. Desai. (1990) Agricultural pollution potential database for mountain castles soil and water conservation district. interim report ISSL 90-6, DSWC. Department of Agricultural Engineering, Virginia Polytechnic Institute and State University, Blacksburg, VA.

Shanholtz, V.O., J.M. Flagg, C.Desai, E.Garland and E.Fox (1993) Agricultural pollution potential database for Southside (Mecklenburg County) Soil and Water Conservation District. Interim Report ISSL 93-3. Department of Agricultural Engineering, Virginia Polytechnic Institute and State University, Blacksburg, VA.

Shanholtz, V.O. and T. M. Younos (1994) A semi-dynamic soil water balance model for no-till and conventional tillage systems. Journal of Agricultural Management, to be published.

Smith, R.E., and J.Y. Parlange. (1978) A parameter-efficient hydrologic infiltration model. Water Resources Research 14(3): 533-538.

Smith, R.E. (1981) A kinematic model for surface mine sediment yield. Transactions of the American Society of Agricultural Engineers 24(6):1508-1514.

Soil Conservation Service. (1972) National engineering handbook. Section 4, hydrology. U.S. Department of Agriculture.

Soil Conservation Service. (1986) Urban hydrology for small watersheds. TR-55, Engineering Division, U.S. Department of Agriculture.

Sorooshian, S. and V.K.Gupta. (1983) Automatic calibration of conceptual rainfall-runoff models: the questions of parameter observability and uniqueness. Water Resources Research, Vol. 19, No.1, pp.260-268.

Storm, D.E. (1986) Modeling phosphorous transport in surface runoff from agricultural watersheds for nonpoint source pollution potential assessment. M.S. Thesis, Virginia Polytechnic Institute and State University, Blacksburg, VA.

Stuebe, M. M. and D. M. Johnston. (1988) Runoff volume estimation using GIS techniques. Water Resources Bulletin. Vol. 26, No.4.

Viessman, W., J.W. Knapp, G.L. Lewis and T.E. Harbaugh (1977) Introduction to Hydrology. Harper and Row. New York, 704pp.

Vieux, B.E., V.F. Bralts and L.J. Segerlind. (1988) Finite element analysis of hydrologic response areas using geographic information systems. In: Proceeding of the international symposium on modeling in agricultural, forest, and rangeland hydrology, Chicago. ASAE, St. Joseph, MI. pp.437-446.

Vieux, B.E. (1991) Geographic information systems and non-point source water quality and quantity modeling. Hydrological Processes, Vol. 5, 101-113.

Wight, J.R. (1988) Potential impact of modeling and systems simulation in rangeland research and management. Paper presented at Fort Koegh Research Symposium on Achieving Efficient Use of Rangeland Resources, Miles City, MI.

Wischmeier, W.H. and D.D. Smith. (1965). *Predicting rainfall erosion losses-- a guide to conservation planning. U.S. Department of Agricultural Handbook 537, pp58.*

Woolhiser, D.A. (1982) Hydrologic system synthesis. In: Hann et al. (ed.) Hydrologic modeling of small watersheds. ASAE, St. Joseph, MI. pp.3-15.

Woolhiser, D.A., R.E. Smith and D.C. Goodrich.(1990) KINEROS, A Kinematic Runoff and Erosion Model: Documentation and User Manual. U.S. Department of Agricultural, Agricultural Research Service, ARS-7.

Woolhiser, D.A. and J.A. Liggett. (1967) Unsteady one-dimensional flow over a plane- the rising hydrograph. Water Resour. Res. 3 (3), 753-771.

Wolfe, M.L. (1982) Sediment detachment and transport functions to simulate soil loss from reclaimed mine spoils. M.S. Thesis, Virginia Polytechnic Institute and State University, Blacksburg, VA.

Wolfe, M.L., V.O. Shanholtz, L.L. Rice and B.B. Ross.(1983) Sediment detachment and transport functions to simulate soil loss from reclaimed mine spoils. Virginia Agricultural Experiment Station. Bulletin 83-5, Virginia Polytechnic Institute and State University, Blacksburg, VA.

Wolfe, M.L. and C.M. U. Neale (1988) Input Data Development for a Distributed Parameter Hydrologic Model (FESHM). In: Proceeding of the international symposium on modeling on agricultural, forest, and Rangeland hydrology, Chicago. ASAE, St. Joseph, MI. pp. 462-463.

Young, R.A., and Onstad C.A., Bosch D.D., and Anderson W.P. (1987) AgNPS: agricultural nonpoint source pollution model: A watershed analysis tool. USDA-ARS. Conservation Research Report 35.

The Soil Map of Foster Creek Watershed

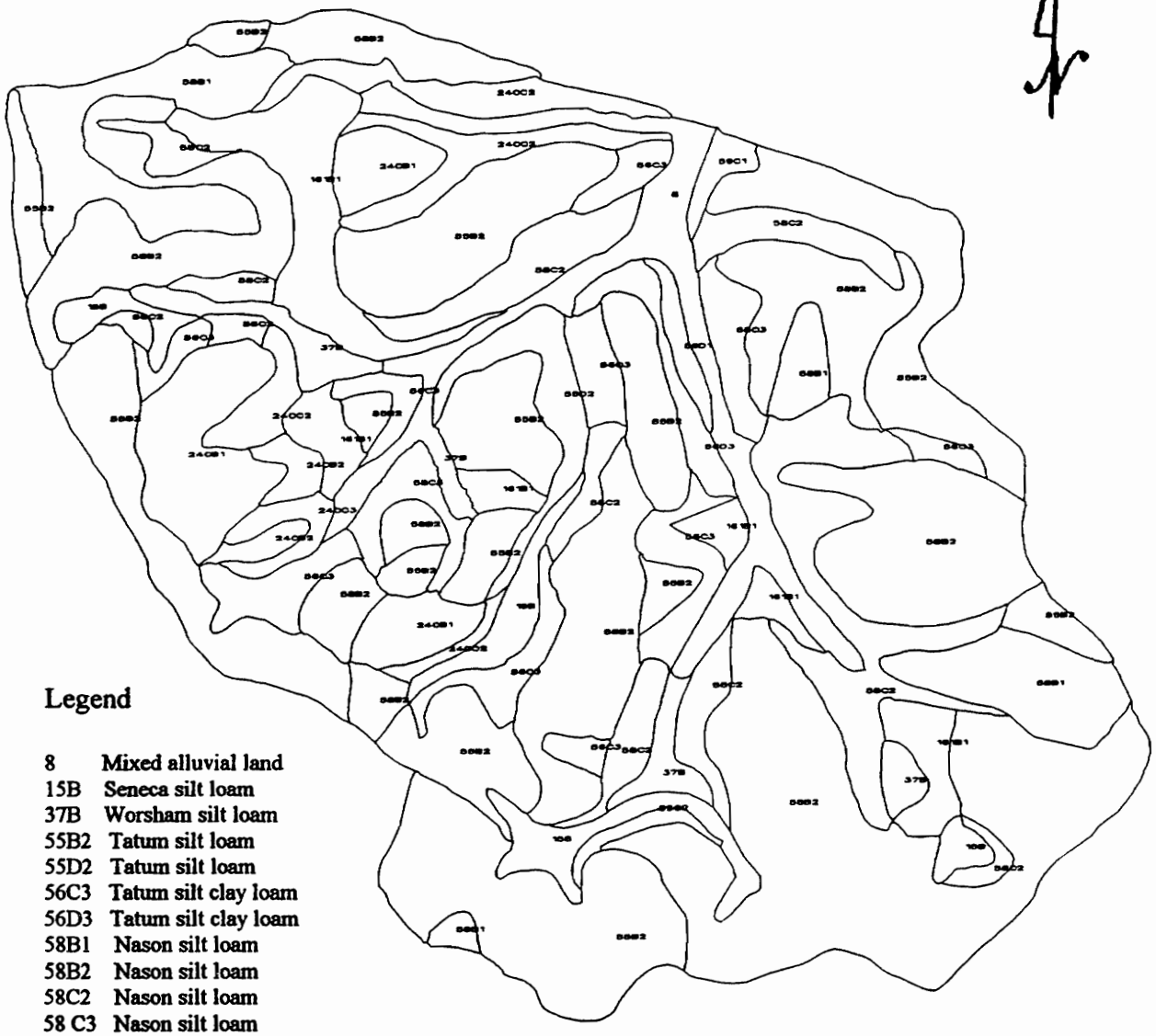

Legend

8 Mixed alluvial land
15B Seneca silt loam
37B Worsham silt loam
55B2 Tatum silt loam
55D2 Tatum silt loam
56C3 Tatum silt clay loam
56D3 Tatum silt clay loam
58B1 Nason silt loam
58B2 Nason silt loam
58C2 Nason silt loam
58 C3 Nason silt loam
59C1 Manteo silt loam
161B1 Ligum loam
240B1 Fluvanna very fine sandy loam
240B2 Fluvanna very fine sandy loam
240C2 Fluvanna very fine sandy loam
240C3 Fluvanna very fine sandy loam

Scale 1:10400

A-1 The digital soil map of Foster Creek Watershed

The Landuse Map of Foster Creek Watershed

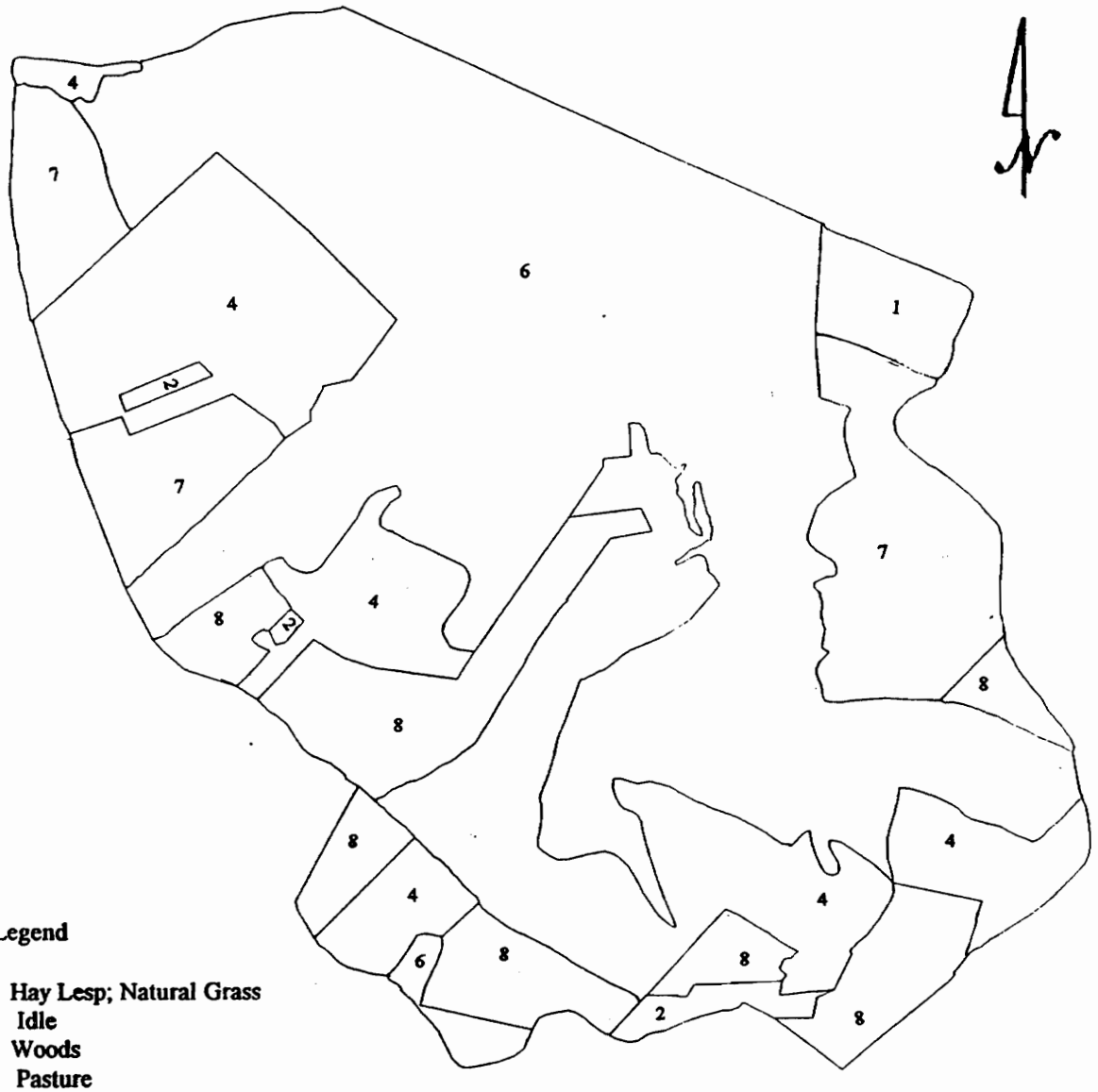

A-2 The digital landuse map of Foster Creek Watershed

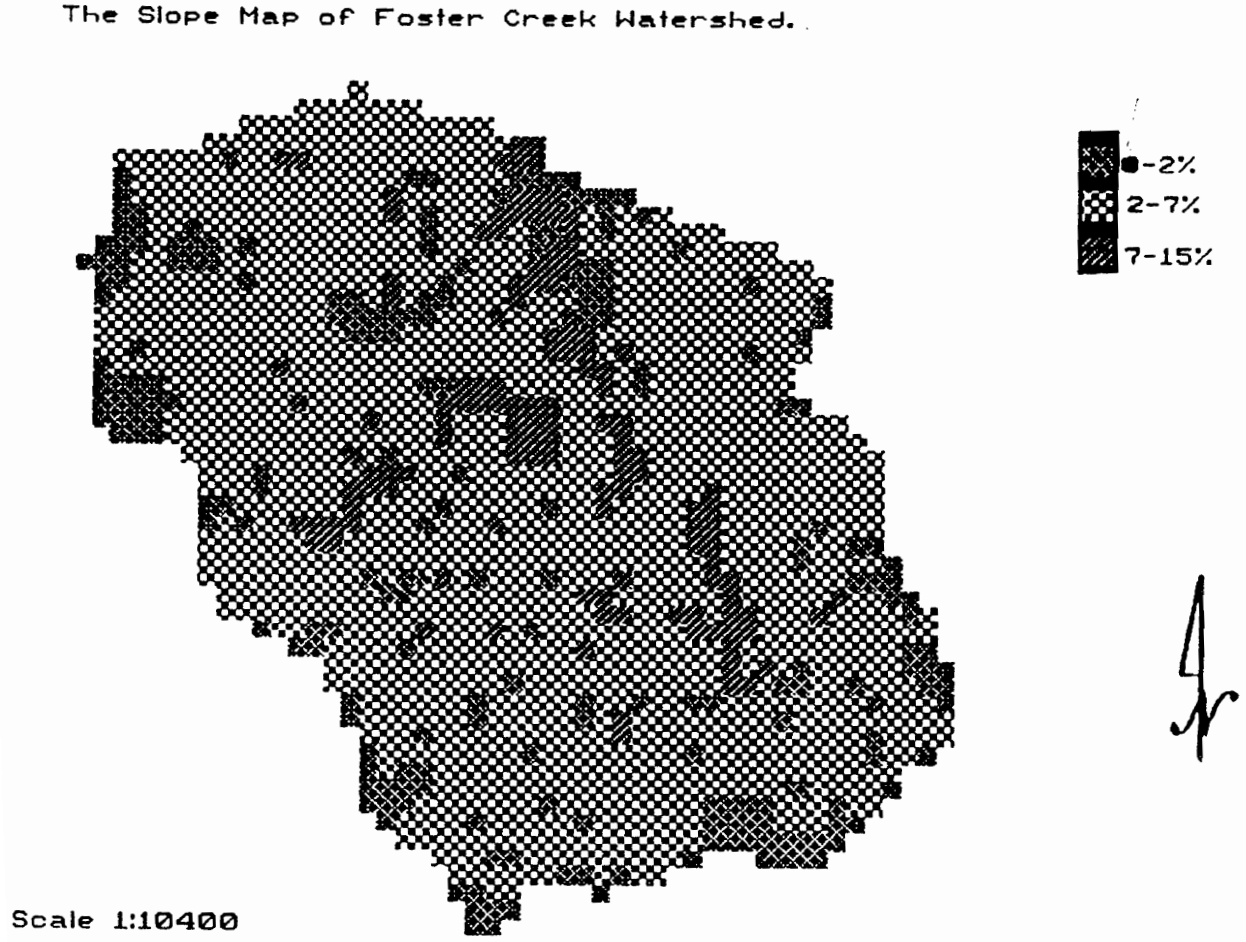

A-3. The digital slope map of Foster Creek Watershed

Table A1 The summary of topographic and hydraulic information for channels

NAME	Channel Elevation Differences (feet)	Channel Lenght (feet)	Channel Slope	Channel Manning 's N
Channel 1	20	780.65	0.03	0.14
Channel 2	20	620.64	0.03	0.14
Channel 3	30	1267.44	0.02	0.14
Channel 4	30	969.76	0.03	0.14
Channel 5	10	433.42	0.02	0.14
Channel 6	5	500.61	0.01	0.14
Channel 7	10	256.59	0.04	0.14
Channel 8	25	630.85	0.04	0.14
Channel 9	15	782.36	0.02	0.14
Channel 10	5	286.09	0.02	0.14
Channel 11	5	251.56	0.02	0.14
Channel 12	5	294.9	0.02	0.14
Channel 13	30	794.8	0.04	0.14
Channel 14	25	1111.78	0.02	0.14
Channel 15	20	852.97	0.02	0.14
Channel 16	25	1040.76	0.02	0.14
Channel 17	45	886.65	0.05	0.14
Channel 18	10	796.78	0.01	0.14
Channel 19	10	315.31	0.03	0.14
Channel 20	10	194.92	0.05	0.14
Channel 21	5	233.17	0.02	0.14
Channel 22	20	897.73	0.02	0.14
Channel 23	5	399.47	0.01	0.14
Channel 24	15	703.59	0.02	0.14
Channel 25	10	687.13	0.01	0.14
Channel 26	5	327.98	0.02	0.14
Channel 27	50	1283.31	0.04	0.14

Continue....

Table A1 The summary of topographic and hydraulic information for channels

Channel 28	5	142.52	0.04	0.14
Channel 29	30	817.87	0.04	0.14
Channel 30	5	775.51	0.01	0.14
Channel 31	20	992.59	0.02	0.14
Channel 32	5	39.04	0.13	0.14

Table A2 Summary of topographic information for each plane of KINEROS

Name	Area (acreas)	Proprotinate Extent (%)	Overland Flow Length (feet)	Width (feet)	Slope (%)
Plane 34	17.571	4.227	516.17	1482.83	2.82
Plane 35	12.904	3.104	632.89	888.15	3.16
Plane 36	4.118	0.991	300	597.93	3.99
Plane 37	11.257	2.708	612.63	800.41	2.83
Plane 38	3.569	0.859	333.64	465.97	4.04
Plane 39	5.491	1.321	388.18	616.18	4.36
Plane 40	15.924	3.831	586.58	1182.53	4.73
Plane 41	7.138	1.717	227.08	1369.26	3.93
Plane 42	1.098	0.264	117.23	407.99	0.43
Plane 43	6.864	1.651	398	751.25	3.22
Plane 44	9.884	2.378	464.54	926.82	2.79
Plane 45	3.844	0.925	409.32	409.08	4.6
Plane 46	4.15	1	226.74	132.27	2.73
Plane 47	8.237	1.982	723.2	496.13	3.66
Plane 48	0.824	0.198	107.25	334.67	4.22
Plane 49	1.922	0.462	175.17	477.95	4.58
Plane 50	1.373	0.33	174.11	343.51	6.31
Plane 51	0.824	0.198	64.8	553.91	7.4
Plane 52	9.335	2.246	402.39	1010.54	2.69
Plane 53	2.471	0.595	153.13	702.91	4.72
Plane 54	3.295	0.793	146.65	978.73	4.42
Plane 55	4.942	1.189	197.71	1088.83	5.31
Plane 56	6.589	1.585	397.57	721.93	5.42
Plane 57	0.275	0.066	116.39	102.92	5.11
Plane 58	6.315	1.519	540.94	508.52	4.47
Plane 59	1.098	0.264	122.98	388.92	6.26

Continue....

Table A2 Summary of topographic information for each plane of KINEROS

Plane 60	0.549	0.132	39.18	610.37	5.59
Plane 61	1.922	0.462	385.22	217.34	6.05
Plane 62	0.549	0.132	830.04	28.81	6.54
Plane 63	11.806	2.84	572.82	897.79	3.31
Plane 64	2.471	0.595	130.14	827.08	4.95
Plane 65	5.491	1.321	268.72	890.1	4.05
Plane 66	4.942	1.189	243.26	884.95	6.58
Plane 67	14.551	3.501	653.57	969.81	4.38
Plane 68	14.277	3.435	866.38	717.82	3.14
Plane 69	4.393	1.057	237.45	805.89	4.33
Plane 70	6.589	1.585	304.27	943.3	4.41
Plane 71	5.491	1.321	331.47	721.6	6.3
Plane 72	7.962	1.916	345.3	1004.42	5.9
Plane 73	2.471	0.595	293.2	367.11	2.15
Plane 74	3.844	0.925	216.88	772.06	4.64
Plane 75	4.118	0.991	204.73	876.18	4.64
Plane 76	12.355	2.972	708.51	759.6	3.91
Plane 77	8.237	1.982	386.5	928.34	4.56
Plane 78	5.491	1.321	293.33	815.42	5.49
Plane 79	1.098	0.264	142.38	335.92	6.49
Plane 80	1.647	0.396	359.59	199.51	6.32
Plane 81	6.589	1.585	667.89	429.74	3.8
Plane 82	1.098	0.264	166.01	288.11	5.59
Plane 83	1.098	0.264	328.93	145.41	3.77
Plane 84	2.471	0.595	287.8	374	4.84
Plane 85	2.196	0.528	276.33	346.17	4.36
Plane 86	20.866	5.02	831.71	1092.84	2.37
Plane 87	6.315	1.519	316.98	867.82	3.74

Continue....

Table A2 Summary of topographic information for each plane of KINEROS

Plane 88	2.746	0.661	158.09	756.63	5.14
Plane 89	3.02	0.727	299.66	439	3.99
Plane 90	0.549	0.132	136.53	175.16	4.72
Plane 91	6.04	1.453	483.72	543.91	4.62
Plane 92	1.373	0.33	173.34	345.03	8.14
Plane 93	1.922	0.462	189.61	441.55	4.64
Plane 94	6.315	1.519	498.21	552.14	5.37
Plane 95	0.275	0.066	617.76	19.39	6.67
Plane 96	2.196	0.528	269.06	355.53	6.59
Plane 97	5.766	1.387	330.34	760.33	2.95
Plane 98	4.667	1.123	215.76	942.23	4.41
Plane 99	4.942	1.189	188.16	1144.1	4.54
Plane 100	0.549	0.132	209.31	114.25	6.88
Plane 101	3.844	0.925	617.25	271.28	4.33
Plane 102	5.217	1.255	406.3	559.32	2.8
Plane 103	2.471	0.595	151.71	709.49	4.33
Plane 104	4.118	0.991	294.92	608.23	4.29
Plane 105	21.964	5.284	1375.48	695.58	3.43
Plane 106	12.629	3.038	541.02	1016.82	3.68
Plane 107	3.844	0.925	307.07	545.3	5.64
Plane 108	6.315	1.519	218.71	1257.74	4.82
Plane 109	4.667	1.123	270.02	752.89	7.34
Plane 110	0.03	0	23.31	56.06	0.01
Plane 111	0.03	0	23.38	55.89	0.01

Table A3 Summary of the hydrologic information for each plane of KINEROS

Plane	Saturated Hydraulic Conductivity (in/hr)	Net Capillary Drive (in)	Total Porosity (cm^3/ cm^3)	Minimum Relative Saturation	Maximum Relative Saturation	Maninng's N	Interception (in)
34	*0.27*	8	0.5	0.03	0.97	0.26	0.05
35	*0.25*	8.19	0.5	0.04	0.96	0.26	0.03
36	*0.27*	8	0.5	0.03	0.97	0.27	0.02
37	*0.27*	8	0.5	0.03	0.97	0.2	0.05
38	*0.27*	8	0.5	0.03	0.97	0.3	0.02
39	*0.27*	8	0.5	0.03	0.97	0.27	0.02
40	*0.21*	8.88	0.48	0.09	0.91	0.3	0.03
41	*0.28*	7.86	0.5	0.04	0.96	0.38	0.03
42	*0.27*	8	0.5	0.03	0.97	0.2	0.08
43	*0.3*	4.89	0.5	0.03	0.97	0.25	0.03
44	*0.28*	7.9	0.5	0.03	0.97	0.22	0.06
45	*0.27*	8	0.5	0.03	0.97	0.36	0.03
46	*0.43*	5.69	0.48	0.05	0.95	0.38	0.03
47	*0.27*	8	0.5	0.03	0.97	0.31	0.02
48	*0.44*	5.52	0.48	0.05	0.95	0.35	0.03
49	*0.31*	7.48	0.5	0.03	0.97	0.4	0.03
50	*0.27*	8	0.5	0.03	0.97	0.4	0.03
51	*0.2*	9.28	0.48	0.1	0.9	0.4	0.03

Continue ....

Table A3 Summary of the hydrologic information for each plane of KINEROS

52	*0.27*	8	0.5	0.03	0.97	0.31	0.04
53	*0.27*	8	0.5	0.03	0.97	0.4	0.03
54	*0.27*	8	0.5	0.03	0.97	0.32	0.01
55	*0.27*	8.03	0.48	0.07	0.93	0.4	0.03
56	*0.23*	8.65	0.49	0.07	0.93	0.38	0.03
57	*0.05*	11.9	0.43	0.25	0.75	0.4	0.03
58	*0.26*	8.17	0.5	0.04	0.96	0.35	0.02
59	*0.24*	8.19	0.47	0.1	0.9	0.25	0.02
60	*0.52*	4.3	0.46	0.06	0.94	0.25	0.02
61	*0.14*	9.81	0.47	0.14	0.86	0.26	0.03
62	*0.16*	9.95	0.47	0.14	0.86	0.4	0.03
63	*0.26*	8.15	0.5	0.04	0.96	0.3	0.01
64	*0.25*	8.43	0.49	0.05	0.95	0.38	0.03
65	*0.27*	8	0.5	0.03	0.97	0.38	0.03
66	*0.19*	9.14	0.48	0.1	0.9	0.37	0.03
67	*0.24*	8.51	0.49	0.06	0.94	0.39	0.03
68	*0.33*	7.95	0.49	0.05	0.95	0.2	0.08
69	*0.42*	7.21	0.49	0.04	0.96	0.33	0.03
70	*0.25*	8.27	0.5	0.05	0.95	0.25	0.06
71	*0.26*	8.11	0.5	0.04	0.96	0.4	0.03
72	*0.2*	8.84	0.49	0.08	0.92	0.37	0.03
73	*0.76*	6	0.47	0.07	0.93	0.23	0.04

Continue....

Table A3 Summary of the hydrologic information for each plane of KINEROS

74	*0.27*	8	0.5	0.03	0.97	0.3	0.02
75	*0.3*	7.51	0.5	0.03	0.97	0.37	0.03
76	*0.34*	8.12	0.48	0.07	0.93	0.26	0.05
77	*0.7*	5.86	0.47	0.07	0.93	0.39	0.03
78	*0.33*	7.92	0.49	0.05	0.95	0.29	0.03
79	*0.17*	9.53	0.47	0.12	0.88	0.4	0.03
80	*0.27*	8	0.5	0.03	0.97	0.4	0.03
81	*1*	5	0.45	0.09	0.91	0.3	0.01
82	*0.82*	5.74	0.47	0.08	0.92	0.26	0.02
83	*0.58*	5.39	0.47	0.06	0.94	0.31	0.02
84	*0.6*	6.66	0.48	0.06	0.94	0.23	0.02
85	*0.32*	7.17	0.48	0.07	0.93	0.38	0.03
86	*0.29*	8	0.5	0.04	0.96	0.26	0.02
87	*0.37*	6.55	0.49	0.04	0.96	0.25	0.02
88	*0.42*	7.25	0.48	0.06	0.94	0.24	0.02
89	*0.28*	8.04	0.48	0.08	0.92	0.35	0.03
90	*0.09*	10.2	0.46	0.16	0.84	0.4	0.03
91	*0.25*	8.36	0.49	0.06	0.94	0.4	0.03
92	*0.27*	8	0.5	0.03	0.97	0.4	0.03
93	*0.09*	11.17	0.44	0.21	0.79	0.4	0.03
94	*0.24*	8.43	0.49	0.05	0.95	0.4	0.03
95	*0.05*	11.9	0.43	0.25	0.75	0.4	0.03

Continue....

Table A3 Summary of the hydrologic information for each plane of KINEROS

96	*0.12*	10.07	0.46	0.15	0.85	0.4	0.03
97	*0.27*	8	0.5	0.03	0.97	0.15	0.12
98	*0.26*	8.23	0.5	0.04	0.96	0.3	0.07
99	*0.25*	8.43	0.49	0.05	0.95	0.28	0.08
100	*0.05*	11.9	0.43	0.25	0.75	0.4	0.03
101	*0.24*	8.56	0.49	0.06	0.94	0.4	0.03
102	*0.46*	6.36	0.48	0.05	0.95	0.28	0.02
103	*1*	5	0.45	0.09	0.91	0.4	0.03
104	*0.51*	7	0.48	0.05	0.95	0.4	0.03
105	*0.36*	7.02	0.49	0.04	0.96	0.36	0.03
106	*0.41*	7.5	0.49	0.05	0.95	0.4	0.03
107	*0.76*	6.43	0.45	0.12	0.88	0.4	0.03
108	*0.61*	6.73	0.47	0.07	0.93	0.4	0.03
109	*0.69*	6.46	0.47	0.08	0.92	0.4	0.03
110	*1*	6.73	0.47	0.07	0.93	0.4	0.03
111	*0.24*	8.56	0.49	0.06	0.94	0.4	0.03

Table A4 Summary of the topographic information for each sub-area of PSRM-QUAL

Name	Areas (arceas)	Proportinate Extent (%)	Overland Flow Lengh (feet)	Slope (%)
Sub-area 1	17.571	4.227	639.7	2.82
Sub-area 2	11.531	2.774	297.1	2.86
Sub-area 3	26.357	6.341	591.8	3.66
Sub-area 4	1.098	0.264	240.5	0.43
Sub-area 5	17.022	4.095	435	2.96
Sub-area 6	8.786	2.114	416	3.48
Sub-area 7	8.786	2.114	398.2	4.11
Sub-area 8	8.511	2.048	335.2	2.77
Sub-area 9	7.962	1.916	321.2	5.15
Sub-area10	11.257	2.708	446.3	5.34
Sub-area 11	22.788	5.482	570.7	4.53
Sub-area 12	7.962	1.916	492.4	4.88
Sub-area 13	11.257	2.708	526.9	3.33
Sub-area 14	10.433	2.51	657.5	4.72
Sub-area 15	14.826	3.567	389.4	3.18
Sub-area 16	11.257	2.708	236.6	4.45
Sub-area 17	2.196	0.528	139.9	2.28
Sub-area 18	13.179	3.17	500.7	4.09
Sub-area 19	21.964	5.284	474.7	4.71
Sub-area 20	7.413	1.783	246.3	3.79
Sub-area 21	1.922	0.462	170.4	4.98
Sub-area 22	22.788	5.482	536.6	2.51
Sub-area 23	12.08	2.906	422.3	4.24
Sub-area 24	6.315	1.519	378.7	4.84
Sub-area 25	20.866	5.02	661.85	5.79
Sub-area 26	28.279	6.803	651.69	4.97
Sub-area 27	5.217	1.255	344.15	2.81

Continue....

Table A4 Summary of the topographic information for each sub-area of PSRM-QUAL

Sub-area 28	11.806	2.84	209	4.94
Sub-area 29	4.393	1.057	258.65	2.93
Sub-area 30	22.239	5.35	435.8	3.49
Sub-area 31	22.513	5.416	660.29	4.21
Sub-area 32	15.1	3.633	298.6	5.43
Sub-area 33	0.03	0	18.7	0.01

Table A 5 Summary of the hydrologic information for each sub-area of PSRM-QUAL

Name	SCS Curve Number	Manning' N	Saturated Hydraulic Conductivity (in/hr)—>	Soil Porosity
Sub-area 1	72	0.25	0.27	0.46
Sub-area 2	80	0.21	0.27	0.45
Sub-area 3	76	0.27	0.26	0.47
Sub-area 4	81	0.2	0.27	0.45
Sub-area 5	80	0.24	0.29	0.46
Sub-area 6	79	0.33	0.27	0.45
Sub-area 7	78	0.37	0.32	0.46
Sub-area 8	74	0.3	0.27	0.45
Sub-area 9	76	0.37	0.27	0.45
Sub-area 10	77	0.39	0.29	0.46
Sub-area 11	76	0.33	0.26	0.46
Sub-area 12	75	0.34	0.28	0.45
Sub-area 13	66	0.3	0.25	0.46
Sub-area 14	73	0.36	0.27	0.46
Sub-area 15	75	0.2	0.32	0.46
Sub-area 16	77	0.28	0.31	0.46
Sub-area 17	78	0.24	0.82	0.45
Sub-area 18	73	0.26	0.32	0.46
Sub-area 19	75	0.35	0.45	0.47
Sub-area 20	73	0.3	0.96	0.45
Sub-area 21	80	0.28	0.65	0.46
Sub-area 22	75	0.26	0.29	0.46
Sub-area 23	78	0.27	0.41	0.46
Sub-area 24	70	0.37	0.26	0.47
Sub-area 25	68	0.39	0.24	0.47

Table A 5 Summary of the hydrologic information for each sub-area of PSRM-QUAL

Sub-area 26	75	0.39	0.27	0.47
Sub-area 27	74	0.14	0.27	0.46
Sub-area 28	73	0.31	0.25	0.46
Sub-area 29	77	0.29	0.5	0.45
Sub-area 30	76	0.36	0.37	0.45
Sub-area 31	74	0.4	0.57	0.45
Sub-area 32	74	0.39	0.54	0.46
Sub-area 33	100	0.9	0.54	0.46

Table A6 Data for day length vs. latitude from Thornthwaite and Mather (1955)

	J	F	M	A	M	J	J	A	S	O	N	D
N. Lat.												
0.00	1.04	0.94	1.04	1.01	1.04	1.01	1.04	1.04	1.01	1.04	1.01	1.04
5.00	1.02	0.93	1.03	1.02	1.06	1.03	1.06	1.05	1.01	1.03	0.99	1.02
10.00	1.00	0.91	1.03	1.03	1.08	1.06	1.08	1.07	1.02	1.02	0.98	0.99
15.00	0.97	0.91	1.03	1.04	1.11	1.08	1.12	1.08	1.02	1.01	0.95	0.97
20.00	0.95	0.90	1.03	1.05	1.13	1.11	1.14	1.11	1.02	1.00	0.93	0.94
25.00	0.93	0.89	1.03	1.06	1.15	1.14	1.17	1.12	1.02	0.99	0.91	0.91
26.00	0.92	0.88	1.03	1.06	1.15	1.15	1.17	1.12	1.02	0.99	0.91	0.91
27.00	0.92	0.88	1.03	1.07	1.16	1.15	1.18	1.13	1.02	0.99	0.90	0.90
28.00	0.91	0.88	1.03	1.07	1.16	1.16	1.18	1.13	1.02	0.98	0.90	0.90
29.00	0.91	0.87	1.03	1.07	1.17	1.16	1.19	1.13	1.03	0.98	0.89	0.89
30.00	0.90	0. 87	1.03	1.08	1.18	1.17	1.20	1.14	1.03	0.98	0.89	0.88
31.00	0.90	0.87	1.03	1.08	1.18	1.18	1.20	1.14	1.03	0.98	0.88	0.88
32.00	0.89	0.86	1.03	1.08	1.19	1.19	1.21	1.15	1.03	0.97	0.88	0.87
33.00	0.88	0.86	1.03	1.09	1.19	1.20	1.22	1.15	1.03	0.97	0.86	0.86
34.00	0.88	0.85	1.03	1.09	1.20	1.20	1.22	1.16	1.03	0.97	0.86	0.86
35.00	0.87	0.85	1.03	1.09	1.21	1.21	1.23	1.16	1.03	0.97	0.86	0.85
36.00	0.87	0.85	1.03	1.10	1.21	1.22	1.24	1.16	1.03	0.97	0.86	0.84
37.00	0.86	0.84	1.03	1.10	1.22	1.23	1.25	1.17	1.03	0.97	0.85	0.83
38.00[1]	0.85	0.84	1.03	1.10	1.23	1.24	1.25	1.17	1.04	0.96	0.84	0.83
39.00	0.85	0.84	1.03	1.11	1.23	1.24	1.26	1.18	1.04	0.96	0.84	0.82
40.00	0.84	0.83	1.03	1.11	1.24	1.25	1.27	1.18	1.04	0.96	0.83	0.81
41.00	0.83	0.83	1.03	1.11	1.25	1.26	1.27	1.19	1.04	0.96	0.83	0.81
42.00	0.82	0.83	1.03	1.12	1.26	1.27	1.28	1.19	1.04	0.96	0.82	0.80
43.00	0.81	0.82	1.02	1.12	1.26	1.27	1.28	1.19	1.04	0.95	0.82	0.79
44.00	0.81	0.82	1.02	1.13	1.27	1.29	1.30	1.20	1.04	0.95	0.80	0.76
45.00	0.80	0.81	1.02	1.13	1.28	1.29	1.31	1.21	1.04	0.94	0.79	0.75
46.00	0.79	0.81	1.02	1.13	1.29	1.31	1.32	1.22	1.04	0.94	0.79	0.74
47.00	0.77	0.80	1.02	1.14	1.30	1.32	1.33	1.22	1.04	0.93	0.78	0.73
48.00	0.76	0.80	1.02	1.14	1.31	1.33	1.34	1.23	1.05	0.93	0.77	0.72
49.00	0.75	0.79	1.02	1.14	1.32	1.34	1.35	1.24	1.05	0.93	0.76	0.71
50.00	0.74	0.78	1.02	1.15	1.33	1.36	1.37	1.25	1.06	0.92	0.76	0.70

[1] The values for this lattitude was used for Foster Creek Watershed

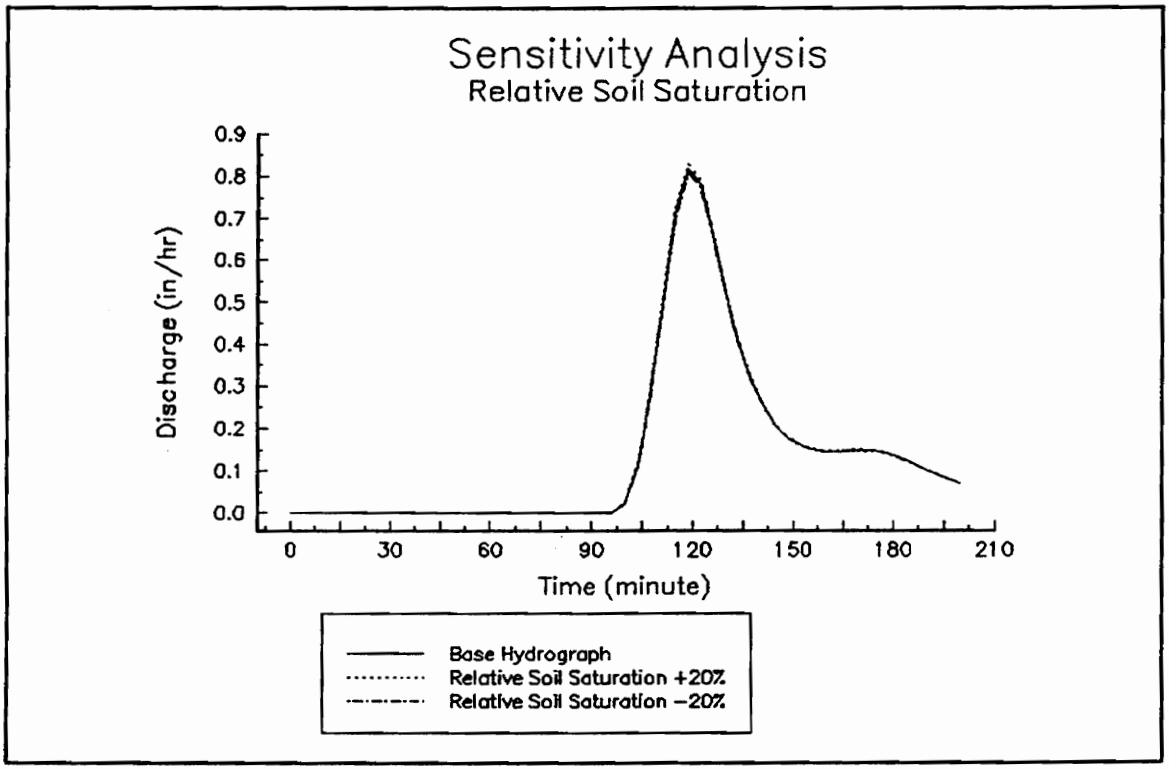

Figure B-1 The effect of relative soil saturation on simulated hydrographs (KINEROS)

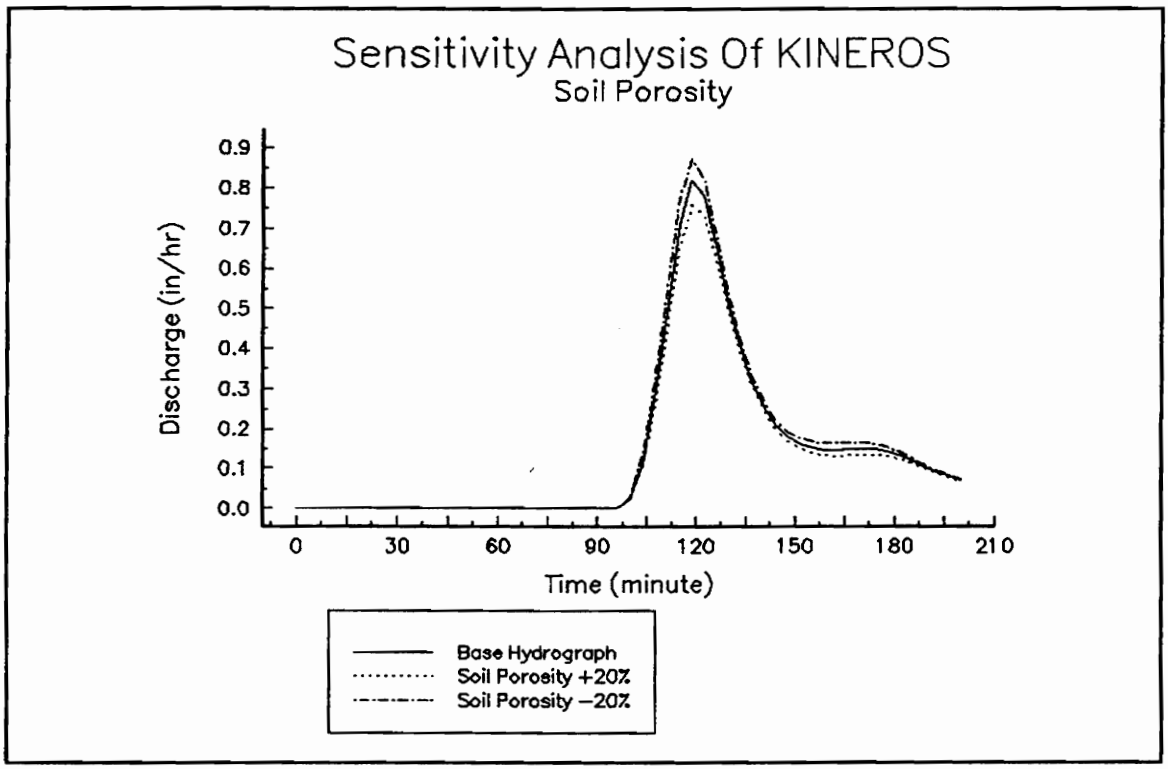

Figure B-2 The effect of soil porosity on simulated hydrographs (KINEROS)

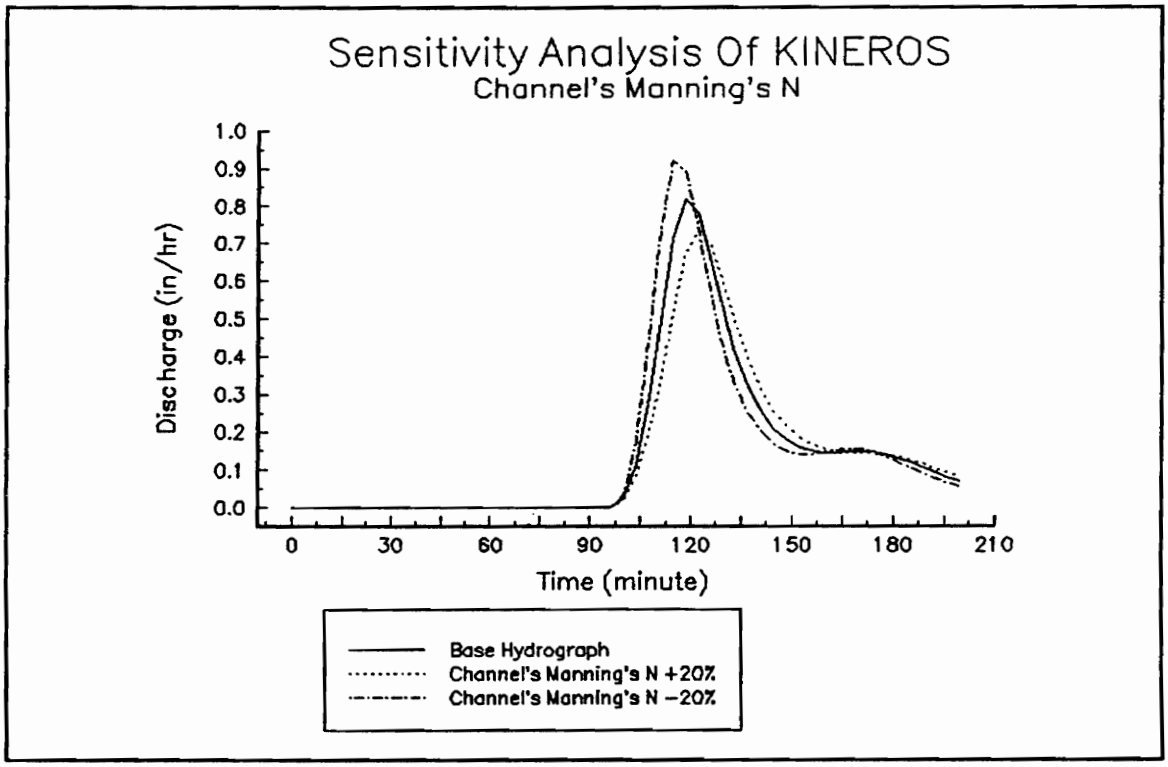

Figure B-3 The effect of channel manning's N on the simulated hydrgraphs (KINEROS)

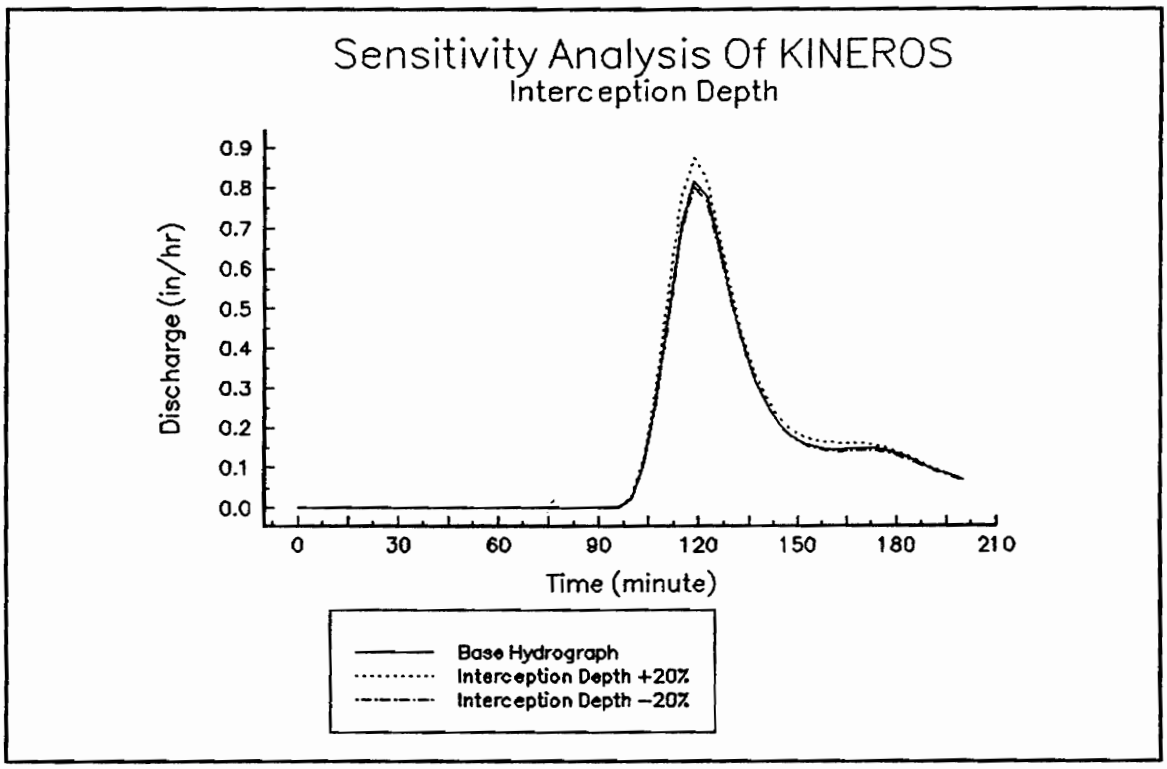

Figure B-4 The effect of interception depth on simulated hydrograph (KINEROS).

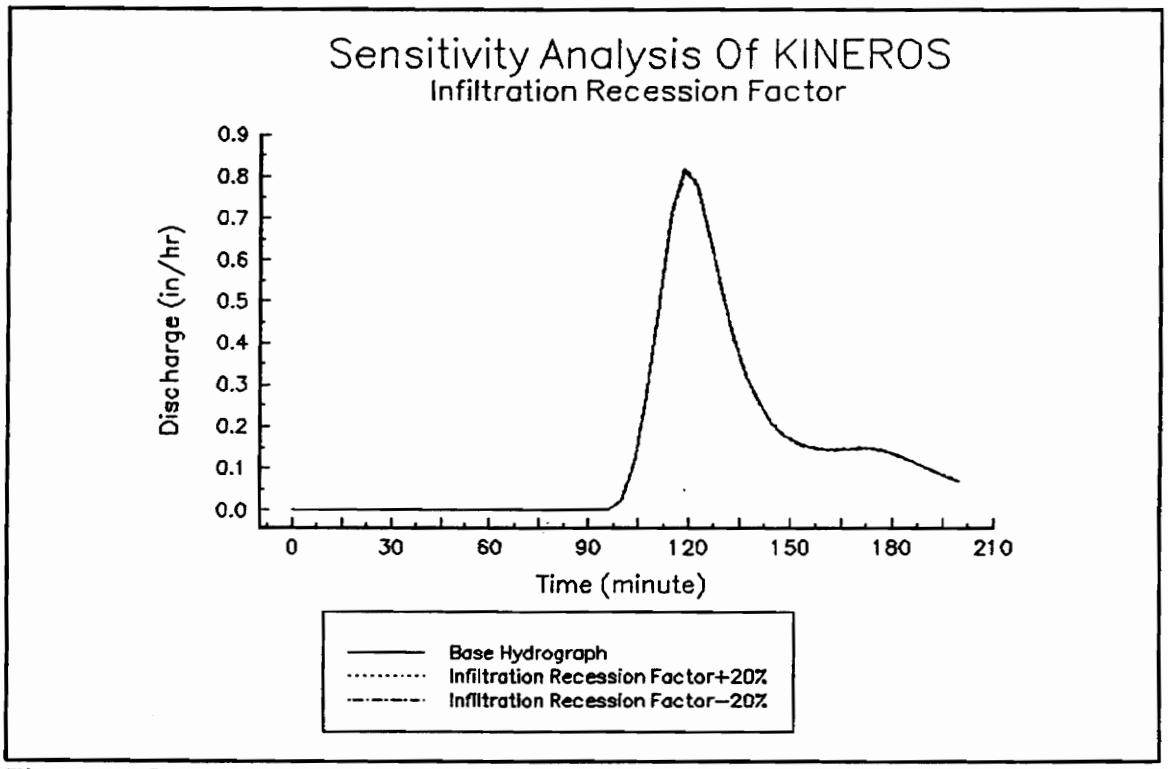

Figure B-5 The effect of infiltration recession factor on simulated hydrographs (KINEROS).

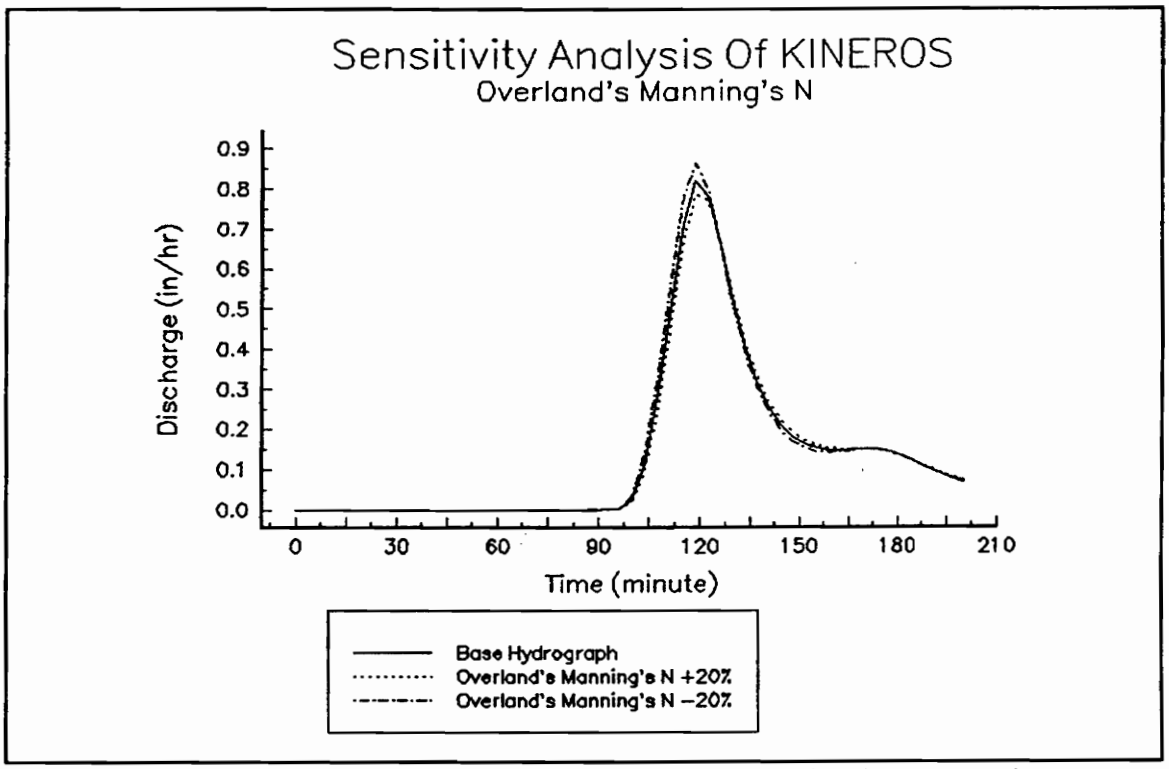

Figure B-6 The effect of overland manning's N on the simulated hydrographs (KINEROS)

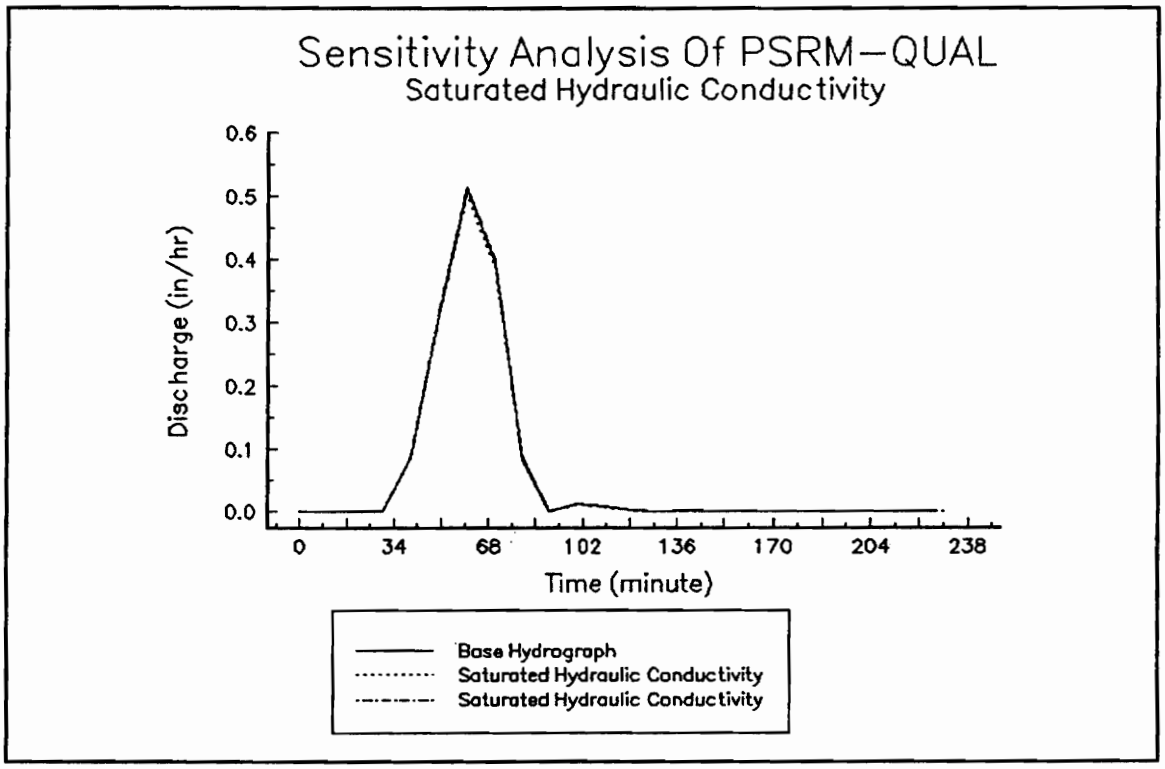

Figure B-7 The effect of saturated hydraulic conductivity on the simulated hydrographs (PSRM-QUAL)

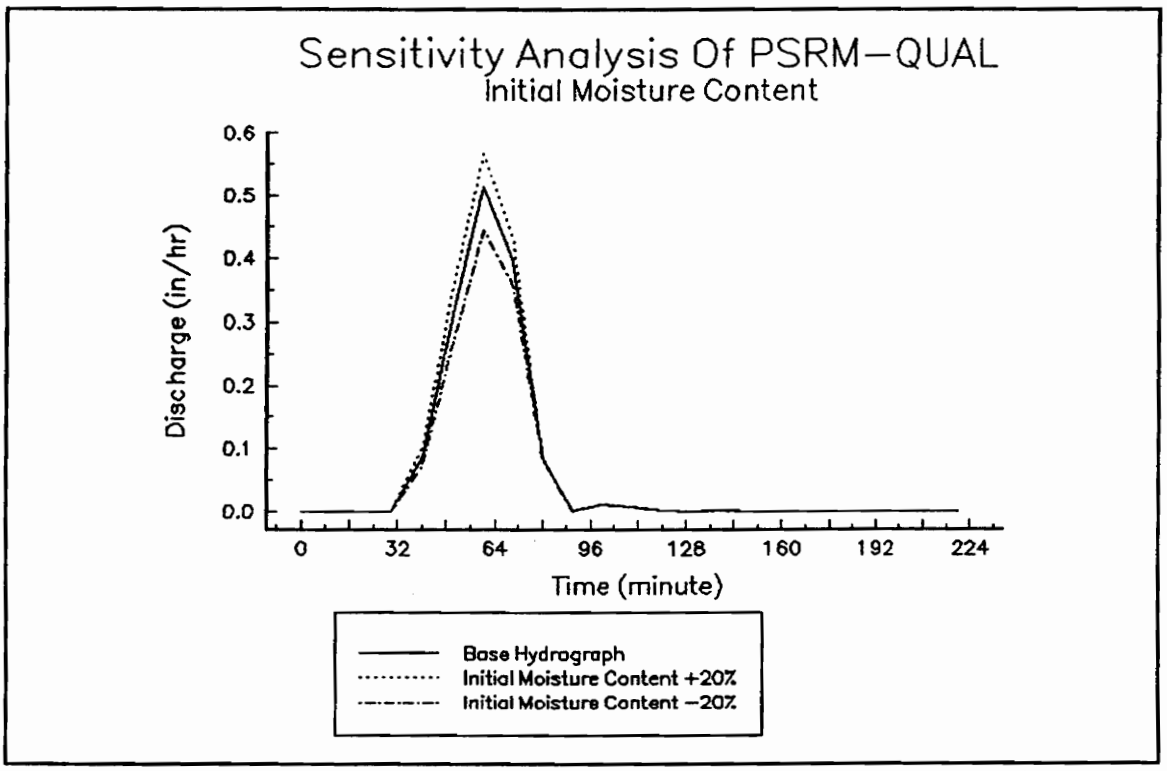

Figure B-8 The effect of initial moisture content on the simulated hydrographs (PSRM-QUAL)

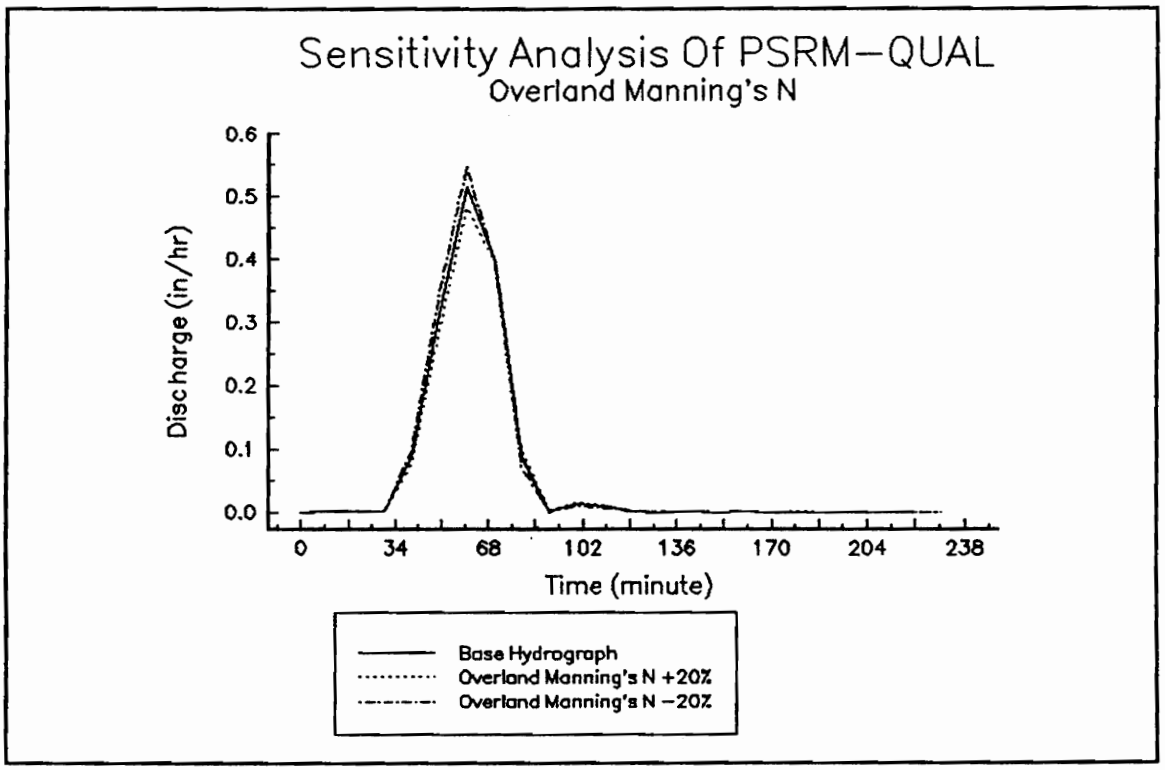

Figure B-9 The effect of the manning's N of overland on the simulated hydrographs (PSRM-QUAL).

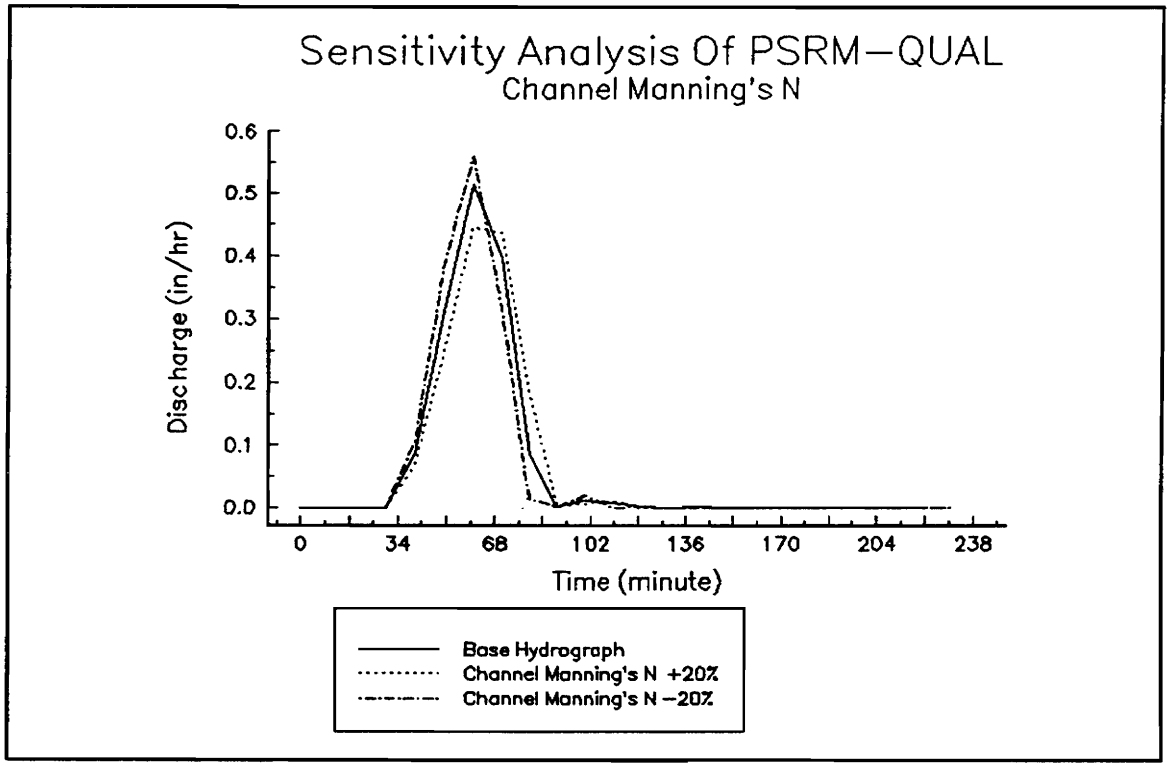

Figure B-10 The effect of the manning's N of channel on the simulated hydrographs (PSRM-QUAL).

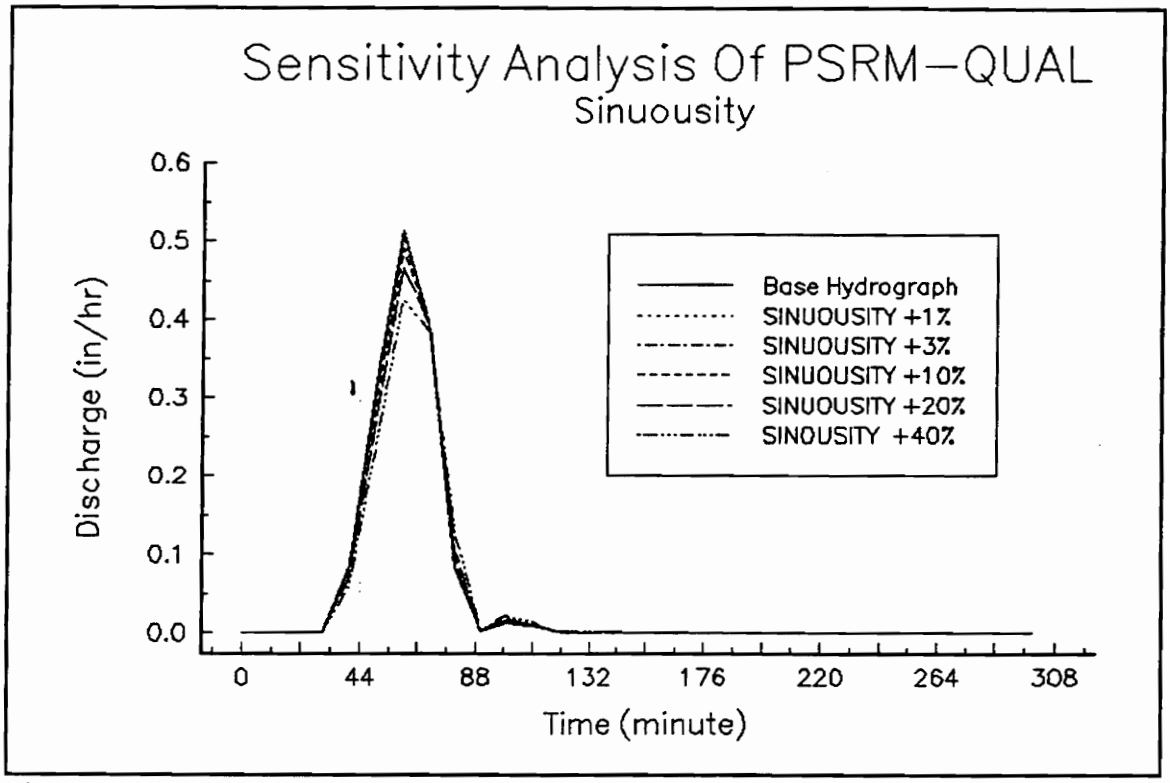

Figure B-11 The effect of sinuousity factor on the simulated hydrographs (PSRM-QUAL).

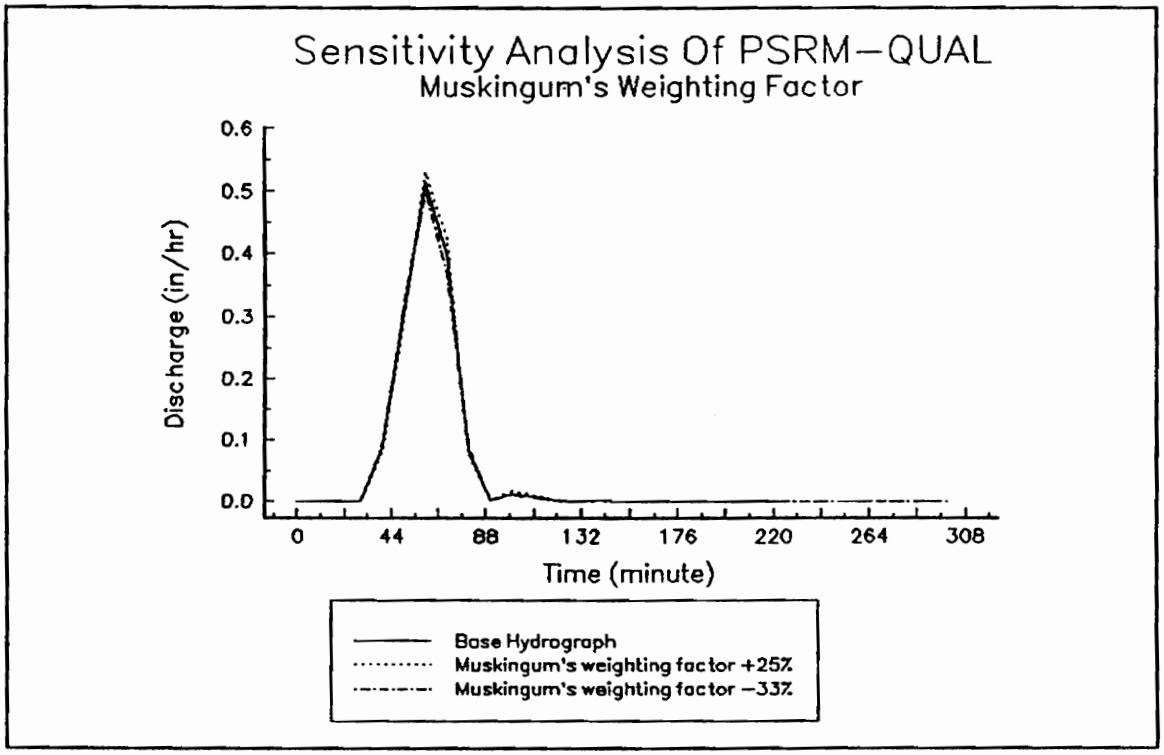

Figure B-12 The effect of Muskingum's weighting factor on the simulated hydrographs (PSRM-QUAL)

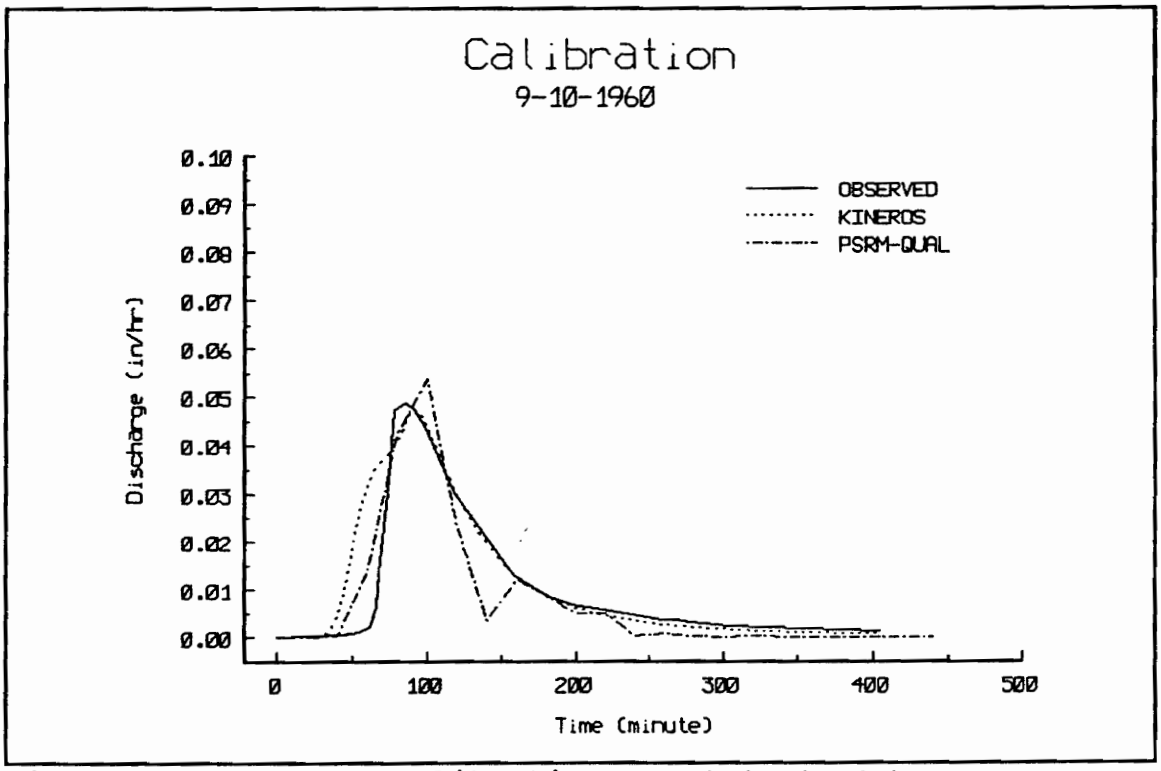

Figure C-1 A sample calibration run (9/10/1960)

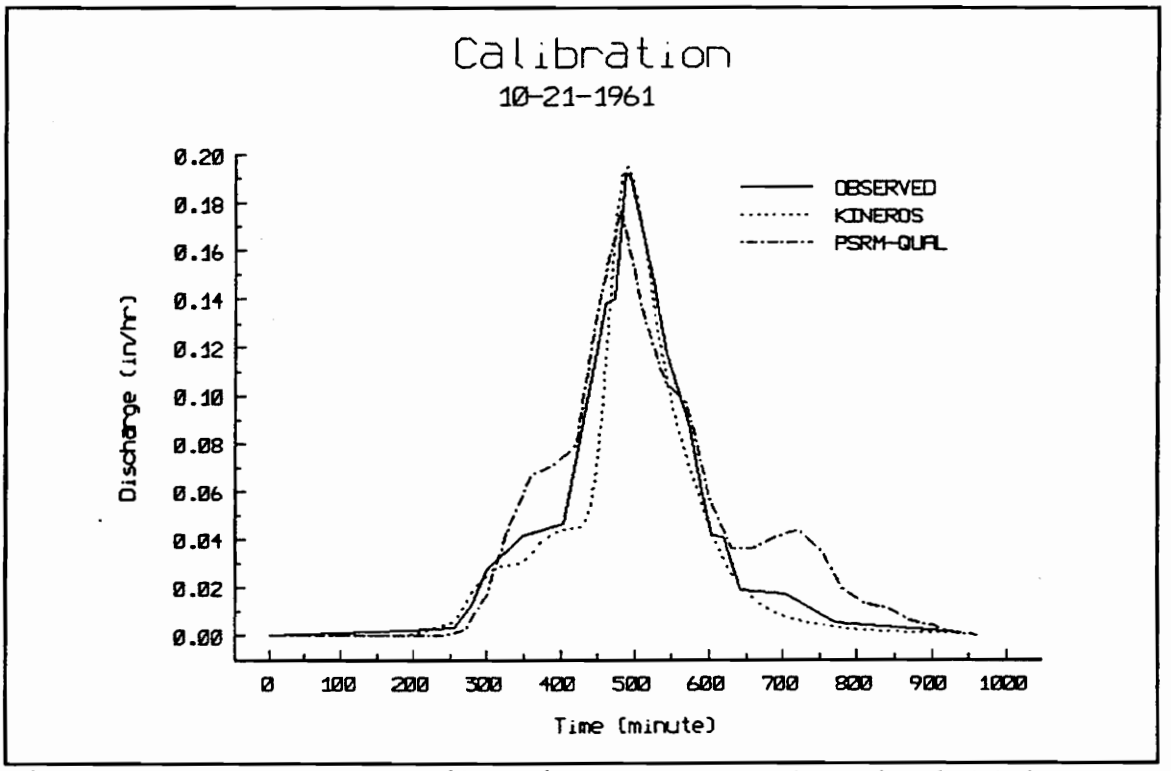

Figure C-2 A sample calibration run (event 10/21/1961)

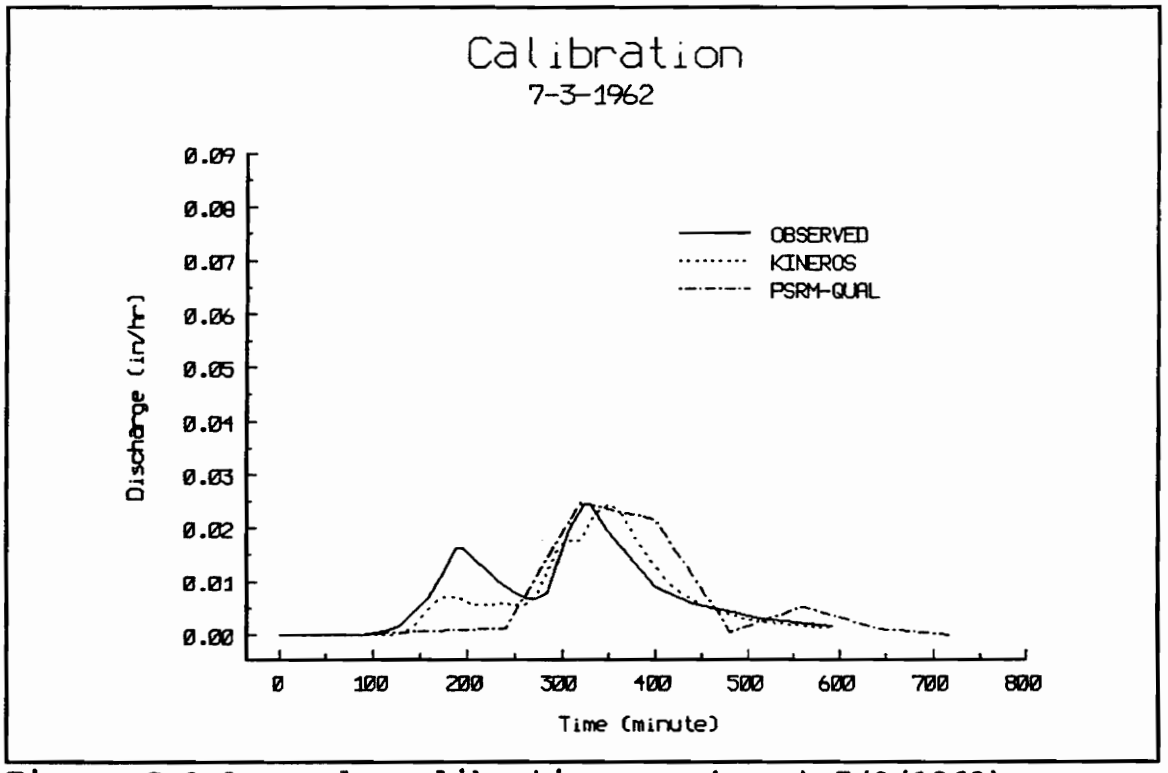

Figure C-3 A sample calibration run (event 7/3/1962)

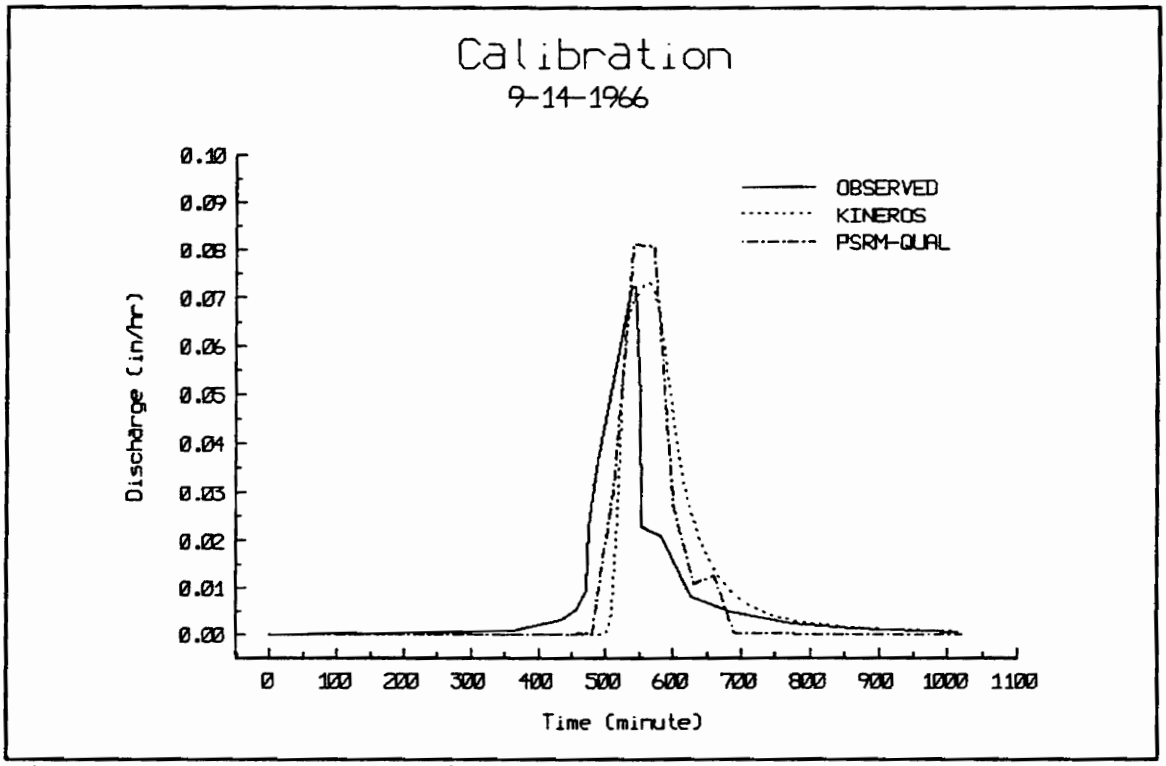

Figure C-4 A sample calibration run (event 9/14/1966)

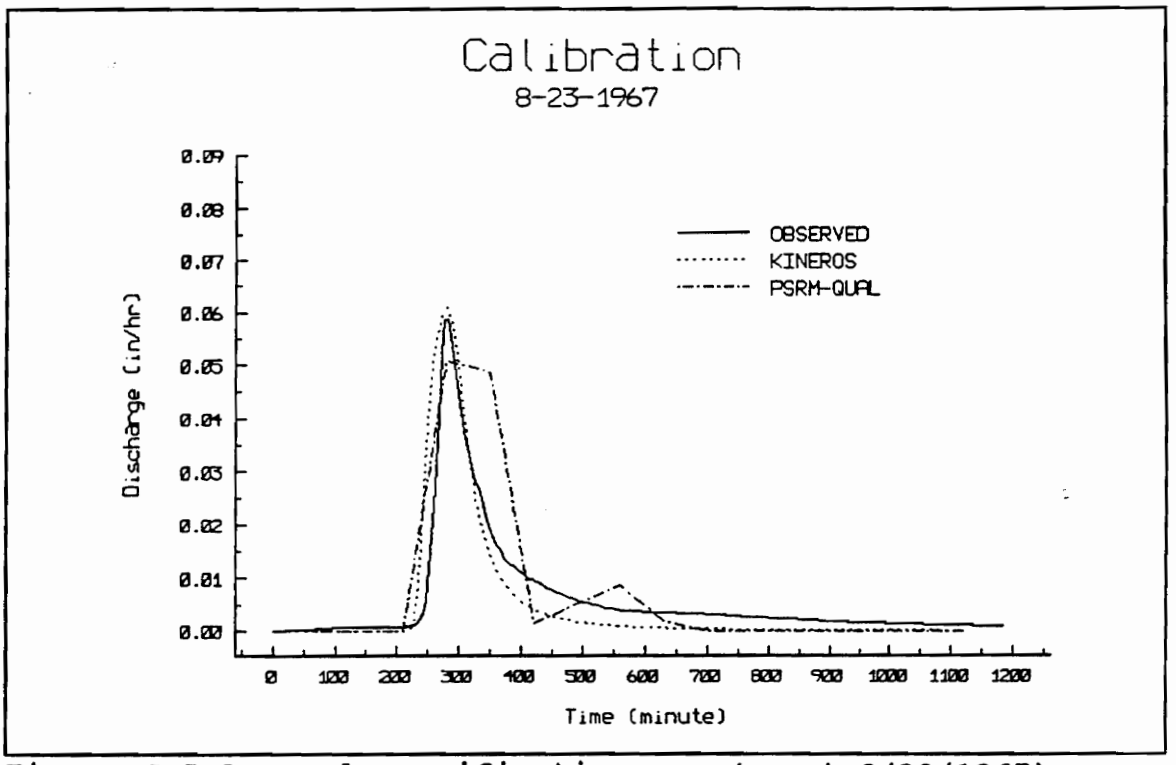

Figure C-5 A sample verification run (event 8/23/1967)

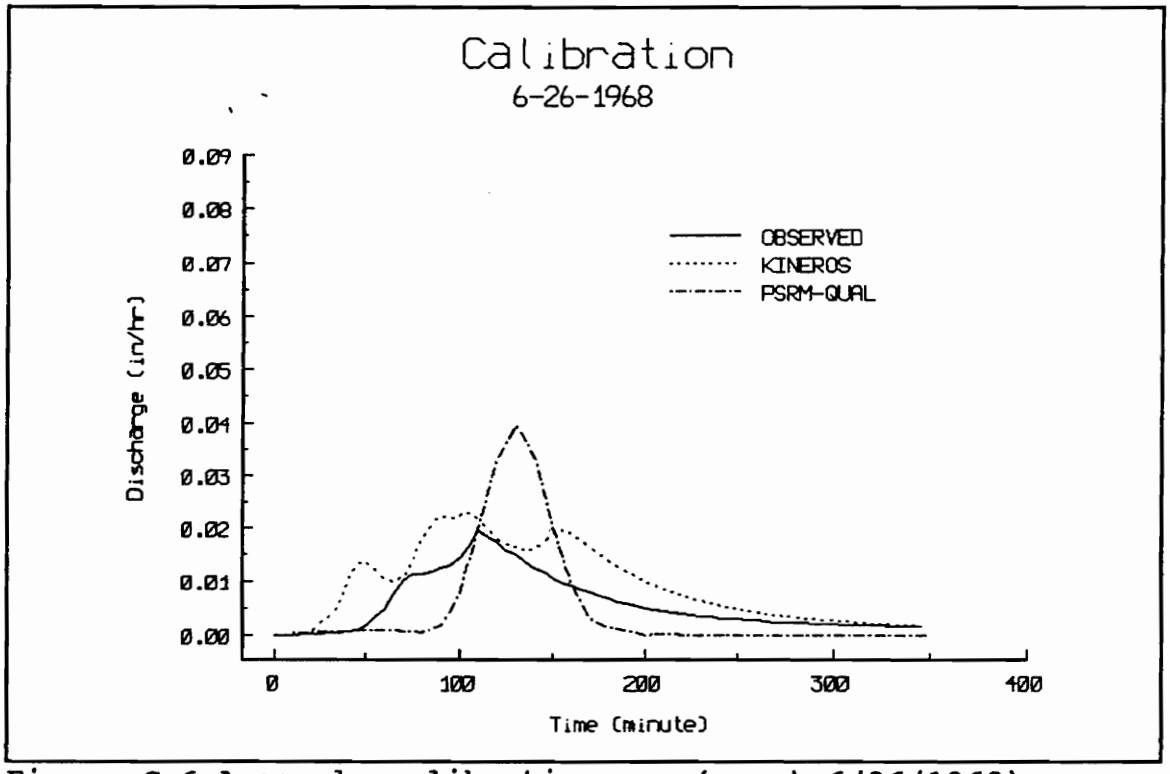

Figure C-6 A sample calibration run (event 6/26/1968)

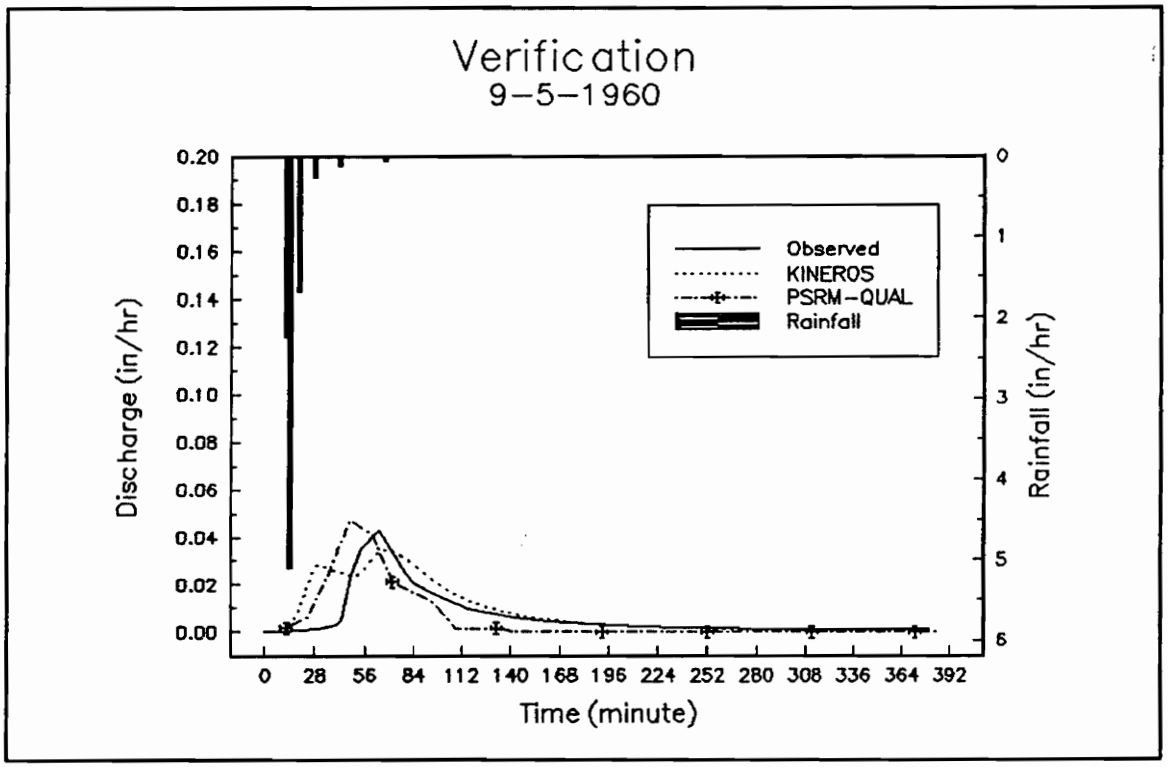

Figure C-7 A sample verification run (event 9/5/1960)

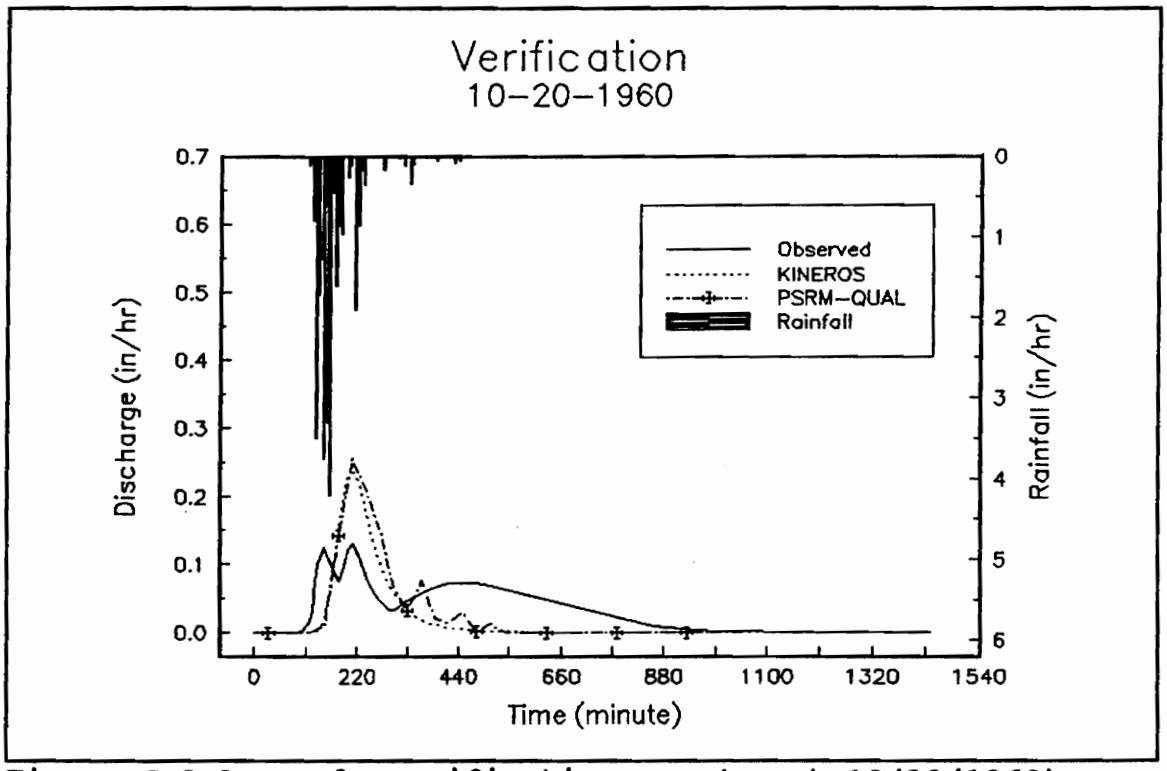

Figure C-8 A sample verification run (event 10/20/1960)

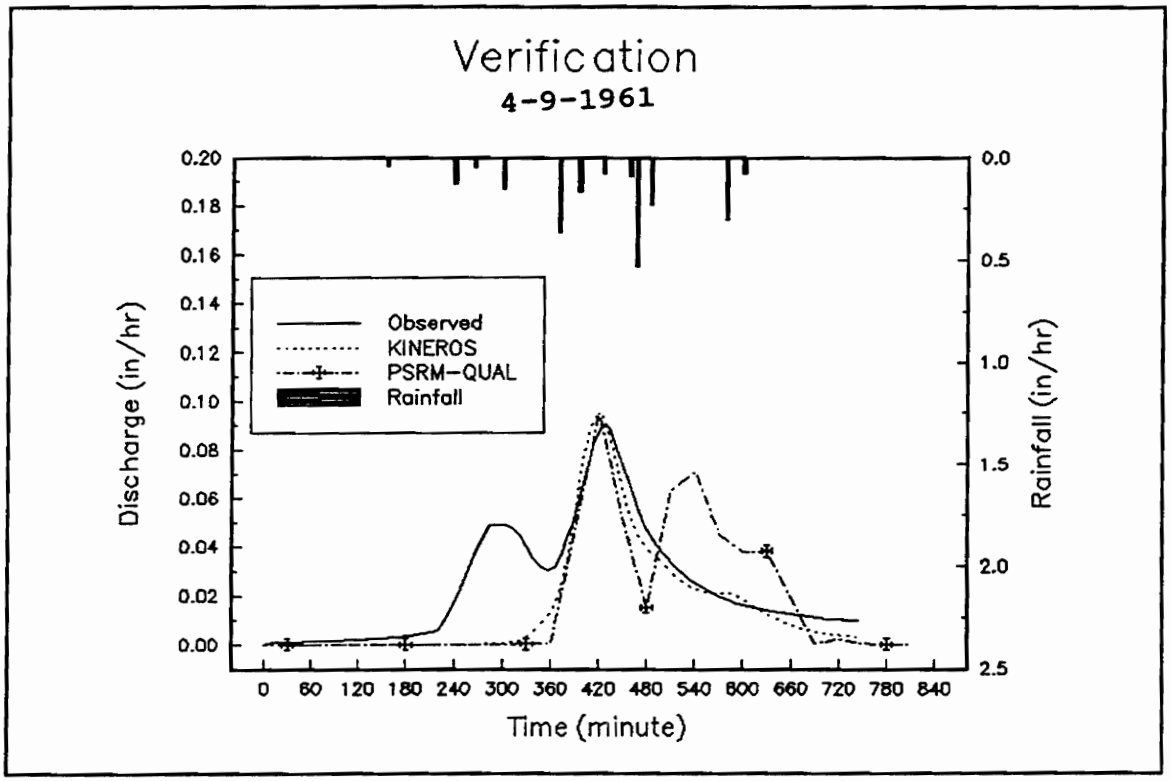

Figure C-9 A sample verification run (4/9/1961)

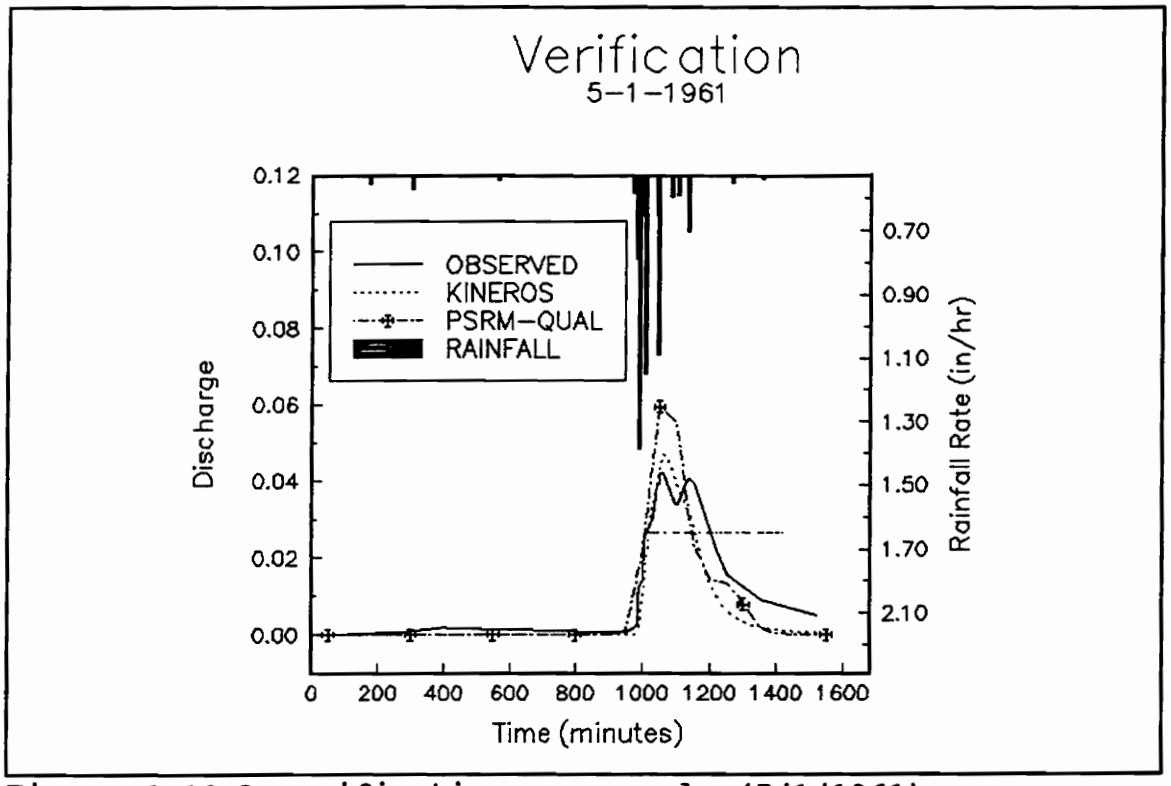

Figure C-10 A verification run sample (5/1/1961)

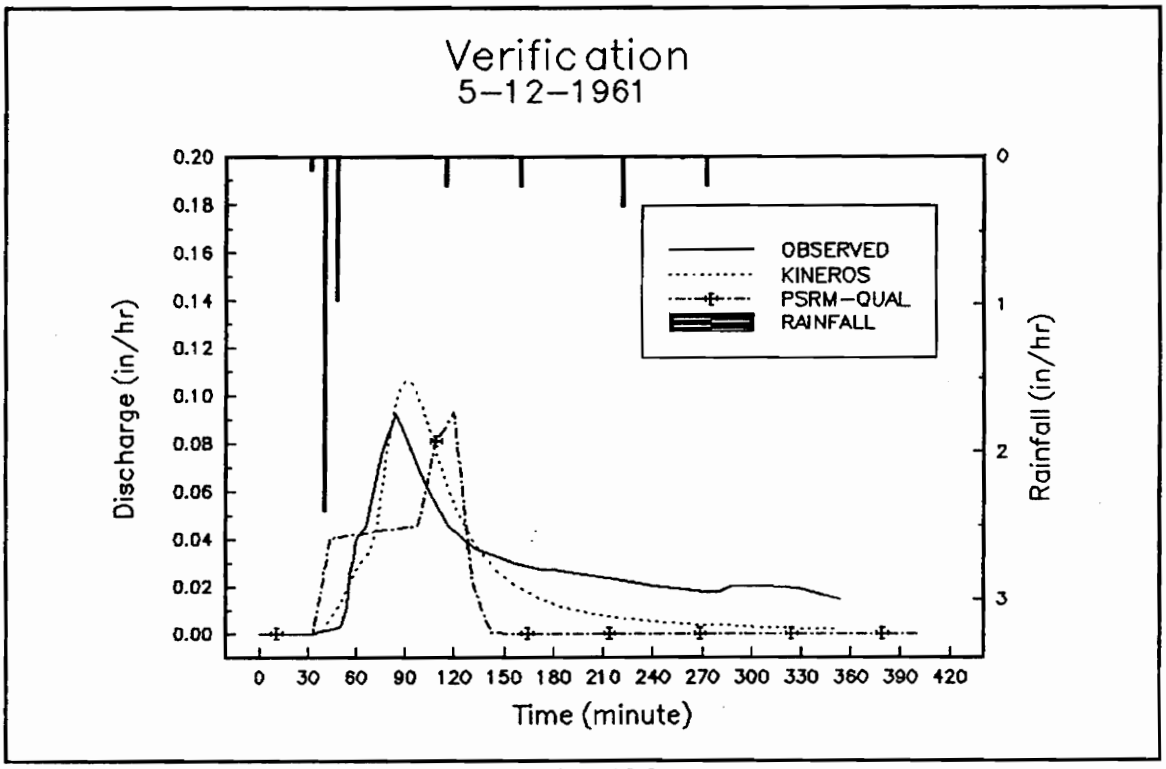

Figure C-11 A sample verification run (5/12/1961)

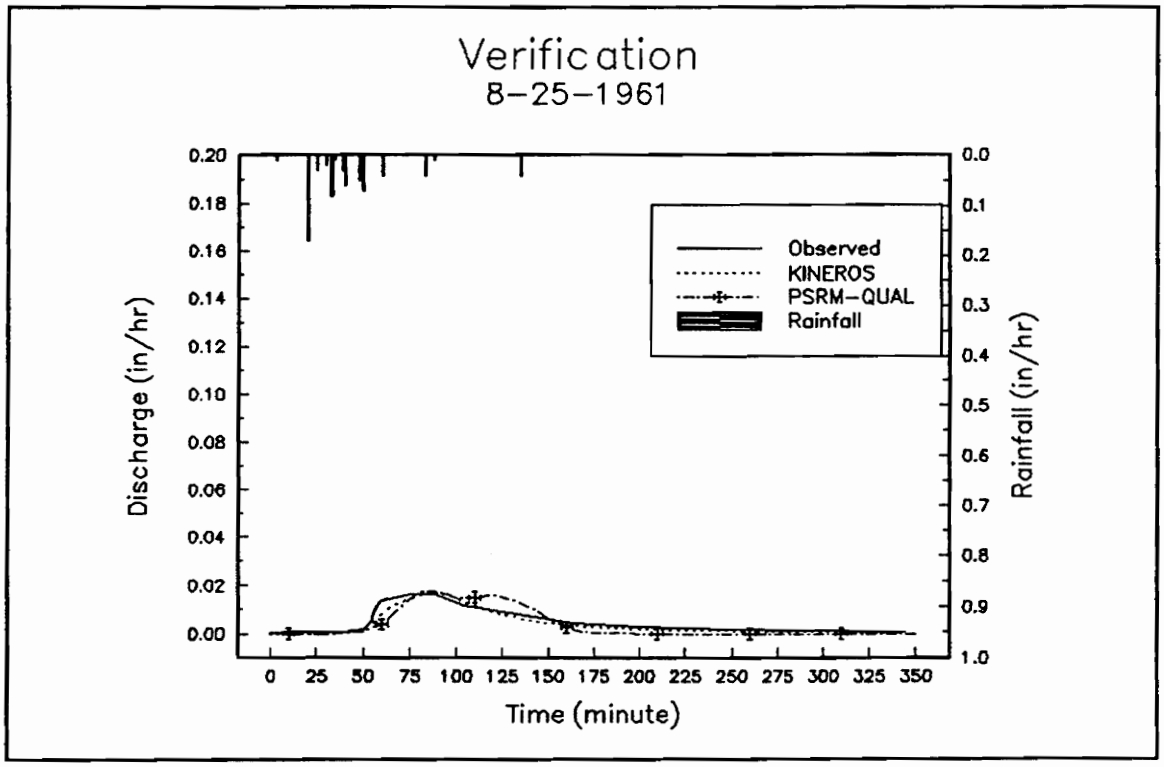

Figure C-12 A sample verification run (8/25/1961)

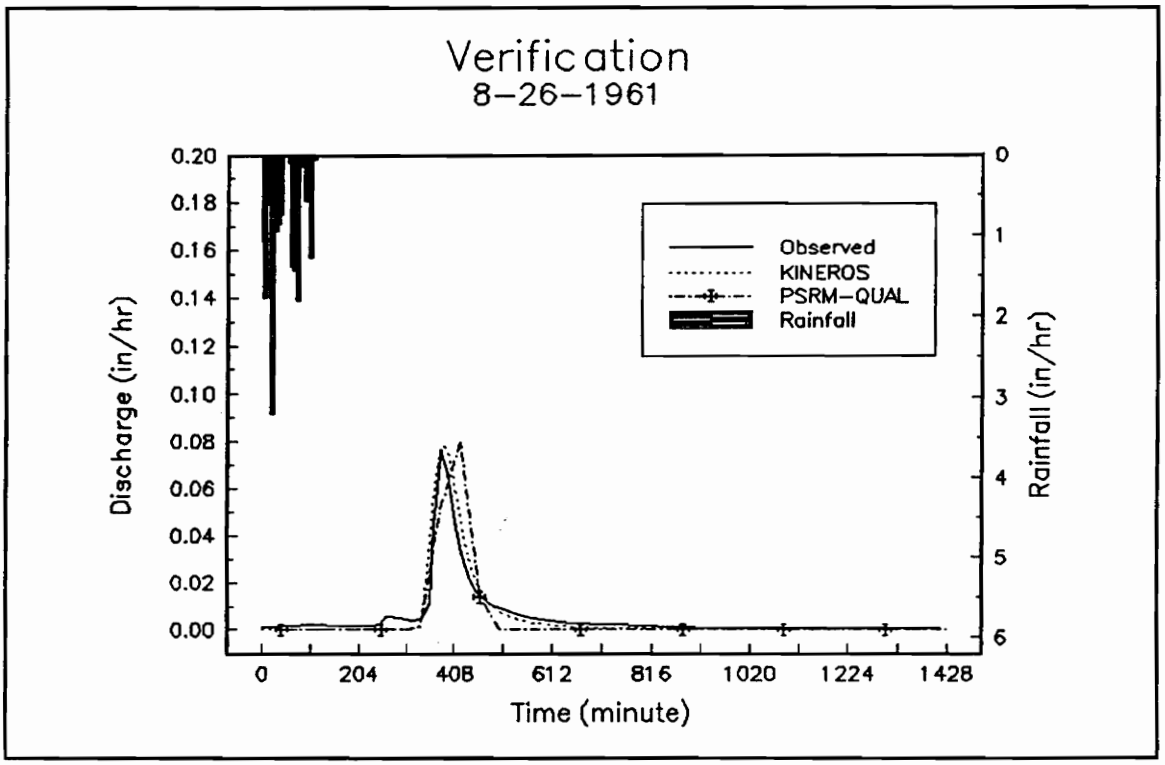

Figure C-13 A sample verification run (8/26/1961)

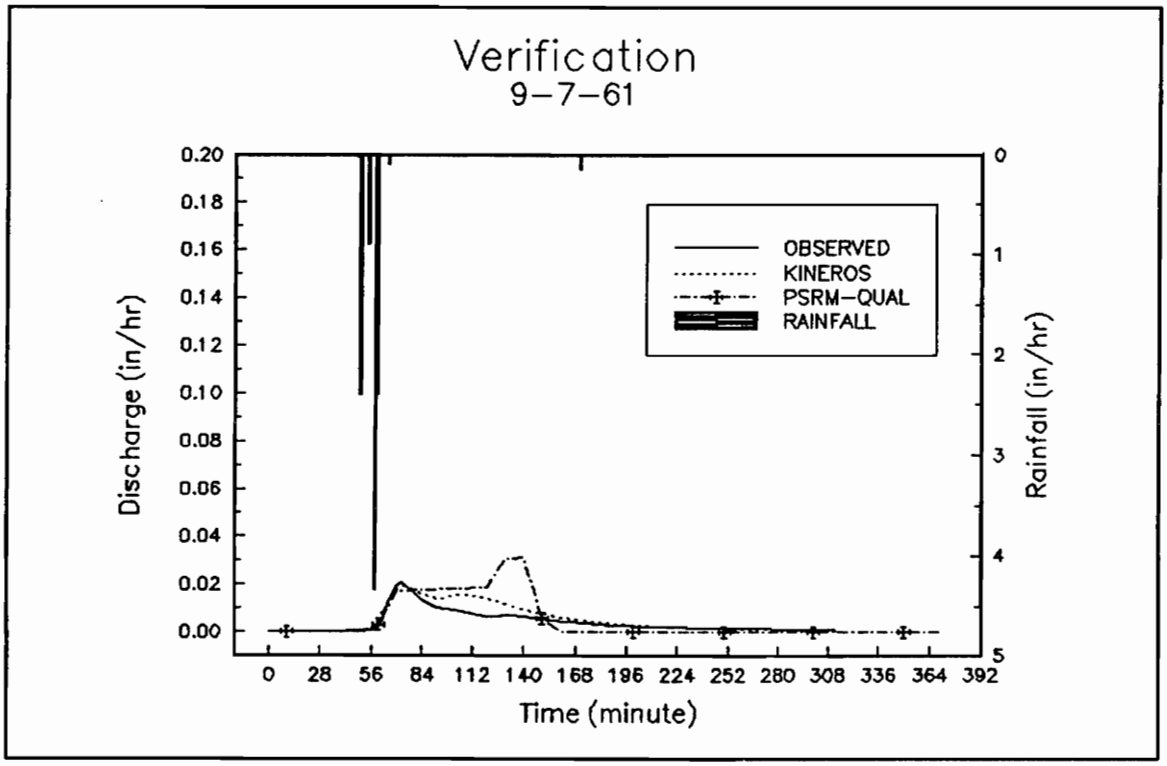

Figure C-14 A sample verification run (9/7/1961)

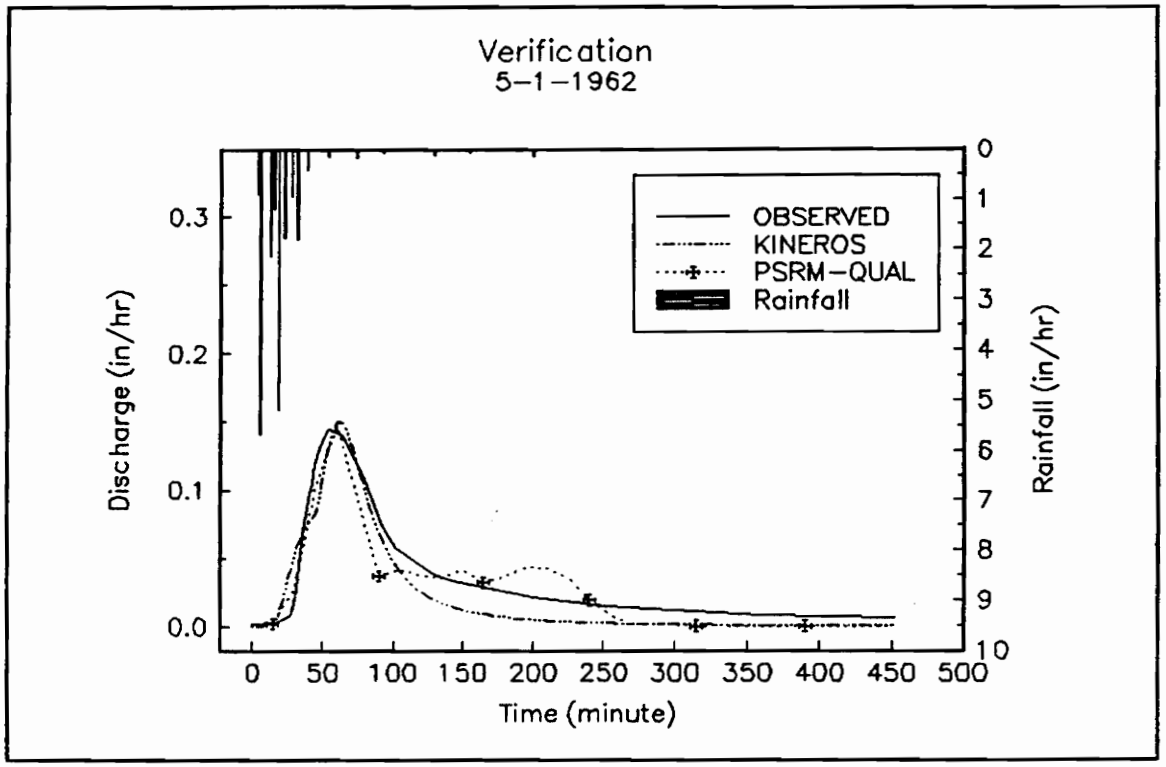

Figure C-15 A sample verification run (event 5/1/1962)

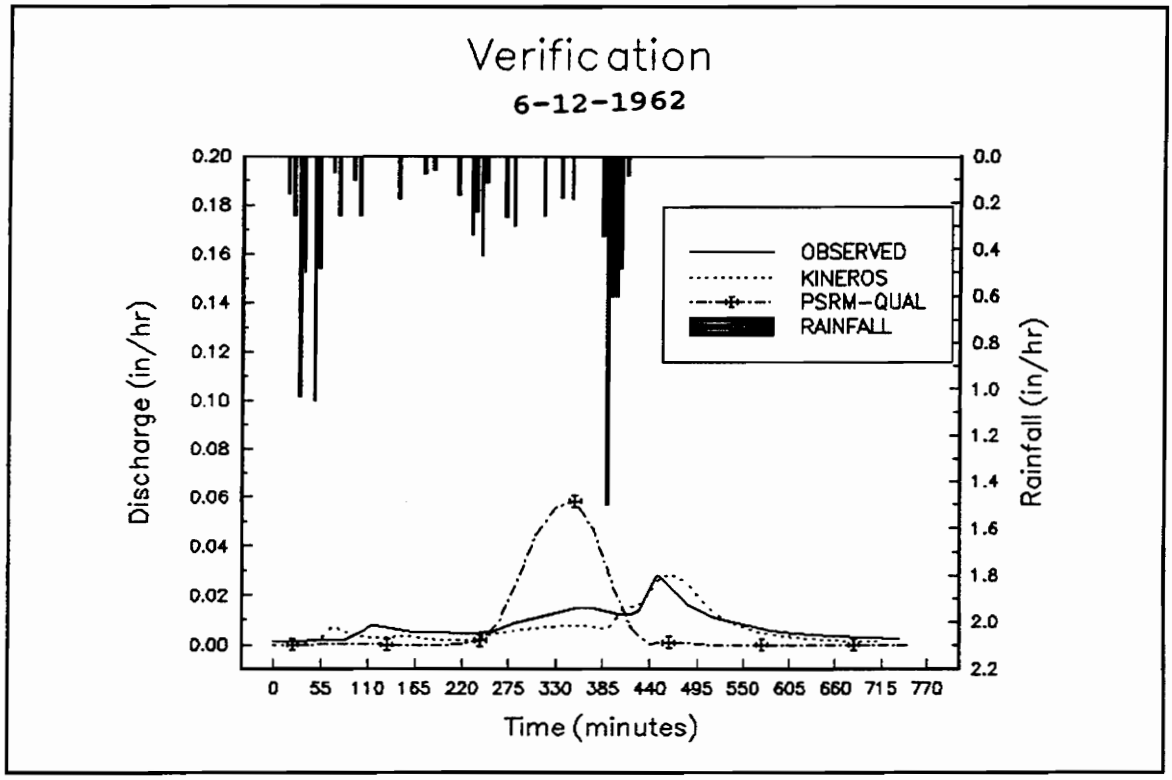

Figure C-16 A sample verification run (6/12/1962)

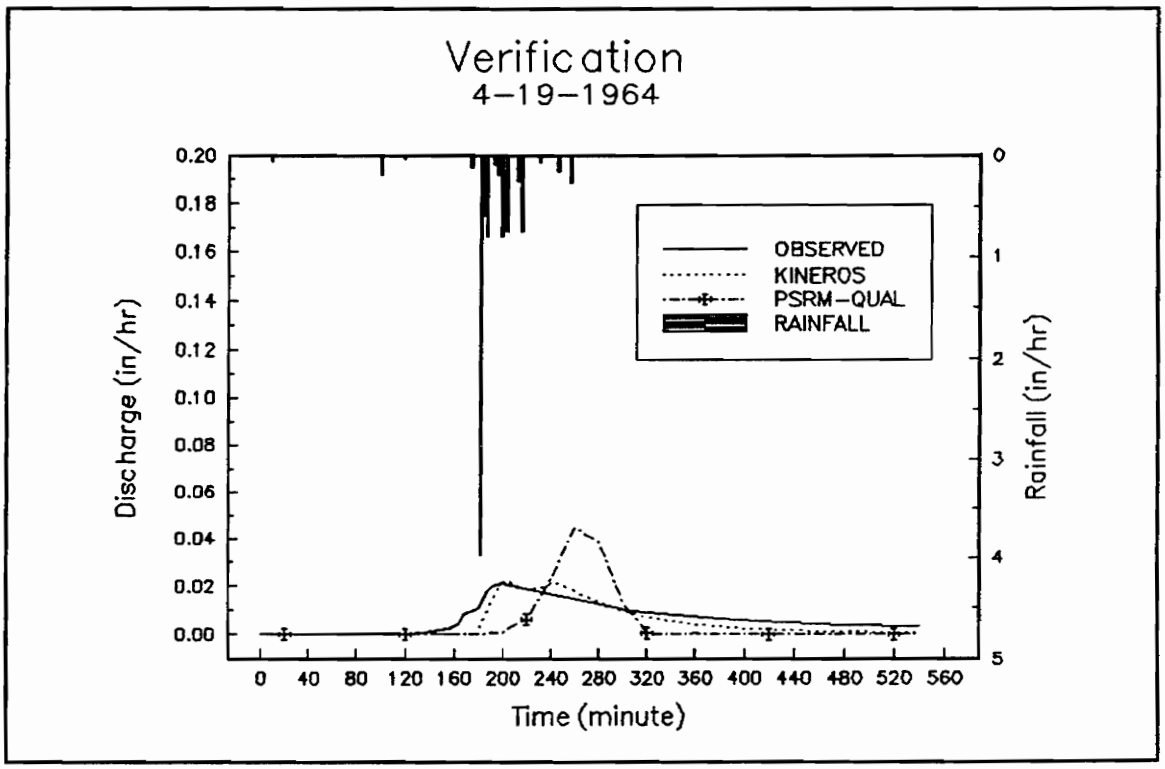

Figure C-17 A sample verification run (4/19/1964)

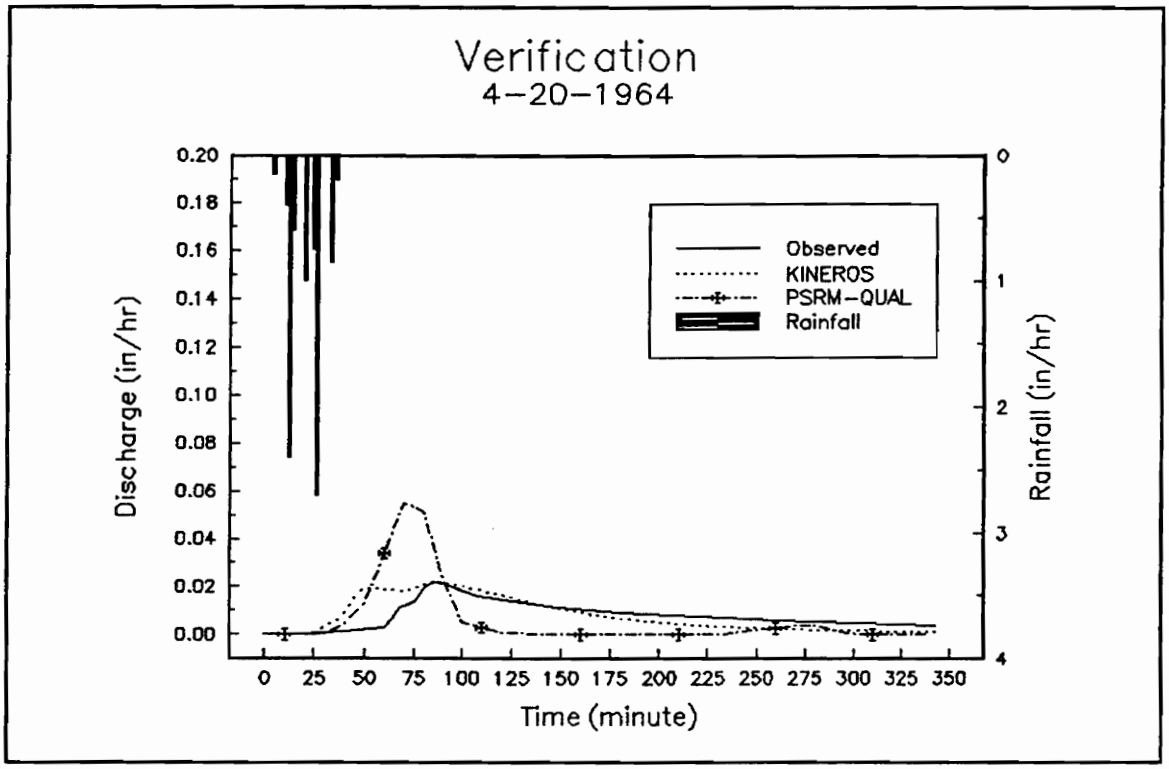

Figure C-18 A sample verification run (4/20/1964)

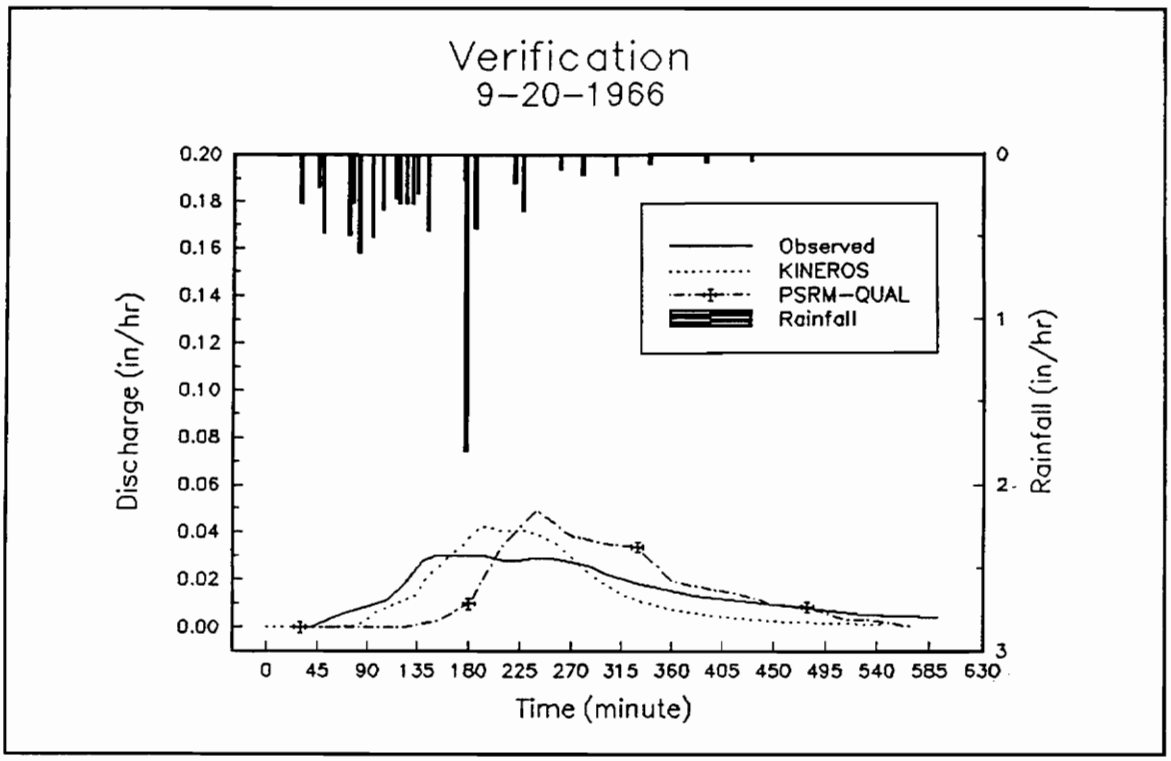

Figure C-19 A sample verification run (9/20/1966)

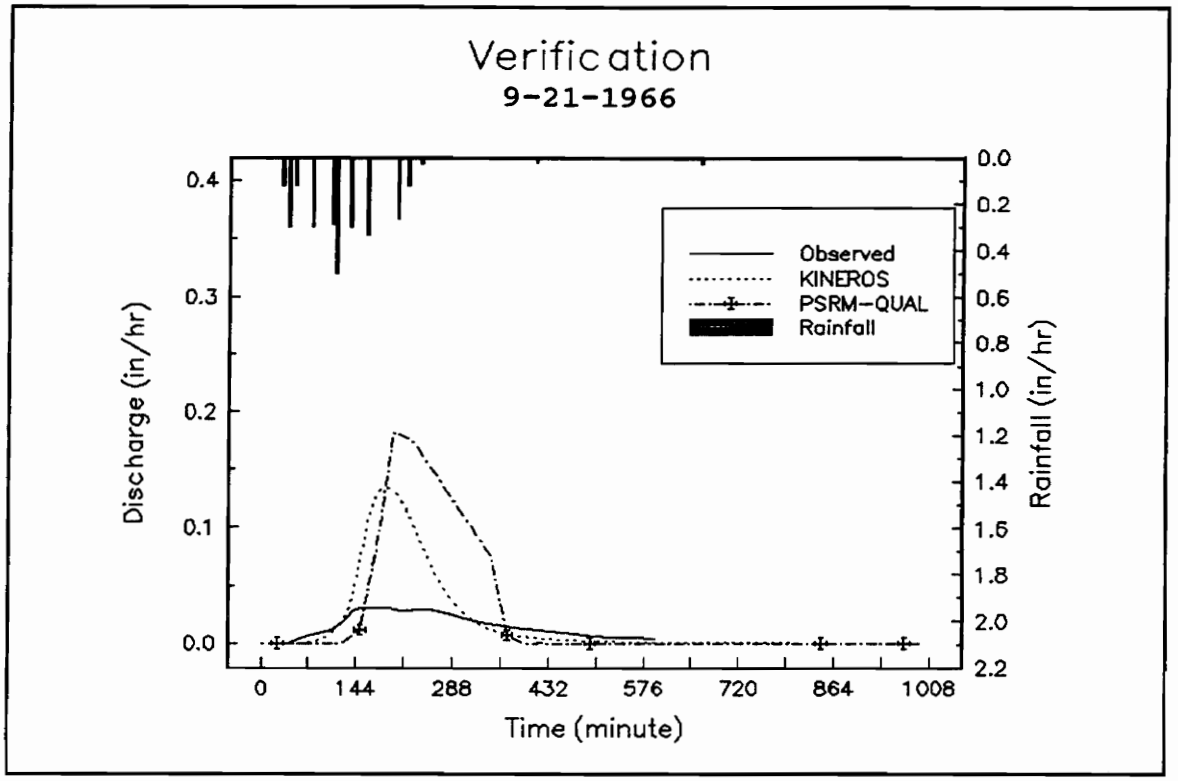

Figure C-20 A sample verification run (9/21/1966)

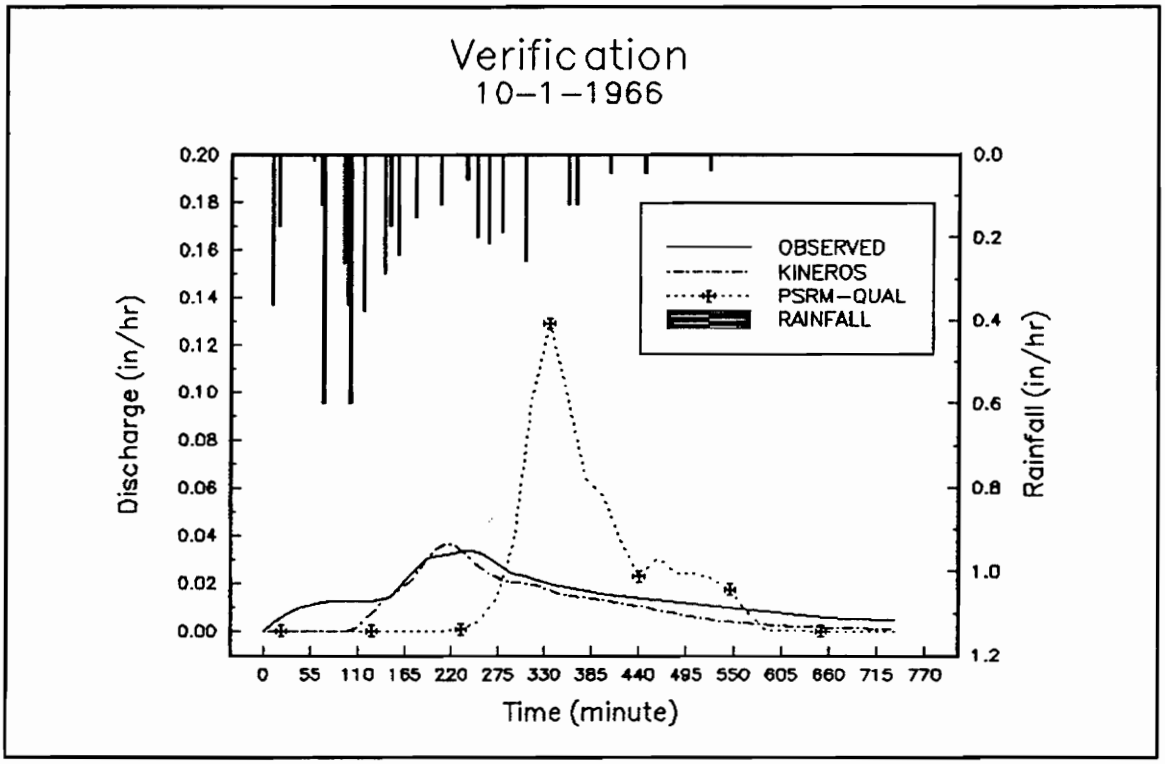

Figure C-21 A sample verification run (10/1/1966)

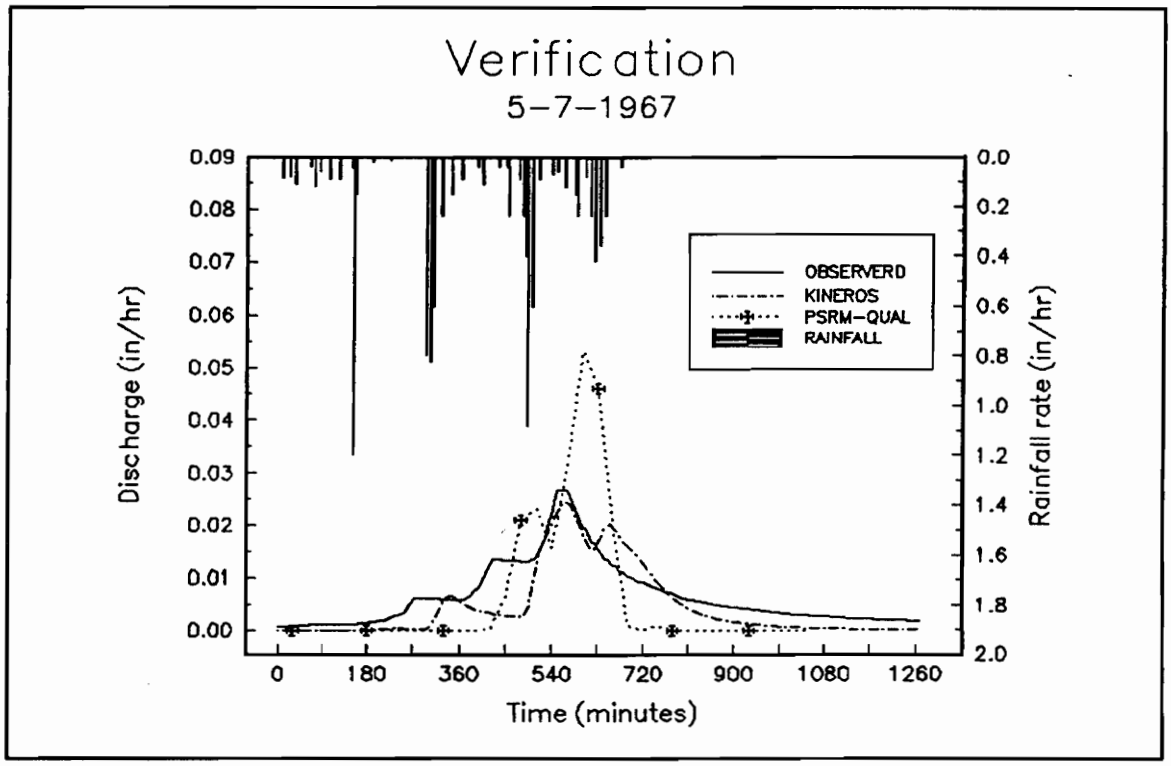

Figure C-22 A sample verification run (5/7/1967)

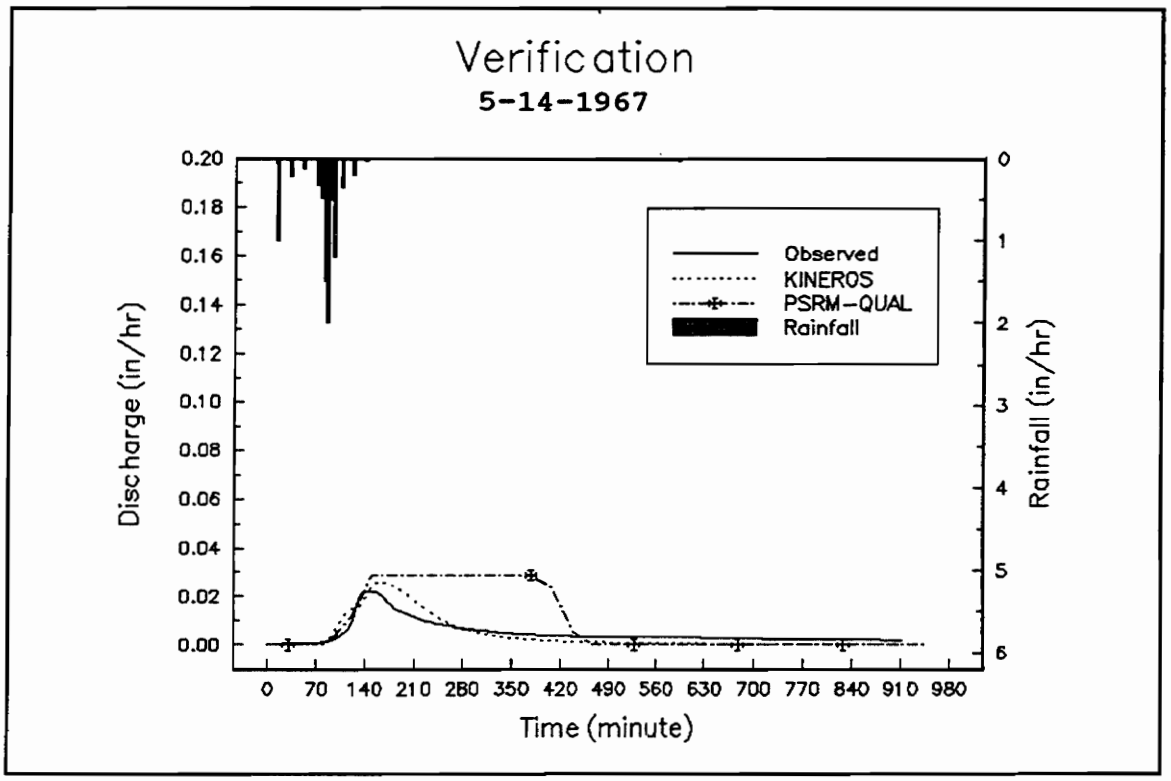

Figure C-23 A sample verification run (5/14/1967)

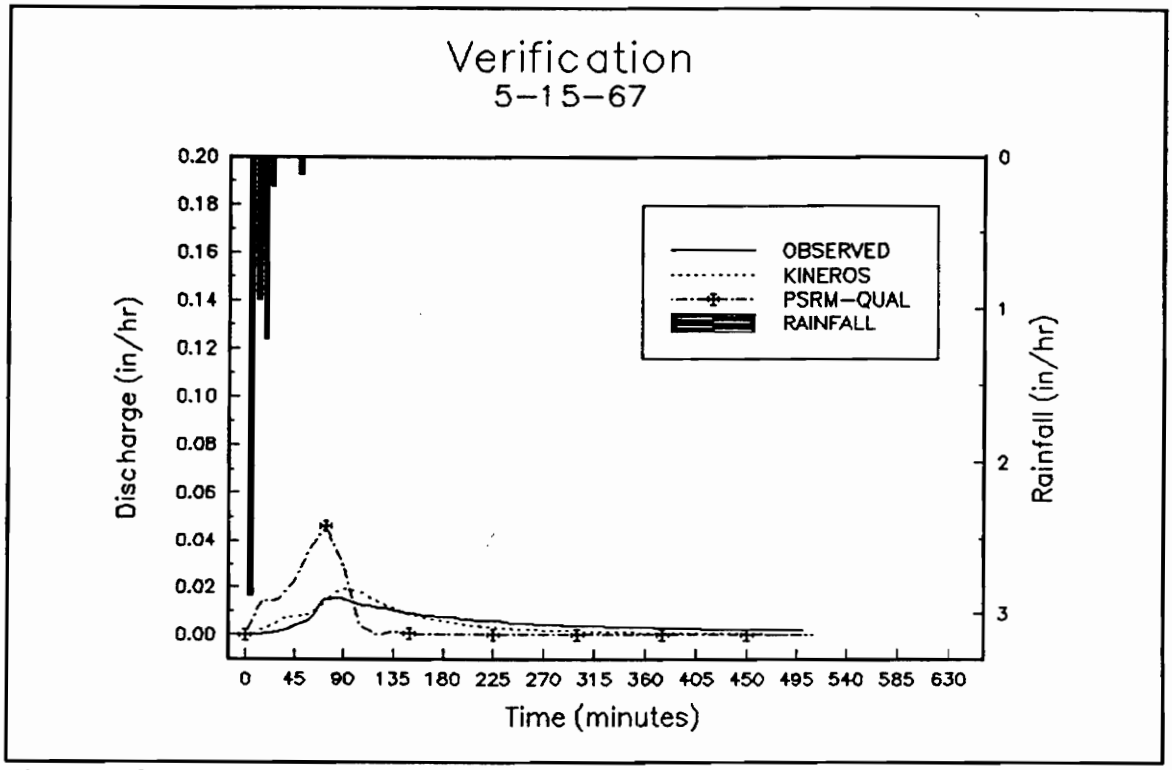

Figure C-24 A sample verification run (5/15/1967)

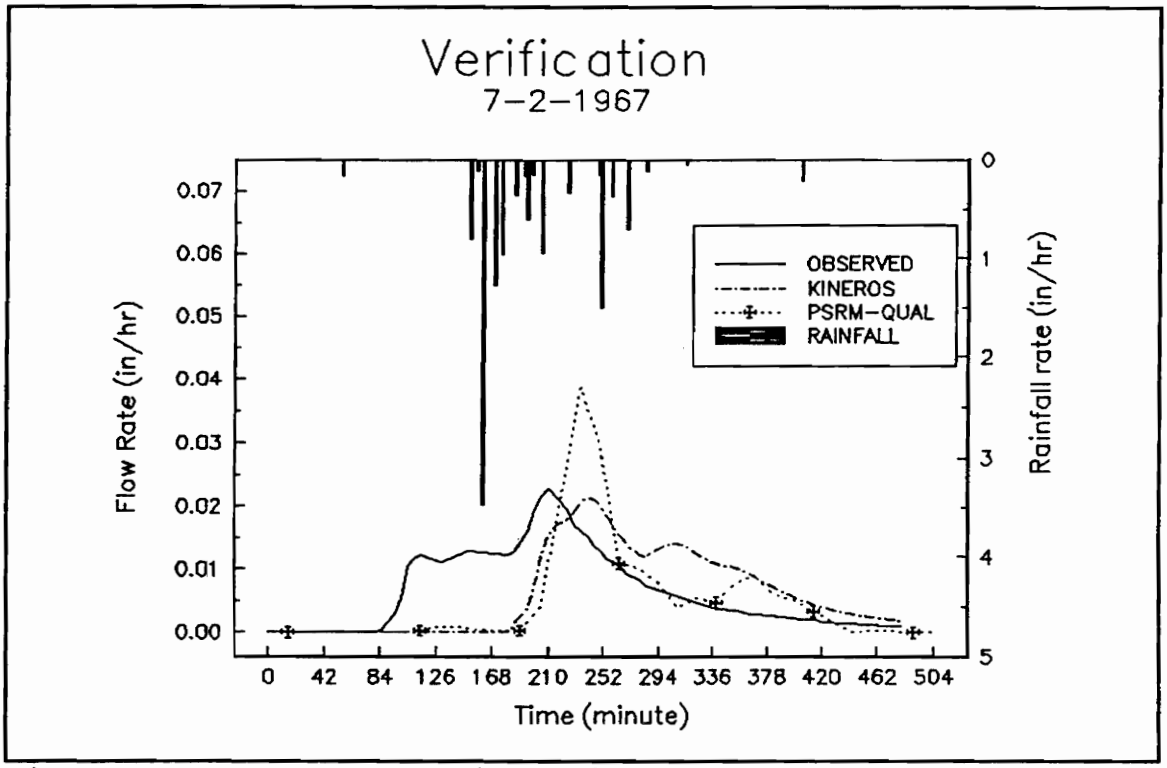

Figure C-25 A sample verification run (7/2/1967)

Table D-1 (a) Parts of Rainfall Input file for KINEROS

```
                              KINEROS   Rainfall Input Data
#
*****************************
      Gage Network Data      RAIN EVENT  0F26-06-68: GAGE 83
*****************************
#
  NUM. OF RAINGAGES     MAX. NUM. OF TIME-DEPTH DATA PAIRS FOR ALL GAGES
      (NGAGES)              (MAXND)
      --------              -------
         1                    20
#
 There must be NELE  pairs of (GAGE  WEIGHT) data
*
 ELE. NUM. (J)      RAINGAGE      WEIGHT
 -------------      --------      ------
       1               1           1.0
       2               1           1.0
       3               1           1.0
       *               *            *
       *               *            *
       *               *            *
     105               1           1.0
     106               1           1.0
     107               1           1.0
     108               1           1.0
     109               1           1.0
     110               1           1.0
     111               1           1.0
   #
*****************************
       Rainfall Data
*****************************
 There must be NGAGES sets of rainfall data. Repeat lines from * to *
 for each gage inserting a variable number of TIME-DEPTH data pairs
 (see example in User Manual).
#
* ALPHA-NUMERIC GAGE ID: WALNUT GULCH GAGE #83 = GAGE NUM. 1
#
  GAGE NUM.      NUM. OF DATA PAIRS (ND)
  ---------      -----------------------
      1                   20
#
 There must be ND pairs of time-depth (T D) data: NOTE: The last time
 must be greater than TFIN (the total computational time)
#
   TIME      ACCUM. DEPTH
  ------     ------------
    0.0          0
    3.0       0.05
    6.0       0.14
   10.0       0.18
   19.0       0.45
   22.0        0.6
   30.0       0.73
   35.0        0.8
   39.0       0.85
   57.0       0.88
   60.0       0.95
   66.0       1.09
   70.0       1.15
   74.0       1.27
   86.0        1.3
   90.0       1.34
   98.0       1.35
  101.0       1.41
  110.0       1.42
  300.0       1.42
*
```

Table D-1 (b) Parts of Parameter Input file For KINEROS

```
                    KINEROS Parameter 260668 Input File
#
************************************
*********** S Y S T E M ********
************************************
*  NELE    NRES   NPART    CLEN    TFIN    DELT  THETA    TEMP
    110       1       0  1283.3  240.     1.9    0.8    -1.
#
************************************
********* O P T I O N S ***********
************************************
  NTIME NUNITS   NEROS
      2       1       0
#
************************************************
****   C O M P U T A T I O N   O R D E R   ****
************************************************
  There must be NELE elements in the list. NLOG
  must be sequential. ELEMENT NUM. need not be.
#
  COMP. ORDER     ELEMENT
     (NLOG)       NUM. (J)
     ------       --------
       1             34
       2             35
       3             36
       4             1
       5             37
       6             38
       7             39
       8             2
       9             40
      10             41
      11             3
      12             42
      13             43
      14             44
      15             4
      16             45
      17             46
      18             5
      19             47
      20             48
      21             49
      22             6
      23             50
      24             51
      25             7
      26             52
      27             53
      28             54
      29             8
      30             55
      31             56
      32             9
      33             57
      34             58
      35             10
      36             59
      37             60
      38             11
      39             61
      40             62
      41             12
      42             63
      43             64
      44             65
      45             13
      46             66
      47             67
      48             14
      49             68
      50             69
      51             70
```

```
        52          15
        53          71
        54          72
        55          16
        56          73
        57          74
        58          75
        59          17
        60          76
        61          77
        62          78
        63          18
        64          79
        65          80
        66          19
        67          81
        68          82
        69          83
        70          20
        71          84
        72          85
        73          21
        74          86
        75          87
        76          88
        77          22
        78          89
        79          90
        80          23
        81          91
        82          92
        83          24
        84          94
        85          93
        86          25
        87          96
        88          95
        89          26
        90          97
        91          98
        92          99
        93          27
        94         100
        95         101
        96          28
        97         102
        98         103
        99         104
       100          29
       101         105
       102         106
       103         107
       104          30
       105         108
       106         109
       107          31
       108         110
       109         111
       110          32
#
************************************************
******   E L E M E N T - W I S E   I N F O  ***
************************************************
    There must be NELE sets of the ELEMENT-WISE  prompts and data
    records; duplicate records from * to * for each element.  The
    elements may be entered in any order.
*
 J      NU      NR      NL     NC1     NC2  NCASE NPRINT    NPNT     NRP
 1      34      36      35       0       0      1       0       0       0
-------------------------------------------------------------------------
       XL       W       S      ZR      ZL      BW    DIAM      R1      R2
   780.65     0.0    0.02    3.0     3.0    12.0     0.0    0.09     0.0
-------------------------------------------------------------------------
     FMIN       G     POR      SI    SMAX     ROC    RECS   DINTR
      0.0     0.0     0.0     0.0     0.0     0.0     0.0     0.0
-------------------------------------------------------------------------
      LAW      CF      CG      CH   CO-CS     D50    RHOS    PAVE SIGMAS
```

```
        0    0.0    0.0    0.0    0.0    0.0    0.0    0.0    0.0
*
*
 J     NU     NR     NL     NC1    NC2   NCASE NPRINT   NPNT    NRP
 2     37     39     38      0      0      1      1      0      0
-------------------------------------------------------------------
       XL      W      S     ZR     ZL     BW   DIAM     R1     R2
    620.6    0.0   0.03    3.0    3.0   12.0    0.0   0.09    0.0
-------------------------------------------------------------------
     FMIN      G    POR     SI   SMAX    ROC   RECS  DINTR
      0.0    0.0    0.0    0.0    0.0    0.0    0.0    0.0
-------------------------------------------------------------------
      LAW     CF     CG     CH  CO-CS    D50   RHOS   PAVE SIGMAS
        0    0.0    0.0    0.0    0.0    0.0    0.0    0.0    0.0
*
*
 J     NU     NR     NL     NC1    NC2   NCASE NPRINT   NPNT    NRP
 3      0     41     40      1      2      1      1      0      0
-------------------------------------------------------------------
       XL      W      S     ZR     ZL     BW   DIAM     R1     R2
   1267.4    0.0   0.02    3.0    3.0   12.0    0.0   0.09    0.0
-------------------------------------------------------------------
     FMIN      G    POR     SI   SMAX    ROC   RECS  DINTR
      0.0    0.0    0.0    0.0    0.0    0.0    0.0    0.0
-------------------------------------------------------------------
      LAW     CF     CG     CH  CO-CS    D50   RHOS   PAVE SIGMAS
        0    0.0    0.0    0.0    0.0    0.0    0.0    0.0    0.0
      3.0    3.0   12.0    0.0   0.09    0.0
-------------------------------------------------------------------
     FMIN      G    POR     SI   SMAX    ROC   RECS  DINTR
      0.0    0.0    0.0    0.0    0.0    0.0    0.0    0.0
-------------------------------------------------------------------
      LAW     CF     CG     CH  CO-CS    D50   RHOS   PAVE SIGMAS
        0    0.0    0.0    0.0    0.0    0.0    0.0    0.0    0.0
*

-------------------------------------------------------------------
      LAW     CF     CG     CH  CO-CS    D50   RHOS   PAVE SIGMAS
        0    0.0    0.0    0.0    0.0    0.0    0.0    0.0    0.0
  *           *              *              *      *
  *           *              *              *      *
  *           *              *              *      *
 J     NU     NR     NL     NC1    NC2   NCASE NPRINT   NPNT    NRP
106     0      0      0      0      0      0      1      0      0
-------------------------------------------------------------------
       XL      W      S     ZR     ZL     BW   DIAM     R1     R2
    541.0 1016.8  0.036    0.0    0.0    0.0    0.0    0.4    0.0
-------------------------------------------------------------------
     FMIN      G    POR     SI   SMAX    ROC   RECS  DINTR
     0.21    7.5   0.49   0.60   0.95    0.0    0.5   0.03
-------------------------------------------------------------------
      LAW     CF     CG     CH  CO-CS    D50   RHOS   PAVE SIGMAS
        0    0.0    0.0    0.0    0.0    0.0    0.0    0.0    0.0
*
*
 J     NU     NR     NL     NC1    NC2   NCASE NPRINT   NPNT    NRP
107     0      0      0      0      0      0      1      0      0
-------------------------------------------------------------------
       XL      W      S     ZR     ZL     BW   DIAM     R1     R2
    307.0  545.3  0.056    0.0    0.0    0.0    0.0    0.4    0.0
-------------------------------------------------------------------
     FMIN      G    POR     SI   SMAX    ROC   RECS  DINTR
     0.38   6.43   0.45   0.62   0.91    0.0    0.5   0.03
-------------------------------------------------------------------
      LAW     CF     CG     CH  CO-CS    D50   RHOS   PAVE SIGMAS
        0    0.0    0.0    0.0    0.0    0.0    0.0    0.0    0.0
*
*
 J     NU     NR     NL     NC1    NC2   NCASE NPRINT   NPNT    NRP
108     0      0      0      0      0      0      1      0      0
-------------------------------------------------------------------
       XL      W      S     ZR     ZL     BW   DIAM     R1     R2
    218.7 1257.7  0.048    0.0    0.0    0.0    0.0    0.4    0.0
-------------------------------------------------------------------
     FMIN      G    POR     SI   SMAX    ROC   RECS  DINTR
     0.31   6.73   0.47   0.05   0.93    0.0    0.5   0.03
-------------------------------------------------------------------
```

LAW	CF	CG	CH	CO-CS	D50	RHOS	PAVE	SIGMAS
0	0.0	0.0	0.0	0.0	0.0	0.0	0.0	0.0

*
*

J	NU	NR	NL	NC1	NC2	NCASE	NPRINT	NPNT	NRP
109	0	0	0	0	0	0	1	0	0

XL	W	S	ZR	ZL	BW	DIAM	R1	R2
270.0	752.8	0.073	0.0	0.0	0.0	0.0	0.4	0.0

FMIN	G	POR	SI	SMAX	ROC	RECS	DINTR
0.35	6.46	0.47	0.05	0.92	0.0	0.5	0.03

LAW	CF	CG	CH	CO-CS	D50	RHOS	PAVE	SIGMAS
0	0.0	0.0	0.0	0.0	0.0	0.0	0.0	0.0

*
*

J	NU	NR	NL	NC1	NC2	NCASE	NPRINT	NPNT	NRP
110	0	0	0	0	0	0	1	0	0

XL	W	S	ZR	ZL	BW	DIAM	R1	R2
23.3	56.0	0.01	0.0	0.0	0.0	0.0	0.4	0.0

FMIN	G	POR	SI	SMAX	ROC	RECS	DINTR
0.03	11.9	0.43	0.57	0.75	0.0	0.5	0.03

LAW	CF	CG	CH	CO-CS	D50	RHOS	PAVE	SIGMAS
0	0.0	0.0	0.0	0.0	0.0	0.0	0.0	0.0

*
*

J	NU	NR	NL	NC1	NC2	NCASE	NPRINT	NPNT	NRP
111	0	0	0	0	0	0	1	0	0

XL	W	S	ZR	ZL	BW	DIAM	R1	R2
23.3	55.8	0.01	0.0	0.0	0.0	0.0	0.4	0.0

FMIN	G	POR	SI	SMAX	ROC	RECS	DINTR
0.03	11.9	0.43	0.59	0.75	0.0	0.5	0.03

LAW	CF	CG	CH	CO-CS	D50	RHOS	PAVE	SIGMAS
0	0.0	0.0	0.0	0.0	0.0	0.0	0.0	0.0

*

Table D-2 Parts of Parameter Input File For PSRM-QUAL

```
NHL  NA  NRES  NRG  NNRG  NPRT  NOBS  NST  NWG  EXW  IPCS
1    33     0    1     0     1     0    1    1  2.0     2
This is the first run
ST     TR        PRI       DT      DTR     TB      STT
1    350.0      10.0     1.03     10.0   0.00      0.0
STDN1  STDN2  STCN1  STCN2  STDIA  STDS1  STDS2  STCTS  STMX
0.110  0.250   99.5   78.0  0.218   0.06   0.00   1.10  0.40
STLU   STML   STIL   STSW   STSI   STFR   STUK   STUC   STUP
   1     30      5    5.0   2.00   0.80  0.200  1.000  1.000
STKS   STIS   STCD   STCF   STCS   STDK   STSF
 0.090 0.40   0.56   0.35   0.67   0.30   1.00
Rain Gage Data  NS ID  NPT     STR     XRG     YRG   Raingage Name
                 1  1   11     0.0    0.00    0.00  a
 0.18  0.32  0.23  0.12  0.02 0.08 0.2 0.14 0.05 0.07 0.01
Subareas for Hydrograph Output
 33
Organic Materials
   a         ,  b
 10.00000  10.00000
Sub.No.  Area    Length  Slope Imp.Fr. X-Coord  Y-Coord
  1       17.57    639.7  0.028  0.00      7.85     2.37
  2       11.53    297.0  0.028  0.00     10.90     2.50
  3       26.36    591.8  0.036  0.00      9.10     4.27
  4        1.10    240.5  0.043  0.00     13.20     2.10
  5       17.00    435.0  0.029  0.00     15.15     3.10
   *       *        *      *      *        *         *
   *       *        *      *      *        *         *
   *       *        *      *      *        *         *
 29        4.40    258.7  0.029  0.00      5.10    12.90
 30       22.20    435.8  0.035  0.00      3.40    14.40
 31       22.50    660.3  0.042  0.00      6.20    14.50
 32       15.10    298.6  0.054  0.00      8.70    14.70
 33        0.01     88.7  0.021  0.00     10.40    14.70
 I.D.      n1       n2    CN1    CN2     IA     DEP1   DEP2   CTS    MX
  1     -1.000  -1.000  -1.0  64.0 -1.00  -1.00  -1.00  -1.00 -1.00
  2     -1.000   0.210  -1.0  67.0 -1.00  -1.00  -1.00  -1.00 -1.00
  3     -1.000   0.270  -1.0  64.0 -1.00  -1.00   0.06  -1.00 -1.00
  4     -1.000   0.200  -1.0  68.0 -1.00  -1.00  -1.00  -1.00 -1.00
  5     -1.000   0.240  -1.0  67.0 -1.00  -1.00  -1.00   0.00 -1.00
  *        *       *      *      *        *          *
  *        *       *      *      *        *          *
  *        *       *      *      *        *          *
 29     -1.000   0.290  -1.0  64.0 -1.00  -1.00  -1.00  -1.00 -1.00
 30     -1.000   0.360  -1.0  64.0 -1.00  -1.00  -1.00  -1.00 -1.00
 31     -1.000   0.400  -1.0  62.0 -1.00  -1.00  -1.00  -1.00 -1.00
 32     -1.000   0.390  -1.0  64.0 -1.00  -1.00  -1.00  -1.00 -1.00
 33     -1.000   0.390  -1.0  65.0 -1.00  -1.00  -1.00  -1.00 -1.00
 I.D.  LU    ML    IL    SW    SI    FR    UK    UC    UP
  1    1.0   30.    5.   5.0  2.00  0.80  0.20  1.00  1.00
  2    1.0   30.    5.   5.0  2.00  0.80  0.20  1.00  1.00
  3    1.0   30.    5.   5.0  2.00  0.80  0.20  1.00  1.00
  4    1.0   30.    5.   5.0  2.00  0.80  0.20  1.00  1.00
  5    1.0   30.    5.   5.0  2.00  0.80  0.20  1.00  1.00
  *       *      *     *     *        *          *
  *       *      *     *     *        *          *
  *       *      *     *     *        *          *
 29    1.0   30.    5.   5.0  2.00  0.80  0.20  1.00  1.00
 30    1.0   30.    5.   5.0  2.00  0.80  0.20  1.00  1.00
 31    1.0   30.    5.   5.0  2.00  0.80  0.20  1.00  1.00
 32    1.0   30.    5.   5.0  2.00  0.80  0.20  1.00  1.00
 33    1.0   30.    5.   5.0  2.00  0.80  0.20  1.00  1.00
I.D.  KS     IS     CD    CF    CS    DK    SF
  1  0.27  0.126  0.56  0.35  0.67  0.30  1.07
  2  0.27  0.199  0.56  0.35  0.67  0.30  1.07
  3  0.26  0.156  0.56  0.35  0.67  0.30  1.07
  4  0.27  0.212  0.56  0.35  0.67  0.30  1.07
  5  0.29  0.190  0.56  0.35  0.67  0.30  1.07
  *        *       *     *     *        *          *
  *        *       *     *     *        *          *
  *        *       *     *     *        *          *
 29  0.50  0.164  0.56  0.35  0.67  0.30  1.07
 30  0.37  0.157  0.56  0.35  0.67  0.30  1.07
 31  0.57  0.140  0.56  0.35  0.67  0.30  1.07
 32  0.54  0.140  0.56  0.35  0.67  0.30  1.07
 33  0.54  0.024  0.56  0.35  0.67  0.30  1.07
DRAIN.ELEM.DATA  KP    CAP    PT   NAP(1)  NAP(2)  NAP(3)
```

1	0	297.3	7.9	0	0	0
2	0	364.8	5.2	0	0	0
3	2	297.3	12.8	1	2	0
4	0	364.0	8.0	0	0	0
5	1	364.0	3.6	4	0	0
6	0	222.2	7.1	0	0	0
7	2	420.4	1.8	5	6	0
8	0	420.4	4.4	0	0	0
9	2	297.3	7.9	7	8	0
10	1	297.2	2.9	9	0	0
11	1	297.3	2.6	3	0	0
12	2	210.3	4.2	10	11	0
13	0	210.2	11.3	0	0	0
14	2	297.3	11.6	12	13	0
15	0	297.3	8.6	0	0	0
16	1	297.3	10.4	15	0	0
17	0	470.1	4.4	0	0	0
18	0	210.3	7.8	0	0	0
19	2	364.0	2.6	17	18	0
20	0	470.1	1.3	0	0	0
21	1	297.3	2.3	20	0	0
22	0	297.3	9.0	0	0	0
23	2	210.3	5.7	21	22	0
24	2	297.3	7.1	19	23	0
25	2	210.3	9.8	16	24	0
26	2	211.2	4.7	14	25	0
27	0	420.4	9.1	0	0	0
28	2	420.4	1.0	26	27	0
29	0	420.4	5.9	0	0	0
30	0	211.0	11.0	0	0	0
31	2	297.3	10.0	29	30	0
32	2	210.2	0.5	28	31	0
33	1	400.0	0.1	32	0	0

* End of Input

VITA

Born:

Nanjing City, People's Republic of China, April 11, 1967.

Parents:

Bijia and Aixue Fu

Married:

Qun Zhuang, August 12,1991.

Education:

Nanjing University

Nanjing, People's Republic of China

B.Sc. in GIS and Computer Cartography, July, 1989.

Professional Experience:

- Research Associate, Virginia Polytechnic Institute and State University, Blacksburg, Virginia. Information Support Systems Laboratory (ISSL), Biological Systems Engineering Department, May, 1994 - present
- Graduate Research Assistant, Virginia Polytechnic Institute and State University, Blacksburg, Virginia. ISSL, Biological Systems Engineering (former Agricultural Engineering) Department, Aug., 1991- Feb.,1994.
- Assistant Researcher, Research Center for Eco-Environmental Studies, Chinese Academy of Science, Beijing, People's Republic of China, Aug., 1989- June, 1991.

Professional Societies:

American Society of Agriculture Engineers

American Geophysical Union

Honorary:

Alpha Epsilon